Study the Dynamic Behavior of Rotor Supported on a Worn Journal Bearings

Adnan Naji Jamil
Professor
Engineering College - Baghdad University
adnanaji2004@yahoo.co

Ahmed Abdul Hussein Ali
Assistant Professor
Engineering College - Baghdad University
ahmedrobot65@yahoo.com

Tariq Mohammad
Ph-student
Engineering College - Baghdad University
gensettariq@yahoo.com

ABSTRACT

In this paper, the effect of wear in the fluid film journal bearings on the dynamic behavior of rotor bearing system has been studied depending on the analytical driven of dynamic stiffness and damping coefficients of worn journal bearing. The finite element method was used to modeling rotor bearing system. The unbalance response, critical speed and natural frequency of rotor bearing system have been studied to determine the changes in these parameters due to wear. MATLAB software was used to find the analytical values of dynamic coefficients of journal bearing. The results of rotor mounted on fluid film journal bearings showed that the wear in journal bearing increases the amplitude of unbalance response and decrease critical speed, stability and the natural frequencies.

Key words: Rotor, Journal Bearing, Wear, Critical Speed,

دراسة السلوك الديناميكي لدوار مستند على كراسي تحميل متآكلة

عدنان ناجي جميل
استاذ
كلية الهندسة – جامعة بغداد

احمد عبد الحسين علي
استاذ مساعد
كلية الهندسة – جامعة بغداد

طارق محمد حمزة
طالب دكتوراه
كلية الهندسة – جامعة بغداد

الخلاصة

في هذه ألورقة تم دراسة تأثير ألتآكل في كراسي ألتحميل ذات ألغشاء ألسائل على ألسلوك ألديناميكي لمنظومة ألدوار وكرسي ألتحميل بالاعتماد على ألحساب النظري لمعاملات الجساءة والتخميد الديناميكية لكرسي تحميل متآكل. أُستخدمت طريقة العناصر المحددة لتمثيل منظومة الدوار وكرسي التحميل. تم دراسة الاستجابة لعدم ألاتزان, السرعة الحرجة والتردد الطبيعي لمنظومة الدوار وكرسي التحميل لتحديد التغيرات في هذه العوامل نتيجة للتآكل. تم استخدام برنامج الماتلاب لايجاد القيم التحليلية للمعاملات الديناميكية لكراسي التحميل. أظهرت النتائج ان التآكل في كراسي التحميل يزيد سعة الاستجابة لعدم الاتزان ويقلل السرعة الحرجة والأستقرارية والتردد الطبيعي للدوارات المستندة على كراسي تحميل ذو غشاء سائل متآكلة.

الكلمات الرئيسية : الدوار, المحمل الأسطواني, التآكل, السرعة الحرجة.

1. INTRODUCTION

The response of a rotor mounted on the fluid film bearings is depended on the material characteristics and geometric of the rotor, the reaction forces and the dynamic coefficients of the journal bearings which support the rotor. The lubrication of the fluid film bearings is described by the Reynolds equation. The wear in the bearing metals is a usual situation in the systems. This wear occurs due to overloads which leading to contact between journal and bearing or due to dry friction between them during the startup or shutdown of the system. In such cases the wear changes the oil thickness and then the pressure distribution, the equilibrium position of the rotor's center and finally the dynamic coefficients of the journal bearing and the response amplitude of the system.

Dufrane, et al., 1983. inspected the worn hydrodynamic journal bearings used in steam turbine generators and established a model of wear geometry for use in analytical studies of the bearings. **Hashimoto, et al., 1986.** examined theoretically and experimentally the effects of geometric change due to wear on the hydrodynamic lubrication of journal bearings in both laminar and turbulent regimes. **Nikolakopoulos and Papadopoulos, 1994**. calculated the full stiffness and damping matrices of a misaligned wear pattern in a fluid film bearing including higher order nonlinear terms. **Kumar and Mishra, 1996**.studied numerically the influences of geometric change due to wear on stability of hydrodynamic journal bearings. **Kumar and Mishra,1996**, studied the non-circular worn journal bearings under condition of non-laminar lubrication regimes, and the influence of wear on friction and load carrying capacity. **Bouyer and Fillon, 2004.** investigated the effect of wear on the thermohydrodynamic performance of a plain journal bearing and they found out that the temperature of lubrication oil is lowering due to wear in journal bearings**. Nikolakopoulos, et al., 2005.** developed and presented a numerical method to identify the clearance defect due to wear in a rotating flexible rotor supported on two misaligned journal bearing, by response identification at any arbitrary point. **Nikolakopoulos and Papadopoulos, 2007** developed an analytical model in order to find out the relationship between the friction coefficient, the misalignment angles, and wear depth. **Gertzos, et al.,2011.** developed a graphical detection method to identify the wear depth correlating with the measured dynamic bearing characteristics. **Chasalevris, et al., 2013.** analyzed a rotor bearing system supported on worn fluid film bearings in order to estimate the progress of specific frequency components in the rotor response during resonance due to the action of an external excitation force. **Desjardins, 2013.** used special software known the COMSOL software to study the Effect of Wear on the maximum Oil Pressure and Load-Carrying Capacity of a Plain Journal Bearing. **Robbersmyr, et al.,2014**. investigated the metallic contact degree and thus wear and tear between bearing bushes and rotating shafts due to the oil whirl and oil whips in oil film journal bearings by measuring electric currents which pass through the oil film.

2. MATHEMATICAL MODEL OF WEAR IN FLUID FILM JOURNAL BEARING

2.1 Wear Model

The wear model used in this work is proposed by **Dufrane, et al., 1983.** The shape of wear model is shown schematically in **Fig 1.**

The region of positive pressure in the state of worn journal bearing can be divided to three sub region as following:

1. First non- worn region where $(0 \leq \theta \leq \theta_s)$ .In this region the lubricant oil fluid thickness at equilibrium position can be described by the following equation, **Cameron, 1981**:

$$h_o = c + e\cos\theta \quad (1)$$

For small amplitude motions about the equilibrium journal position the fluid film thickness can be rewritten as shown in the following equation and this represents a new approach adopted in this paper to determine the wear effect on the fluid film thickness

$$h = C + e(t)\cos(\theta); \quad (2)$$

Where,

$\theta = \gamma - \emptyset_0$, γ is an angle measured from y axis.

$e(t) = e_0 + \Delta e(t)$; $\emptyset(t) = \emptyset_0 + \Delta\emptyset(t)$, where Δe and $\Delta\emptyset$ are small radial and angular displacement quantities, respectively. Eq. (2) can be rewritten as in the following equation

$$h = C + (e_0 + \Delta e)\{\cos\theta\cos\Delta\emptyset + \sin\theta\sin\Delta\emptyset\}, \quad (3)$$

And, for small amplitude motions, $\cos(\Delta\emptyset)\sim 1, \sin(\Delta\emptyset)\sim\Delta\emptyset$. Small values products such as $(\Delta e\Delta\emptyset)$ should be neglected (considered equal to zero)

$$h = C + e_0\cos\theta + \Delta e\cos\theta + e_0\Delta\emptyset\sin\theta = h_0 + h_1 \quad (4)$$

Where,

$$h_0 = C + e_0\cos\theta\,;\ h_1 = \Delta e\cos\theta + e_0\Delta\emptyset\sin\theta$$

2. Worn region where ($\theta_s \le \theta \le \theta_f$).The thickness of lubricant oil fluid (h_{ow}) in the journal bearing wear region at equilibrium position can be described by the following equation **Dufrane, et al., 1983.**

$$h_{ow} = d_0 + e\cos\theta - c\cos(\theta + \emptyset_o) \quad (5)$$

Where, c is the journal bearing radial clearance.

By using the same procedures mentioned above for non worn region the thickness fluid film for worn region (h_w) can be written as following

$$h_w = do + (e_0 + \Delta e)\cos(\gamma - \emptyset_0 - \Delta\emptyset) - c\cos(\theta + \emptyset_0)$$

$$h_w = do + e_0\cos\theta - c\cos(\theta + \emptyset_0) + e_0\Delta\emptyset\sin\theta + \Delta e\cos\theta$$

$$= h_{0w} + h_1 \quad (6)$$

3. Second non-worn region where ($\theta_f \le \theta \le \pi$). In this region the thickness of lubricant oil fluid as in the first non-worn region.

The starting and final angles of the region where the wear take place (θ_s and θ_f) are given by the solution of the following equation **Nikolakopoulos and Papadopoulos, 2009**

$$\cos(\theta + \emptyset_o) = \frac{d_0}{c} - 1 = \delta - 1 \quad (7)$$

Where $\delta = \frac{d_0}{c}$

So the values of starting and final angles of the region where the wear take place are

$$\theta_s = \pi - \emptyset_o - arcos(1-\delta) \ , \ \theta_f = \pi - \emptyset_o + arcos(1-\delta) \tag{8}$$

2.2 Reynolds Equation

For a laminar flow and isoviscous incompressible fluid the Reynolds equation with some necessary assumptions **Kramer, 1993.** And for short journal bearing can be written as below

$$\frac{\partial}{\partial x}\left(\frac{h^3}{12\mu}\frac{\partial P}{\partial x}\right) + \frac{\partial}{\partial z}\left(\frac{h^3}{12\mu}\frac{\partial P}{\partial z}\right) = \frac{\partial h}{\partial t} + \frac{\Omega}{2}\frac{\partial h}{\partial \theta} \tag{9}$$

By integrating Eq. (9) with respect to the journal bearing length (z), the pressure distribution for non worn region can be described by the following equation

$$P(\theta, z, t) = \frac{6\mu}{h^3}\left(\frac{\partial h}{\partial t} + \frac{\Omega}{2}\frac{\partial h}{\partial \theta}\right)\left(Z^2 - \frac{L^2}{4}\right) \tag{10}$$

And for worn region in journal bearing above equation becomes

$$P_w(\theta, z, t) = \frac{6\mu}{h^3}\left(\frac{\partial h_w}{\partial t} + \frac{\Omega}{2}\frac{\partial h_w}{\partial \theta}\right)\left(Z^2 - \frac{L^2}{4}\right) \tag{11}$$

Where P_w and h_w are the pressure and fluid film thickness in the worn region of journal bearing respectively.

2.3 Calculation of Dynamic Coefficients of Worn Journal Bearings

The radial and tangential components of fluid film journal bearing force are **Chen and Gunter, 2007**

$$\begin{Bmatrix} F_r \\ F_t \end{Bmatrix} = 2\int_0^{L/2}\int_0^{\pi} P(\theta, z, t) R \begin{pmatrix} \cos\theta \\ \sin\theta \end{pmatrix} d\theta dz \tag{12}$$

According to the above divided of positive pressure in journal bearing, by using Eq. (10) and Eq.(11) for pressure in non worn region and worn region of fluid film journal bearing respectively , Eq. (12) becomes

$$\begin{Bmatrix} F_r \\ F_t \end{Bmatrix} = \frac{12\mu}{h^3}\int_0^{L/2}\left\{\int_0^{\theta_s}\left(\frac{\partial h}{\partial t} + \frac{\Omega}{2}\frac{\partial h}{\partial \theta}\right) + \int_{\theta_s}^{\theta_f}\left(\frac{\partial h_w}{\partial t} + \frac{\Omega}{2}\frac{\partial h_w}{\partial \theta}\right) + \int_{\theta_f}^{\pi}\left(\frac{\partial h}{\partial t} + \frac{\Omega}{2}\frac{\partial h}{\partial \theta}\right)\right\}\begin{pmatrix} cos\,\theta \\ sin\,\theta \end{pmatrix}$$
$$\left(Z^2 - \frac{L^2}{4}\right) d\theta dz \tag{13}$$

Substitute the derivative of fluid film thickness for worn and non worn region of journal bearing in the Eq. (13) and integrate it with respect to the bearing length (Z) with limits (0 to L/2), and let $H = \frac{h}{c}$, $H_w = \frac{h_w}{c}$ therefore Eq. (13) can be rewritten as following

$$\begin{Bmatrix} F_r \\ F_t \end{Bmatrix} = -\frac{\Omega}{2}\frac{\mu L^3 R}{c^3 H^3}\int_0^{\theta_s}\begin{Bmatrix} -e_0 \sin\theta\cos\theta \\ -e_0 \sin^2(\theta) \end{Bmatrix} d\theta - \frac{\Omega}{2}\frac{\mu L^3 R}{c^3 H^3}\int_{\theta_f}^{\pi}\begin{Bmatrix} -e_0 \sin\theta\cos\theta \\ -e_0 \sin^2(\theta) \end{Bmatrix} d\theta$$

$$-\frac{\Omega}{2}\frac{\mu L^3 R}{c^3 H_w^3}\int_{\theta_s}^{\theta_f}\begin{Bmatrix} -e_0 \sin\theta\cos\theta + c\sin(\theta+\emptyset_0)\cos\theta \\ -e_0 \sin^2(\theta) + c\sin\theta\sin(\theta+\emptyset_0) \end{Bmatrix} d\theta$$

$$-\frac{\Omega}{2}\frac{\mu L^3 R}{c^3 H^3}\left[\int_0^{\theta_s}\begin{Bmatrix} -\sin\theta\cos\theta \\ -\sin^2\theta \end{Bmatrix} d\theta\right]\Delta e - \frac{\Omega}{2}\frac{\mu L^3 R}{c^3 H^3}\left[\int_0^{\theta_s}\begin{Bmatrix} \cos^2\theta \\ \sin\theta\cos\theta \end{Bmatrix} d\theta\right] e_0 \Delta\emptyset$$

$$-\frac{\Omega}{2}\frac{\mu L^3 R}{c^3 H_w^3}\left[\int_{\theta_s}^{\theta_f}\begin{Bmatrix} -\sin\theta\cos\theta \\ -\sin^2(\theta) \end{Bmatrix} d\theta\right]\Delta e - \frac{\Omega}{2}\frac{\mu L^3 R}{c^3 H_w^3}\left[\int_{\theta_s}^{\theta_f}\begin{Bmatrix} \cos^2\theta \\ \sin\theta\cos\theta \end{Bmatrix} d\theta\right] e_0 \Delta\emptyset$$

$$-\frac{\Omega}{2}\frac{\mu L^3 R}{c^3 H^3}\left[\int_{\theta_f}^{\pi}\begin{Bmatrix} -\sin\theta\cos\theta \\ -\sin^2\theta \end{Bmatrix} d\theta\right]\Delta e - \frac{\Omega}{2}\frac{\mu L^3 R}{c^3 H^3}\left[\int_{\theta_f}^{\pi}\begin{Bmatrix} \cos^2\theta \\ \sin\theta\cos\theta \end{Bmatrix} d\theta\right] e_0 \Delta\emptyset$$

$$-\frac{\mu L^3 R}{c^3 H^3}\left[\int_0^{\theta_s}\begin{Bmatrix} \cos^2\theta \\ \sin\theta\cos\theta \end{Bmatrix} d\theta\right]\Delta\dot{e} - \frac{\mu L^3 R}{c^3 H^3}\left[\int_0^{\theta_s}\begin{Bmatrix} \sin\theta\cos\theta \\ \sin^2\theta \end{Bmatrix} d\theta\right] e_0 \Delta\dot{\emptyset}$$

$$-\frac{\mu L^3 R}{c^3 H_w^3}\left[\int_{\theta_s}^{\theta_f}\begin{Bmatrix} \cos^2\theta \\ \sin\theta\cos\theta \end{Bmatrix} d\theta\right]\Delta\dot{e} - \frac{\mu L^3 R}{c^3 H_w^3}\left[\int_{\theta_s}^{\theta_f}\begin{Bmatrix} \sin\theta\cos\theta \\ \sin^2\theta \end{Bmatrix} d\theta\right] e_0 \Delta\dot{\emptyset}$$

$$-\frac{\mu L^3 R}{c^3 H^3}\left[\int_{\theta_f}^{\pi}\begin{Bmatrix} \cos^2\theta \\ \sin\theta\cos\theta \end{Bmatrix} d\theta\right]\Delta\dot{e} - \frac{\mu L^3 R}{c^3 H^3}\left[\int_{\theta_f}^{\pi}\begin{Bmatrix} \sin\theta\cos\theta \\ \sin^2\theta \end{Bmatrix} d\theta\right] e_0 \Delta\dot{\emptyset}$$

(14)

The solution of Eq. (14) has the following form **Andres, 2006**.

$$\begin{bmatrix} F_r \\ F_t \end{bmatrix} = \begin{bmatrix} F_{ro} \\ F_{to} \end{bmatrix} - \begin{bmatrix} K_{rr} & K_{rt} \\ K_{tr} & K_{tt} \end{bmatrix}\begin{bmatrix} \Delta e \\ e_0\,\Delta\emptyset \end{bmatrix} - \begin{bmatrix} C_{rr} & C_{rt} \\ C_{tr} & C_{tt} \end{bmatrix}\begin{bmatrix} \Delta\dot{e} \\ e_0\,\Delta\dot{\emptyset} \end{bmatrix} \tag{15}$$

So as to solve equation (14) a first order Tyler series expansion has been used

$$H^{-3} = H_0^{-3} - 3H_0^{-4}.H_1 \quad , \; H_w^{-3} = H_{0w}^{-3} - 3H_{0w}^{-4}.H_1 \tag{16}$$

After long algebraic operations, the solution of Eq. (14) can be described as in the following equation

$$\begin{Bmatrix} F_r \\ F_t \end{Bmatrix} = \begin{bmatrix} I_1 \\ I_2 \end{bmatrix} - \begin{bmatrix} I_3 & I_4 \\ I_5 & I_6 \end{bmatrix}\begin{Bmatrix} \Delta e \\ e\Delta\emptyset \end{Bmatrix} - \begin{bmatrix} I_7 & I_8 \\ I_9 & I_{10} \end{bmatrix}\begin{Bmatrix} \Delta\dot{e} \\ e\Delta\dot{\emptyset} \end{Bmatrix} \tag{17}$$

Where

$$I_1 = c.F_s\begin{Bmatrix} \int_0^{\theta_S}\frac{\varepsilon_o \sin\theta\cos\theta}{H_O^3}d\theta + \int_{\theta_s}^{\theta_f}\frac{\varepsilon_o \sin\theta\cos\theta - \cos\theta\sin(\theta+\emptyset_o)}{H_{0w}^3}d\theta \\ + \int_{\theta_f}^{\pi}\frac{\varepsilon_o \sin\theta\cos\theta}{H_O^3}d\theta \end{Bmatrix}$$

$$I_2 = c.F_s \left\{ \begin{array}{c} \int_0^{\theta_S} \frac{\varepsilon_o (sin\theta)^2}{H_O^3} d\theta + \int_{\theta_s}^{\theta_f} \frac{\varepsilon_o (sin\theta)^2 - sin\theta\, sin(\theta+\emptyset_o)}{H_{0w}^3} d\theta \\ + \int_{\theta_f}^{\pi} \frac{\varepsilon_o (sin\theta)^2}{H_O^3} d\theta \end{array} \right\}$$

$$I_3 = F_s \left\{ \begin{array}{c} -\int_0^{\theta_S} \frac{sin\theta\, cos\theta}{H_O^3} d\theta + 3.\varepsilon_o.\int_0^{\theta_S} \frac{sin\theta\, (cos\theta)^2}{H_O^4} d\theta \\ -\int_{\theta_s}^{\theta_f} \frac{sin\theta\, cos\theta}{H_{0w}^3} d\theta + 3.\varepsilon_o.\int_{\theta_s}^{\theta_f} \frac{sin\theta\, (cos\theta)^2}{H_{0w}^4} d\theta - 3.\int_{\theta_s}^{\theta_f} \frac{(cos\theta)^2\, sin(\theta+\emptyset_o)}{H_{0w}^4} d\theta \\ -\int_{\theta_f}^{\pi} \frac{sin\theta\, cos\theta}{H_O^3} d\theta + 3.\varepsilon_o.\int_{\theta_f}^{\pi} \frac{sin\theta\, (cos\theta)^2}{H_O^4} d\theta \end{array} \right\}$$

$$I_4 = F_s \left\{ \begin{array}{c} \int_0^{\theta_S} \frac{(cos\theta)^2}{H_O^3} d\theta + 3.\varepsilon_o.\int_0^{\theta_S} \frac{cos\theta\, (sin)^2}{H_O^4} d\theta \\ +3.\varepsilon_o.\int_{\theta_s}^{\theta_f} \frac{(sin\theta)^2\, cos\theta}{H_{0w}^4} d\theta + \int_{\theta_s}^{\theta_f} \frac{(cos\theta)^2}{H_{0w}^3} d\theta - 3.\int_{\theta_s}^{\theta_f} \frac{cos\theta\, sin(\theta+\emptyset_o)}{H_{0w}^4} d\theta \\ + \int_{\theta_f}^{\pi} \frac{(cos\theta)^2}{H_O^3} d\theta + 3.\varepsilon_o.\int_{\theta_f}^{\pi} \frac{cos\theta\, (sin\theta)^2}{H_O^4} d\theta \end{array} \right\}$$

$$I_5 = F_s \left\{ \begin{array}{c} -\int_0^{\theta_S} \frac{(sin\theta)^2}{H_O^3} d\theta + 3.\varepsilon_o.\int_0^{\theta_S} \frac{cos\theta\, (sin)^2}{H_O^4} d\theta \\ +3.\varepsilon_o.\int_{\theta_s}^{\theta_f} \frac{(sin\theta)^2\, cos\theta}{H_{0w}^4} d\theta - \int_{\theta_s}^{\theta_f} \frac{(sin\theta)^2}{H_{0w}^3} d\theta - 3.\int_{\theta_s}^{\theta_f} \frac{sin\theta\, cos\theta\, sin(\theta+\emptyset_o)}{H_{0w}^4} d\theta \\ -\int_{\theta_f}^{\pi} \frac{(sin\theta)^2}{H_O^3} d\theta + 3.\varepsilon_o.\int_{\theta_f}^{\pi} \frac{cos\theta\, (sin\theta)^2}{H_O^4} d\theta \end{array} \right\}$$

$$I_6 = F_s \left\{ \begin{array}{c} \int_0^{\theta_S} \frac{sin\theta\, cos\theta}{H_O^3} d\theta + 3.\varepsilon_o.\int_0^{\theta_S} \frac{(sin)^3}{H_O^4} d\theta \\ +3.\varepsilon_o.\int_{\theta_s}^{\theta_f} \frac{(sin)^3}{H_{0w}^4} d\theta + \int_{\theta_s}^{\theta_f} \frac{sin\theta\, cos\theta}{H_{0w}^3} d\theta - 3.\int_{\theta_s}^{\theta_f} \frac{(sin\theta)^2\, sin(\theta+\emptyset_o)}{H_{0w}^4} d\theta \\ + \int_{\theta_f}^{\pi} \frac{sin\theta\, cos\theta}{H_O^3} d\theta + 3.\varepsilon_o.\int_{\theta_f}^{\pi} \frac{(sin)^3}{H_O^4} d\theta \end{array} \right\}$$

$$I_7 = \frac{2F_s}{\Omega} \left\{ \int_0^{\theta_S} \frac{(cos\theta)^2}{H_O^3} d\theta + \int_{\theta_s}^{\theta_f} \frac{(cos\theta)^2}{H_{0w}^3} d\theta + \int_{\theta_f}^{\pi} \frac{(cos\theta)^2}{H_O^3} d\theta \right\}$$

$$I_8 = \frac{2F_s}{\Omega} \left\{ \int_0^{\theta_S} \frac{sin\theta\, cos\theta}{H_O^3} d\theta + \int_{\theta_s}^{\theta_f} \frac{sin\theta\, cos\theta}{H_{0w}^3} d\theta + \int_{\theta_f}^{\pi} \frac{sin\theta\, cos\theta}{H_O^3} d\theta \right\}$$

$$I_9 = \frac{2F_s}{\Omega} \left\{ \int_0^{\theta_S} \frac{sin\theta\, cos\theta}{H_O^3} d\theta + \int_{\theta_s}^{\theta_f} \frac{sin\theta\, cos\theta}{H_{0w}^3} d\theta + \int_{\theta_f}^{\pi} \frac{sin\theta\, cos\theta}{H_O^3} d\theta \right\}$$

$$I_{10} = \frac{2F_s}{\Omega} \left\{ \int_0^{\theta_S} \frac{(sin\theta)^2}{H_O^3} d\theta + \int_{\theta_s}^{\theta_f} \frac{(sin\theta)^2}{H_{0w}^3} d\theta + \int_{\theta_f}^{\pi} \frac{(sin\theta)^2}{H_O^3} d\theta \right\}$$

$$F_s = \frac{\mu \Omega R L^3}{2c^3} \quad ,$$

By comparison between Eq. (15) and Eq. (17) get the values of dynamic coefficients in rotating coordinates system

$F_{ro} = I_1$, $F_{to} = I_2$, $K_{rr} = I_3$, $K_{rt} = I_4$, $K_{tr} = I_5$, $K_{tt} = I_6$

$C_{rr} = I_7$, $C_{rt} = I_8$, $C_{tr} = I_9$, $C_{tt} = I_{10}$

For dynamic coefficients in fixed coordinate system the following equation can be used to convert from the rotating coordinates to the fixed coordinates **Andres, 2006**.

$$\begin{bmatrix} K_{XX} & K_{XY} \\ K_{YX} & K_{YY} \end{bmatrix} = \begin{bmatrix} \sin\emptyset_o & \cos\emptyset_o \\ -\cos\emptyset_o & \sin\emptyset_o \end{bmatrix} \begin{bmatrix} K_{rr} & K_{rt} \\ K_{tr} & K_{tt} \end{bmatrix} \begin{bmatrix} \sin\emptyset_o & -\cos\emptyset_o \\ \cos\emptyset_o & \sin\emptyset_o \end{bmatrix}$$

(18)

$$\begin{bmatrix} C_{XX} & C_{XY} \\ C_{YX} & C_{YY} \end{bmatrix} = \begin{bmatrix} \sin\emptyset_o & \cos\emptyset_o \\ -\cos\emptyset_o & \sin\emptyset_o \end{bmatrix} \begin{bmatrix} C_{rr} & C_{rt} \\ C_{tr} & C_{tt} \end{bmatrix} \begin{bmatrix} \sin\emptyset_o & -\cos\emptyset_o \\ \cos\emptyset_o & \sin\emptyset_o \end{bmatrix}$$

The integrals in Eq. (17) can be calculated by using table of journal bearings integrals **Booker, 1965.** for integrals of non worn regions and by using Simpsons 1/3 rule with multiple divisions for integrals in the worn regions. Many Matlab scripts have been written to calculate dynamic coefficients for non worn journal bearing and worn journal bearings. The dynamic coefficients of non worn journal bearings can be calculated by using the same equations of worn journal bearings except the value of wear depth (do) equal zero.

The following steps were followed to calculate dynamic coefficients for journal bearings in state of non worn and worn case

1. Writing Matlab script to calculate iteratively (using Newton – Raphson method) the eccentricity ratio of journal bearing by using the balancing between the film reaction force components and applied static load which represented in the following equation **Friswell, et al, 2010**.

$$\varepsilon^8 - 4\varepsilon^6 + \left(6 - S_s^2(16 - \pi^2)\right)\varepsilon^2 - (4 + \pi^2 S_s^2)\varepsilon^2 + 1 = 0 \qquad (19)$$

   Where S_s is modified Sommerfeld Number $S_s = \frac{\mu\Omega L^3 R}{4c^2 F_0}$ and R, L, Ω, μ,c and F_0 are journal radius , bearing length, rotor rotational speed, lubricant oil viscosity, radial clearance and external applied load (the part of rotor weight supported by every bearing) respectively.

2. Writing Matlab script is used to calculate iteratively the attitude angle in state of worn journal bearing by using the following equation

$$\left({F_{ro}}^2 + {F_{to}}^2\right)^{0.5} - F_0 = 0 \qquad (20)$$

3. Writing Matlab script is used to calculate dynamic coefficients for non worn journal bearing by using Eq.(17) with (substitute do = 0 in Eq.(6) then substitute resultant equation in Eq.(17))
4. Writing Matlab script is used to calculate dynamic coefficients for worn journal bearing by using Eq. (17). For bearing number one as shown in the **Fig.1** while bearing number two still without wear.

3. ROTOR BEARING SYSTEM ANALYSIS USING ANSYS

3-D Solid model rotor bearing system gives more accurate results than in the case of one dimensional beam model as well as there are many advantages in adopting this model **Rao and Sreenivas, 2003.** Therefore it is used in this work, Solid187 element has been used to model shaft and disk as shown in the **Fig.2. (a),** as well as comi214 element used to model journal bearing **ANSYS Guide, 2012**. The eight dynamic coefficients of journal bearing are depending on the rotational speed therefore when these coefficients represent in ANSYS must be changed with rotor speed. The dimensions of rotor and bearings which used in this work are shown in **Fia.2. (b),** and **Table.1.**

4. RESULTS AND DISCUSSION

4.1 Effect of Wear on the Dynamic Coefficients of Journal Bearings

The eccentricity ratio for fluid film journal bearing decreases with the increasing the modified Sommerfeld number (S_s) and with increasing the rotor spin speed due to the inverse relationship between modified Sommerfeld number and rotational speed of rotor and then with eccentricity ratio as shown in the **Fig.3**.

Fig.4 and **Fig.5** describe the variation of the intact rotor dimensionless stiffness and damping coefficients respectively with the modified Sommerfeld number (duty number) and rotational speed of rotor, these figures showed that the direct dynamic coefficients (stiffness and damping) become somewhat fixed value when the rotor spin speed reach about 2000 rpm, because the eccentricity ratio becomes somewhat fixed and eccentricity ratio represents the important parameter in the dynamic coefficients calculations.

Fig .6 shows the variation of attitude angle with wear depth and eccentricity ratio, the attitude angle under the constant eccentricity ratio decreases with increasing in the wear depth parameter.

Fig.7 demonstrated that the direct dynamic coefficients ($K_{xx}, K_{yy}, C_{xx}, C_{yy}$) have fixed value when rotational speed of the rotor becomes higher than the 2000 rpm approximately, also cross coupling dynamic coefficients ($K_{xy}, K_{yx}, C_{xy}, C_{yx}$) have no significant changes when rotor speed becomes higher than the 2000 rpm this is because the change in the value of the eccentricity ratio becomes small at this speed.

Fig .8 and **Fig.9** clearly show that the dynamic coefficients decrease with the increasing of wear depth parameter except the direct stiffness coefficient in the y- direction increases with the increasing in wear depth parameter that means the stability of rotor supported on worn journal bearing will decreases with increasing in the wear depth parameter.

4.2 Effect of Wear on the Dynamic Behavior of Rotor

The critical speed of rotor supported on fluid film journal bearings is speed dependence, **Childs, 1993.** Therefore the location of the critical speed is at maximum unbalance response, **Rao, 1996.** The ANSYS results showed that the using of fluid film journal bearing in the rotor bearing system increases the instability at the critical speed due to existence of cross coupling coefficients as shown in the **Fig.10**. The wear in the journal bearing with the wear depth parameter ($\delta = 0.2\,, do = 0.02\ mm$) decreases the critical speed by about 2.3% and increases the amplitude by about 50% at the critical speed as shown in the **Fig.11** this is due to the high decreasing in the cross coupling (K_{xy}) with low decreasing in the direct damping coefficients and less increasing in the cross coupling damping coefficients but this state increases the stability of rotor after critical speed as shown in the **Fig.11** where there is smooth decay beyond maximum response.

The additional increase in the wear depth parameter ($\delta = 0.4\,, do = 0.04\,mm$) led to decrease the critical speed by about 8.87 % and decrease the amplitude of unbalance response by 8.9 % due to high increasing in the K_{yy} as well as high increasing in the cross coupling damping coefficients as shown in the **Table 2**., but The important point that deserves to be mentioned here the system become more instable as shown in the **Fig.12,** and this is undesirable case

5. CONCLUSIONS

1. Wear in journal bearing is generally decreasing the critical speed of rotor bearing system and that means decreasing the natural frequency.
2. Low wear depth is increasing the stability of rotor bearing system but in the same time increasing unbalance response amplitude.
3. High wear depth led to increasing in the instability of the rotor bearing system.
4. Measuring of unbalance response can be used to on line wear detection in the rotor journal bearing system and develop a monitoring system for rotating machine can be applied in the virtual system at early wear detection and prevent the sudden failure that could lead to full system break down.

REFERENCES

- Andres, L. S., 2006, *Hydrodynamic Fluid Film Bearings and Their Effect on the Stability of Rotating Machinery*, Turbomachinery Laboratory, Texas A&M University College Station, TX 77843-3123 USA.

- ANSYS, Inc.2012, *ANSYS Mechanical APDL Rotordynamic Analysis Guide*, Release 14.5.

- Booker, J. F., 1965, *A Table of the Journal Bearing Integral", Journal of Basic Engineering* ,ASME,1965/533

- Cameron, A., 1981, *Basic Lubrication Theory*, 3rd Edition, Ellis Harwood Limited Publishers.

- Childs, D., 1993, *Turbomachinery Rotordynamics, Phenomena, Modeling, and Analysis*, Copyright by John Wiley and Sons, Inc.

- Chasalevris, A. C., Nikolakopoulos, P. G., and Papadopoulos, C. A., 2013, *Dynamic Effect of Bearing Wear on Rotor-Bearing System Response*, Journal of Vibration and Acoustics Copyright by ASME, Vol. 135 / 011008-1, DOI: 10.1115/1.4007264.

- Chen, W. J. and Gunter, E. J., 2007, *Introduction to Dynamics of Rotor – Bearing Systems*, Copyright Eigen Technologies Inc. printed in Victoria, BC, Canada.

- Desjardins, M., 2013, *The Effect of Wear on the Load-Carrying Capacity and Maximum Oil Pressure of a Plain Journal Bearing*, a Project Submitted to the Graduate Faculty of Rensselaer Polytechnic Institute in Partial Fulfillment of the Requirements for the degree of master of engineering in mechanical engineering, Rensselaer Polytechnic Institute Hartford, CT US.

- Dufrane K.F., Kannel J.W., and McCloskey T.H., 1983, *Wear of Steam Turbine Journal Bearings at Low Operating Speeds*, Journal of Lubrication Technology, ASME, and Vol.105/313.

- Fillon, M., and Bouyer, J., 2004, *Thermohydrodynamic Analysis of a Worn Plain Journal Bearing*, Tribology International 37 (2004) 129–136, doi: 10.1016/S0301-679X (03)00051-3, Elsevier Ltd.

- Friswell, M. I., Penny, J.E.T., Garvey, S.D., and Lees, A.W., 2010, *Dynamics of Rotating Machines*, Cambridge Aerospace Series, Cambridge University Press.

- Gertzos, K.P., Nikolakopoulos , P.G., Chasalevris, A.C., and Papadopoulos, C.A.,2011, *Wear Identification in Rotor-Bearing Systems by Measurements of Dynamic Bearing Characteristics*, Computers and Structures, 89 (2011) 55–66, Elsevier Ltd. doi:10.1016/j.compstruc.2010.08.006, (2011).

- Hashimoto, H., Wada, S., and Nojima, K., 1986, *Performance Characteristics of Worn Journal Bearings in both Laminar and Turbulent Regimes, Part I: Steady-State Characteristics*, A S L E Transactions, 29:4, 565-571, DOI: 10.1080/05698198608981721.

- Kjell G. R., Oslen, H., Karimi, H.R. and Tender, K., 2014, *Oil Whip-Induced Wear in Journal Bearings*, Springer-Verlag London.

- Kramer, E., 1993, *Dynamics of Rotors and Foundations*, Springer.

- Kumar A., and Mishra S.S., 1996, *Stability of a Rigid Rotor in Turbulent Hydrodynamic Worn Journal Bearings*, Wear, 193(1):25-30. DOI: 10.1016/0043-1648(95)06654-3.

- Kumar A., and Mishra S.S., 1996, *Steady State Analysis of Non-Circular Worn Journal Bearings in Non-Laminar Lubrication Regimes*, Tribology International, (1996) 29 (6) 493-498.

- Nikolakopoulos, P.G., Papadopoulos, C.A., 1994, *Nonlinearities in Misaligned Journal Bearings*, Tribology International, Butterworth Heinemann Ltd, DOI: 10.1016/0301-679X(94)90004-3.

- Nikolakopoulos, P.G., Papadopoulos C.A., and Gounaris, G.D., 2005, *Wear Identification in Misaligned Journal Bearings*, Proceedings of the 3rd IASME/WSEAS Int. Conf. on Fluid Dynamics and Aerodynamics, Corfu, Greece, (pp293-298), August 20-22.

- Nikolakopoulos, P.G., Papadopoulos, C.A., 20007, *A study of Friction in Worn Misaligned Journal Bearings under Severe Hydrodynamic Lubrication*, Elsevier Ltd. doi:10.1016/j.triboint.2007.10.005

- Nikolakopoulos, P.G., Papadopoulos, C.A., 20009, *Wear Model Evaluation in Misaligned Journal Bearings* , researchgate,

- http://www.researchgate.net/publication/257638054_Wear_Model_Evaluation_in_Misaligned_Journal_Bearings

- Rao, J. S., and Sreenivas, R., 2003, *Dynamics of Asymmetric Rotors using Solid Models*, Proceedings of the International Gas Turbine Congress 2003 Tokyo, November 2-7.

- Rao, J. S., 1996, *Rotor Dynamics*, New Age International (P) Ltd., Publishers.

NOMENCLATURE

c = radial clearance, m
do = wear depth, m
e = eccentricity between journal center and bearing center, m
e_0 = eccentricity between journal center and bearing center at equilibrium position, m
F_0 = journal bearing external applied force = weight of rotor applied on every bearing , N
F_r = radial component of fluid film journal bearing force, N
F_t = tangential component of fluid film journal bearing force, N
F_{r0} = radial component of fluid film journal bearing force at equilibrium position, N
F_{t0} = tangential component of fluid film journal bearing force at equilibrium position, N
K_{ij} = dynamic coefficients in rotating coordinates , i,j = r,t
K_{ij} = dynamic coefficients in fixed coordinates , i,j = x,y
h = fluid film thickness non- worn region, m
H = nondimensional fluid film thickness of non- worn region =h/c
h_0 = non- worn fluid film thickness at equilibrium position, m
h_w = worn fluid film thickness, m
H_w = nondimensional fluid film thickness of worn region = h_w/c
h_{0w} = worn fluid film thickness at equilibrium position, m
L = bearing length, m
P = lubricant oil pressure of non- worn region, pa
P_w = lubricant oil pressure of worn region, pa
R = journal radius, m
γ = circumferential coordinate from Y-axis, **Fig. 1**
δ = wear depth parameter = do/c
ε = eccentricity ratio = e/c
θ = circumferential coordinate, **Fig 1.**
θ_s= circumferential location of the starting point of the worn region, **Fig. 1**
θ_f= circumferential location of the final point of the worn region, **Fig. 1**
μ = viscosity pa s
$\emptyset_0$ = attitude angle, **Fig. 1**
Δe = small displacement at equilibrium position
$\Delta\emptyset$ = small variation of attitude angle
Ω = rotational speed of rotor, rad/s

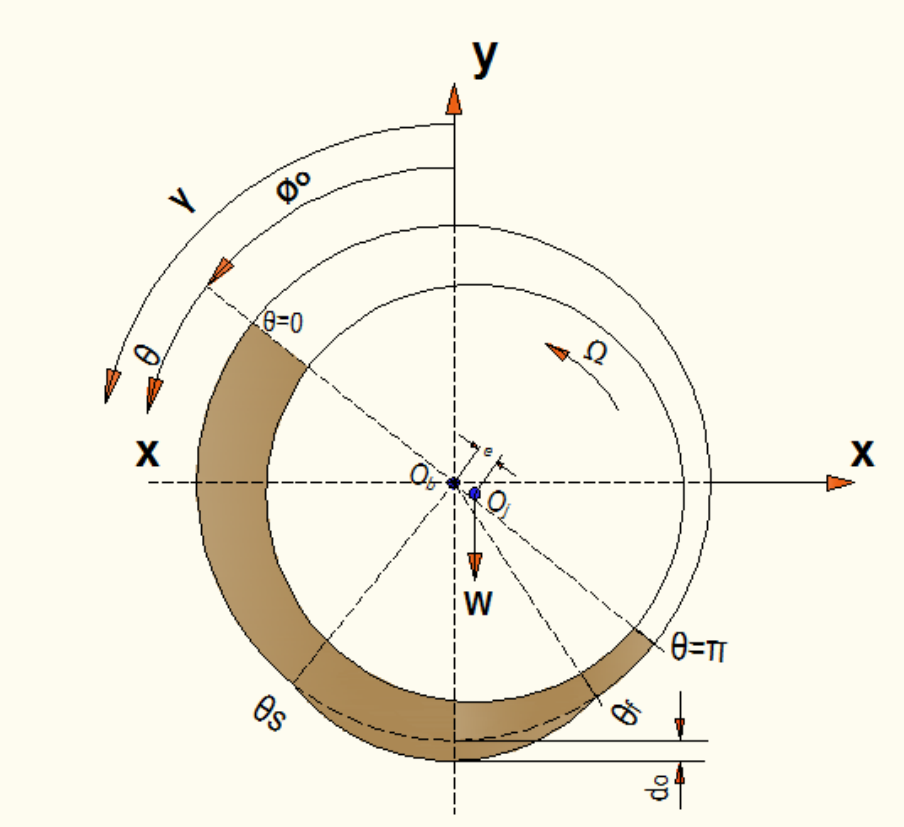

Figure 1. Worn journal bearing.

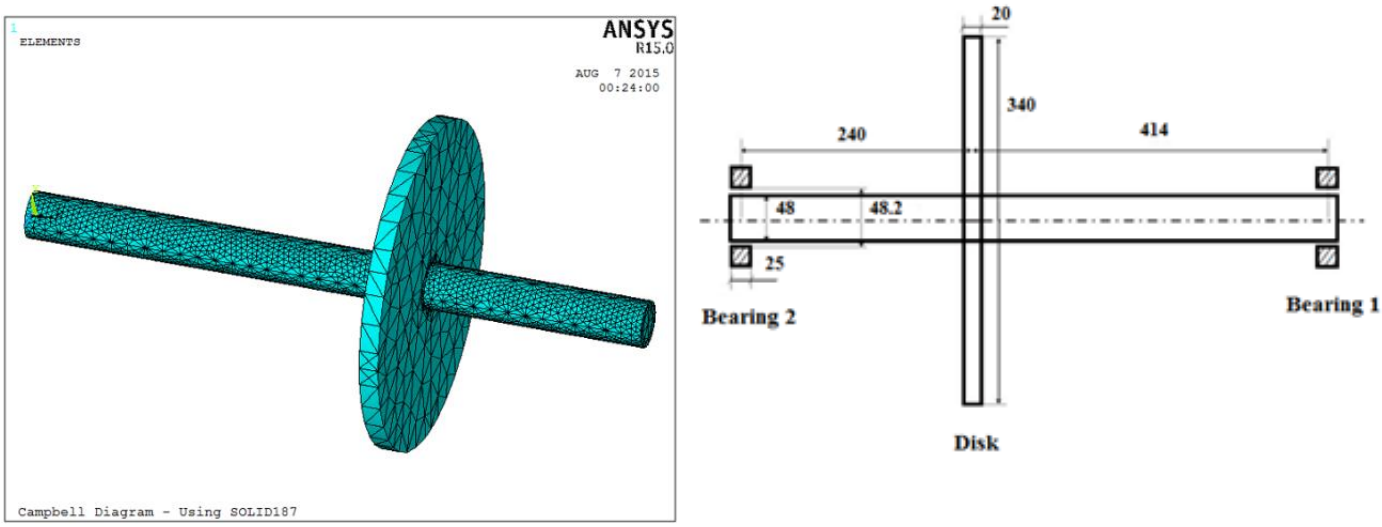

(a) (b)

Figure 2. (a) Ansys rotor model (b) Mechanical drawing of present rotor bearing system.

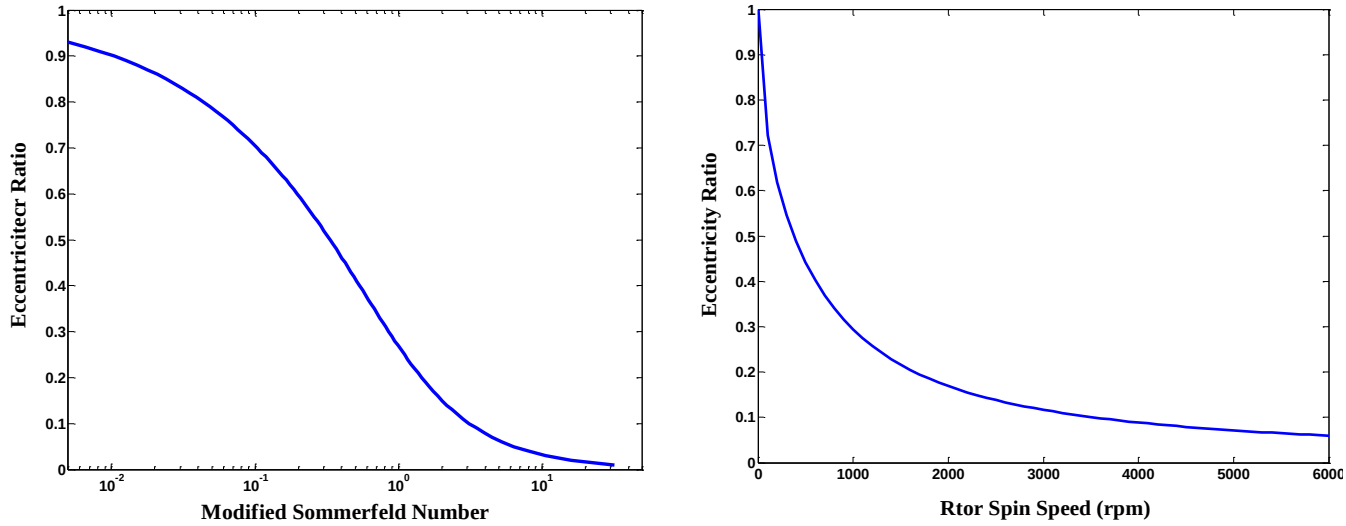

(a) (b)

Figure 3. Bearing eccentricity ratio (a) as a function of the modified Sommerfeld number (b) as a function of the Rotor Spin Speed.

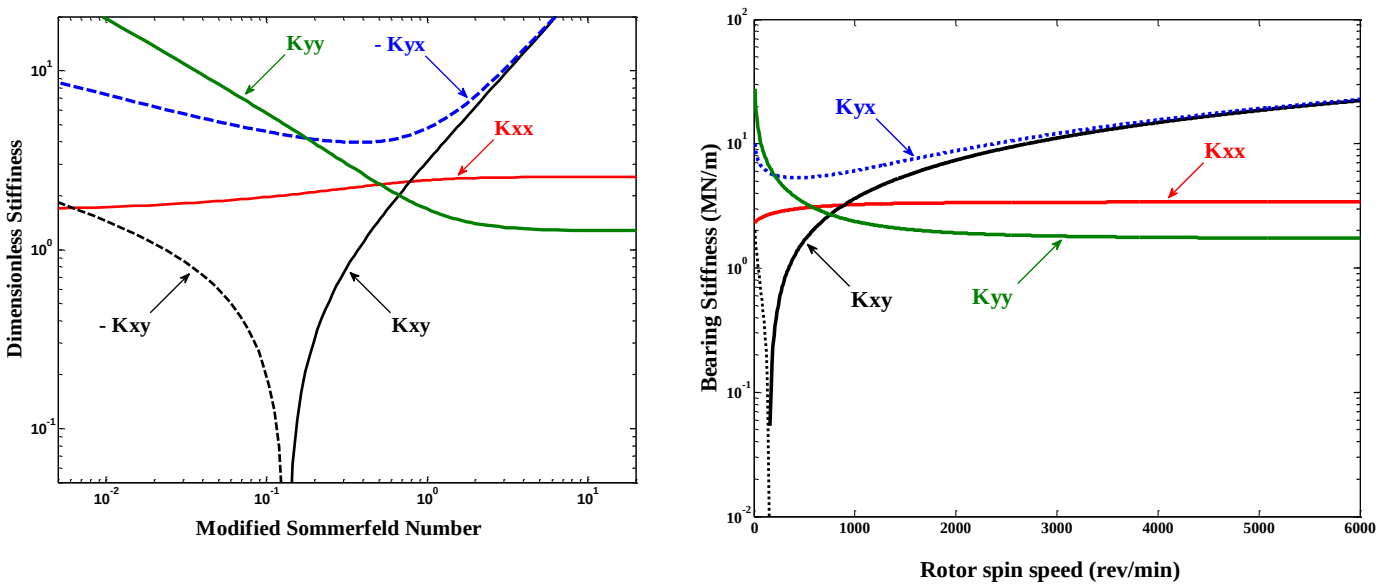

(a) (b)

Figure 4. Nondimensional stiffness of an intact fluid film bearing (a) as a function of the modified Sommerfeld number (b) as a function of the rotor spin speed, (negative coefficients are shown as dashed lines).

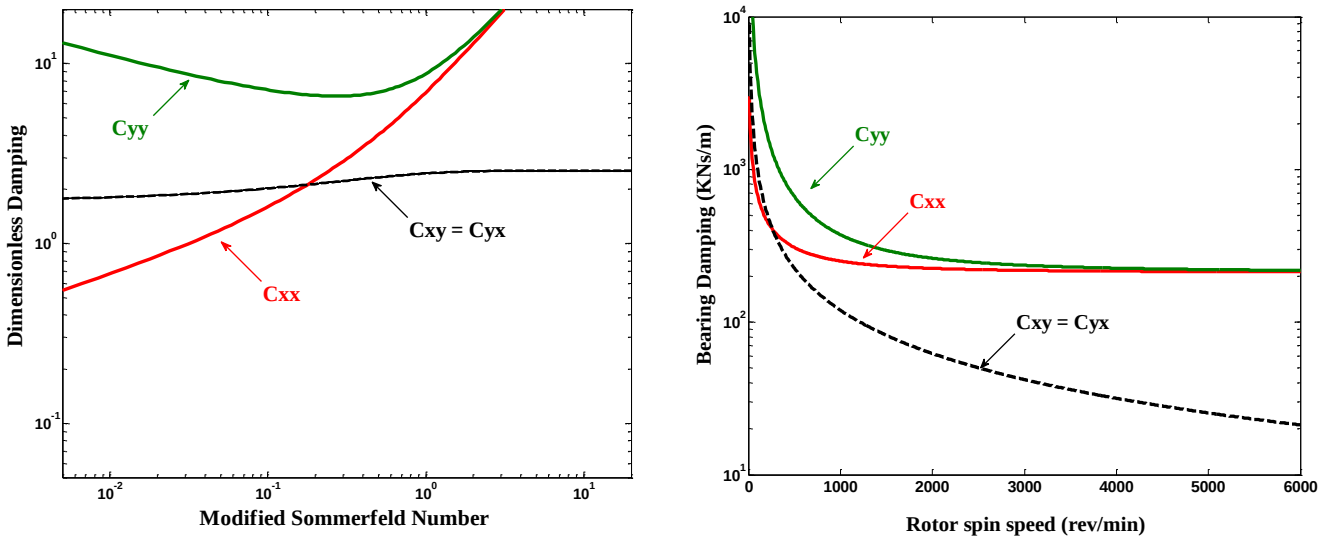

(a) (b)

Figure 5. Nondimensional damping of an intact fluid film bearing (a) as a function of the modified Sommerfeld number (b) as a function of the rotor spin speed, (negative coefficients are shown as dashed lines).

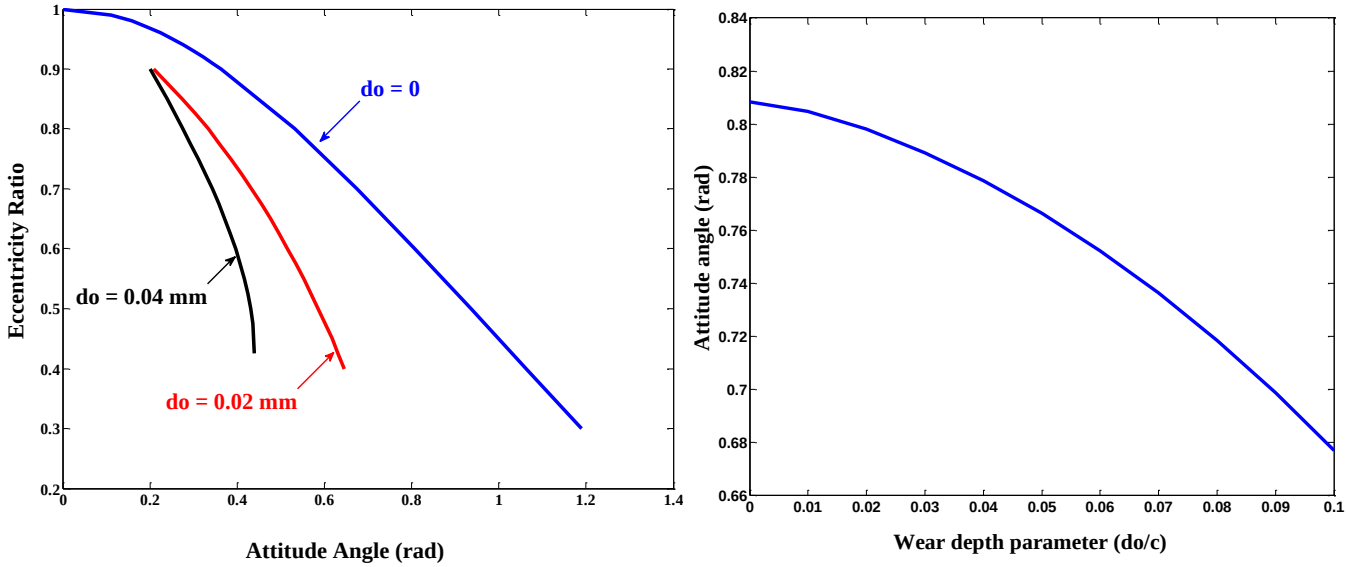

(a) (b)

Figure 6. Variation of attitude angle (a) with the eccentricity ratio and depth wear parameter, (b) with depth wear parameter (do/c).

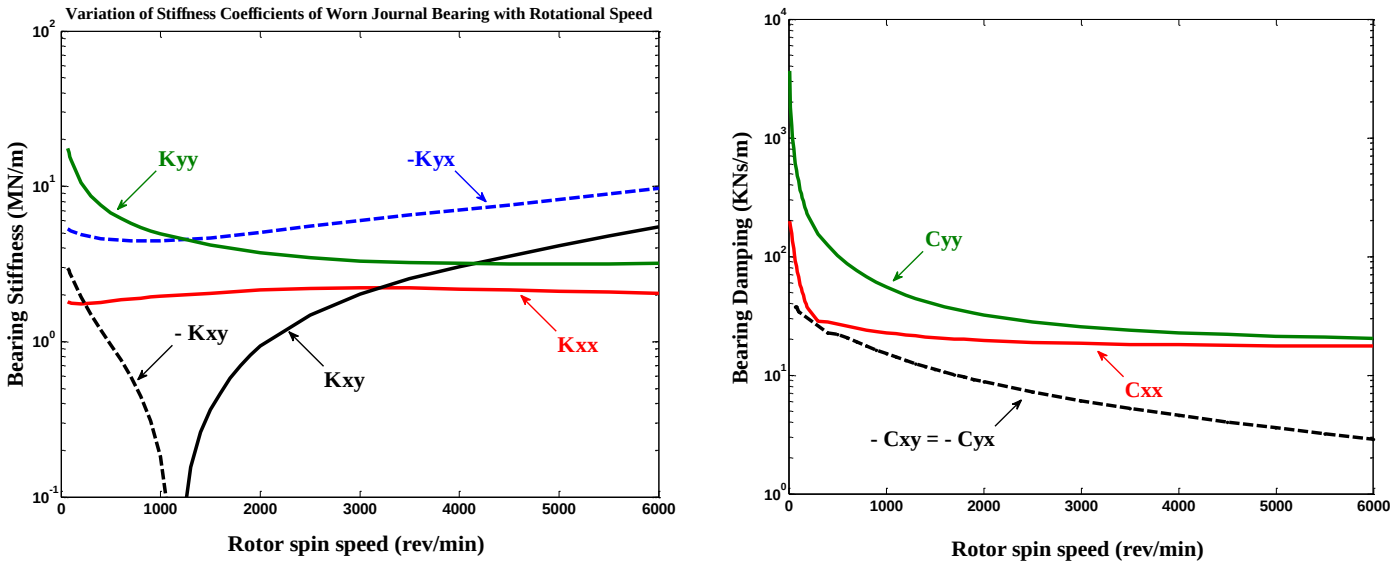

(a) (b)

Figure 7. Nondimensional dynamic coefficients of a worn fluid film bearing (a): stiffness as a function of the rotor spin speed (b): damping as a function of the rotor spin speed, (negative coefficients are shown as dashed lines).

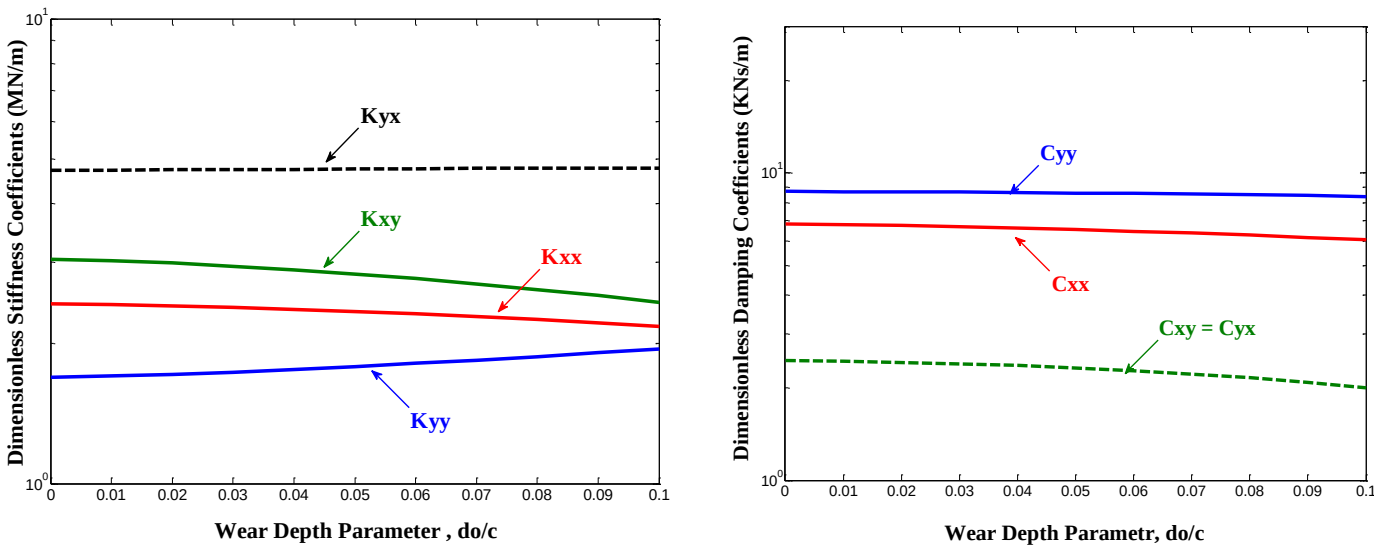

(a) (b)

Figure 8. Nondimensional dynamic coefficients of a worn fluid film bearing (a): stiffness as a function of the wear depth parameter (b) damping as the wear depth parameter, (negative coefficients are shown as dashed lines).

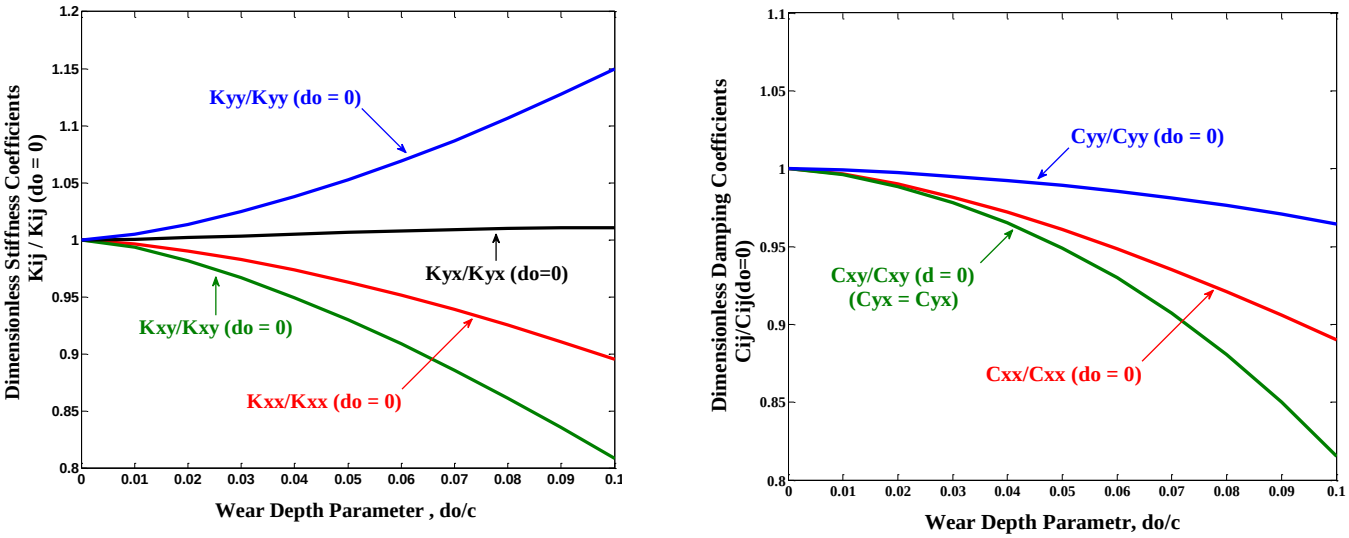

(a) (b)

Figure 9. Nondimensional dynamic coefficients ratio of a worn fluid film bearing (a): stiffness ratio as a function of the wear depth parameter (b) damping ratio as the wear depth parameter, (negative coefficients are shown as dashed lines).

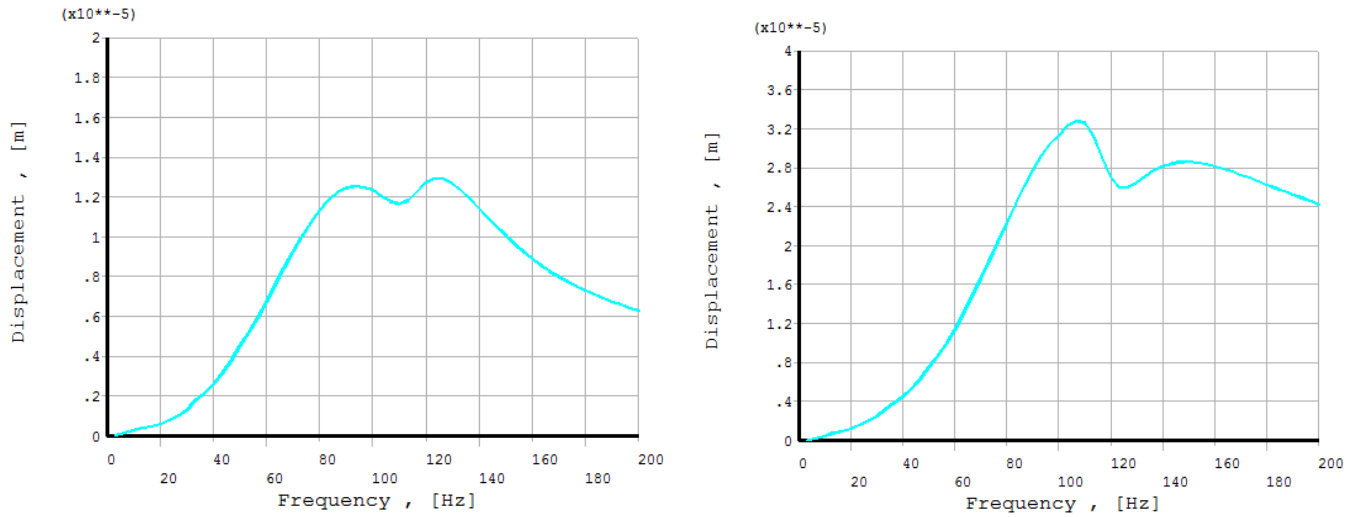

(a) (b)

Figure 10. Unbalance response of rotor supported on fluid film journal bearings (a): at bearing No.1 (b): at disc center.

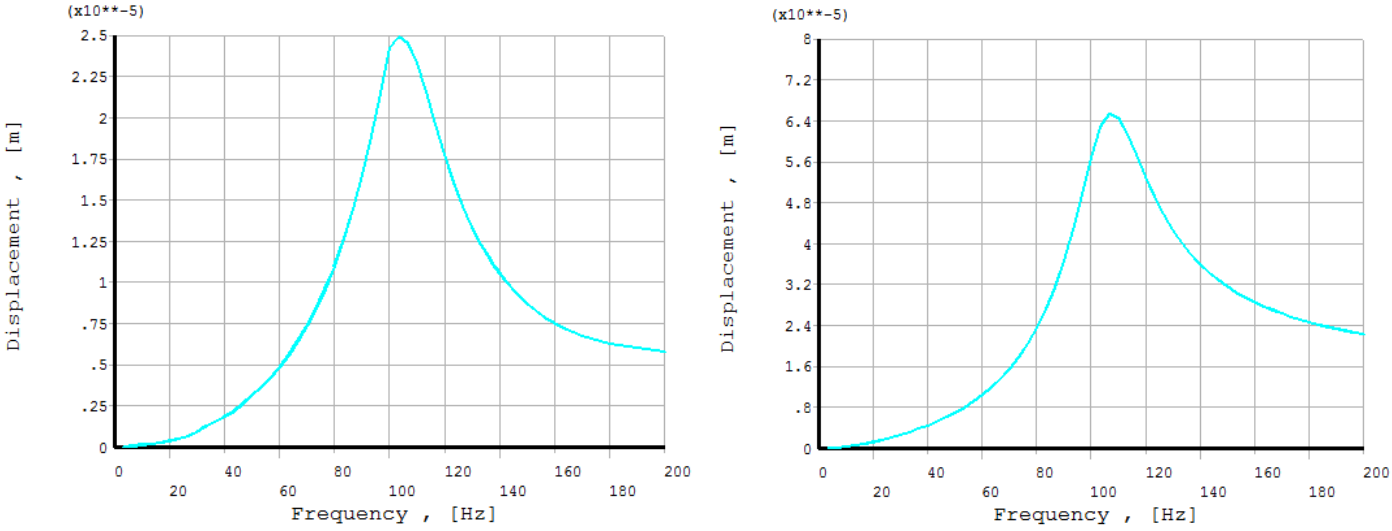

(a) (b)

Figure 11. Unbalance response of rotor supported on worn journal bearings (do= 0.02 mm) (a): at bearing No.1 (b): at disc center.

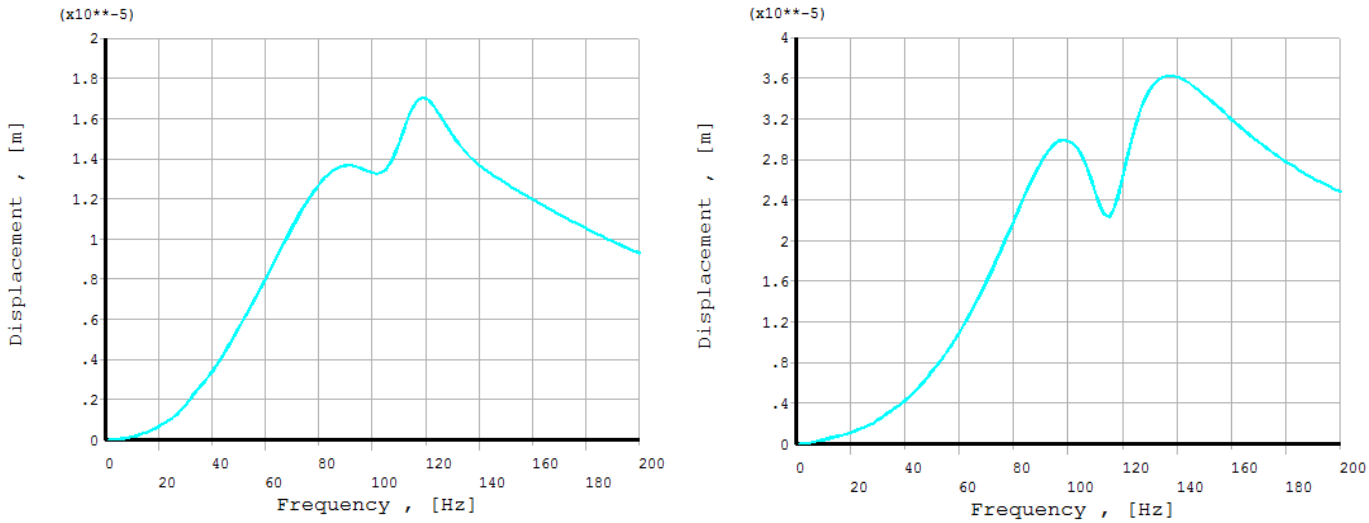

(a) (b)

Figure 12. Unbalance response of rotor supported on worn journal bearings (do= 0.04 mm) (a): at bearing No.1 (b): at disc center.

Table 1. Shows rotor material and lubricant oil specifications

Shaft length m	Shaft diam. m	Disc diam. m	Disc thickness m	Modulus of Elasticity pa	Shaft and Disk Density Kg/m^3	Lubricant oil viscosity Pa s	Unbalance force Kg - m
o.654	0.048	0.34	0.02	$2.1x10^{11}$	7850	0.032	$0.323x10^{-6}$

Table .2 Variation of journal bearing coefficients with wear depth

δ	K_{xx} $x10^6$	K_{xy} $x10^6$	K_{yx} $x10^6$	K_{yy} $x10^6$	C_{xx} $x10^4$	C_{xy} $x10^4$	C_{yx} $x10^4$	C_{yy} $x10^4$
0	2.4	5.9	-6.81	1.34	1.94	-0.38	-0.38	2.1
0.2	2.1	3.93	-6.86	1.6	1.69	-0.25	-0.25	1.7
0.4	1.5	3.37	-7.77	2.2	1.94	0.176	0.176	1.59

Experimental Evaluation Use of Semifluidized Bed Adsorber for the Treatment of P-chlorophenol and O-cresol in Wastewater using Activated Carbon as Adsorbent

Dr. Saad Hanash Ammar
Lecturer
Department of Chemical Engineering, Al-Nahrain University
Email: saad_cheminet@yahoo.com

ABSTRACT

In the present work the performance of semifluidized bed adsorber was evaluated for removal of phenolic compound from wastewater using commercial activated carbon as adsorbent. P-chlorophenol (4-Chlorophenol) and o-cresol (2-methylphenol) was selected as a phenolic compound for that purpose. The phenols percent removal, in term of breakthrough curves were studied as affected by hydrodynamics limitations which include minimum and maximum semifluidization velocities and packed bed formation in the column by varying various parameters such as inlet liquid superficial velocity (from U_{minsf} to $8U_{minsf}$ m/s), and retaining grid (sometimes referred to as adsorbent loading) to initial static bed height ratio (from 3-4.5). Inlet phenols concentration (50-400 mg/l) and initial pH of the liquid solutions feed (from 4 to 10) were also studied. The experimental semifluidized adsorber unit was designed and constructed in Chem. Eng. labs at Al-Nahrain University (consisted of a QVF glass tube 2.54 cm inside diameter, and 70cm length). The results showed that the initial percent removal of phenolic compounds (P-chlorophenol and o-cresol) decrease with increasing the superficial liquid velocity while the time required reaching equilibrium state decreased. Also it slightly affected with the increase in the retaining grid height and the time required to reach the equilibrium value decreased.

Keywords: wastewater; p-chlorophenol; o-cresol; Semi-fluidized bed; adsorption; activated carbon.

تقييم استخدام العمود الماز شبه المميع مختبريا لمعالجة باراكلوروفينول و اورثوكريسول من المياه الملوثة بأستخدام الكاربون المنشط كمادة ممتزة

م.د. سعد حنش عمار
قسم الهندسة الكيمياوية – جامعة النهرين

الخلاصة

في هذا البحث تم تقييم استخدام العمود الماز شبه المميع مختبريا لازالة مركبات الفينول من المياه الملوثة باستخدام الكاربون المنشط التجاري كمادة ممتزة وقد اختير الباراكلوروفينول و اورثوكريسول كمواد فينولية ملوثة لهذا الغرض. تم دراسة نسبة الازالة مع الزمن وتأثرها بالحدود الهيدروديناميكية والتي تتضمن سرعة شبه التميع الدنيا والعظمى وتكون الطبقة الثابتة في العمود وذلك بتغيير عدة متغيرات وهي سرعة السائل الداخلة (من 1 الى 8 مرات من سرعة شبه التميع الدنيا) ونسبة ارتفاع الشبكة الحابسة الى ارتفاع العمود الساكن الابتدائي (من 3 الى 4.5). التركيز الابتدائي للفينولات المستخدمة (من 50 الى 400 ملغم / لتر) والدالة الحامضية للمحلول ابتداءا (من 4 الى 10) ايضا تم دراستها. وحدة العمود شبه المميع المختبرية تم تصميمها

وبنائها في مختبرات قسسم الهندسة الكيمياوية جامعة النهرين وتتألف من عمود زجاجي بقطر 2.54 سم وارتفاع 70 سم. بينت النتائج بأن نسبة الازالة الابتدائية تقل بزيادة سرعة السائل الداخلة بينما الزمن اللازم للوصول الى حالة التوازن يقل. وايضا تتأثر قليلا بزيادة نسبة ارتفاع الشبكة الحابسة الى ارتفاع العمود الساكن الابتدائي وكذلك الزمن اللازم للوصول الى حالة التوازن يقل.

الكلمات الرئيسية: المياه الملوثة, باراكلوروفينول, اورثوكريسول, الطبقة شبه المميعة, الامتزاز, الكاربون المنشط.

1. INTRODUCTION

Wastewater from chemical and petrochemical industries containing toxic pollutants such as phenolic compounds, dyes and heavy metals can have a several impacts on many organisms that live not only in aquatic ecosystem but also in the body of the human beings. The surface and ground waters are polluted by these compounds therefore the environmental concerns make it is necessary to remove these pollutants from the wastewater ,**Parida and Amaresh, 2010**.

Presence of phenol and its derivatives even at low concentration in the industrial wastewater adversely affects aquatic as well as human life directly or indirectly when disposed off to public sewage, river or surface water. The toxicity imparted by phenolic compounds is responsible for health hazards and dangerous to aquatic life ,**Meikap, 1997**.

Phenols are being discharged into the wastewater from various industrial processes such as oil refineries, petrochemical plants, ceramic plants, coal conversion processes and phenolic resin industries (such as phenol-formaldehyde and bisphenol-A plants) and other synthetic resin manufacturing units ,**Monteiro, 2000 and Vinod and Reddy, 2003**.

Removal of phenols from industrial effluents is required before sewage disposal. For that purpose, various methods have been suggested. According to, **Kulkarni and Kaware, 2013** review on the research for removal of phenolic compounds from wastewater several physicochemical and biological treatment methods such as polymerization, electro coagulation, solvent extraction, photodecomposition, ion exchange by resins, electro-fenton (EF-Fere) method, chemical oxidation by ozone, aerobic or anaerobic biodegradation and adsorption onto active solid materials has been used **,Senturk et al., 2009.**

Activated carbon has been employed widely by numerous researchers as an adsorbent to remove phenol and its compounds from wastewater. Activated carbon is synthesized from various carbon containing raw materials such as coke, palm shell, rice hulls, and coconut shell by a process including dehydration of the raw material and carbonization and then activation **Singh and Srivastava, 2002.**

In the other words, various aspects of liquid-solid semifluidization which have been studied and reported earlier by different authors include packed bed formation, pressure drop, fluidized bed heights, and minimum and maximum semi-fluidization velocities are determined according to a number of variables such as the retaining grid height from inlet fluid distributer, inlet fluid velocity, density and viscosity of the liquid, static bed height, expansion ratio, and particle size.

When semi-fluidized bed is compared with both fluidized bed and fixed bed; there are some problems in fluidized and fixed beds such as back-mixing of solids particles, attrition and elutriation of particles, the necessity of considerable free board above the bed and erosion of surfaces in fluidized bed and high pressure drop, non-uniform bed temperatures, segregation of solids and channeling and blockage in fixed bed therefore the semi-fluidized bed merits when it compared to the fluidized bed and fixed bed **,Younk, et al., 1999**.

The main objective of this work is to study and evaluates the removal process of phenolic compounds P-chlorophenol and o-cresol from wastewater in semifluidized bed adsorber as a novel system. Single aqueous solutions of p-chlorophenol and o-cresol were passed through the column packed with activated carbon to get their breakthrough curves at different experimental conditions these conditions include inlet liquid superficial velocity, initial phenols concentration, and pH in addition to the hydrodynamic characteristics such as retaining grid height, static bed height and minimum and maximum semiflidization velocities.

2. EXPERIMENTAL

2.1 Materials

Commercial granular activated carbon supplied by Didactic company of purity 99.9% with surface area 1080 (m^2/g) and solid density 1.153 (g/ml) was tested as an adsorbent. The GAC solid was milled and screened to the range of 200-600 µm.

Analytical grade p-chlorophenol (powder state, ≥ 99.0 % purity, formula C_6H_5ClO, molecular weight 128.5) and o-cresol (solid powder state, ≥ 99.0 % purity, formula C_7H_8O, molecular weight 108.14) were provided from Sigma-Aldrich, Inc. and used without any further treatment. Firstly phenols (p-chlorophenol or o-cresol) solution was prepared by dissolving 1 gm of p-chlorophenol or o-cresol in 1 L of distilled water to obtain stock solution of concentration 1000 mg phenols/l. The stock solutions were diluted if necessary to get the required concentrations of 50, 100, 200, and 400 mg/l.

The pH of the solutions was adjusted by addition of 0.1M HCl or 0.1M NaOH solutions as needed at initial solution pH study.

2.2 Experimental Unit

The experimental unit used in this work consists of a semi-fluidized column equipped with a top retaining plate, and liquid distributor, liquid pump, two liquid rotameters and two tanks for feed and product. The semifluidized bed column used in this work is transparent QVF glass column of 2.54 cm. inside diameter and 70 cm. long with an expanding end of 10.16 cm diameter. A movable retaining grid made up of 100 mesh stainless steel screen is fixed on a Perspex perforated plate with outside diameter of which is very nearly the same as the inside diameter of the column. The retaining grid can be moved up and down to any position along the column by using a 4 mm diameter metal rod. **Fig.1** shows the schematic and photographic view of the experimental unit.

2.3 Procedure

As a preliminary study the hydrodynamic limits (such as minimum U_{minsf} and maximum U_{maxsf} semifluidization velocities and height of packed h_{pa} bed formation in the semi-fluidizer) were determined.

The minimum and maximum semiflidization velocities and packed bed formation h_{pa} were determined at each (h_r/h_s) ratio visually and compared with estimated value from equations given by **,Jena et. Al, 2009**.

In the first set of experiments the retaining grid to static bed height ratio (h_r/h_s) and the initial static bed height (h_s) were fixed and selected as 3.5 and 5 cm respectively, therefore the height of grid h_r = 17.5 cm then the superficial liquid velocity was changed from one to eight times the value of minimum semiflidization velocity (i.e. $U_{minsf} - 8U_{minsf}$) to find its effect on the percent removal of p-chlorophenol. The determined value of minimum semiflidization velocity and the other experimental conditions were fixed as shown in **Table.1.** At this step the semifluidized bed was operated under continuous mode and the breakthrough curves of p-chlorophenol were generated. All experiments were performed at constant temperature of 30 ^{o}C.

After determining liquid superficial velocity that gives the best breakthrough curve of p-chlorophenol, the retaining grid to initial static bed height ratio (from 3 to 4.5) and by the way the initial static bed height (from 3 to 8 cm) were examined at particle size, initial p-chlorophenol concentration, and initial pH of (200-600) µm, 100 mg/l, and 6 respectively. The aim of this step is to determine the best value of the retaining grid to initial static bed height ratio. The best value of retaining grid to initial static bed height ratio which gives higher removal of p-chlorophenol will be selected for the next step.

In the next step the initial concentration of p-chlorophenol and o-cresol (50, 100, 200, and 400 mg/l) was tested at best values of liquid superficial velocity and retaining grid to initial static bed height ratio.

In the final step of the experimental procedure the initial pH (varied as 4, 6, 8 and 10) was studied on the removal of p-chlorophenol and o-cresol and new breakthrough curve will be generated.

Each sample of phenols was analyzed using UV-Vis. spectrophotometer at wavelengths of 279 for p-chlorophenol and 271 nm for o-cresol **(Thomas, 2007)**. The pH was measured using pH meter manufactured by HANNA Instruments Company (range 2 to 16 ± 0.01).

3. RESULTS AND DISCUSSION

3.1 Hydrodynamics

Fig.2 shows the experimental relationship between the retaining grid to initial static bed height ratio (h_r/h_s) and minimum U_{minsf} and maximum U_{maxsf} semifluidization velocities for the activated carbon of range of (200-600) µm particle diameter in water- solid carbon system. The benefit of this run was to know the limits of velocities at different (h_r/h_s) ratios in order to select the appropriate (h_r/h_s) ratio. It is seen from this figure that the minimum and maximum semifluidization velocities increase with the increasing of (h_r/h_s) ratio.

3.2 Effect of Liquid Superficial Velocity

Figs.3 and **4** show the effect of the superficial liquid velocity on the removal of p-chlorophenol. It is clear from this figure when C_o=100 mg/l, d_p=(200-600) µm, h_s=5 cm, h_r=17.5, U_{minsf} = 0.05 m/s, pH=6 and liquid superficial velocity was varied from U_{minsf} to $8U_{minsf}$ the initial percent removal decrease with increasing the superficial liquid velocity while the time required reaching equilibrium state decreased. The increase in superficial liquid velocity leads to decrease the contacting rate between the activated carbon adsorbent and phenols aqueous solution **,Younk G.P. et al., 1999**. The equilibrium time for adsorption of p-chlorophenol at superficial liquid velocity of U_{minsf}, $2U_{minsf}$, $4U_{minsf}$, $6U_{minsf}$ and $8U_{minsf}$ were 60, 75, 80, 90 and 100 min respectively.

3.3 Effect of Retaining Grid to Initial Static Bed Height Ratio (h_r/h_s)

To determine the effect of the retaining grid to initial static bed height ratio, the liquid superficial velocity was selected as (8 Uminsf) and the retaining grid to initial static bed height ratio was varied from 3 to 4.5 (initial static bed height varied from 3 to 8 cm), the other parameters were fixed as C_o=100 mg/l, d_p= (200-600) µm, and pH=6. **Table.2** shows the variation of hydrodynamic characteristics at this section.

Fig.5 shows the effect of retaining grid to initial static bed height (h_r/h_s) ratio on the breakthrough curve of p-chlorophenol. It can be seen from this figure that the initial removal of p-chlorophenol slightly affected with the increase in the retaining grid height also the time required to reach the equilibrium value decreased. For example when the initial static bed height was 5 cm and the height of retaining grid varied from 17.5 cm to 20 cm as shown in **Table.2** the percent removal increase from 0.71 to 0.8.

Increasing the retaining grid height leads to a slight increase in the value of minimum semifluidization velocity required therefore there is no big change in percent removal.

3.4 Effect of Initial Concentration of P-chlorophenol and O-cresol

Figs.6 and **7** show the effect of initial concentration of p-chlorophenol and o-cresol respectively on the breakthrough of these two compounds at retaining grid to initial static bed height ratio of 4, static bed height of 5 cm, superficial liquid velocity of 8 Uminsf, particle size of (200-600) µm, and pH= 6.

The initial percent removal decrease with increasing the initial concentration while the time required reaching equilibrium state decreased, this is due to increasing the amount of p-chlorophenol and o-cresol to be adsorbed onto activated carbon particles. This result is agree with numerous investigators such as **, Shabiimam and Dikshit , 2012),** Singh D. K. **(Singh D. K. and Bhavana Srivastava, 2002)** and Kulkarni S. J. **(Kulkarni and Kaware, 2013)** whose studied the removal of several phenolic compounds onto activated carbon using fixed and fluidized bed adsorber but not semifluidized bed.

3.5 Effect of Initial pH

Fig.8 shows the effect of initial pH of the solution in the bed on the percent removal of both p-chlorophenol and o-cresol after 40 min of operation at retaining grid to initial static bed height ratio of 4, static bed height of 5 cm, superficial liquid velocity of 8 Uminsf, particle size of (200-600) µm, and finally the initial concentration was selected for each component as 200 mg/l. It can be seen that the percent removal was highly dependent on the pH of the solution. The percent removal for both phenols increases with increasing pH of the solution up to about pH 7 then decreases with further increasing in pH. The maximum removal percent was at pH between 7 and 8. When increasing pH above 8 this is leads to affect the surface charge of the adsorbent and degree of ionization therefore the percent removal decrease. In other words, this effect can explain that because of the aqua-complex formation and it's following acid-base disintegration in the solid-liquid interface **(Singh and Srivastava, 2002, Amit and Minocha, 2006**).

4. CONCLUSIONS

Semifluidized bed adsorber was used and evaluated experimentally for removal of two phenolic compounds p-chlorophenol and o-cresol at different conditions. It is claimed that the use of semifluidized bed was very successful when use high to moderate superficial liquid velocity above minimum semifluidization velocity and initial pH between 7 and 8 and any retaining grid to initial static bed height ratio to enhance the percentage removal of these pollutants.

REFERENCES

- Amit B. and Minocha A. K., 2006, *Conventional and non-conventional adsorbents for removal of pollutants from water- A review*, Indian Journal of chemical technology, Vol. 13, May.
- Jena H. M., G. K. Roy and B. C. Meikap, 2009, *Hydrodynamics of regular particles in a liquid-solid semifluidized bed*, Powder Technology.
- Kulkarni S. J. and Kaware J. P., 2013, *Review on Research for Removal of Phenol from Wastewater*, International Journal of Scientific and Research Publications, Volume 3, Issue 4, April.
- Meikap B. C., 1997, *Removal of Phenolic Compounds From Industrial Waste Water by Semifluidized Bed Bio-Reactor*, Journal of the 1PHE, India, Vol.1997, No. 3
- Monteiro A. A. M. G., R. A. R. Boaventura, A. E. Rodrigues, 2000, *Phenol biodegradation by Pseudomonas Putida DSM 548 in a batch reactor*, Biochemical Engineering Journal 6, 45-49.
- Parida K.M., and Amaresh C. P., 2010, *Removal of phenolic compounds from aqueous solutions by adsorption onto manganese nodule leached residue*, Journal of Hazardous Materials 173, 758–764.
- Roy G. K. and K. J. R. Sarma, 1973, *Dynamics of Liquid-Solid Semi-fluidization: Prediction of Semi-fluidization Velocity & Packed Bed Formation*, Indian Journal of Technology Vol. 11, June, pp. 237-241

- Senturk H. B., Duygu O., Ali G., Celal D., Mustafa S., 2009, *Removal of phenol from aqueous solutions by adsorption onto organomodified Tirebolu bentonite: Equilibrium, kinetic and thermodynamic study*, Journal of Hazardous Materials 172, 353–362.
- Shabiimam M. A. and Dikshit A. K., 2012, *Adsorption of o-Cresol Using Activated Carbon, 2012 International Conference on Clean and Green Energy IPCBEE vol.27.*
- Singh D. K. and Srivastava B., 2002, *Removal of phenol pollutants from aqueous solutions using various adsorbents*, Journal of Scientific and Industrial Research, Vol. 61, March.
- Thomas O. and Burgess C. editors, 2007, *UV-visible Spectrophotometry of Water and Wastewater*, Elsevier, Oxford.
- Vinod A. V., and G. V. Reddy, 2003, *Dynamic behaviour of a fluidised bed bioreactor treating wastewater*, Indian Chem. Engr., Section A, Vol.45, No.1, Jan-Mar, 20-27.
- Younk G. P., Sung Yong Cho, Seung Jai Kim, Byung Gwon Lee, Byung Hoon Kim and Song-Ja Park, 1999, *Mass Transfer in Semifluidized and Fluidized Ion-Exchange Beds*, Environ. Eng. Res. Vol. 4, No. 2, pp. 71-80.

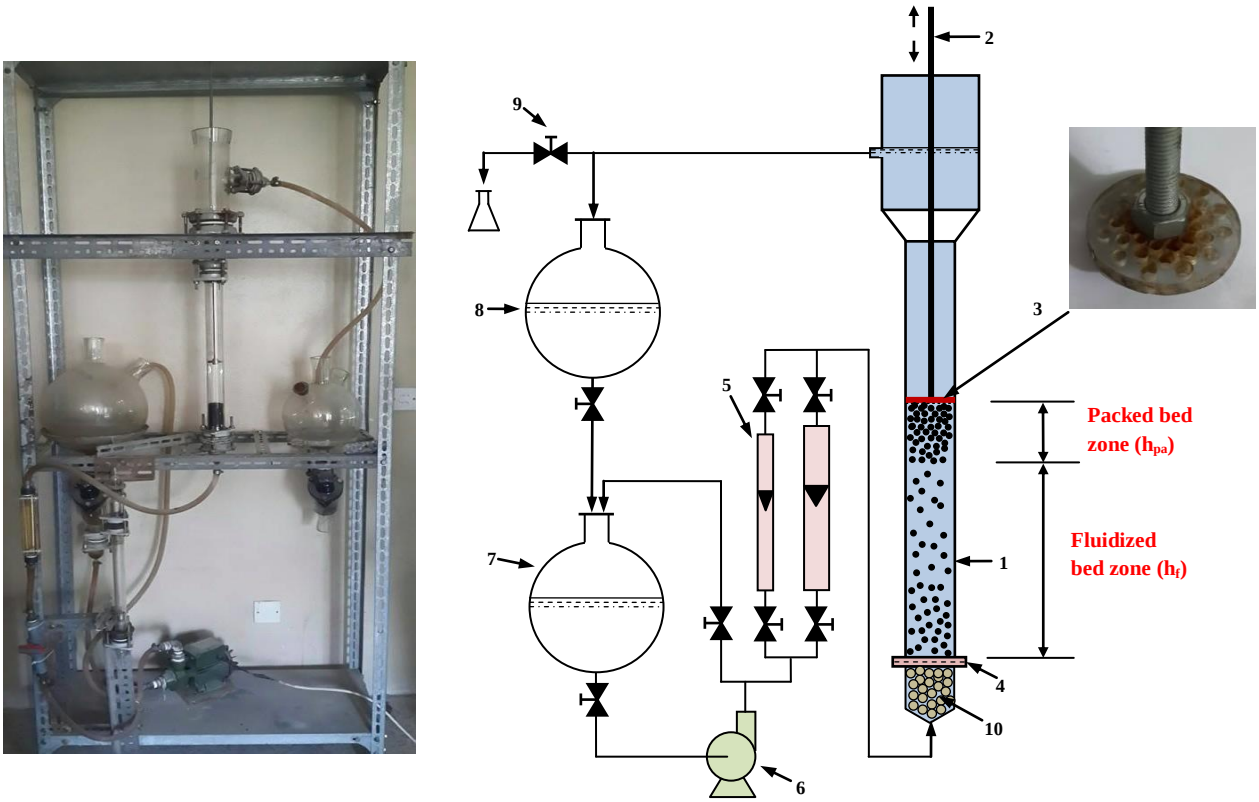

Figure 1. Schematic diagram and photographic view of the semi-fluidized bed unit. (1): Semi-fluidizer. (2): Movable retaining grid (3): Retaining grid (4): Liquid distributor (5): Rotameters (6): Pump (7): Feed tank (8): Liquid reservoir (9): Sampling valve (10) inert packing for distribution.

Table1. Experimental conditions of the preliminary study.

Parameter	**Value**
Phenolic compound	P-chlorophenol
Initial concentration (C_o), mg/l	100
Particle size (d_p), µm	200-600
Initial static bed height (h_s), cm	5
Retaining grid height (h_s), cm	17.5
(h_r/h_s)	3.5
Minimum semiflidization velocity (U_{minsf}), m/s	0.05
pH	6

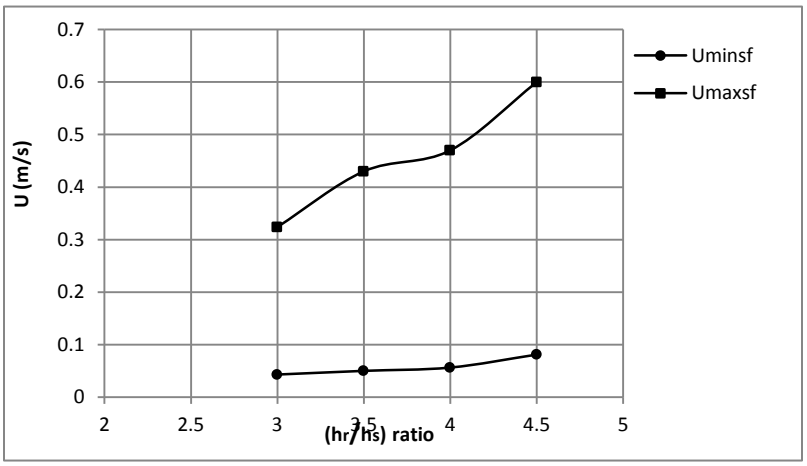

Figure2. The relation between (hr/hs) and minimum and maximum semifluidization velocities **.**

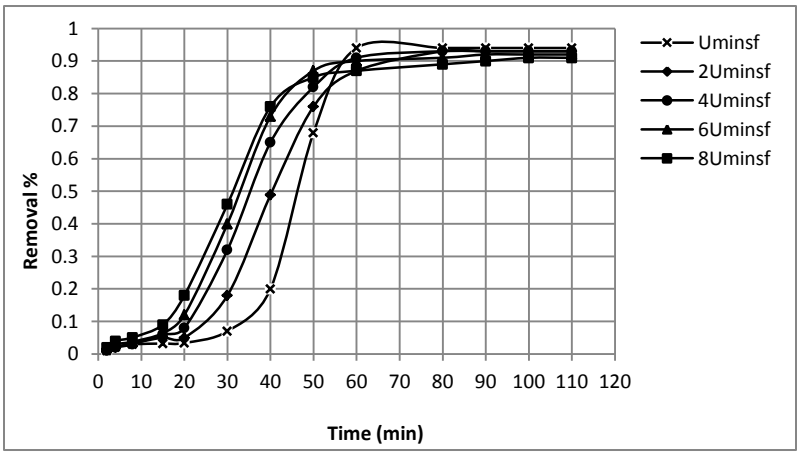

Figure3. Effect of liquid superficial velocity on the breakthrough curve of p-chlorophenol **.**

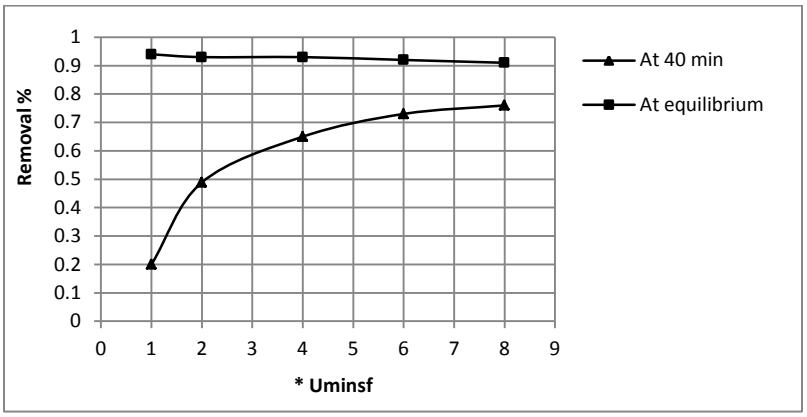

Figure4. Effect of superficial liquid velocity on the p-chlorophenol removal percent at 40 min and at equilibrium **.**

Table2. The hydrodynamic characteristics for determination (h_r/h_s) ratio.

Run #	(h_r/h_s)	h_s (cm)	h_r (cm)	U_{minsf} (m/s)	$U=8U_{minsf}$	h_{pa} (cm)
1	3	3	9	0.043452	0.347	2.5
2	3.5	5	17.5	0.049918	0.4	3
3	4	5	20	0.056293	0.45	2.5
4	4.5	8	36	0.062588	0.5	4.5

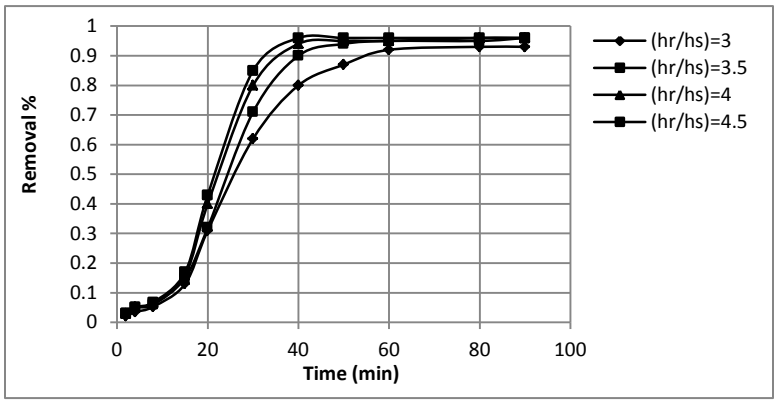

Figure5. Effect of retaining grid to initial static bed height ratio **.**

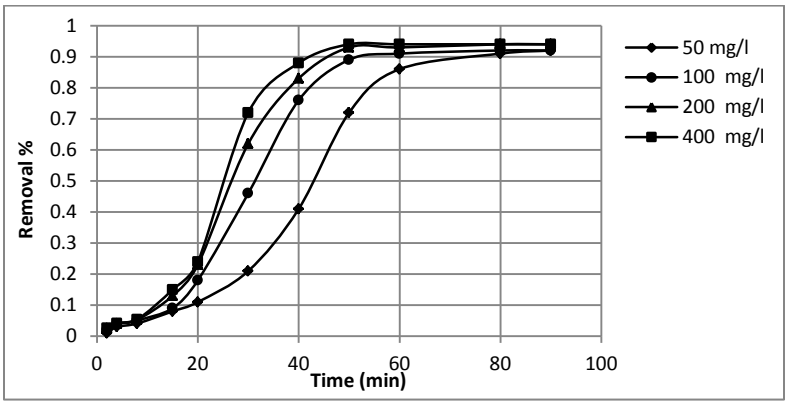

Figure6. Effect of initial p-chlorophenol concentration on the percent removal.

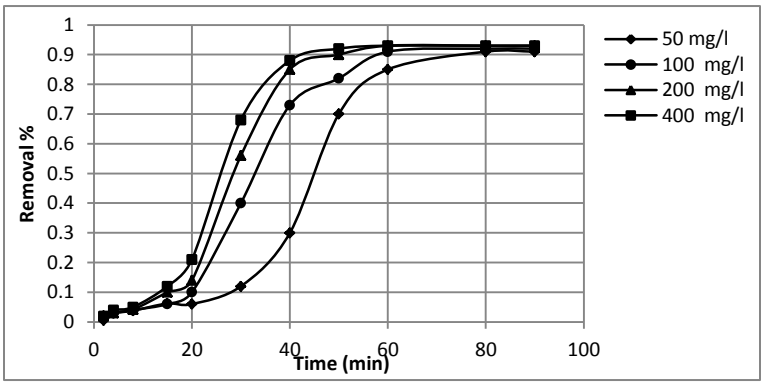

Figure7. Effect of initial o-cresol concentration on the percent removal.

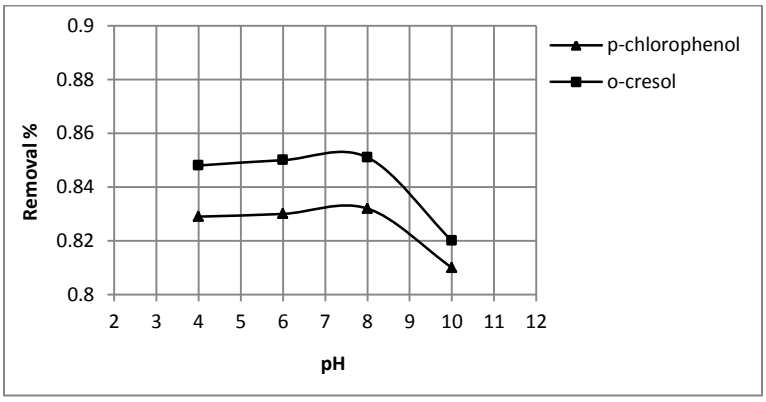

Figure8. Effect of initial pH on the percent removal of p-chlorophenol and o-cresol after 40 min.

Effect of Metakaolin on the geotechnical properties of Expansive Soil

Mahmoud D. Ahmed
Asst. Prof., Civil Engineering Department
University of Baghdad
Mahmood_baghdad@yahoo.com

Nisreen A. Hamza
Department of Civil Engineering
College of Engineering, University of Baghdad
Email: heart_owen1077@yahoo.com

ABSTRACT

Expansive soil spreads in Iraq and some countries of the world. But there are many problems can be occurred to the structures that built on, so we must study the characteristics of these soils due to the problems that may be caused to these structures which built on these kinds of soil and then study the methods of treatment. The present study focuses on improving the geotechnical properties of expansive soils by treating it Metakaolin(M). Metakaolin (M) has never been used before as an improvement material for stabilizing the expansive soil . Metakaolin is a pozzolanic material. It's obtained by calcination of kaolinite clay at temperatures from 700°C to 800°C. Kaolin chemical composition is basically aluminous silicates hydrates associated with Mn, Fe, Ca, K, Na. Its crystal has a lattice structure of tetrahedral and octahedral layers with interplanar distance of 7.2 Å. The soil used in the present study can be classified according to the Unified Soil Classification System as clay with high plasticity (CH) .

Key words: expansive soil, improvement ,swelling, , swelling pressure, metakaolin

تأثير الميتاكولين على الخواص الهندسيه للتربه الانتفاخيه

أ.م.د. محمود ذياب احمد
استاذ مساعد في قسم الهندسة المدنية
جامعة بغداد

نسرين عبد الجبار حمزه
قسم الهندسة المدنية
جامعة بغداد

الخلاصة

تنتشر الترب الانتفاخية في العراق و بعض بلدان العالم غير أن هناك العديد من المشاكل التي من الممكن أن تسببها للمنشآت المستندة عليها لذا فأن دراسة خواص تلك الترب يجب ان يتم بسبب المشاكل التي من الممكن ان تحدثها للمنشات المستندة عليها ومن ثم يتم تحديد طرق معالجتها. حيث تناول البحث أمكانيه تحسين الخواص الهندسية للترب الانتفاخية بمادة الميتاكؤلين. الميتاكؤلين لم يتم استخدامها من قبل كمادة محسنه لتثبيت التربة الانتفاخيه . الميتاكؤلين هي مادة بوزولانية . تم الحصول علبها من قبل التكليس من الطين الكاؤليني في درجات الحرارة من 700 درجة مئوية إلى 800 درجة مئوية. التركيب الكيميائي للكاؤلين هو في الأساس هيدرات سيليكات المرتبطة بالمنغنيز ، الحديد ، الكالسيوم ، البوتاسيوم، الصوديوم . من الواضح ان لديها بنية من طبقات رباعية السطوح و ثمانية السطوح مع مسافة داخليه 7.2 Å . التربة المستخدمة في هذه الدراسة يمكن تصنيفها على انها تربة طينيه ذات لدونة عالية تبعا لنظام تصنيف التربة الموحد.

الكلمات المفتاحية : تربة انتفاخية , معالجة , انتفاخ , ضغط الانتفاخ, الميتاكؤلين .

1. INTRODUCTION

Expansive soil is one of the problematic soils that face many geotechnical engineers in the field (others include collapsible soil, quick clays, etc.). The expansive soil is known to cause severe damage structures that are founded on it. In Iraq, there is no confirmed information about the economic losses due to structures founded on expansive soils. However, there are several well-documented cases of studying the behavior of expansive soil in Iraq. Expansive soils are very sensitive to variations in water content and show excessive volume changes because of an increase in their water contents. Expansive soils have the tendency to swell when they become in contact with moisture and to shrink if moisture is removed from them. Expansive soils are a worldwide problem **, Seed et al., 1962, and Kormonik and David, 1969.** This highly plastic soil may create cracks and damage on the pavements, railways, highway embankments, roadways, building foundations, channel and reservoir, water lines, sewer lines etc.**,Gromko, 1974.** Swell response of expansive soils has been investigated by researchers since the 1950s based on Atterberg limits, index properties, and other soil tests carried out in the laboratory **,Seed et al., 1962.** These studies were a major success but they have failed to determine the associated engineering properties. This is mainly because soils with the same atterberg limits and index properties show different engineering properties. In order to control the volume change in expansive soils, many admixtures are adequately used in the researches **, Kehew,1995.** Metakaolin has never been studied its effect on the expansive soils. Metakaolin is a dehydroxylated form of the clay mineral kaolinite. Rocks that are rich in kaolinite are known as kaolin, traditionally used in the manufacture of porcelain. The particle size of metakaolin is smaller than cement particles, but not as fine as silica fume. Metakaolin is a pozzolanic material and has never been used before as an additive to improve the expansive soil therefore studying its effect will give us the way to use it as pozzolanic material to reduce the swelling potential. The standard chemical requirements of **ASTM C618-03** include the sum of SiO_2 , Al_2O_3 and Fe_2O_3 content ($\geq$ 70%) for class F and ($\geq$ 50%) for class C to define the material as pozzolanic.

2. MECHANISM OF SWELL

Mitchell, 1993 showed that soil swelling happens due to several factors:

1-Capillary Imbibition: The surface tension caused by air in the unsaturated soil and the soil suction caused water adsorption to the soil system.

2-Osmotic Imbibition: The double layer acts as semi permeable membrane with difference in the ion's concentration inside and outside of it causing the flow of water and increase in the soil volume.

3- Hydration of Exchangeable Cations: as described previously the cations attracted to the negatively charged soil surface causing an increase in the volume of the double layer. Then these cations will be hydrated causing an increase in the ion's volume and as a result an increase in the soil volume.

4-Van Der Waals forces: these forces are secondary in-directional forces and less strong than the hydrogen bonding and they connect the montmorillonite sheets, when adsorption of water happens a repulsion between these forces will happen leading to an increase in the volume of soil.

The objectives of this study are

1- Improve the properties of expansive soil to be used as construction material in the pavements, railways, highway embankments, roadways, building foundations, channel and reservoir linings, irrigation systems, water lines, sewer lines etc.
2- Reduce the industrial wastes, this reduction is considered one of the concept used in contamination control.
3- Use local materials in soil treatment which reduces the costs.

3. EXPERIMENTAL WORKS AND MATERIALS USED

3.1 Materials used

The materials used during the experiments were bentonite, sand, and metakaolin. **Table 1.** shows the physical properties of the materials that have been used in the study.

1-**Prepared soil**: mixture of bentonite (Ca-based bentonite manufactured by Al-Fallujah Cement Factory is used as the expansive soil) with sand (from Ali Al-Gharbi city south of Baghdad) were tested till getting the mixture of 85% of bentonite to 15% of sand (B-S) by dry weight depending on the required plasticity indices.

2- **Metakaolin (M)** is a pozzolanic material. It's obtained by calcination of kaolinite clay at temperatures from 700°C to 800°C as shown in Eq.(1).Kaolin chemical composition is basically aluminous silicates hydrates associated with Mn, Fe, Ca, K, Na. Its crystal has a lattice structure of tetrahedral and octahedral layers with interplanar distance of 7.2 ,**Cited, et al., 2004.**

$$\underset{\text{Kaolin}}{Al_2Si_2O_5(OH_4)} \xrightarrow{700°C} \underset{\text{Metakaolin}}{Al_2O_{3.}2SiO_{2+}2H_2O} \qquad (1)$$

The chemical properties of these materials are presented **Table 2**.

3.2 Physical Tests

3.2.1 Grain size distribution tests

The test was carried according to **,BS 1377: 1975.** and the prepared soil is composed of 72% of clay , 24% of silt ,and 4% of sand.

3.2.2 Specific gravity tests

The specific gravity of specimens was determined in accordance with the **(ASTM D-854).**

3.2.3 Compaction tests

Compaction tests were conducted using "standard" compaction test according to **(ASTM D-1557).**

3.3 Shear Strength Tests

3.3.1 Sample preparation

Remolded specimens were prepared in the laboratory depending on the proctors data at the required molding water content according to **(ASTM D 2850 – 03a) .**

3.3.2 Unconfined compression tests

The specimens were compacted statically for the maximum dry density and optimum moisture content values then sealed and allowed to cure for one day. The test has been carried according to **(ASTM D-2166).**

3.4 The Swelling Test

Three types of swelling tests have been made (free swell test, constant volume test, and consolidation test). The tests were done according to **Head 1984 and ASTM D 4829-03**. In these tests, the oven dried soil passing 2mm sieve was mixed with the required amount of water and were remolded at the oedometer ring (75 mm in diameter and 19 mm in height) but the sample was prepared by a height equal to 14 mm to insure that the specimen will be laterally confined , **Al-Omari, et al., 2010**. A load of about 7 KPa was applied as seating pressure, left for ten minutes then an initial reading was recorded. The soil sample was submerged with distilled water for 24 hours then the final reading was recorded. To measure the swelling pressure, weights will be added in increments to the soil sample to get the dial gage reading zero again.

4. RESULTS OF TESTS

4.1 Results of Grain Size Distribution

Fig. 1 shows the effect of metakaolin on the grain size analysis of the prepared soil. It can be noticed that metakaolin affects the prepared soil at the beginning and causes a reduction in the percentages of clay particles but eventually remains constant and causes a reduction in percentages of sand between 4% and 12% of M and that is due to the particle size of M which represents a fine material with diameter size less than 0.00325 mm. Soil M10 gives 31% reduction in the clay content , 42% increment in the silt content and 300% increment in the sand content, therefore 10% of M gives the best results for the grain size distribution. Soil M12 gives different behavior which shows 3% increment in the clay content (an increment more than Soil A) and 25% reduction in the Silt content, this behavior could be related to the pozzolanic reaction of M which take place during the process (The standard chemical requirements of **ASTM C618-03** include the sum of SiO_2 , Al_2O_3 and Fe_2O_3 content ($\geq$ 70%) for class F and ($\geq$ 50%) for class C to define the material as pozzolanic).**Table 3** shows the results of the grain size distribution test.

4.2 Results of Specific Gravity Tests

Fig. 2 shows the effect of metakaolin on the specific gravity results. it can be noticed that M causes a linearly reduction in the specific gravity of mixture. The reduction of specific gravity is because of lower specific gravity of M. Linear decrease in specific gravity indicate that no mineralogical alterations have occurred with M alone. At 12% replacement the specific gravity of mixture reduces to 2.72 **,Kumar, 2012.**

4.3 Results of the Compaction Tests

Fig. 3 shows the effect of metakaolin on the compaction results. Metakaolin increases the max dry unit weight from (13.5 to 13.66) KN/m^3 and decreases the optimum moisture content from (36 to 34.5) . As water is added to a soil (at low moisture content) it becomes easier for the particles to

move past one another during the application of compacting forces. **Table 4** shows the results of the compaction and specific gravity tests results.

4.4 Results of Unconfined Compression Test

Fig. 4 shows effect of M on the unconfined compression strength of the expansive soil**.** This Figure illustrate the stress-strain behavior of prepared and treated soil under vertical load. Initially the stress gradually increases with the increase in strain. After attaining the peak stress, it decreases with the increase in strain for all the combinations of replacement materials and soil. Approximately all the specimens show shear failure after the failure of plane of specimens. Fig. 5 shows the effect of M on the c_u and **Table 5** shows the results of the unconfined compression tests .it can be noticed that the replacement material M causes a linear increment in c_u from (160.73 to 315.00) KPa for soil samples from (M4 to M10). This increment was due to the reactive silica which reacts and produce cementations material and binds soil particles together to increase strength **,Kumar, 2012.** The reduction in c_u at M12 to 258.90 KPa may be due to the excess M introduced to the soil and therefore forming weak bonds between the soil and the cementations compounds formed.

4.2 Results of Swelling Tests

Fig. 6 shows time – percent swell for the prepared soil and soil treated with M**.** The prepared soil shows a high rate of swell within the 11 days and then reaches a fix point ,whereas the treated soil reaches its point with less than that. It is due to the electrical equilibrium when the double layer arrives to its full required thickness to balance the net negative charges at the faces of clay particles. The swell percent decreases due to the effect of pozzolanic reaction for the replacement materials that have been used which take place during the process. **Fig. 7** shows the effect of metakaolin on the swelling pressure, it can be noticed that the metakaolin causes a reduction in the swelling pressure while the sudden increment in the swelling pressure at M8 and M12 were due to the reduction in water content from 32.5% at M6 to 30% at M8 and from 35% at M10 to 34.5% at M12 which means more adsorb water and that lead to more swelling potential. Swelling pressure obtained from free swell tests is higher than that obtained from the constant volume test .That is because the free swell test allows an increase in volume and that causes random arrangement for the parallel particles of the soil, in reloading an additional pressure was needed to rearrange the particles. **Fig. 8** shows e- $\log\sigma_v$ for the prepared soil and **Fig. 9** shows e- $\log\sigma_v$ for soils treated with M. **Fig. 10** shows the effect of metakaolin on the consolidation parameters, one can notice that M causes a linear reduction in the void ratio which can be related to the reduction in water content from 36% to 34.5%. the compression index decreased due to the reduction in the clay content from 72% to 50%. **Table 6** shows the results of the free swell and constant volume tests. The potential expansion has been classified according to **ASTM- D (4829 – 03)** as shown in **Table 7.** The soils samples turned from very high expansive to moderate and even very low expansion potential due to the effect of pozzolanic materials which could be due to the pozzolanic and cation exchange reactions which occurred between the soil and replacement materials. Eq.(2) shows the calculation of the expansion index according to **ASTM- D (4829-0).**

$$EI=(\Delta H/H)* 1000 \quad (2)$$

Where:

EI: Expansion Index,

ΔH = change in height, D2 − D1, mm,
H1 = initial height, mm,
D1 = initial dial reading, mm, and
D2 = final dial reading, mm.

Based on the results of consolidation ,the coefficient of permeability of the soil can be calculated from Eq. 3:

$$K = C_v \, m_v \, \gamma_w \tag{3}$$

where:
C_v = Coefficient of consolidation,
m_v = Coefficient of volume change, and
γ_w = Unit weight of water.

Fig .11 shows the effect of M on the coefficient of permeability. **Fig. 12** shows the effect of M on the coefficient of c of consolidation. **Fig .13** shows the effect of M on the coefficient of volume change. The calculation of m_v, C_v, and the coefficient of permeability were at stress equal to 400 Kpa. The coefficient of consolidation and the coefficient of permeability various from one soil to another for soils samples M4 to M12 in and this variation could be easily related to the variation in the sand content (increasing in sand content causes an increment in the permeability due to the coarser size of sand) ,for example at soils samples from M4 to M6 the coefficient of consolidation increased from (3.920 to 8.187) m^2/sec and the coefficient of permeability increased from (0.0087 to 0.0154) m/sec due to the increment in sand content from (4 to 20)% then the coefficient of consolidation and the coefficient of permeability began to decrease at M8 due to the reduction in sand content to 4%. And finally the coefficient of consolidation and the coefficient of permeability began to increase at M10 and then decrease at M12 due to the increment in sand content for M10 from (4 to 16) % and then the reduction in sand content from (16 to 8)% for M8. **Table 8** shows the results of the consolidation test.

5. CONCLUSIONS

Based on the experimental results of the experimental work, the following conclusions may be obtained:

1- The grain size distribution shows that the soil turn to more coarser size due to the pozzolanic reaction between the expansive soil and metakaolin.
2- The specific gravity decreased with the addition of M from 2.78 to 2.72
3- The compaction curves shows that, the addition of M increases the maximum dry density and decreases the optimum moisture content.
4- From the unconfined compression tests results show that the prepared soil A has (C_u=94.76 KPa). The optimum unconfined compressive strength was obtained for 10% of M content. The cohesion of soil shows an increasing order for first percentages of M and after that this value decreases at 12% of M to 258.90 KPa but it is still higher than the prepared soil type A.
5- From free swell tests, the following conclusions can be drawn.
   a- Soil sample M10 causes a reduction in the free swell about 91%. and after the addition of R (5, 8 and 11%), the reduction various to about (91%, 89%, 82%) respectively.
   b- The results of swelling pressure test using constant volume method show that the addition of the addition of (10%) M causes a reduction of about (87%).

c- From the consolidation test results, it can be concluded that the values of compression index increases and a linear reduction in the void ratio. The coefficient of permeability increases for all soil samples which is considered acceptable for construction of water retention and irrigation projects. It is evident from the test results that the soil sample M10 revealed a better improvement to the consolidation parameters.

6- It is worth mentioning that the best type of replacement from these five soils samples is soil sample M10 due to maximum reduction in the swelling potential.

REFERENCES

- Al-Omari, R. R., Ibrahim, S. F. and Al-Bayati, I. K., 2010 *Effect of Potassium Chloride on Cyclic Behavior of Expansive Clays*, International Journal of Geotechnical Engineering, Vol. 4, No.2, pp. 231-239.
- ASTM C 618-03, Standard Specification for Coal Fly Ash and Raw or Calcined Natural Pozzolan for Use in Concrete, Reprinted from the Annual Book of ASTM Standards. Copyright ASTM, Vol.4, No.2.
- ASTM D 1140-00, *Standard Test Methods for Amount of Material in Soils Finer Than the No. 200 Sieve*, Reprinted from the Annual Book of ASTM Standards. Copyright ASTM, Vol.4, No.8.
- ASTM D 2166-00, *Standard Test Method for Unconfined Compressive Strength of Cohesive Soil*, Reprinted from the Annual Book of ASTM Standards. Copyright ASTM, Vol.4, No.8.
- ASTM D 2487-00, *Standard Practice for Classification of Soils for Engineering Purposes (Unified Soil Classification System)*, Reprinted from the Annual Book of ASTM Standards. Copyright ASTM, Vol.4, No.8.
- ASTM D 422-02, *Standard Test Method for Particle-Size Analysis of Soils*, Reprinted from the Annual Book of ASTM Standards. Copyright ASTM, Vol.4, No.8.
- ASTM D 4318-00, *Standard Test Methods for Liquid Limit, Plastic Limit and Plasticity Index of Soils*, Reprinted from the Annual Book of ASTM Standards. Copyright ASTM, Vol.4, No.8.
- ASTM D 4829-03, *Standard Test Method for Expansion Index of Soils*, Reprinted from the Annual Book of ASTM Standards. Copyright ASTM, Vol.4, No.8.

- ASTM D 698-12, Standard Test Methods for Laboratory Compaction Characteristics of Soil Using Standard Effort (600KN-m/m^3), Reprinted from the Annual Book of ASTM Standards. Copyright ASTM, Vol.4, No.8.
- ASTM D 854-00, *Standard Test Methods for Specific Gravity of Soil Solids by Water Pycnometer*, Reprinted from the Annual Book of ASTM Standards. Copyright ASTM, Vol.4, No.8.
- Clovis N. , Vanderley M. J. , Cleber M. R. D., Holmer S. Jr. , and Mario S. T. , 2004, *Effect of Metakaolin on the Performance of Pva and Cellulose Fiber Reinforced Cement.*
- Gromko, G. J., 1974, *Review of Expansive Soils*, Journal of the Geotechnical Engineering Division, ASCE, Vol. 100, No. GT6, pp. 667-687.
- Head, K. H., 1984, *Manual of Soil Laboratory Testing*, Pentech Press, London, Vol. 1.
- Kehew, E.A., 1995, *Geology for Engineers and Environmental Scientists, 2nd ed*. Prentice Hall Englewood Cliffs, New Jersey, pp. 295-302.
- Kormonik, A., and David, D., 1969, *Prediction of Swelling Pressure of Clays, Journal of Soil Mechanics and Foundation Division* ASCE, Vol. 95 (SM1), pp. 209–225.
- Kumar S. M. P. , 2012, *Silica and Calcium effect on Geo-Technical Properties of Expansive soil Extracted from Rice Husk Ash and Lime,* International Conference on Environment Science and Engineering, *Singapore* , Vol. 32 , pp. 119-123.
- Mitchell, J. K. 1993, *Fundamentals of Soil Behavior*, 3rd edition, John Wiley and Sons, New York, USA.
- Seed, H. B., Mitchell, J. K., and Chan, C. K., 1962, *Studies of Swell and Swell Pressure Characteristics of Compacted Clays*, Highway Research Board, Bulletin No. 313 ,1962, pp. 12-39.

Table 1. The physical properties of materials used.

Physical properties	Index properties	Prepared soil	Bentonite	Sand	M	specification
Atterberg limits	Liquid limit,L.L(%)	112	150	NP	39	ASTM D-4318
	Plastic limit,L.L(%)	45	45	NP	22	
	Plasticity index,P.I(%)	67	105	NP	17	
Grain size analysis	% sand (0.06-2)mm	4	0	97.68	0	BS 1377-1975
	% silt (0.002-0.06)mm	24	5	2.32	0	
	% clay (<0.002)mm	72	95		100	
Specific gravity,Gs	-	2.78	2.89	2.63	2.57	ASTM D-854
Compaction test	Max dry density,(KN/m³)	13.4	12.64	15.15	-	ASTM D-1557
	Optimum moisture content,%	36	37	12.5	-	
USCS*		CH	CH	SP	-	ASTM D-2487

Table 2. Chemical properties of materials used.

Materials / Chemical properties	Bentonite	Sand	Metakaolin
SiO_2 %	51.92	55.55	59.62
Fe_2O_3 %	5.45	0.08	1.629
Al_2O_3 %	14.23	0.5	26.63
CaO %	8.24	11.25	0.74
MgO %	2.86	3.9	0.0034
Na_2O %	0.96	1.73	-
K_2O %	0.69		0.43
TiO_2 %	0.8	-	1.875
PH	7.7	7.6	-
SO_3 %	1.3	1.33	-
Gypsum %	2.64	2.86	-
T.S.S %	5.25	0.7	-
O.M %	0.7	1.3	-

Table 3. Results of the grain size distribution tests.

Soil Sample	% Sand	% Silt	%Clay
A	4	24	72
M4	4	26	70
M6	20	14	66
M8	4	36	60
M10	16	34	50
M12	8	18	74

Table 4. Results of the compaction and specific gravity tests.

Soil sample	Compaction characteristics		*Specific gravity*
	O.M.C %	Max. dry unit weight KN/m^3	
A	36.00	13.20	2.78
M4	35.00	13.50	2.78
M6	32.50	13.50	2.77
M8	30.00	13.66	2.76
M10	35.00	13.66	2.73
M12	35.00	13.50	2.72

Table 5. Results of the unconfined compression tests.

Soil Sample	Cu(KPa)
A	94.76
M4	160.73
M6	182.10
M8	283.82
M10	315.00
M12	258.90

Table 5. The results of the free swell and constant volume tests.

Soil Sample	Free Swell Test			Constant Volume Test			Potential Expansion for Constant Volume Test
	Free Swell, %	Expansion Index	Swelling pressure, kpa	Free Swell, %	Expansion Index	Swelling Pressure, KPa	
A	83	825	882	46	458	588	very high
M4	34	340	638	29	285	425	very high
M6	23	234	225	20	195	150	very high
M8	26	257	450	21	215	300	very high
M10	7	72	113	6	60	75	medium
M12	22	220	210	18	184	140	very high

Table 6. The classification of a potentially expansive soil **(ASTM- D 4829 – 03).**

Expansion Index, EI	Potential Expansion
0–20	Very Low
21–50	Low
51–90	Medium
91–130	High
>130	Very High

Table 7 . Results of Consolidation Tests.

Soil samples	e_o	C_C	Cs	m_v x10^{-4} m^2/KN	C_v x10^{-8} m^2/sec	K x 10^{-8} m/sec
A	1.106	0.290	0.032	2.030	1.949	0.004
M4	1.059	0.269	0.026	2.259	3.920	0.009
M6	1.046	0.167	0.029	1.919	8.187	0.015
M8	1.013	0.155	0.009	2.852	2.187	0.006
M10	0.999	0.116	0.019	3.711	19.125	0.070
M12	0.991	0.119	0.038	1.415	23.173	0.032

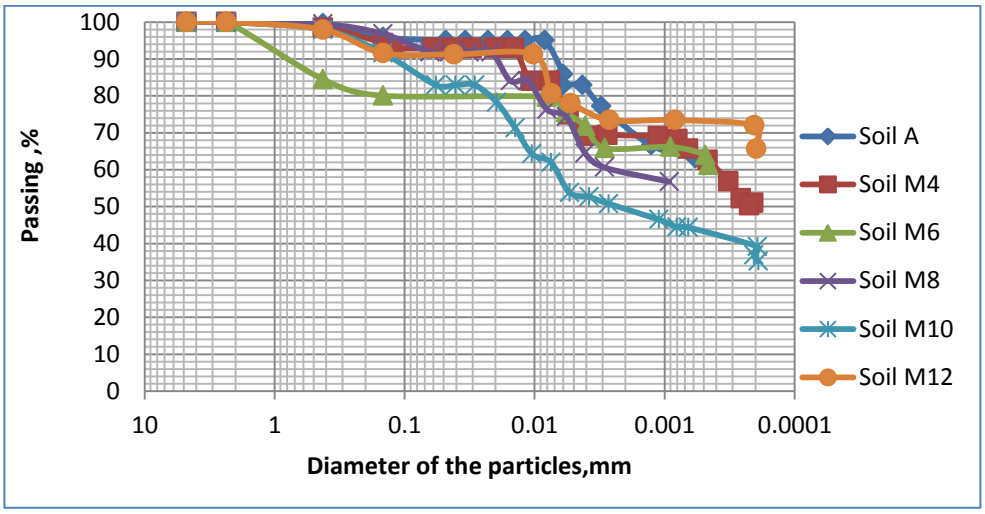

Figure 1. Effect of metakaolin on the grain size distribution.

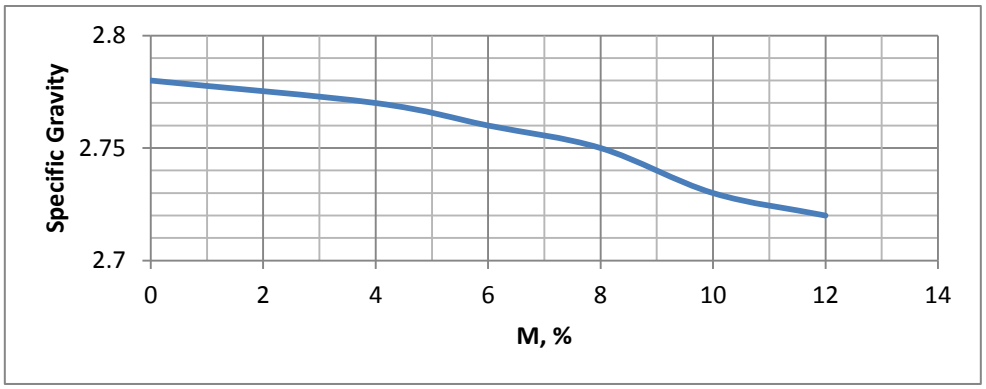

Figure 2. Effect of metakaolin on the specific gravity.

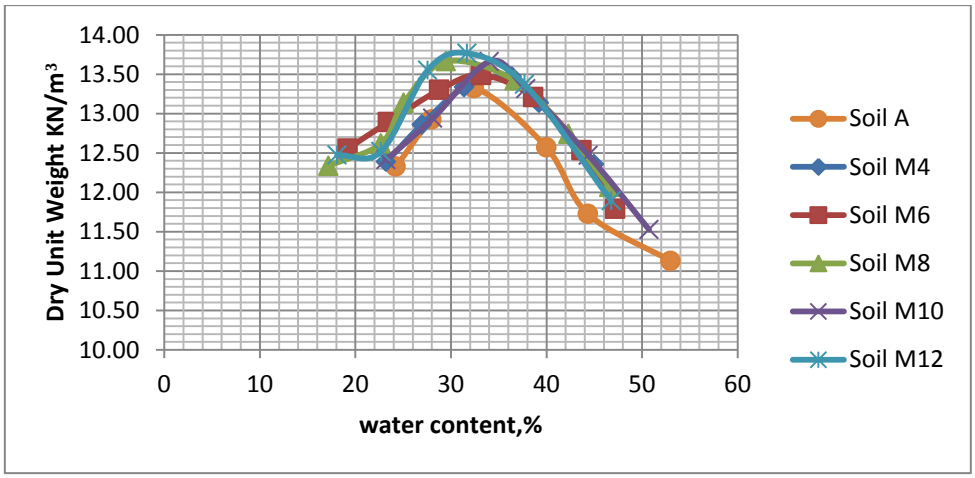

Figure 3 . Effect of metakaolin on the compaction test.

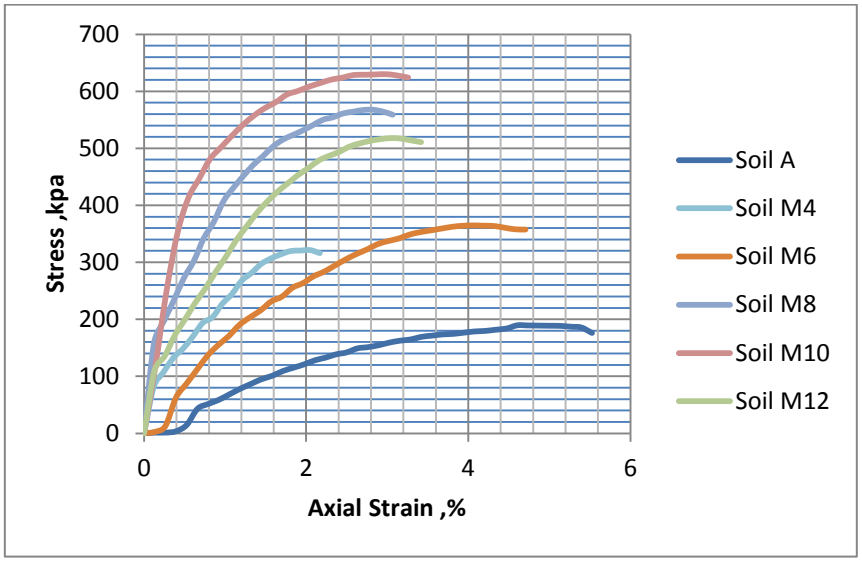

Figure 4. Effect of metakaolin on unconfined compression test results.

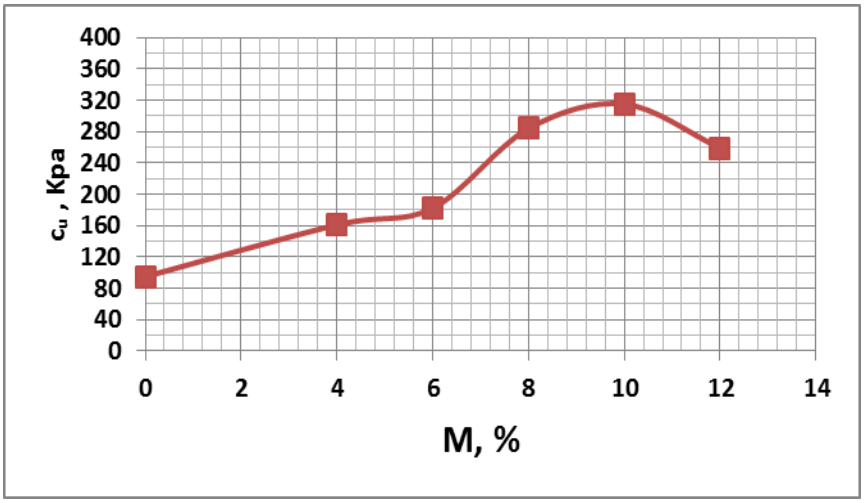

Figure 5. Effect of metakaolin on undrained cohesion.

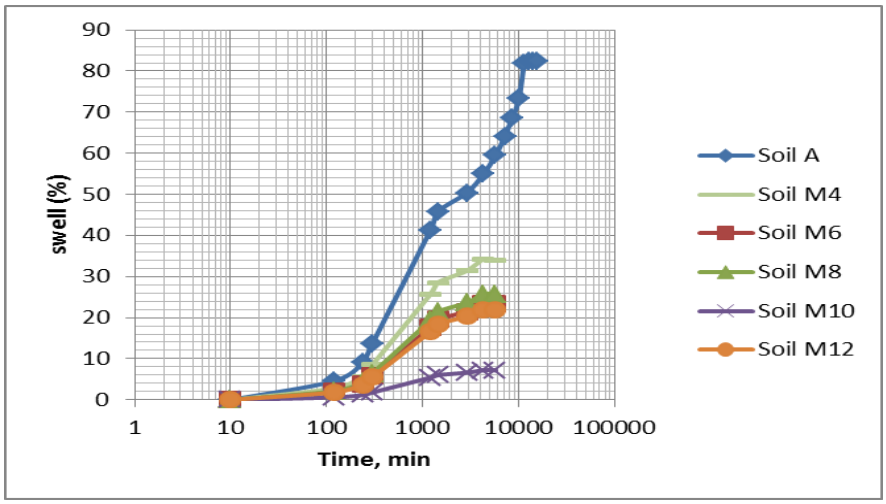

Figure 6 . Time – Percent Swell for the Prepared Soil and Soil Treated with M**.**

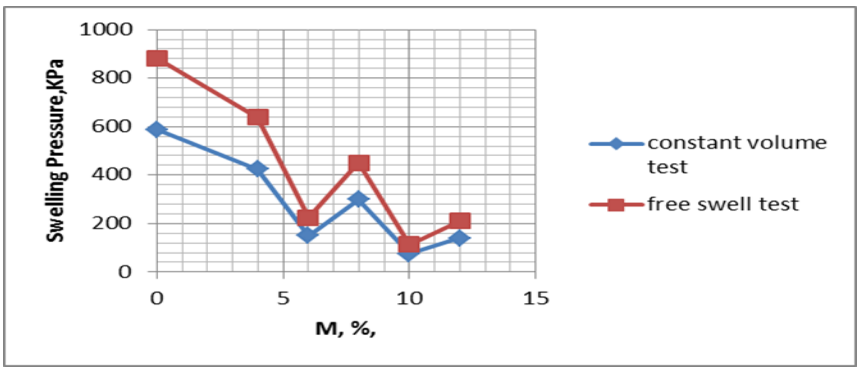

Figure 7. Effect of metakaolin on the swelling pressure.

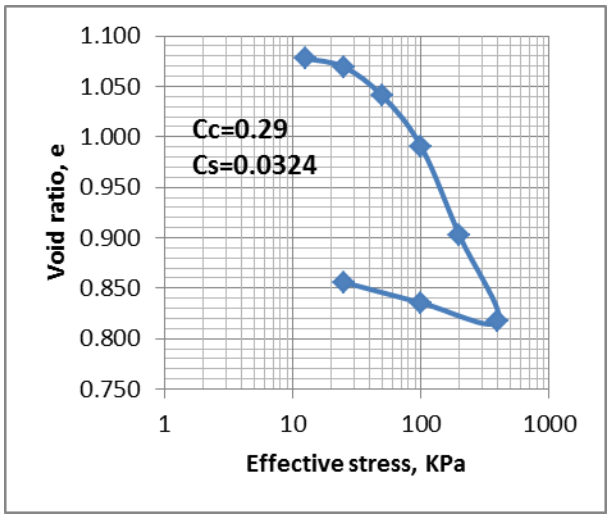

Figure 8. e- $\log\overline{\sigma}_v$ for prepared soil sample A.

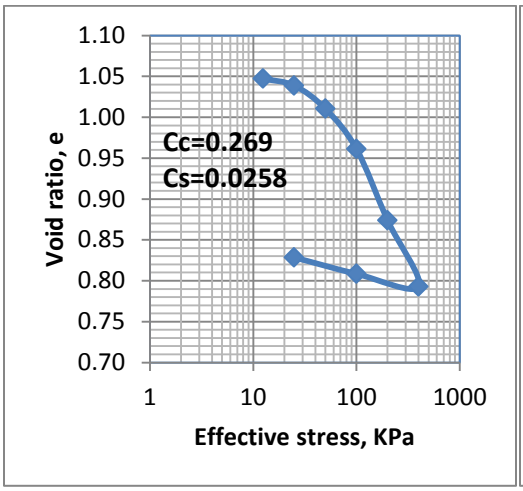

Soil Sample M4

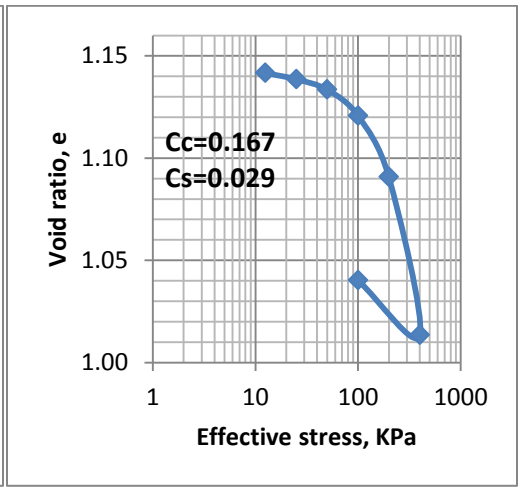

Soil Sample M6

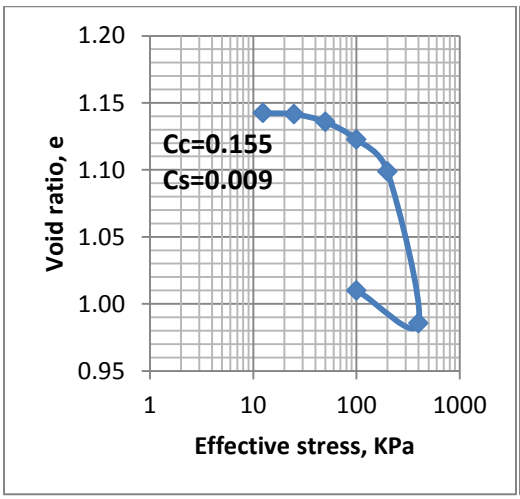

Soil Sample M8

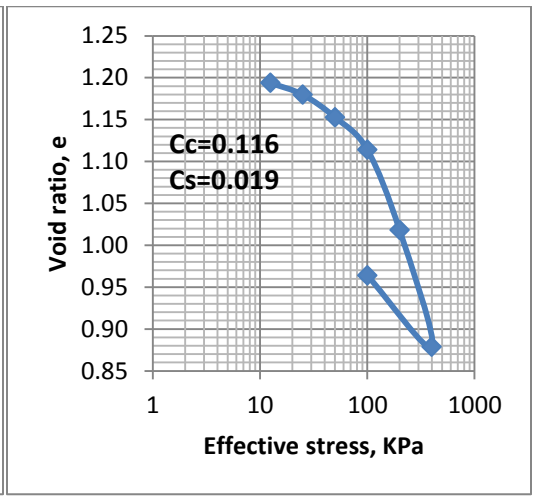

Soil Sample M10

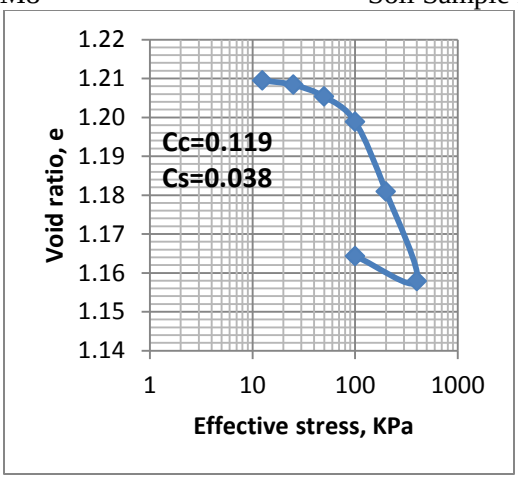

Soil Sample M12

Figure 9 . e- log$\bar{\sigma}_v$ for soils treated with M.

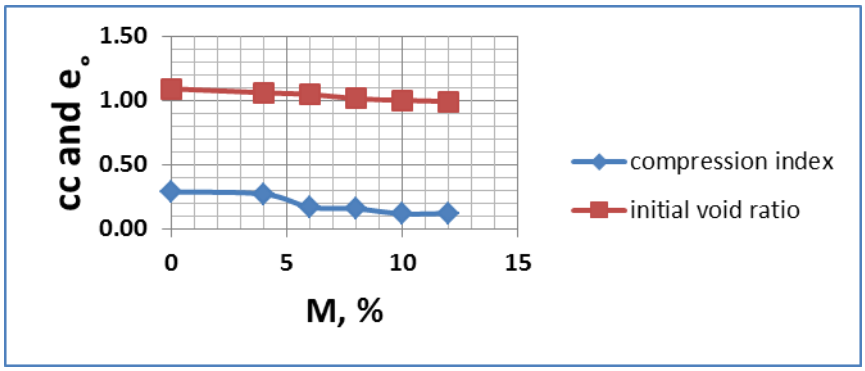

Figure 10. The effect of metakaolin on the consolidation parameters.

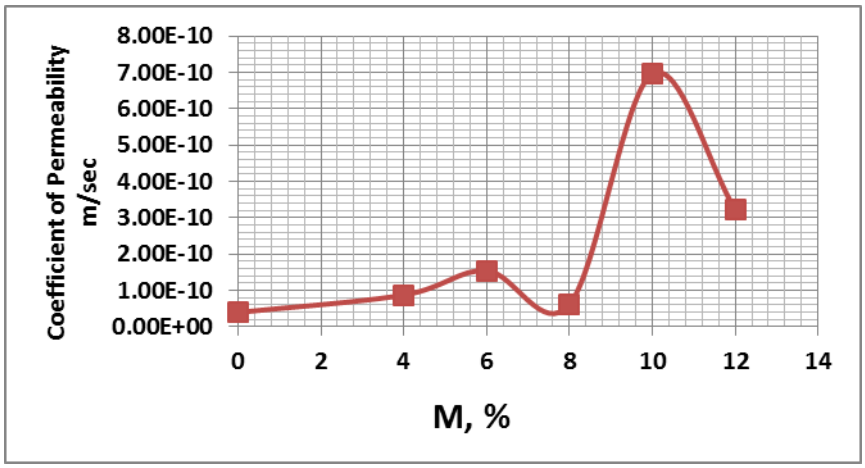

Figure 11. The effect of metakaolin on the coefficient of permeability.

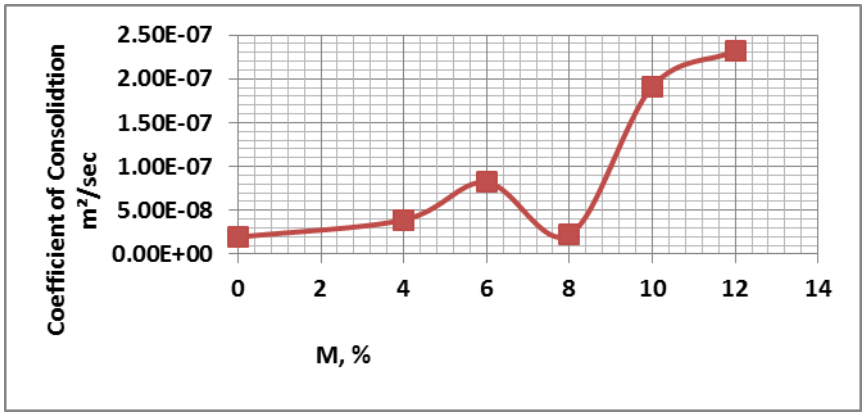

Figure 12. The effect of metakaolin on the coefficient of consolidation.

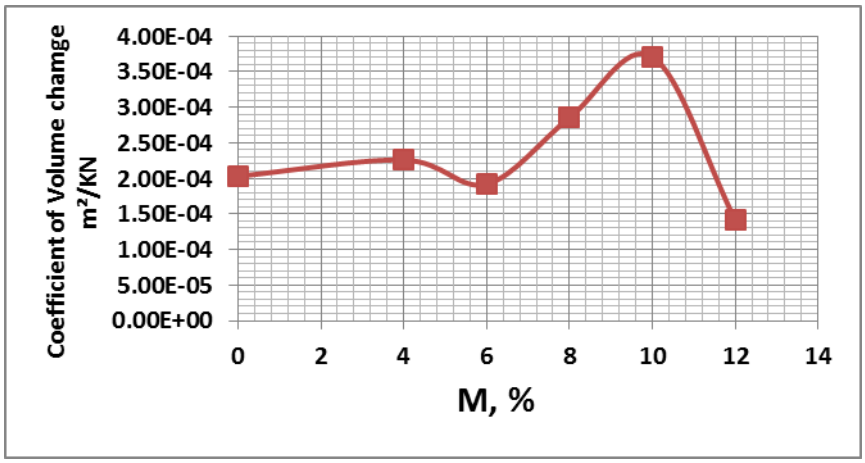

Figure 13. The effect of metakaolin on the coefficient of volume change.

Calibration and Verification of the Hydraulic Model for Blue Nile River from Roseires Dam to Khartoum City

Prof. Kamal edin ELsidig Bashar
Department of civil engineering
College of Engineering
Omdurman Islamic University, Sudan
E-mail:basharke@hotmail.com

Asst. Prof. Basim Hussein Khudair
Department of civil engineering
College of Engineering
University of Baghdad, Iraq
E-mail:basim22003@yahoo.com

Lect. Ghassn khalaf khalid
Department of civil engineering
College of Engineering
University of Diyala, Iraq
E-mail:ghassan75khalid@yahoo.com

ABSTRACT

This research represents a practical attempt applied to calibrate and verify a hydraulic model for the Blue Nile River. The calibration procedures are performed using the observed data for a previous period and comparing them with the calibration results while verification requirements are achieved with the application of the observed data for another future period and comparing them with the verification results. The study objective covered a relationship of the river terrain with the distance between the assumed points of the dam failures along the river length. The computed model values and the observed data should conform to the theoretical analysis and the overall verification performance of the model by comparing it with another set of data. The model was calibrated using data from gauging stations (Khartoum, Wad Medani, downstream Sennar, and downstream Roseires) during the period from the 1st of May to 31 of October 1988 and the verification was done using the data of the same gauging stations for years 2003 and 2010 for the same period. The required available data from these stations were collected, processed and used in the model calibration. The geometry input files for the HEC-RAS models were created using a combination of ArcGIS and HEC-GeoRAS. The results revealed high correlation ($R^2 > 0.9$) between the observed and calibrated water levels in all gauging stations during 1988 and also high correlation between the observed and verification water levels was obtained in years 2003 and 2010. Verification results with the equation and degree of correlation can be used to predict future data of any expected data for the same stations.

Keywords: calibration, verification, Blue Nile, Roseires dam, hydraulic model.

المعايرة والتحقق للنموذج الهيدروليكي لنهر النيل الأزرق من سد الروصيرص إلى مدينة الخرطوم

أ.د كمال الدين الصديق بشار
قسم الهندسة المدنية
كلية الهندسة/جامعة ام درمان الاسلامية،السودان

أ.م..د باسم حسين خضير
قسم الهندسة المدنية
كلية الهندسة/جامعة بغداد،، العراق

م.د غسان خلف خالد
قسم الهندسة المدنية
كلية الهندسة/جامعة ديالى،العراق

الخلاصة

يمثل هذا البحث محاولة تطبيقية للمعايرة والتحقق من النموذج الهيدروليكي لنهر النيل الأزرق حيث تمت إجراءات المعايرة باستخدام البيانات المرصودة لفترة سابقة ومقارنتها مع نتائج المعايرة بينما يتم التحقق مع مقارنة البيانات المرصودة لفترة أخرى في المستقبل، ومقارنتها مع نتائج التحقق. يغطي هدف الدراسة وجود علاقة مع تضاريس النهر والمسافة بين النقاط المفترضة من فشل السد على طول النهر. يجب ان تتوافق القيم المحسوبة من النموذج والبيانات المرصودة مع التحليل النظري وأداء

التحقق الشامل للنموذج من خلال مقارنتها مع مجموعة أخرى من البيانات. وتمت معايرة النموذج باستخدام البيانات من محطات القياس (الخرطوم، ود المدني، موخر سد سنار، موخر سد الروصيرص) خلال الفترة من 1 ايار الى 31 تشرين الاول 1988 اما التحقق فقد تم من خلال استخدام بيانات لنفس محطات القياس للسنوات 2003 و 2010 لنفس الفترة. البيانات المتاحة المطلوبة لكل من هذه المحطات تم جمعها ومعالجتها واستخدامها في معايرة النموذج. تم إنشاء ملفات الإدخال للنموذج HEC–RAS باستخدام مزيج من نظام ArcGIS و HEC–GeoRAS حيث أظهرت النتائج ارتباط عالية ($R^2 > 0.9$) بين مستويات المياه الحقلية والمعايرة في جميع محطات القياس خلال عام 1988 وكذلك ارتباط وثيق بين مستويات المياه الحقلية والمتحققة لنفس المحطات وانفس الفترة لعامي 2003 و 2010 وبذلك يمكن استخدام النموذج للتنبؤ بالبيانات المستقبلية لاي معطيات متوقعة لنفس محطات القياس.

الكلمات الرئيسية: المعايرة ، التحقق ، النيل الأزرق، سد الروصيرص، النموذج الهيدروليكي.

1. INTRODUCTION

The Calibration of a hydraulic model aims to reflect the field measurements of water bodies that are to be used in the prediction of the system performance and to evaluate alternative projects. While the verification is to ensure that the adjustments done during calibration are appropriate and the calibrated model will give reliable results ,**Victore, 1995**.

For low flow rates, Manning's roughness coefficient and the associated data are used in model calibration and validation processes. The achieved calibrated coefficients are then used with the high flow rates ,**Federal Highway Administration, 1984**. Friction and turbulent diffusion/dispersion coefficients are also important parameters in most hydraulic models that affect water surface elevation calculations, velocity and salinity distribution ,**Chao** and **Guofu, 2000**. **Ming-Hsi Hsu, et al., 1999** had used a vertical two-dimensional model on a branched estuarine river system to study calibration procedures and verification requirements. The barotropic flow simulation model was used to calibrate and verify the friction coefficient while a salinity distribution model was used to calibrate the turbulent diffusion and dispersion coefficients. They found a qualitatively agreement of the computed and measured residual currents with theoretical analysis. **Peter, 2009** found that storm water models application have important considerations in calibration and verification processes. An infinite number of combinations and permutations of parameters that directly affect the behavior of the model appeared. Hence the results may be complex and daunting when used to evaluate the effectiveness of altering parameters.

May, et al., 2000 indicated the validation of the Hydrological Engineering centers River Analysis System (HEC-RAS). The water surface profile of the model was compared with two study models of straight uniform reaches with two different flow rates**. Crampton, 2007** studied the dam's failure result in potential flood risks which are tougher and can behave differently from the events of natural floods by using the unsteady HEC-RAS models for dam break analysis. Careful modifications were required to converse from a steady state flood study model to a dynamic dam break model with consideration of the differences in flood routing methodologies between the two model states. Flood inundation maps are created from models which include peak elevation, flood wave arrival time and flood wave time to the peak for both sunny day and storm in progress failures. **Al-Kazwini, et al., 2009** studied AlHusa'chi River which is one of three main branches of Al Ka'hla River in Moissan Governorate, Iraq with a length of 25 km. They ran a steady one dimensional hydraulic model at a location 1.5 km upstream its tail to simulate the flow in the river using the HEC-RAS software. The field measurements were used in the calibration and verification processes to obtain the maximum allowable flow rates and water surface elevation in the river. **Khassaf and Ameera,**

2015 used HEC-RAS to develop the hydraulic model for Al- Kahlaa river system, south of Iraq using the observed weekly stage and flow data .The results showed that a good agreement is achieved between the model predicted and the observed data. The model demonstrated that in the case of high flow discharges, it is found that cross sections flooded are inadequate for such flows and the flows remained within the cross section extents during the drought season.

UNESCO-CWR, 2011 performed a field survey to supplement the available data and verify the accuracy of existing river cross-sections. The United States Corp of Engineers River Analysis System Model (HEC-RAS) was utilized to develop the hydraulic routing model for the Blue Nile River to reveal the shape of Roseires dam failure which covered the shape of the failure and its relationship with the dam height. It also included the capacity of the canal at the end of the dam. The objective of this study to evaluate the calibration and verification of the unsteady flow model through available field data for four gauging stations (Khartoum, Wad Medani, D/S Sennar, D/S Roseires) of Blue Nile River.

2. MATERIAL AND METHODS

2.1 Study Area Description

River Nile consists of three main tributaries, Atbara, White Nile and Blue Nile Rivers. The Blue Nile River system in this study covers about 76% of the total irrigated agriculture of the three Nile tributaries. **Fig.1** illustrates Blue Nile River system schematically of the study area ,**Ministry of Irrigation and Water Resources Sudan's, MOIWRS, 2014**. Blue Nile River has a major characteristic of a remarkable seasonality flow. More than 80% of the Blue Nile River flow is during the period from June to October, which is the flood period .Two Dams were built across the Blue Nile River, Sennar in 1925 and Roseires in 1966 ,**Ministry Of Irrigation Sudan, 1968.** The two dams control the flow, that irrigate about 1.134 million hectares of the Sudan agriculture area, as well as supplying more than 40% of the total hydropower generation in Sudan. The Roseires dam, which spans the Blue Nile River, is at 630 km upstream of Khartoum, it is 1000 m long and 68 m high concrete dam with the crest at 482.2 m amsl (above mean sea level). The dam was completed in 1966 with an initial capacity of 3.024 km^3 at level 480 m amsl to be used for irrigation water as the first priority, and hydropower generation as the second priority. The dam contains five deep sluices and a gated spillway, consisting of seven units, with a maximum discharge capacity of 16500 m^3/s at 480 m amsl. The hydro-electrical generation power approaches 212 MW. Sennar Dam is the second dam on the Blue Nile River near Sennar Town, as shown in **Fig. 2**. It was built by the British engineer, (desert explorer and adventurer), Stephen "Roy" Sherlock, under the direction of Weed man Pearson. The dam is 3025 meters long, with a maximum height of 40 meters. It provides water for crop irrigation in the Gezira scheme. ,**UNESCO-CWR, 2011 and ENTRO 2013**.

2.2 Requirements and Data Collection

Analysis of the system requires upper boundary conditions that specifies the inflow to the system which is considered as lateral inflow hydrograph. Eddiem gauging station, 170 km upstream Roseires dam observes the flow which is used as the upper boundary condition. The downstream boundary condition at Khartoum was taken as the downstream end of the study area which was considered the normal depth. The effects of Rahad and Dindir Rivers, the tributaries of the Blue Nile River were accounted as lateral inflows at their respective confluences with the Blue Nile River. In addition nine internal boundary conditions were observed stages, flow hydrographs at upstream, flow hydrographs at downstream of the two reservoirs, Roseires village, Wad Alaies village in the Roseires-Sennar reach, Wad Medani, Kamlin, and Soba in Sennar-Khartoum reach. **Fig. 3** shows location and type of each flow gauging station for

modeling purpose. The required available data for each of these stations were collected by the Ministry of water resources and electricity. These data were processed and used in the model calibration, **Dam Implementation Unit, 2012, Sudan**.

3. HEC-RAS MODEL APPLICATION METHOD

The geometry input files for the HEC-RAS models were created using a combination of ArcGIS and HEC-GeoRAS. The Blue Nile River centerline, bank lines, flow paths, and cross sections were digitized in HEC-GeoRAS. The Blue Nile River centerline was digitized to similitude the proposed field channel centerline as indicated by the field survey. This was necessarily supplemented by reference to satellite images. The bank lines represented the point where the river was considered as a flood plain and the Blue Nile River was accessing its flood plain for active flow. In addition, these lines determine the change in Manning's roughness coefficients (n) in the hydraulic model and the possibility to be adjusted in the model ,**Federal Highway Administration, 1984**,. The channel bank lines were also digitized using the field survey as a reference. Three flow path lines were setup in HEC-GeoRAS to represent the direction of flow within the channel centerline and banks in the left and right flood plains. These lines also determine the cross sections limits of the stations together with the right and left overbank flow between these cross sections. Finally, the cross sections were oriented perpendicular to the flow and located to represent areas in the reach where physical changes occur ,**HEC-RAS, 2005 and USGS, 2004**.

The steps followed in configuring the HEC-RAS Model for the Blue Nile River could be summarized as follows ,**HEC-RAS, 2005**.

Step 1: Validate geometric data and time series to be used in the model

a- Pre-process time series data using HEC-DSS (Data Storage System) to check for missing data, unit conversion and create an input time series file in DSS format.

b- Pre-process geometric data with the aid of ARC-GIS and Excel, to establish Left Over Bank (LOB), Right Over Bank (ROB) locations for each section, and decide on in-effective areas to be included as part of each section. This also includes decision on roughness coefficients, contraction and expansion coefficients. The purpose of this is to examine the coverage of the field surveyed cross-section and establish the need for modeling meandering effect and bend for certain reaches in the HEC-RAS model.

Step 2: Configure the River basin schematically and input geometric data for the Blue Nile River:

a- Using the geometric data editor in HEC-RAS establish the connectivity and draw the schematic river basin for the Blue Nile River.

b- Enter the reach length for the LOB, ROB for the channel.

c- Enter Station - Elevation data for each cross section.

d- Establish the frictional loss coefficient, expansion and contraction loss coefficient for each cross-section.

Step 3: Determine the initial condition for the model by running HEC-RAS under steady state version.

Step 4: Establish upstream and downstream boundary conditions. The upstream boundary condition is chosen as the daily time series discharge hydrograph at Eddiem station and the downstream boundary condition is taken as the rating curve for Khartoum Station.

Step 5: Perform Unsteady State Simulation.

a- Decide on the time step used for the simulation (1 hr)

b- Decide on the time step used in producing the output results (1 Day).

4. RESULTS AND DISCUSSION

Hydraulic models are used to estimate hydraulic characteristics of the flow in the rivers and channels that would result from passing the discharge through them. Running a steady state model may take seconds, while unsteady flow simulations can take many hours. The results of a model are validated by calibrating one or more known events. Observed points can be entered into the model as inputs for direct comparison with prototype results. The scaled model output should match the prototype output observed points. To arrive at a fully calibrated model the input that has the most uncertainty must be adjusted. Once the digitization process is complete, the HEC-GeoRAS data are imported into HEC-RAS. The transition between the pre-processor and the hydraulic model should be smoothened. The results identical to that created in the pre-processor were visualized in the model presentation, as shown in **Fig. 4**.

One of the main challenges of hydraulic modeling in areas with broad flood plains adjacent to rivers are to represent accurately the conveyance of water and the extent of inundation through hydraulic connections with the river channel. In many cases, there is a direct and continuous connection between the river and the flood plains. In other cases, there is an interruption in the water surface. For the flow to access a floodplain area beyond a high point in the topography, it must be accessible to the main channel or another area of the floodplain from either an upstream or a downstream cross section. This can best be determined through an iterative process of simulating the flow, generating an inundation map, and then adjusting hydraulic constraints in the model to limit or extend flow to areas that can be observed as hydraulically connected. **Fig. 5** and **Fig. 6**, show the relationship between cross sections and inundated areas for connected and disconnected flow areas. They also demonstrate how inundation mapping can provide guidance on placement of hydraulic model constraints. The hydraulic model builders use judgment to define three conditions. The first case is when the levees flow does not enter the flood plain until it exceeds the height of the levee. The second case is when the flow is not simulated. The third case when there are ineffective flow areas that may be inundated but do not contribute to conveyance in the river system ,**HEC-RAS, 2005 and HEC, 1995**.

The model was calibrated using data of each stations (Khartoum, Wad Medani, downstream D/S Sennar, D/S Roseires) during the period from the 1st of May to 31st of October1988.The results of the model are shown in a comparative manner in **Figs. 7a to 10 b**. The results revealed high correlation ($R^2 > 0.9$) between the observed and calibrated water levels in all gauging stations. The verification was done using the data of the same gauging stations in years 2003 and 2010 for the same period. The results of the model are shown in a comparative manner in **Figs. 11a to 14b**. Also high correlation ($R^2 > 0.9$) between the observed and verification water levels was achieved. Verification model performed by comparing the results derived and observed data to predict the equation and degree of correlation, also can be used for future prediction. The study revealed the relationship with the terrain of the river and the distance between the gauging stations of the dam failure on the rivers length. Also it was clearly observed in the downstream direction where terrain became higher there was no effect on both bank sides.

6. CONCLUSION

The HEC-RAS models were used to evaluate the calibration and verification of the unsteady flow model through available field data for four gauging stations (Khartoum, Wad Medani, D/S Sennar, D/S Roseires) of Blue Nile River. The results of the model showed:

1. The study revealed the relationship with the terrain of the river and the distance between the gauging stations of the dam failure on the rivers length. Also it was clearly observed in the downstream direction where terrain became higher there was no effect on both bank sides.
2. High correlation ($R^2 > 0.9$) between the observed and calibrated water levels in all gauging stations during 1988.
3. High correlation ($R^2 > 0.9$) between the observed and verification water levels for years 2003 and 2010.
4. Verification results with the equation and degree of correlation can be used to predict future data for same stations.

ACKNOWLEDGMENT

The authors would like to express their deep appreciation and gratitude to **Sudan and Egyptian Irrigation Centers** for the distinguished efforts and for applying the required data for the models.

REFERENCES:

- Al-Kazwini, Muhannad J., Al Saady, Ali S. and Numa, Ala'a H., 2009, *Developing the Discharge Capacity of Al Husa'chi River*, Eng. & Tech. Journal ,Vol. 27 , No. 2.
- Chao Wu and Guofu Huang, 2000, *Theoretical Solution of Dam-Break Shock Wave*, Journal of Hydraulic Engineering, Vol. 125, No. 11, PP.1210-1215.
- Crampton, Sam, 2007, *HEC-RAS Dam Break modeling of Gwinnett County's NRCS Facilities*, Proceeding of the 2007 Georgia Water Resources Conference, held March 27-29, Athens, University Of Georgia.
- Dam Implementation Unit, 2012, Sudan.
- Eastern Nile Technical Regional office (ENTRO) 2013.
- Federal Highway Administration, 1984, *Guide for Selecting Manning's Roughness Coefficients for Natural Channels and Flood Plains*, Report No. FHWA-TS-84-204, McLean, Virginia.
- HEC (Hydrologic Engineering Center, RD-42), 1995, *Flow Transient in Bridge Back water Analysis*, U.S. Army Croup of Engineers, Davis, California.
- HEC-RAS River Analysis System, 2005, *Hydraulic Reference Manual*, Version 4.1.0, U.S. Army Corps of Engineers Hydrologic Engineering Center, Davis, California.
- Khassaf , Saleh I. and Ameera Mohamad Awad, 2015, *Mathematical Modeling of Unsteady Flow for AL- Kahlaa Regulator River*, IOSR Journal of Engineering, Vol. 05, Issue 02, ||V2|| PP 09-20.

- May, D.R., Lopez, A., Brown, L., 2000, *Validation of the Hydraulic–open channel Flow Model HEC-RAS with observed data*.

- Ming-Hsi Hsu, Albert Y. Kuo, Jan-Tai Kuo, and Wen-Cheng Liu, 1999, *Procedure to Calibrate and Verify Numerical Models of Estuarine Hydrodynamics*, Journal of Hydraulic Engineering, Vol. 125, No. 2, pp. 166-182.

- Ministry Of Irrigation Sudan, 1968, *Manual of irrigation in Sudan*.

- Peter, J. Singhofen, 2009, *Multiple Ponds in Close Proximity Using ICPR, Modeling Percolation from Multiple Ponds in Close Proximity Using ICPR*" Proceed at the 25th Annual ASCE Water Resources Seminar in Orlando, Florida and at an ASCE Suncoast Branch Water Resources Luncheon.

- UNESCO-CWR, 2011**,** *Chair in Water Resources Omdurman Islamic University, Sudan*.

- USGS (United State Geological Survey), 2004, *Shuttle Radar Topography Mission (SRTM)*, Internet Web Site, http://edcsns17.cr.usgs.gov/srtmbil/ 8/9/2007.

- Victore, E., 1995, *Assessing The Threat To Life From Dam Failure*, Water Resources Bulletin,

Figure 1. Blue Nile River system schematic in the study area.

Figure 2. Location of the Sennar dam within Blue Nile River.

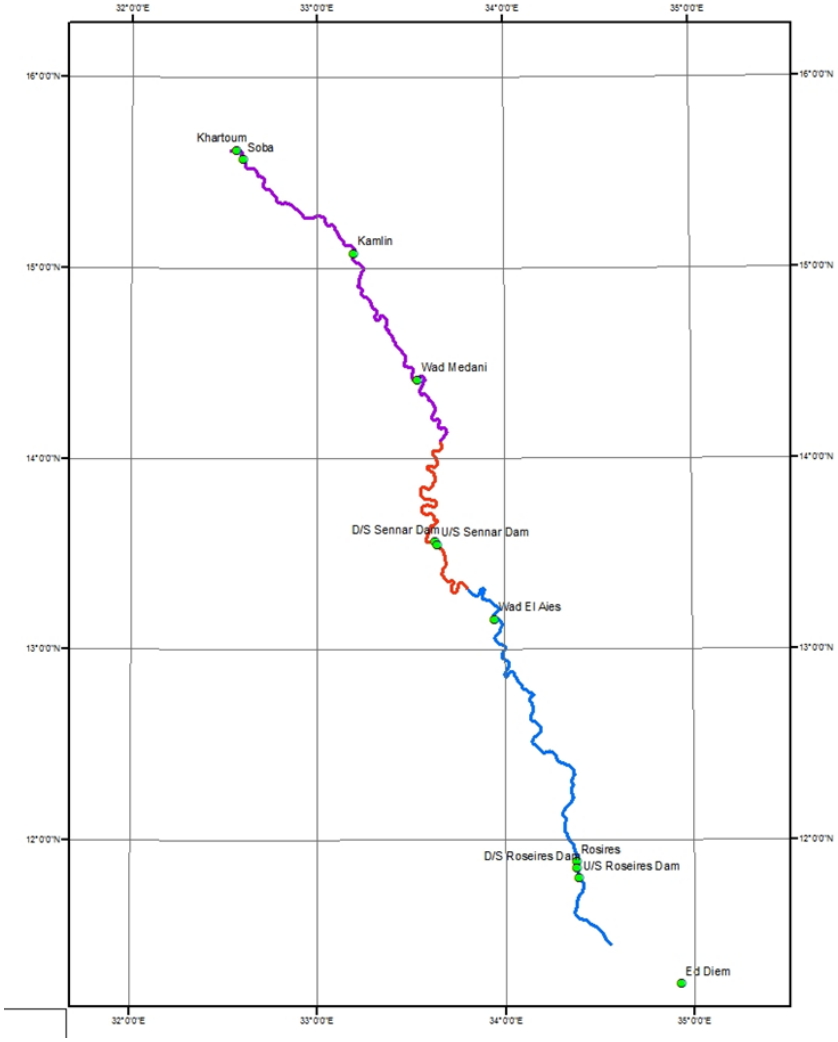

Figure 3. Location and type of each flow gauging station for modeling purpose.

- Structures (Internal Boundaries
- Lateral Inflow Hydrograph Points
- Internal Observation Points
- Normal Boundary Condition Point

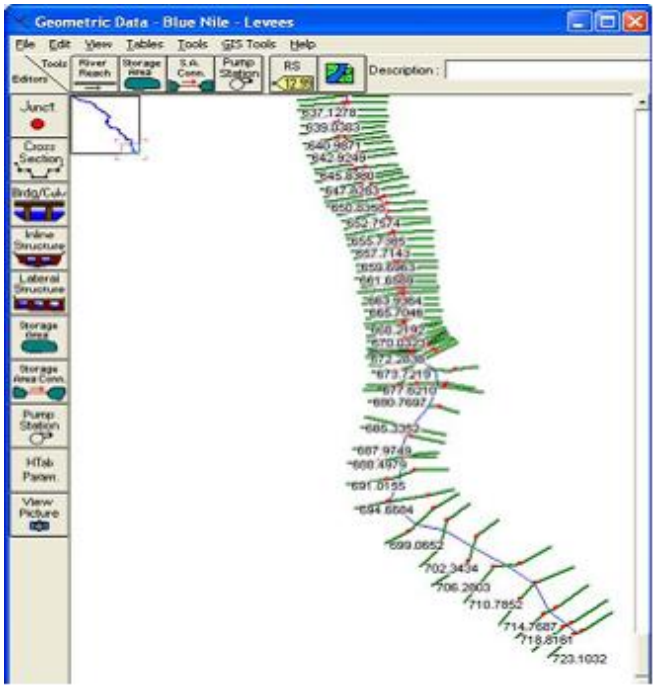

Figure 4. Illustration of HEC-RAS model development.

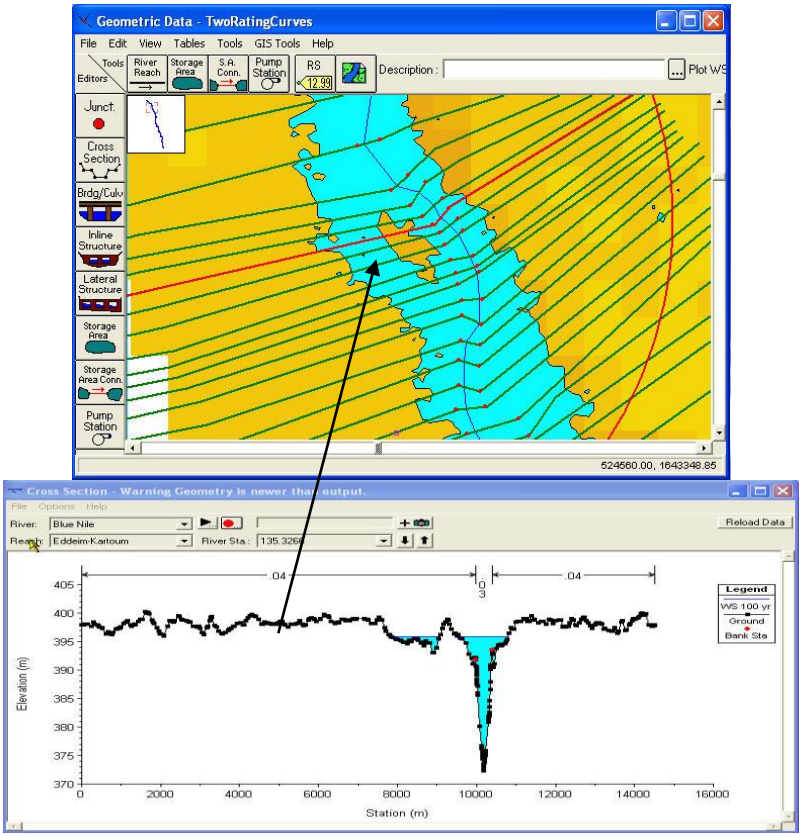

Figure 5. Example of hydraulic connected area.

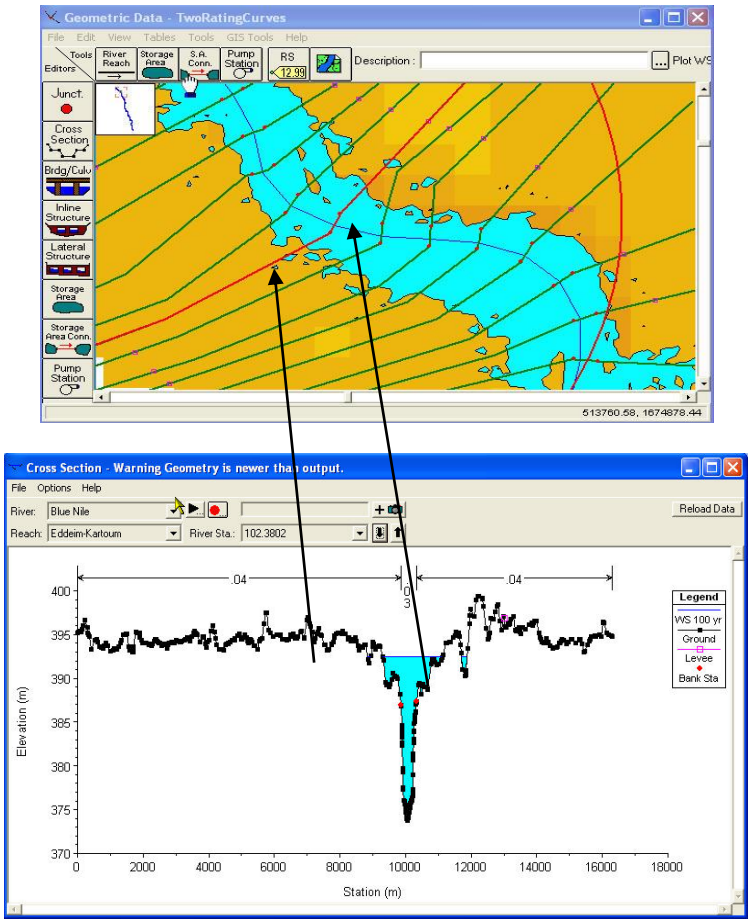

Figure 6. Example of a lack of hydraulic disconnected area.

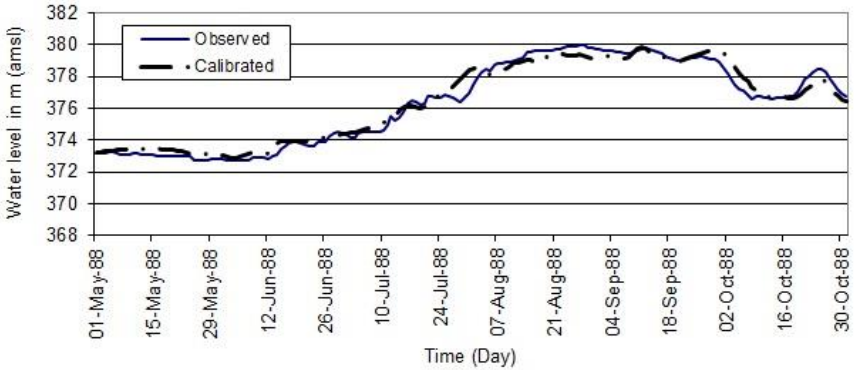

Figure 7a. HEC-RAS forecast calibration for Khartoum, 1988.

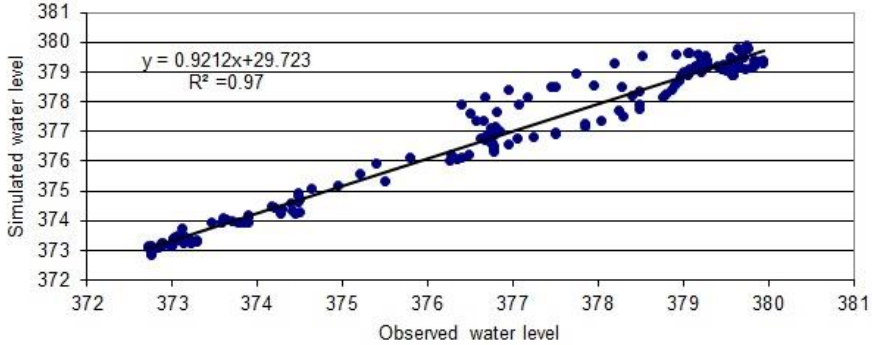

Figure 7b. HEC-RAS calibration-observed flows for Khartoum, 1988.

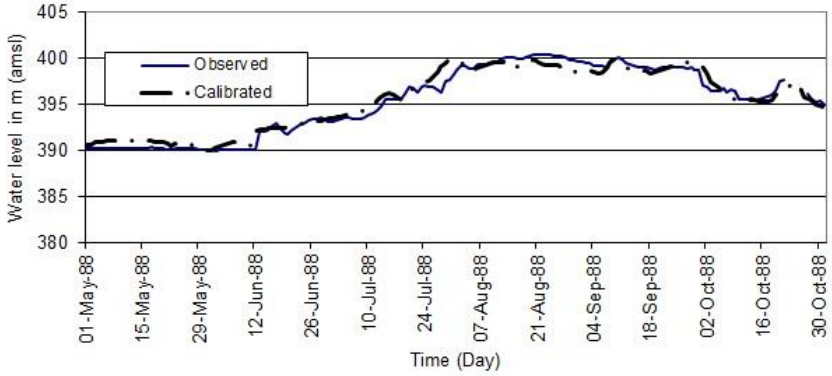

Figure 8a. HEC-RAS forecast calibration for Wad Medani, 1988.

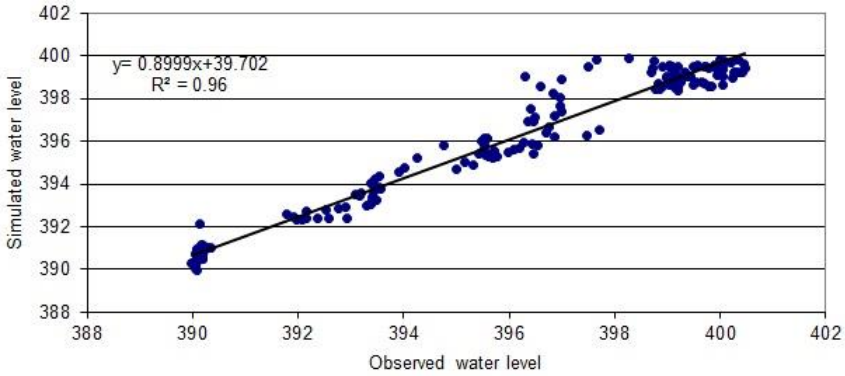

Figure 8b. HEC-RAS calibration-observed flows for Wad Medani, 1988.

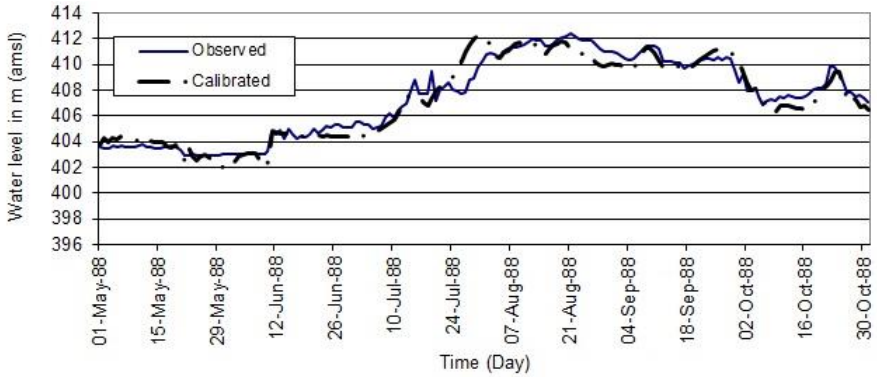

Figure 9a. HEC-RAS forecast calibration for D/S Sennar, 1988.

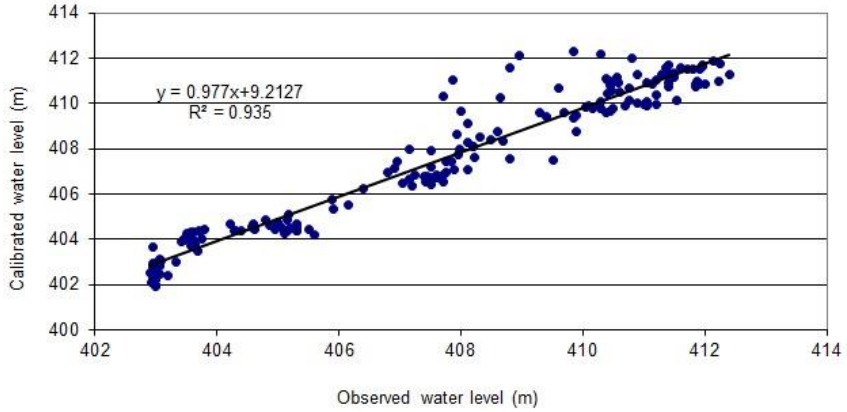

Figure 9b. HEC-RAS calibration-observed flows for D/S Sennar, 1988.

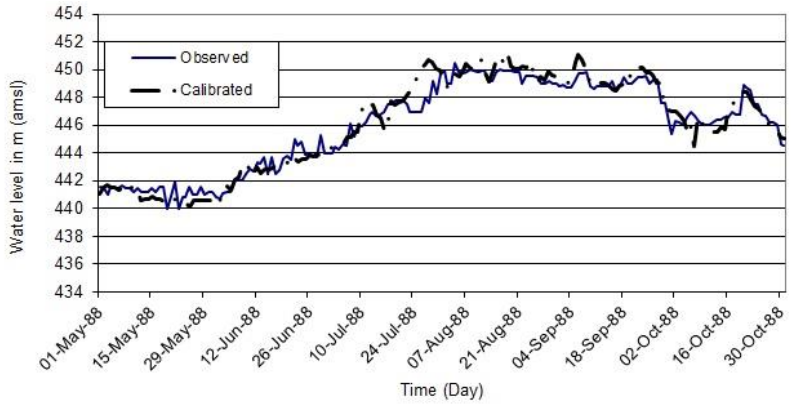

Figure 10a. HEC-RAS forecast calibration for D/S Roseires, 1988.

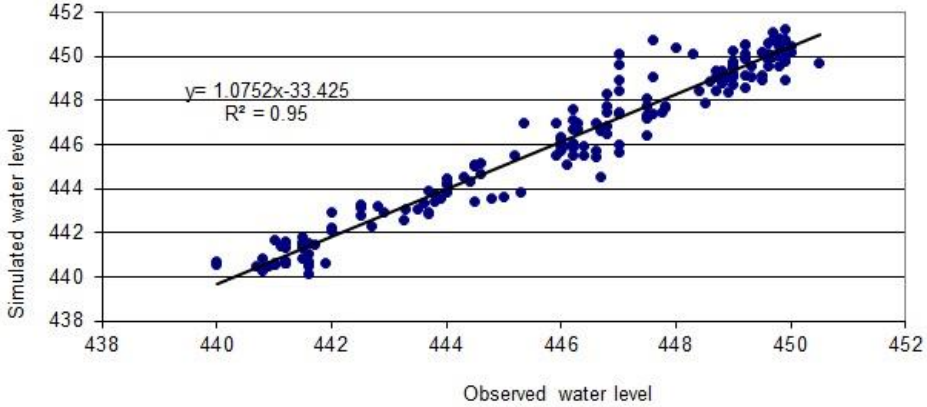

Figure 10b. HEC-RAS calibration-observed flows for D/S Roseires, 1988.

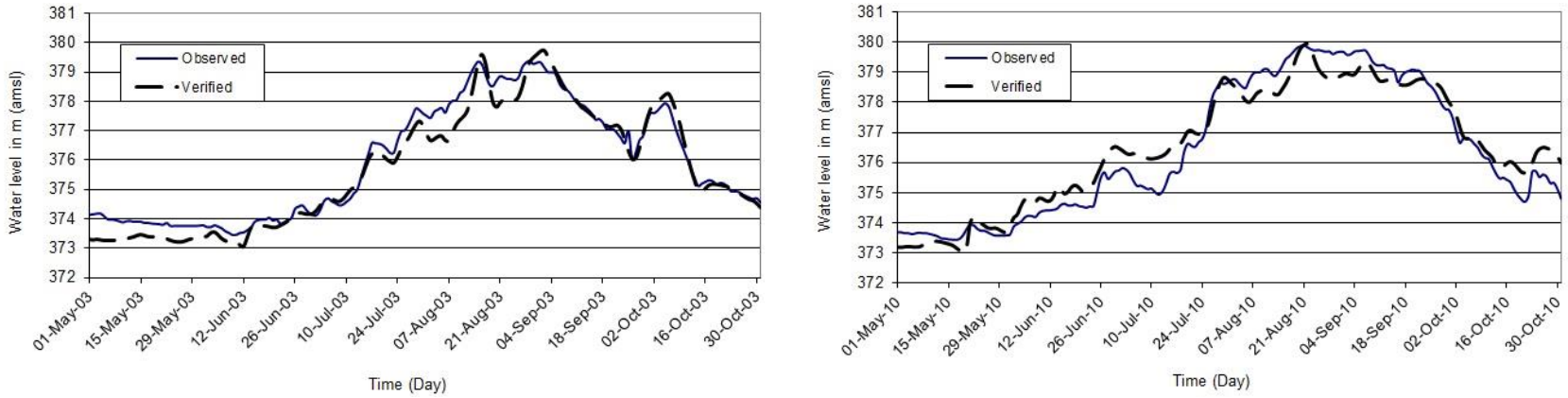

Figure 11a. HEC-RAS forecast verification results for Khartoum during 2003 and 2010.

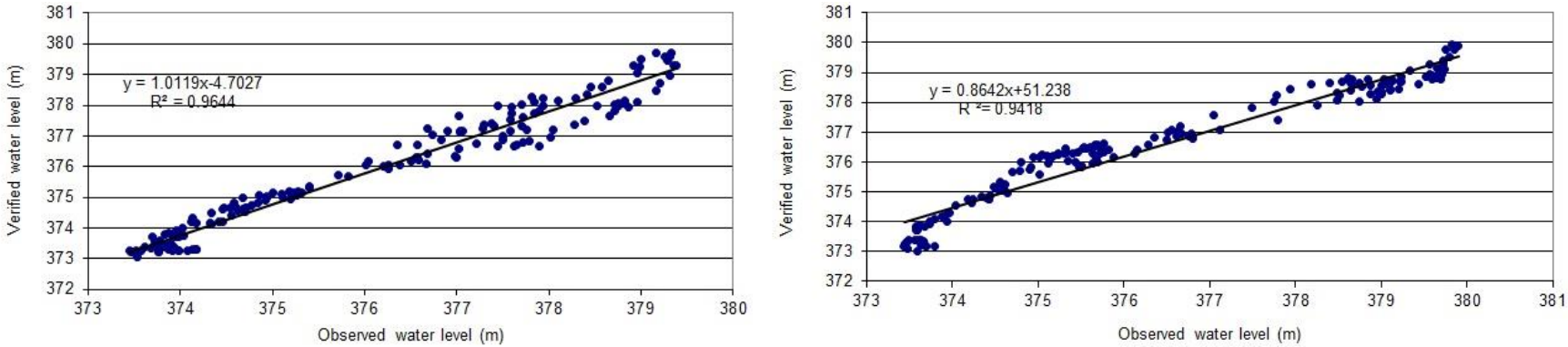

Figure 11b. HEC-RAS verification- observed flows results for Khartoum during 2003 and 2010.

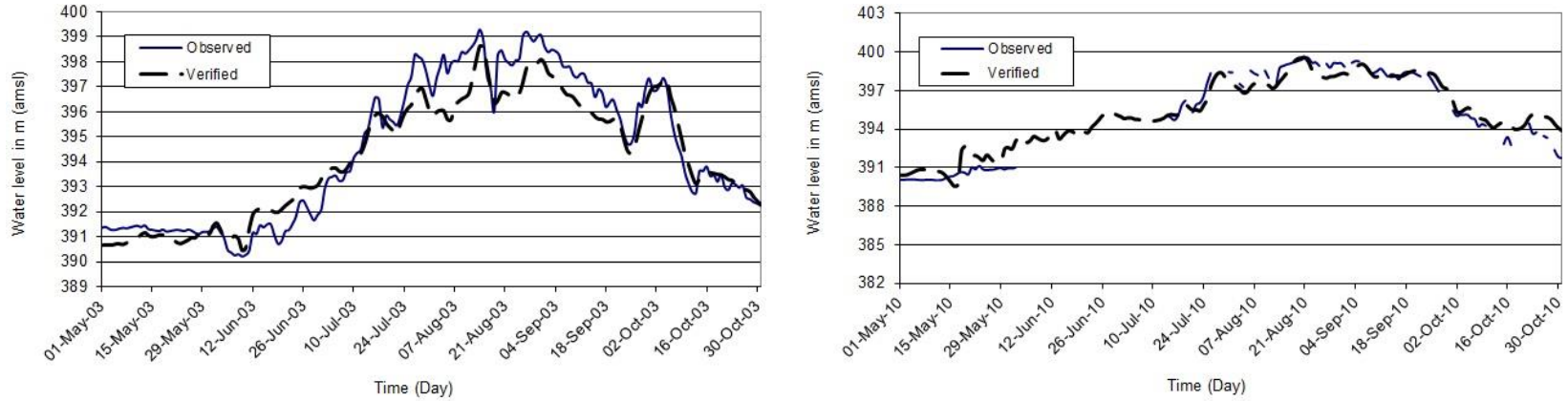

Figure 12a. HEC-RAS forecast verification results for Wad Medani during 2003 and 2010.

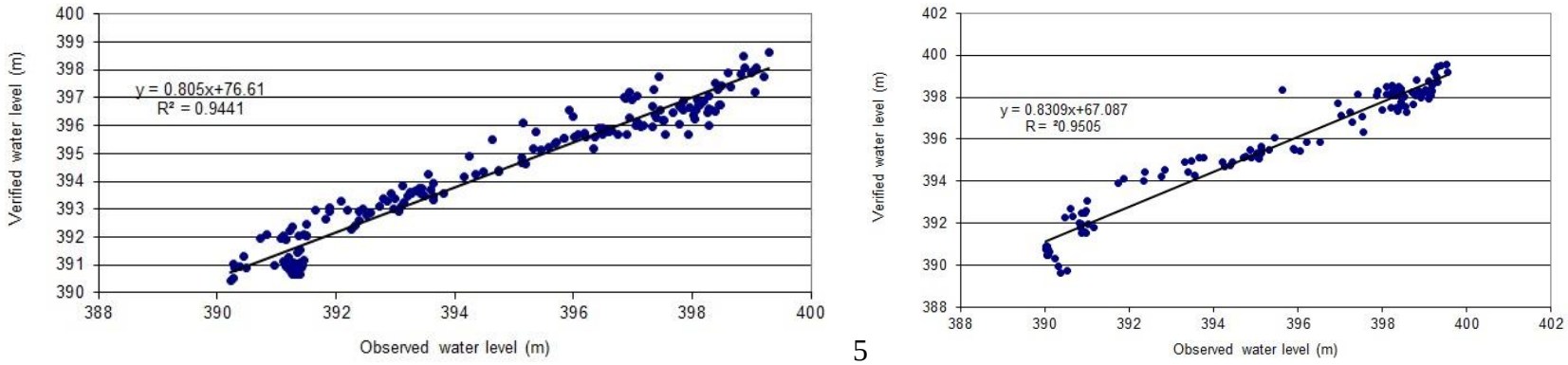

5

Figure 12b. HEC-RAS verification-observed flows results for Wad Medani during 2003 and 2010.

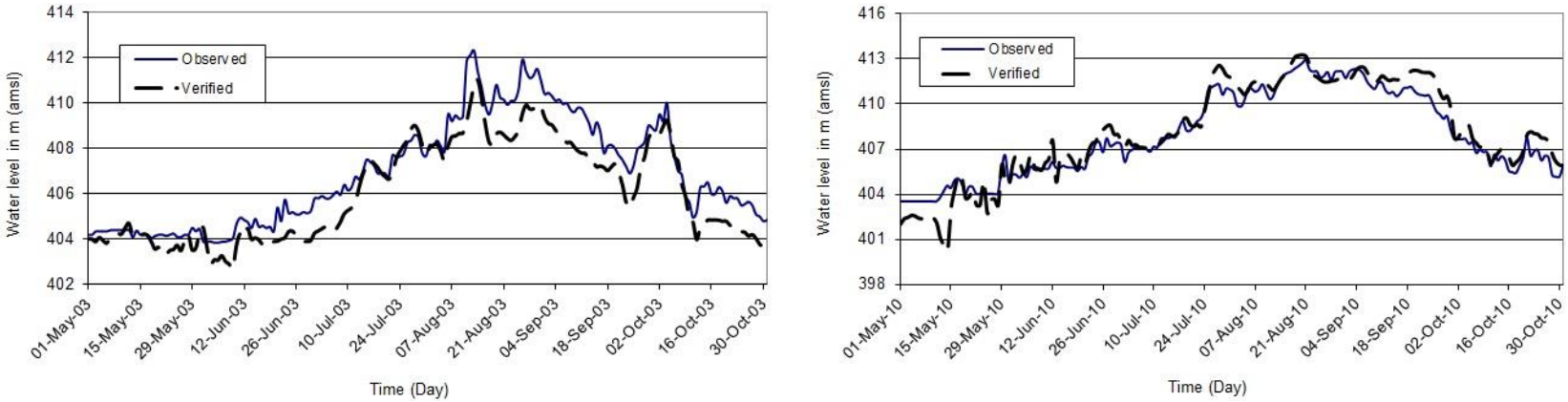

Figure 13a. HEC-RAS forecast verification results for D/S Sennar during 2003 and 2010.

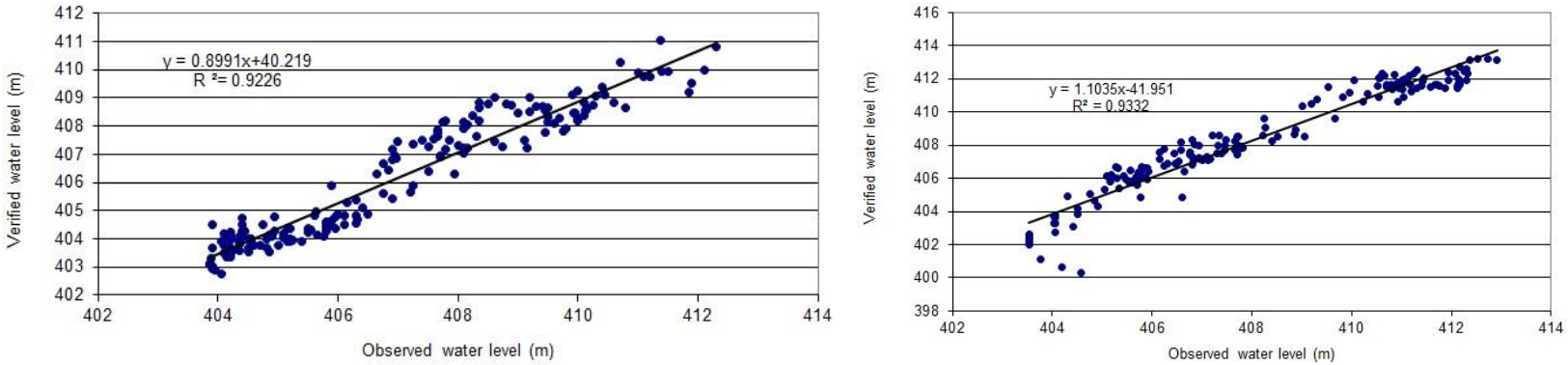

Figure 13b. HEC-RAS verification-observed flows results for D/S Sennar during 2003 and 2010.

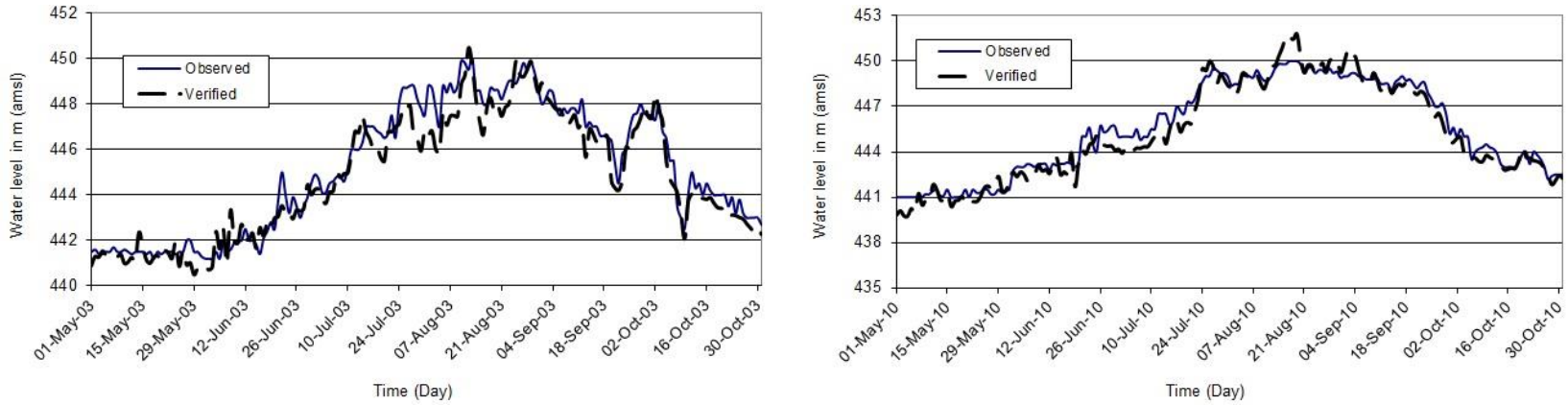

Figure 14a. HEC-RAS forecast verification results for D/S Roseires during 2003 and 2010.

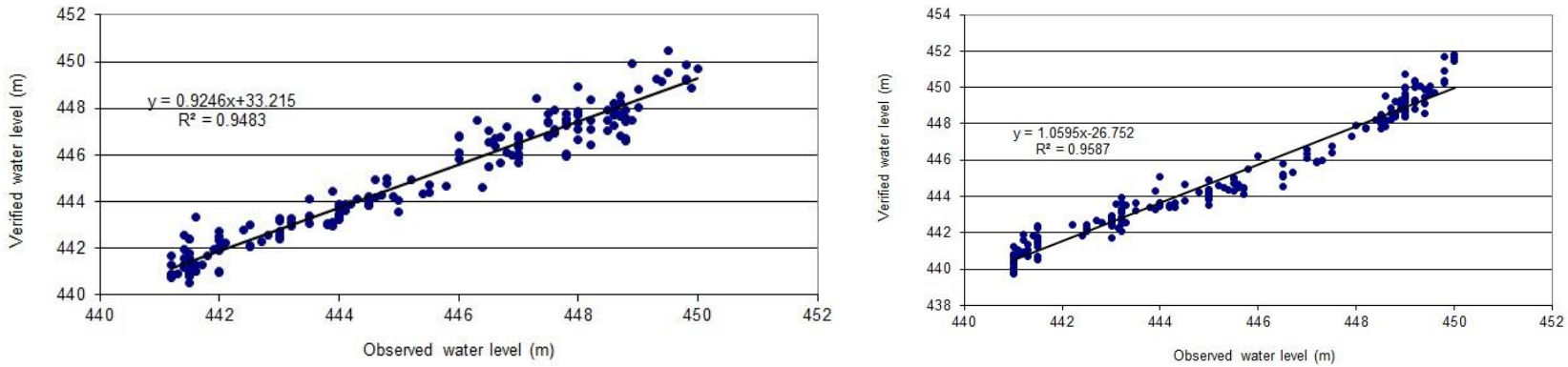

Figure 14b. HEC-RAS verification-observed flows results for D/S Roseires during 2003 and 2010.

The Role of Transition of Workforce between Companies in Transferring Technology

Asst. Prof. Dr. Sedki Esmaeel Rezouki
Department of Civil Engineering College of Engineering- University of Baghdad
Email: sedki_razqi@yahoo.com

Lect. Dr. Ibrahim Fadhil Muhsin
Department of Engineering Affairs
University of Baghdad
Email: ebraheemfad363@yahoo.com

ABSTRACT

The transition of professionals between different sectors is considered as one of sources of acquisition of technology and will lead to add the practical experience to them. This experience depending on different factors like: the scientific degree and practical experience by the professionals, the technology possessed by the transferor sector, the duration that spent by experienced in transferor sector, the type of work performed by professional….etc.
The research aims to verify the affect of these factors in technology transfer process.
Research reached that the technology transfer process which is depending on the Iraqi competencies in work is unsatisfied level between Iraqi organizations because there are different obstacles behind this. Research diagnosed such obstacles as well as the procedures that followed-up by professionals to serve this process.
Key words: technology transfer, foreign company, public sector, private sector.

دور انتقال القوى العاملة بين الشركات في نقل التقنية

أ.م.د. صدقي إسماعيل رزوقي
قسم الهندسة المدنية
جامعة بغداد/ كلية الهندسة

م.د. إبراهيم فاضل محسن
قسم الشؤون الهندسية
جامعة بغداد

الخلاصة

يعد انتقال المهنيين بين مختلف القطاعات كأحد مصادر الحصول على التقنية ويؤدي إلى إضافة الخبرة العملية لهم. هذه الخبرة تعتمد على عوامل مختلفة مثل: الدرجة العلمية والخبرة العملية من قبل المهنيين، والتقنية التي يمتلكها القطاع الناقل، والمدة التي يقضيها ذوي الخبرة في القطاع الناقل، ونوع العمل المنجز من قبلهم ... الخ

يهدف البحث للتحقق من تأثير هذه العوامل في عملية نقل التقنية. لقد توصل البحث إلى أن عملية نقل التقنية المعتمدة على الكفاءات العراقية في العمل بمستوى غير مرضٍ بين المنظمات العراقية لأن هناك عقبات مختلفة وراء ذلك. شخص البحث هذه العقبات، فضلا عن الإجراءات التي قام بإتباعها المهنيين التي تخدم عملية نقل التقنية.

- **الكلمات الرئيسة :** نقل التقنية ، الشركة الأجنبية, القطاع العام, القطاع الخاص.

1. INTRODUCTION

The scientific and technical communication became today a justified subject, so Iraqi companies have to work on investigating and exploring the continued progress of this important industry in economics.

Workforces have role in technology transfer and could be achieved into two main factors by training the workforces either in the workplace or outside it, as well as encouraging the movement of professionals between different sectors, and this improves the exchange of experiences between workforces that need it. This paper focuses on the second factor in transition of professionals.

2. DEFINITION OF TECHNOLOGY TRANSFER

Analyzing technology transfer is difficult, in part because of numerous conceptual and measurement problems in defining technology, understanding the many concurrent processes in its transfer, and conceptualizing and measuring the impacts of technology transfer, **Rubenstein and Heisey,2005**.

Before understanding the term of (Technology Transfer), it is necessary to identify separately each of Technology and Technology Transfer.

2.1 Definition of Technology

Technology is defined as: 1. the science or study of the practical industrial arts; 2. the terms used in a science, technical terminology; 3. applied science, **Bozeman,2000.**

Technology "can be broadly defined as the process of acquisition, adaptation, integration and use of technological knowledge by a nation other than the one that develops the technology and has different political, economic, social, and cultural contexts, **Salem,2011.**

Technology is indeed an interdisciplinary area covering the broader (comprehensive) conceptual framework of scientific, managerial and engineering aspects of knowledge. Therefore, technology can be defined as a study of how humans use the environment to meet their needs, **Tesfayohannes and Temtime, 2002.**

2.2 Definition of Technology Transfer

Technology transfer can be defined in different approaches based on adaptability and utilization for specific purposes.

Technology transfer should be seen in terms of achieving three main objectives: first, introduction of a new technology by investing in new products, improvement of existing techniques and generation of a new knowledge **Vutsova and Ignatova,2013**.

Through technology transfer, ideas and skills could be shared between countries, thus increasing the stock of ideas in the receiving country and reducing the idea gap, **Murshid,2014.**

Or the concept of technology transfer is defined as the process through which technological know-how is adopted by the user through practices that improves and enhances the performance or delivery requirements of an enterprise or an individual, **Ashekele and Matengu, 2008.**

3. METHODS OF TECHNOLOGY TRANSFER

Below are three approaches for selecting a knowledge transfer method.

☒ Select a knowledge transfer method by user needs - can be used when an individual, team, or organization has specific needs in mind.

☒ Select a knowledge transfer method by context and types of knowledge—can be used when an individual, team, or organization has a specific type of knowledge to be transferred.
☒ Select a knowledge transfer method by level of experience - can be used when the potential receiver of the knowledge has a specific level of experience, **Piktialis and Greenes ,2008.**
☒

3.1 Element of Technology Transfer

Three elements of technology transfer: hardware, know-how and know-why, **Memo,2000.**
The three types of flows identified in the above definition are in the literature on technology transfer usually termed:
(1) **Hardware:** equipment, machinery, capital goods, product design etc.
(2) **Know-how:** Competence and skills to absorb and adapt techniques to local circumstances, to fulfill intended tasks.
(3) **Know-why**: Ability to generate and manage technological change.

3.2 Role of Human in Technology Transfer

The empirical studies show "that more highly-educated individuals tend to adopt innovations earlier and implement and adapt them sooner than less-educated individuals". This applies both to the consumption of new technologies. More educated and skilled workers are argued to have greater 'functional flexibility' in that their greater stock of knowledge increases the rate at which they learn and develop higher order problem solving skills, **Toner,2011**.
Technology and knowledge may also be transferred through the movement of people –employees, **Wahab et al.,2012.**
Human capital is an essential element of the technology transfer process, **IFPMA, 2011.** The successful absorption of technology or know-how in the recipient country and its translation into greater economic development hinges on the availability in the host country of an educated workforce with, for example, engineering and management skills.
People are the key to successful technology transfer, **Willis and Ashworth,2002:** as people and not papers transfer technology. This implies that the people in the transfer process have to be:
➢ informed about the process
➢ consulted about their needs, concerns, perceptions, attitudes and expectations
➢ trained/mentored to understand and utilize the technology to its fullest extent.

3.2.1 How skill and knowledge are being transferred

The collaborations with foreign firms had a positive impact on the efficiency and productivity of employees, **Murshid,2014.** There are different ways for achieving knowledge for instance:
▪ Labor turnovers: Labor turnover occurs when workers trained by foreign firms or managers transfer their knowledge to other firms when switching employers.
▪ Labor spin-offs: Labor spin-offs happen when an employee of a foreign firm starts up a new firm based on the know-how gained from previous experience, **Murshid,2014.**

3.2.2 How to improve the employees' skills

The benefits of training and education not only accrue to the individuals receiving the training, but also to the firms that employ the workers and the economies in which the workers are employed, **Rounds,2013**.

❖ Firms that implement employee training programs increase their labor productivity and can eliminate productivity gaps with competitors.

❖ Countries that provide quality education and job-training programs that improve the skills of their workforce tend to have more economic growth and higher levels of economic development than those that do not.

Developing countries, **Ogunade,2011** have over time, adopted myriad strategies to train and develop their workforces to meet global economic challenges and rise out of the cycles of low skills and poverty.

Over the last decade, companies have changed how they tap into the extended workforce. Initially, they did so as a tactical response to an immediate need. But then they began making this workforce a key component of corporate strategy. This shift has enabled organizations to achieve two of the most sought-after competitive capabilities: agility in the face of a highly turbulent business environment and access to high-performing, highly skilled talent, **Silverstone et al., 2015.**

The outcomes of employee's ability and motivation, **Omar et al., 2011** would influence the measurement on the absorptive capacity of TT in the form of knowledge, skills and tools into organizations via construction projects. Knowledge, skills and tools could be transferred and shared among employees and extensive intra organizational communication is likely to contribute to employees' motivation.

4. TACIT AND EXPLICIT KNOWLEDGE

As mentioned in technology transfer definition previously for transferring the ideas, skills and information, so there is a connection and a strong relationship between the technology and achieved knowledge. It is necessary to distinguish the types of acquired technology depending on kinds of knowledge; there are two major types of technologies: Tacit Knowledge and Explicit Knowledge

Tacit Knowledge: in a practical direction, segmenting it into two dimensions, technical and cognitive. Technical dimensions encompass craft and skills captured in concrete 'know-how' exemplified by the master craftsman who is often unable to articulate what he or she knows. 'Knowhow' cannot always be codified since it often has important tacit dimensions, **Kakabadse et al., 2001.**

Tacit knowledge refers to the undocumented and unarticulated (but nevertheless important) knowledge held by practitioners. It is also known as "inarticulate intelligence," "collective wisdom," or "elusive knowledge." The phrase "tacit knowledge" an influential of epistemology, but in recent years it has been used by management theorists as a key piece in the process of knowledge management. Tacit knowledge is contrasted with explicit knowledge, which is expressed knowledge that is communicated to others. When explicit knowledge is documented, it becomes "codified."

Codified knowledge is usually quite structured and appears in written reports, databases, and other media, **Stover-2004.**

On another word the major difference between them defines as follows, **Smith-2001**: Tacit knowledge is technical or cognitive and is made up of mental models, values, beliefs, perceptions, insights and assumptions. Technical tacit knowledge is demonstrated when people master a specific body of knowledge or use skills like those gradually developed by master craftsmen.

Most explicit knowledge is technical or academic data or information that is described in formal language, like manuals, mathematical expressions, copyright and patents. This ''knows-what,'' or systematic knowledge is readily communicated and shared through print, electronic methods and other formal means.

5. DATA COLLECTION

According to hypothesis of this paper of the important role of the human capital for transferring technology, so this paper has guessed the greatest role will be done by human capital in this process.

The questionnaire was prepared for different purposes including the role of human capital in case of professionals' transition between different sectors and the importance level of this transition for transferring technology.

5.1 Size and Nature of Specimen: The specimen has different jobs, specializations, scientific degrees, practical experiences as well as they are working in different sectors either public or private sectors. **Table 1** describes these characteristics. This variety in this specimen will provide a good chance for verifying their responses in this matter as follows:

1- The scientific degree possessed by respondent has the greatest level for enable to evaluating the types and importance of technology or for the best utilizing it.

2- The practical experiences possessed by respondent; this experience can evaluate the advanced technology for executing the project.

3- The Nature of job occupied by respondent, this reflect the complexity of technology needed and seeking for utilizing the adequate technology.

4- The ready to accept or to be familiar with on technology and willing to transfer it to other

Table 1 shows the different of specializations for respondents as well as the different occupied sectors either public or private.

In additional to classification mentioned above, research has used the other categories depending on Engineering Ranks and Functional Ranks: their practical experiences or the practical title regarding to numbers of years in their job. In other hand the other category is used according on the classification of Iraqi Engineers Union, this classification was used for two reasons the first; it should be depended on years of achieved the specialty, second; the research assumes this party has to take its role for improving the professionals technical skills and knowledge. **Fig. 1** describes the last two classifications. The functional description has (7) seven degrees: An expert, Senior of Chief of Engineers, Chief of Engineers, Assistant Chief of Engineers, Senior Engineer, Engineer and Assistant Engineer.

5.2 Transition of Professionals: Fig.2 shows the transition (movement) of professionals from public to private sector or vice versa or such movement did not happen. the ways to get the technology either by importing technology, and then developing the imported technology, or through accessing technology and self-development by relying on existing technical experts and scientific talent who have long experience. The process of technology transfer happens during a transition or exchanging between institutions, by equipments and plants, or the exchanging in skills and knowledge between the professionals.

The Human Resources Management in each ministry or in their organizations (establishments) has to study this transition in consideration to achieve the technology skills.

However, there is 50% proportion of transition of professionals that have no changed their sectors; this rate refers to respondents who still in their job in both public and private, but they got the foreign skill from contracts which signed between their organizations and foreign companies previously or recently.

This gives a rate of a transition case of employees for this specimen in leaving the public sector and settling down at private sector or vice versa.

5.3 Agreement in Variance of the Level of Technology: This section of questionnaire asked respondents for their opinion about differences between the sectors in technology. Technology includes and will always refer to the Mechanization, Scientific and administration in this research. The answers ranging from '1 = strongly disagree' to '5 = strongly agree'. **Fig.3** displays those answers, and will lead to verifying the reasons for the difference in technology between sectors and how to raise the level of the sector and access to technology of (mechanization, scientific and administration).

Fig. 3`displays the mode of these readings turns to (Strongly Agree) with readings 31 by range 5, and it is the upper among them.

The statistical calculations (Mean and Standard Division) explain in **Table 2,** the table shows these statistics descriptive.

5.4 What Sector is Technically Better than Other?: Research provided 4 (four) choices; **Fig. 4** shows those opinions as percentage. Analysis will be discussed.

Research performed the statistic analysis between this Answers group and the answers group of (Transition of Professionals between Public and Private Sectors) as displaying in **Table 3.**

The result refers to the low forward correlation, between the Private and Public Sectors (raw 1 and raw 3), but in the same time the correlation value refers to high forward correlation between the Private and Public Sectors which have the contracts with foreign companies; it means to support them to contracting with foreign companies.

Discussing these answers is as follows:

i. The private sector is seeking for profitability before everything else, and therefore, all employees must have the professional expertise, prior work in this sector, as well as the incentives offered by sector, so employees who are familiar with modern techniques are performed.

ii. The public sector is subject to the acceptance of new graduates (mostly) and even if they were not experienced enough. Thus, this sector is the source of scientific and practical experiences and will be a loser for the departure of professionals to another sector.

iii.The contracts of private sector are (mostly) for small projects or just for parts of projects or for some activities. The quality could be more controlled; thus this may use a new and the best technology.

iv.The public sector is already subjected to the administrative laws; most of that legislation does not currently target knowing new technology; the major target is to complete the project with available facilities.

v. For all mentioned in the preceding paragraphs, the questionnaire result showed that the private sector is technically better than the public sector, both with the partnership with foreign companies or without; this is the opinion of the staff working in the government sector.

vi.The field discussions have stated the need of public sector involvement with foreign companies to get modern technology; this partnership will improve the technical skills of professionals.

vii.The previous contracts in the eighties of the last century adopted by the public sector with large foreign firms yielded good results for both the public and private sectors in Iraq. In that time, there was a significant role for transferring technology.

5.5 Working Previously / Recently with Foreign Company and Related to Construction Sector (Tasks): This question has two parts (working with foreign company and related this job to the construction sector) as follows in **Table 4.**

Although there are some of readings show absences of relationship between the work with foreign company and construction sector, they identified the need to modern technology, however; more than half of the respondents worked in the construction sector and this is a chance for transferring technology.

5.6 The level of Technology Utilized by the Foreign Company: This question was answered as expected with between very high level of technology and high, but some answers were provided as medium because the respondents see that technology presented by foreign companies was limited with scientific procedures or administrative systems and conformed with Iraq environment, so there is no high technology. **Fig. 5** shows the various responses for this question.

Although the largest rate (42 professionals) of respondents answers have unanimously agreed that the technology level was high, but there is a group of (15) professionals that referred to technology level with very high. This refers that more of the half of specimen confirm to the technical gab or need to bridge this gab. **Table 5** illustrates the statistics information for the technology level utilized by foreign companies. It is clear the (Mode) reading refers to results of (very high and high) respectively as well as the other readings (Std. Deviation and Variance).

5.7 Sorting and Arranging the Best Technical (Techniques, Procedures and Systems)

This question gives credence to the previous one, or complements it. There are four choices as follows:

a- The technology with modern mechanization and methods for use;

b- The scientific skills possessed by work team;

c- systematic Administration and managing the work according to authorities and responsibilities;

d- Following up the codes and standards.

The obtained results displaying in **Fig. 6** The largest rate was for the choice administrative system and work management in the division of responsibilities and authorities. This response came from groups who worked in years ago because no technical machines were used by foreign companies. **Fig. 6** shows also the proportion for each selection of the best technologies according to the professionals' assessment.

5.8Technology of Foreign Companies is Outweighing the Technology of Companies in Public Sector: This is a comparison on technology level between the foreign companies and companies in public sector; and the same comparison in the next question of the private sector and foreign companies; there are five levels for this comparison: 1-Very Low, 2- Low, 3- Medium, 4- High, and 5- Very High**.** The results are displayed in **Fig. 7** which shows respondents evaluation. The evaluation shows that foreign technology outweighed the public technology as well as the private technology. The rates of (very high) are (25) and (24) for public and private sectors respectively; and the same comparison rates of (high) are (41) and (40) respectively. These results can be considered as evidence of the superiority of foreign technology to technology in both public and private sectors.

5.9 Technology of Foreign Companies is Outweighing the Technology of Companies in Private Sector: The same previous comparison is conducted on technology level between the foreign companies and companies of the private sector. **Fig. 7** shows respondents evaluation; this chart presents three values of comparison.

Now, the result of the two Iraqi sectors (Public and Private) confirmed the necessary need for modern technology.

5.10The Transferring or Exchanging of Technology is Adopted When Contracts are signed **Fig. 8** illustrates this adoption and shows the lack of adoption of Transferring Technology as an important term for signing the contracts; it also trends to the normal situation in Iraq for this matter.

The degree of legal importance appears in adopting the technology transfer as one of contracts terms.

5.11 The Transferring or Exchanging of Technology is Adopted When Contracts are Concluded. Fig. 9 shows the horizontal transferring in Iraqi environment and the level of available technologies by these organizations;

It seems the effect of contribution of Iraqi contracts trends to (Occasionally, Low and Very low) with score 24, 27 and 2 respectively.

5.12 The Achievement of Technologies between Iraqi Organizations: This is another scale for evaluating and achieving the Iraqi technologies (scientific, mechanization and administration) from local environment. **Fig. 10** shows the technology acquirement level from public and private sectors alike.

5.13 Personal Procedures for Supporting or Encouraging the Technology Transfer

Fig. 11 displays the respondents contribution or (their procedures) to support or transfer technology (the first group)**.** The high percentage for: Submitting proposals for use the modern machineries to raise the level of production and the second was for: Submitting studies and periodic reports about work, and recommending changing the work methods if needed…, and etc. that means the professionals going on following-up the new technologies which utilized in the world as well as the method of work performance.

5.14 The Reasons for Absence of the Personal Role for Transferring Technology

Fig. 12 shows the second group that has the role (weak and non-existent) for major obstacles or barriers that prevent to technology transfer. The Figure shows the major obstacles to prevent technology transfer is the role of top management for supporting the modern technology and with the close percentage the reason of lack of work team, while the other reasons have the same percentage.

6. CONCLUSIONS

Several conclusions were reached (for instance but not limited) as follows:

1- The variety of respondents in (Public and Private) sectors as well as the respondents from different Ministries, with different specializations and different scientific degrees, this led to get a respected view for evaluating the technology and its importance in construction sector.

2- The major obstacles for adopting the modern technology were: Absence of motivation in the (some) top management for accepting it, as well as a lack of capable work team for receiving and absorbing and applying it….etc.

3- The results strongly supported the contracts with foreign companies to improve the skills in public and private sectors alike to bridge the technical gap.

4- There is no clearly legal term in Iraqi contracts for transferring technology which signed between different sectors.

5- The utilized technologies recently do not meet the required specifications for executing the projects.

6- Respondents have contribution for transferring technology and in contrast there are different obstacles for preventing this process.

7- Last but not least; there is no care to the professionals who worked with foreign companies, to get benefits, and the interesting should be paid to them and encouraging to improve the work.

REFERNCES

- Ashekele, H. M. and Kenneth M. 2008, *Success Factors in Technology Transfer to SME's: Rundu Woodwork Common Facility Center* PICMET University of Namibia, Windhoek, Namibia, Cape Town, South Africa (c) PICMET. P.2191.
- Bozeman, B. 2000, *Technology Transfer and Public Policy: A Review of Research and Theory* School of Public Policy, Georgia Tech, Atlanta, GA 30332 USA Center for Science, Policy, and Outcomes, 201 Pennsylvania Avenue, SE, Washington, DC. USA. P. 628.
- IFPMA –International Federation of Pharmaceutical Manufacturers and Associations 2011, *Technology Transfer: A Collaborative Approach to Improve Global Health* Geneva Switzerland. P.22.
- Kakabadse, N. K., Alexander K. and Andrew K. 2001 *From Tacit Knowledge to Knowledge Management: Leveraging Invisible Assets* Knowledge and Process Management Volume 8 Number 3. Cranfield School of Management, UK. P. 140.
- Kelly D. R. and Paul W. H. 2005, *Can Technology Transfer Help Public-Sector Researchers Do More with Less? The Case of the USDA's Agricultural Research Service* United States Department of Agriculture Economic Research Service. P.134
- Memo -ECON Centre for Economic Analysis- 2000, *Issues An Option in Technology Transfer* ECON-Memo no. 53/2000, Project no.20711 Restricted HLi/MDa/mbh, THa, 20. 0130 Oslo, Norway Commissioned by Norwegian Foreign Ministry. P. 4.
- Murshid, N.2014, *Technology Transfers and Their Effect on Human Capital* Lambert Fellowships in Public Affairs - Department of Political Science. Ameetosri Basu. P. 11.
- Ogunade, A. O. 2011, *Human Capital Investment in the Developing World: An Analysis of Praxis* Schmidt Labor Research Center Seminar Series. University of Rhode Island. P. 13.
- Omer R., Takim R. and Abdul Hadi N. 2011, *Measuring Absorptive Capacity in Technology Transfer (TT) Projects* Dept. Postgraduate Studies University Technology MARA (UiTM) Shah Alam, Selangor. P.331.
- Piktialis, D. and Greenes, K. A. 2008, *Bridging the Gaps How to Transfer Knowledge in Today's Multigenerational Workplace* Trusted Insights for Business Worldwide: by The Conference Board. Printed in the U.S.A. ISBN No. 0-8237-0925-6 The Conference Board and the torch logo are registered trademarks of The Conference Board, Inc. P. 19.
- Rounds, D. 2013, *To Train or Not to Train: Is Workforce Training a Good Public Investment?* California Senate Office of Research, 1020 N Street, Suite 200 Sacramento,
- Rubenstein Kelly Day and Paul W. Heisey 2005, *Can Technology Transfer Help Public-Sector Researchers Do More with Less? The Case of the USDA's Agricultural Research Service* United States Department of Agriculture Economic Research. Ag Bio Forum.
- Salem, A. 2011, *An Investigation on Foreign Direct Investment and Technology Transfer Comparative Study of Libya and Egypt* International Review of Business Research Papers Vol. 7. No. 2. P. 214.

- Silverstone, Y., Tambe, H. and Cantrell, S. 2015, *The Rise of the Extended Workforce* Strategy, Digital, Technology and Operations – Accenture Strategy – High Performance US .
- Smith, E. A. 2001, *The Role of Tacit and Explicit Knowledge in the Workplace* Journal of Knowledge Management Volume 5. Number 4. School of Business and Public Administration at the University of Houston Clear Lake. P.P.314 and 315.
- Stover, M. 2004, *Making Tacit Knowledge Explicit: The Ready Reference Database as Codified Knowledge* This item was retrieved from CSUN Scholar Works, the open-access, institutional repository of California State University, Northridge. P.2.
- Tesfayohannes, M. and Temtime, Z. T. 2002, *Problems and Prospects of Technology Transfer in Developing Economies: A Review* Pakistan Journal of Applied Sciences 2(3):
- Toner, P. 2011, *Workforce Skills and Innovation: An Overview of Major Themes in the Literature* OECD Directorate for Science, Technology and Industry (STI) Centre for Educational Research and Innovation (CERI). Paris, France. P.32.
- Vutsova, A. and Ignatova, O. 2013, *The Role of Public-Private Partnership for Effective Technology Transfer* Technology Transfer and Innovations, 2nd Annual Conference & Networking Volume 2. Issue 2. P. 12.
- Wahab, S. A., Che R. R. and Osman, S. I. W. 2012, *Exploring the Technology Transfer Mechanisms by the Multinational Corporations: A Literature Review* National Defense University of Malaysia, Kuala Lumpur 57000, Malaysia. P. 147.
- Willis, R.P.H. and Ashworth. S. G. E. 2002, *Technology and Knowledge Transfer— Good Practice Guidelines* The Journal of The South African Institute of Mining and Metallurgy, P.

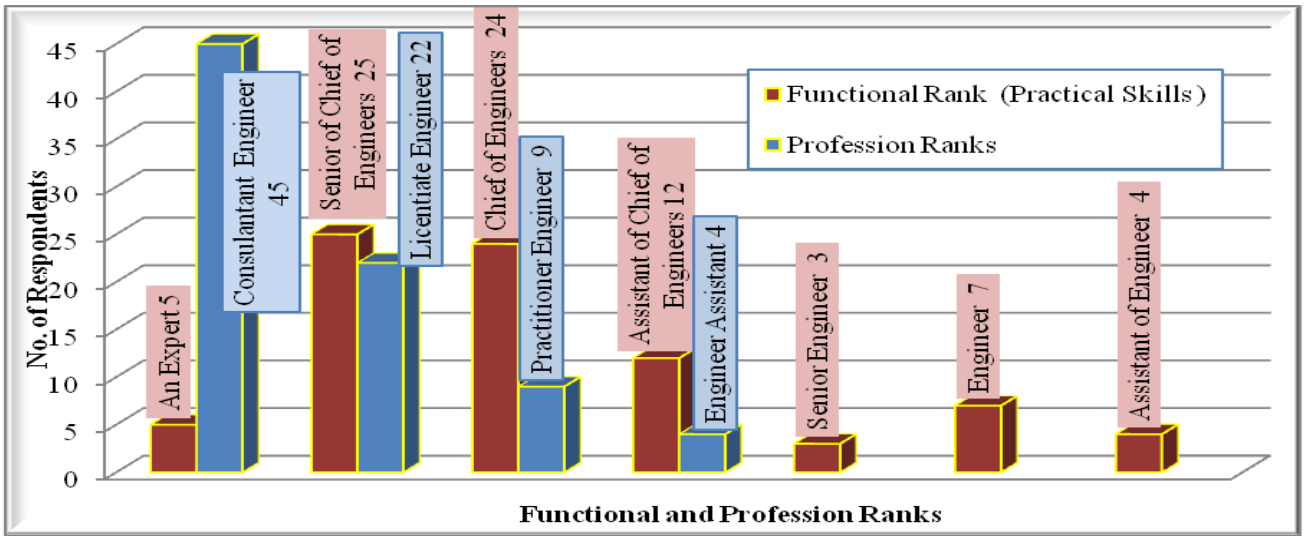

Figure 1. Functional and profession ranks of the respondents.

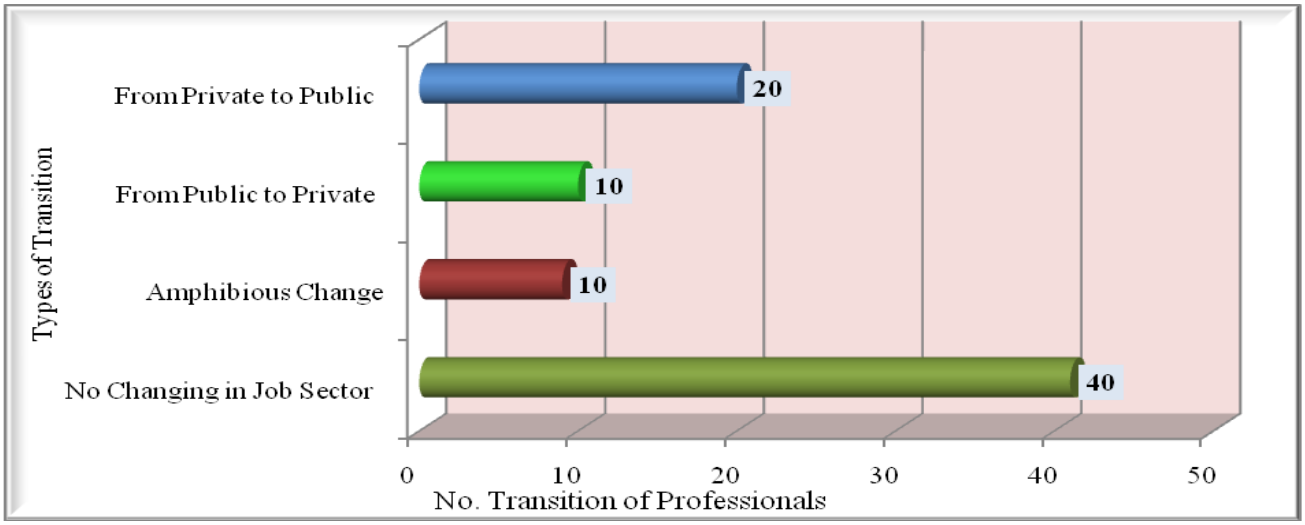

Figure 2. Transition of professionals between public and private sectors.

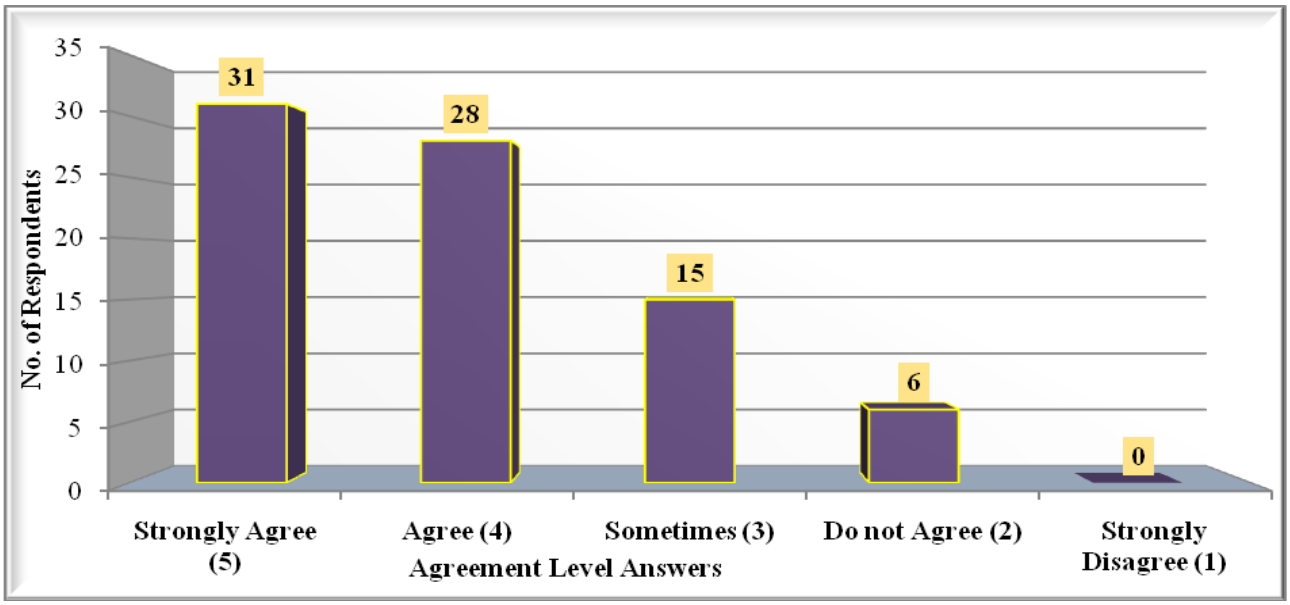

Figure 3. Respondents' opinion of the technology differences between sectors.

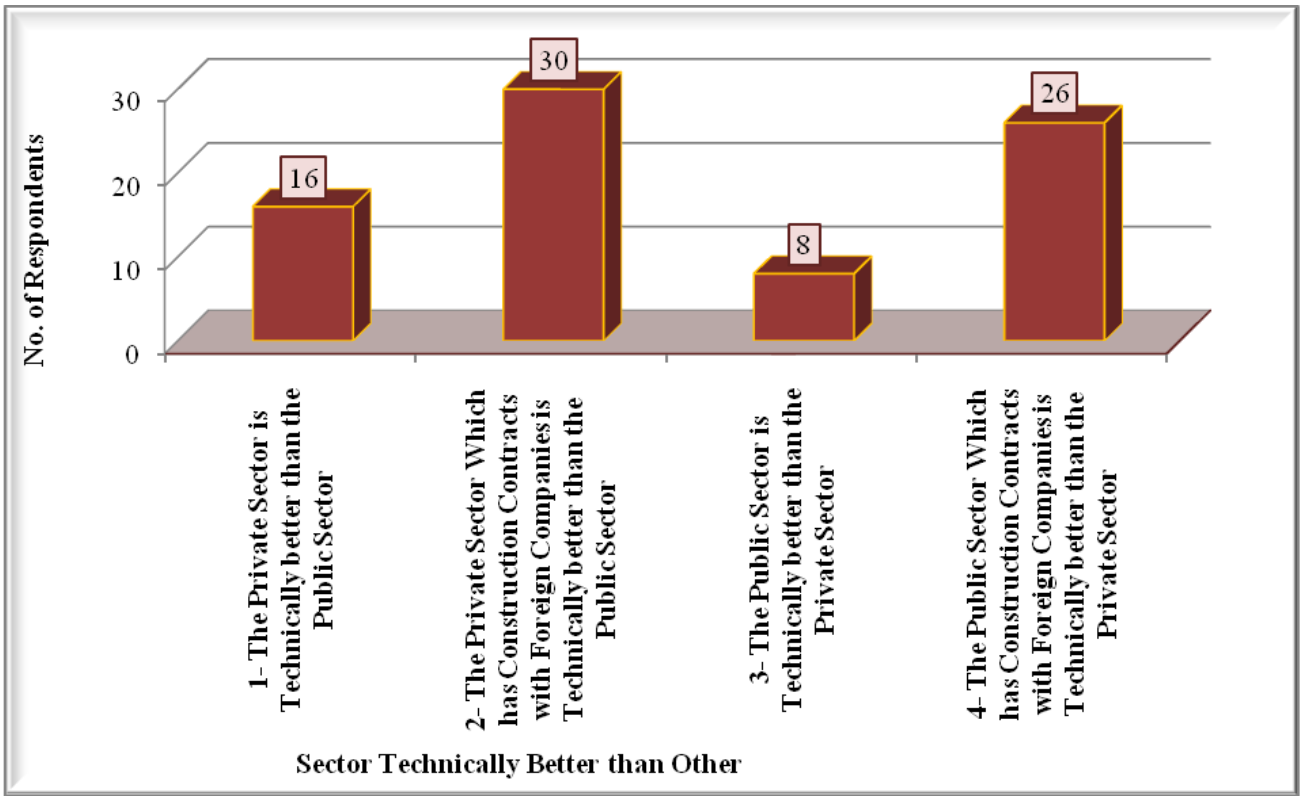

Figure 4. Comparison for selection of the technical sector.

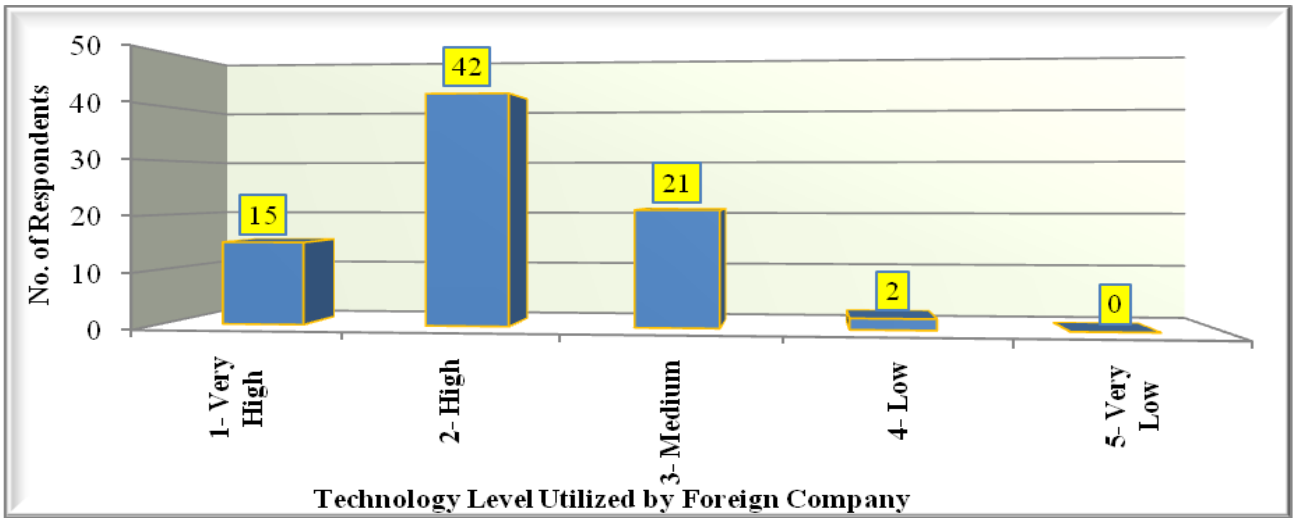

Figure 5. Technical level of foreign companies in previous work.

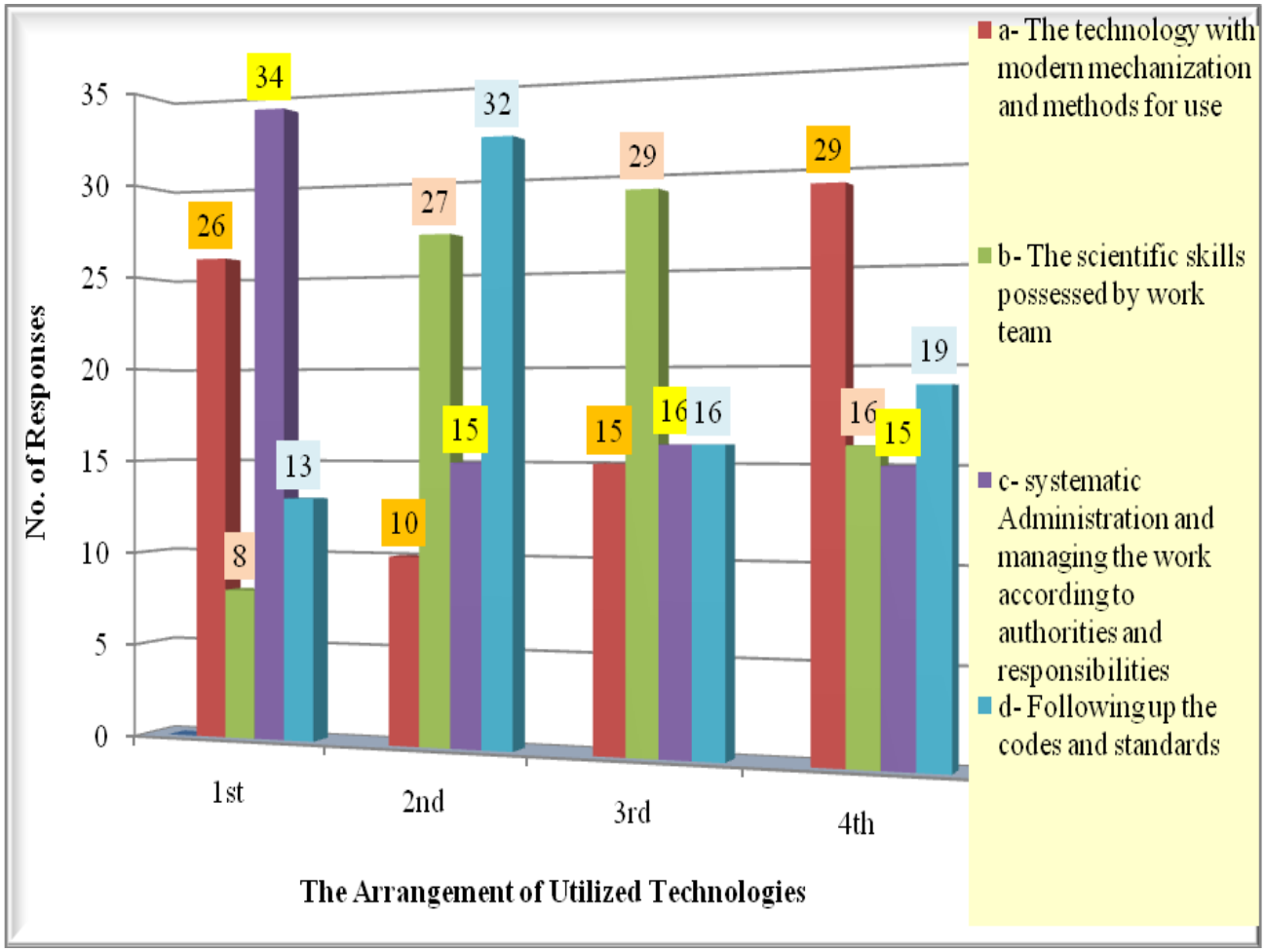

Figure 6. The arrangement of the best technologies.

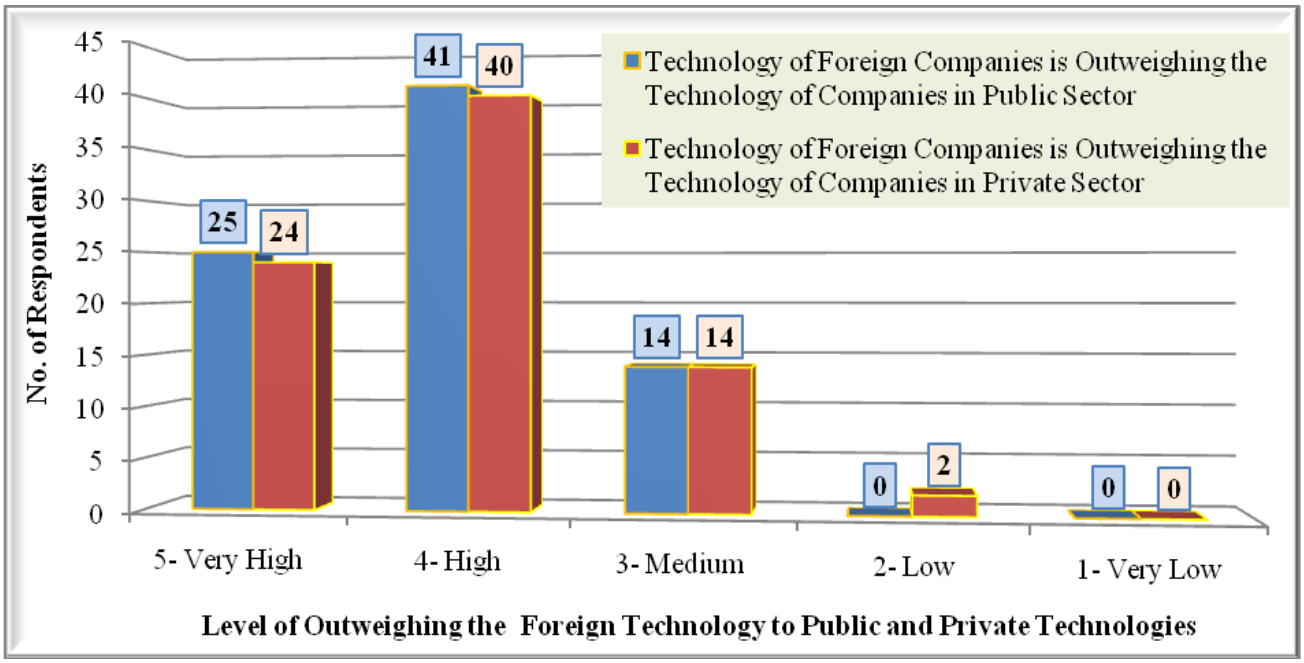

Figure 7. Weighting the foreign technology to public and private technologies.

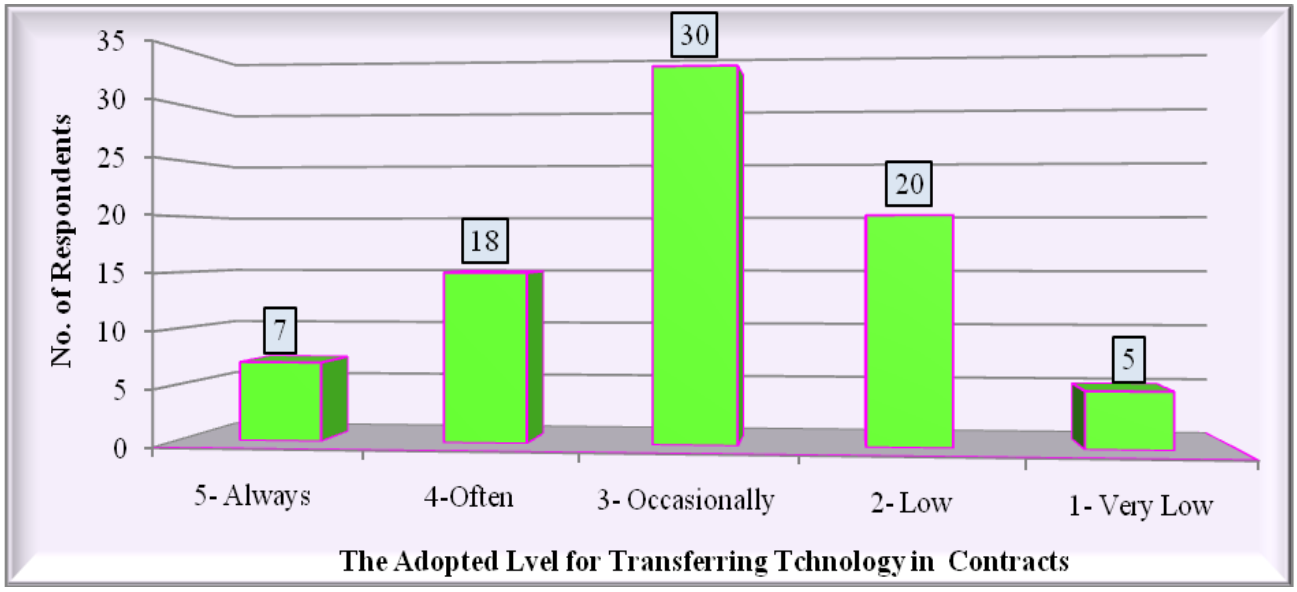

Figure 8. The legal term in a contract for transferring technology.

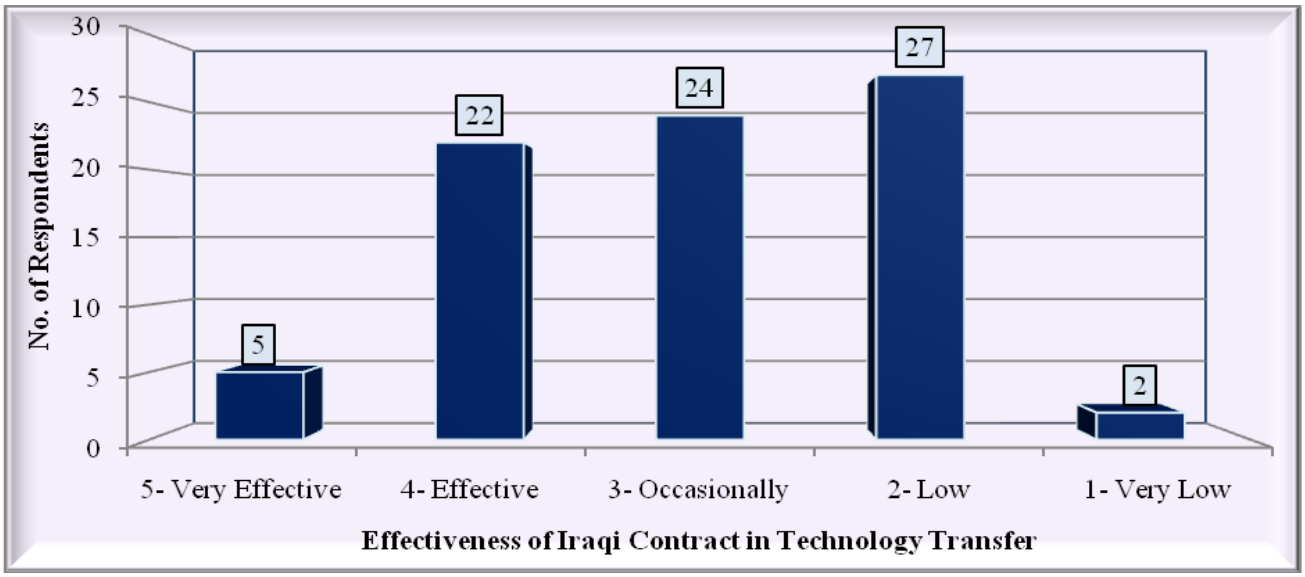

Figure 9. Contribution degree for technology transfer in iraqi contracts.

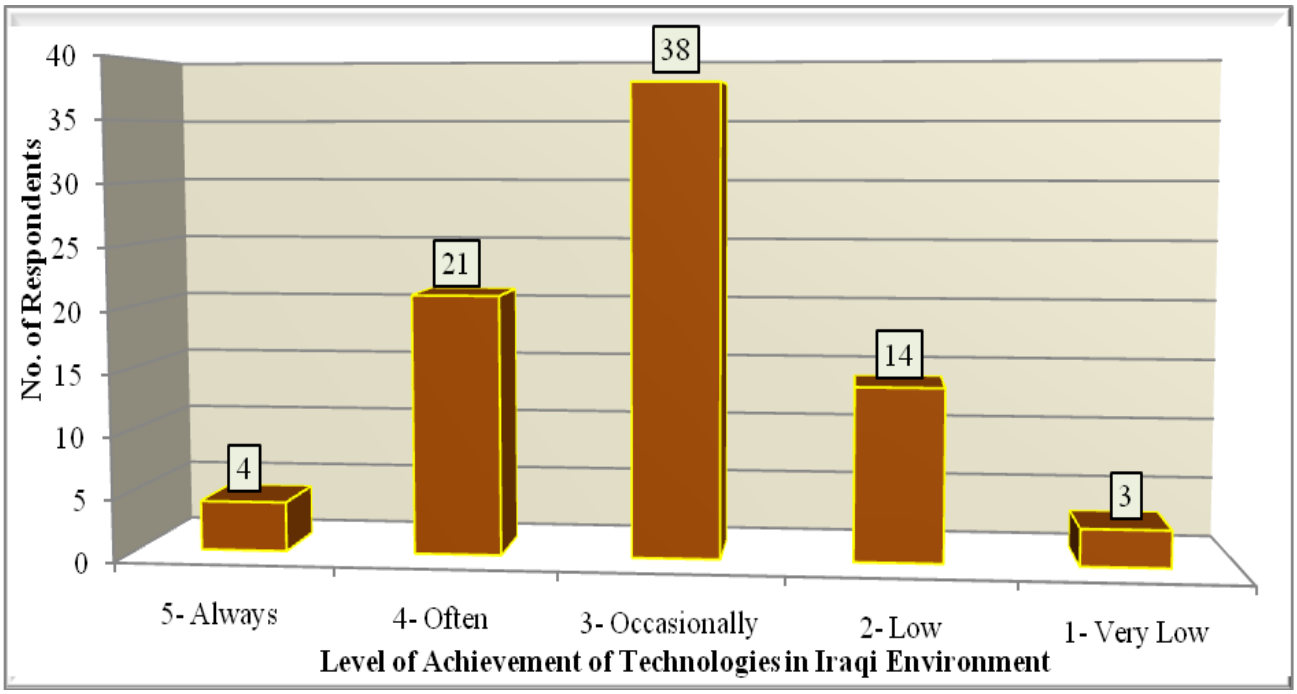

Figure 10. Technology achievement level from local environment.

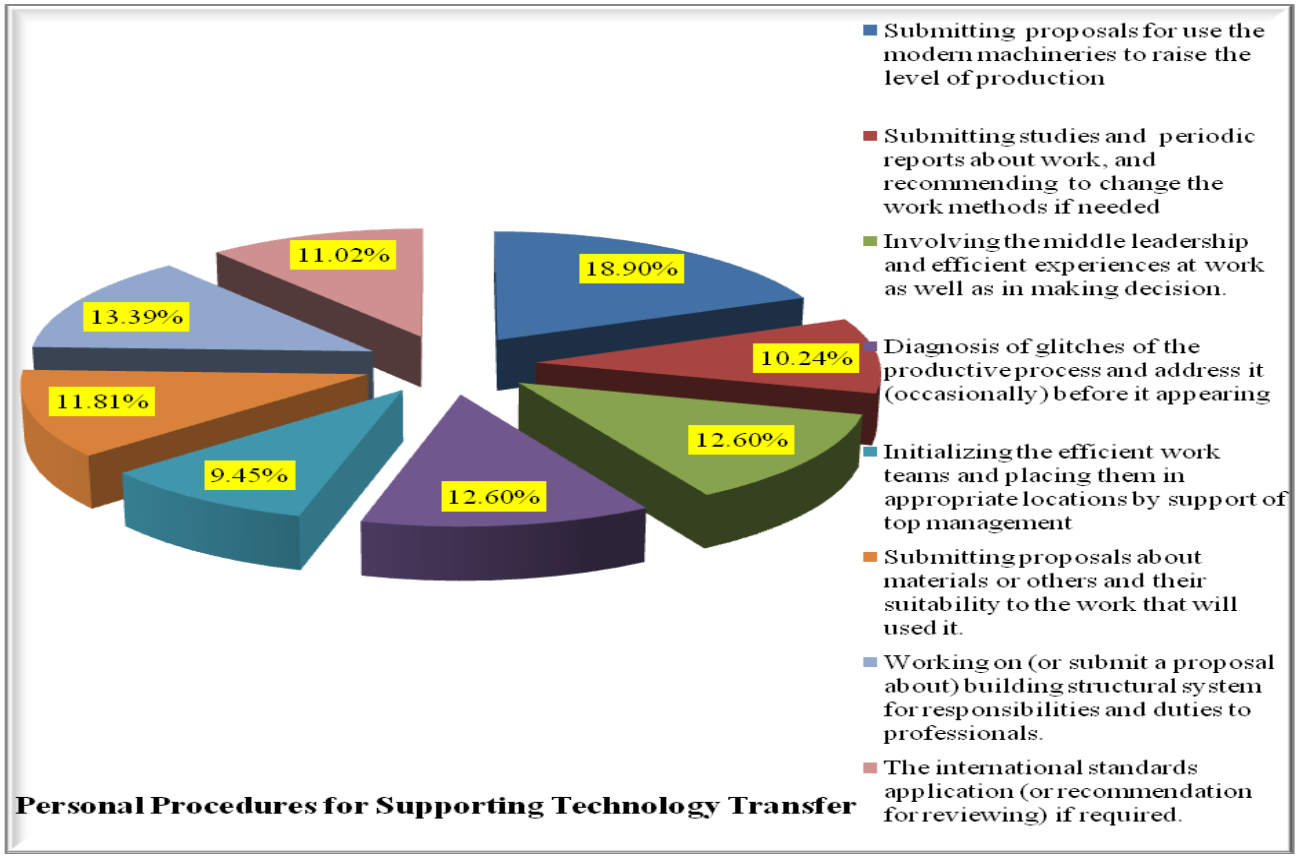

Figure 11. Personal procedures for supporting the transferring technology (the first group).

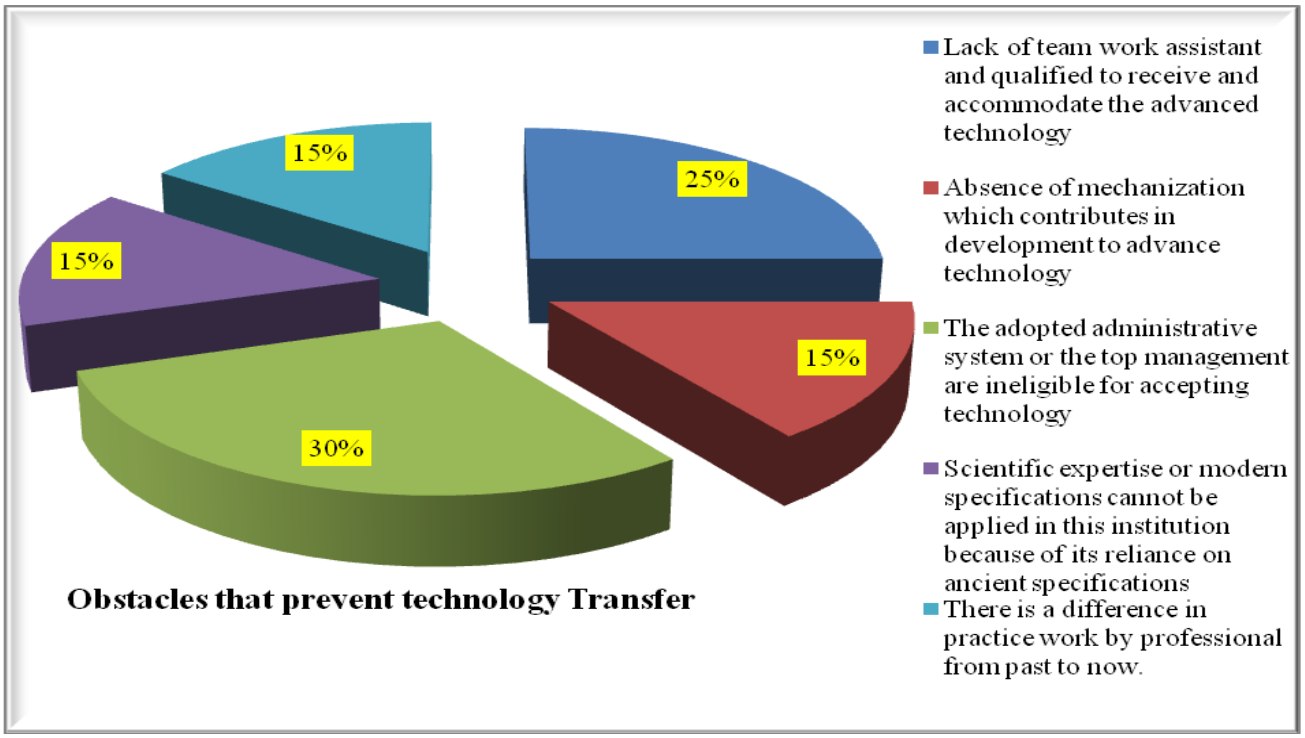

Figure 12. Obstacles or barriers that prevent the transfer of technology (second group).

Table 1. Different Specialization for Respondents in Public and Private Sector.

Specialization / Public and Private Sectors	Civil			Mechanical			Electrical	Architectural			Chemical			Environmental			Urban & Regional Planning		Production & Minerals	Total
	B	M	D	B	M	D	B	B	M	D	B	M	D	B	M	D	HD	D	B	
Ministry of Higher Education and Scientific Research	2	5	3	2	2	1									1	2		2		**20**
Ministry of Construction and Housing	7	4							1	1										**13**
Ministry of Water Resources	2	1																		**3**
Ministry of Health	2						1				2									**5**
Mayoralty of Baghdad				3														1		**4**
Ministry of Science and Technology					1						1								1	**3**
Ministry of Industry and Minerals	3										3									**6**
Ministry of Electricity						1	3													**5**
Ministry of Oil	1										1									**2**
Ministry of Youth and Sport							1										1			**2**
Different Private Companies	6	5		1				4			1									**17**
Total	**23**	**15**	**3**	**6**	**3**	**2**	**5**	**4**	**2**	**1**	**8**				**1**	**2**	**1**	**3**	**1**	**80**

Where B: Bachelor, H.D: High Diploma, M: Master and D: Doctorate

Table 2. Statistic descriptive for the agreement level in technology.

Descriptive Statistics								
	N	Mean	Std. Deviation	Variance	Skewness		Kurtosis	
	Statistic	Statistic	Statistic	Statistic	Statistic	Std. Error	Statistic	Std. Error
Specialization	80	2.50	1.981	3.924	1.117	.269	.042	.532
Scientific Degree	80	1.93	1.188	1.412	.659	.269	-1.297-	.532
Functional Ranks	80	3.30	1.546	2.390	.871	.269	.125	.532
Engineering Ranks	80	1.65	.873	.762	1.223	.269	.652	.532
Agree Level	80	4.05	.940	.884	-.664-	.269	-.503-	.532
Valid N (list wise)	80							

Table 3. Transition of professionals and the better technical sector .

Better Technically / Transition	Transition of Professionals					Correlation
	1- From Private to Public	2- From Public to Private	3- Amphibious Change	4- No Changing in Job Sector	**Total**	
1- The Private Sector is Technically better than the Public Sector	4	4	2	3	13	
2- The Private Sector Which has Contracts with Foreign Companies is Technically better than other	8	5	4	16	33	0.0580259
3- The Public Sector is Technically better than the Private Sector	3	0	1	3	7	
4- The Public Sector Which has Contracts with Foreign Companies is Technically better than other	5	1	3	18	27	0.976079
Total	20	10	10	40	**80**	

Table 4. Work in / with foreign company.

Respondents Answers for Part 1	Yes (Directly)	Yes (Indirectly)	No	Total
work with Foreign Company	39	41	0	80
Respondents Answers for Part 2	**Yes**	**Sometimes**	**No**	**Total**
Related to Construction Sector	59	12	9	80

Table 5. Statistic information for the technology level .

		Sector	Specialization	Scientific Degree	Functional Ranks	Engineering Ranks	Technology Level
N	Valid	80	80	80	80	80	80
	Missing	0	0	0	0	0	0
Mean			2.50	1.93	3.30	1.65	3.88
Median			1.00	1.00	3.00	1.00	4.00
Mode			1	1	3	1	4
Std. Deviation			1.981	1.188	1.546	.873	.736
Variance			3.924	1.412	2.390	.762	.541

Operation of the Iraqi Part of Al-Huweizah Marsh

Asst. Prof. Dr. Hayder Abdulameer AL-Thamiry
Department of Water Resources Engineering
College of Engineering-Baghdad University
E-mail: dr_hydr @yahoo.com

Ahmed Kamil Hassani
Department of Water Resources Engineering
College of Engineering -Baghdad University
E-mail: ahmed_khm@yahoo.com

ABSTRACT

Al-Huweizah Marsh is considered as the largest in Iraq. This research aims to maintain the sustainability of Al-Huweizah Marsh under all circumstances and within the limits of the available natural resources from the Iraqi side and the absence of feeding from the Iranian side due to the recent Iranian separation dike along the international boundaries within the marsh. Twelve scenarios have been suggested as a first step to restore the whole marsh. But the uncontrolled Iranian feeders and exiguity of their discharges recently, it was necessary to study only the northern part of the marsh as an alternative case to ensure reasonable amounts of water for the purpose of maintaining and restore the marsh. Hydrological routing model was used to calculate the quantities required to restore the whole marsh, as well as the northern part. In this research, the total dissolved solid (TDS) was adopted as the water quality parameter considering, three concentrations of TDS (1500, 1750, and 2000*ppm*). A two-dimensional flow mathematical simulation model was prepared using the SMS package (surface water modeling system) where RMA-2 and RMA-4 software's are used to study the flow and water quality patterns, respectively. In order to improve the water quality in the marsh according to the acceptable water quality determinants and the current conditions, we studied diverting some of Tigris River water, which is one of Shatt-Al-Arab feeders, into the marsh and releasing this amount into Tigris River through Al-Kassara control structure into Shatt-Al-Arab. A significant water quality improvement in the marsh was noticed as a result of mixing 25% or 50% of the Tigris River water which is suppose to go to Shatt Al-Arab. According to the results of this study, it was found that the restoration of the whole marsh cannot be achieved under the current circumstances because of the limited water discharges from Iraqi feeders of the marsh and receding of feeding from Iranian side. The best scenario was that of 3650*million cubic meters/year* for an area 338km^2 and water surface elevation of 3*m.a.m.s.l.* The results also show that Al-Kassara control structure is unable to pass the required outflow at low level to improve water quality according to the required standard determinants.

Key words: Al-Huweizah Marsh; hydrological routing model; discharge; TDS; SMS.

تشغيل الجزء العراقي من هور الحويزه

الأستاذ المساعد الدكتور حيدر عبد الامير الثامري
قسم هندسة الموارد المائية
كلية الهندسه - جامعة بغداد

احمد كامل حساني
قسم هندسة الموارد المائية
كلية الهندسه - جامعة بغداد

الخلاصة

يعد هور الحويزه من اكبر الاهوار الواقعة في العراق. يهدف هذا البحث الى ايجاد وسائل للمحافظه على ديمومة هور الحويزه في كافة الظروف مع الاخذ بنظر الاعتبار محدودية مصادر المياه المتوفره من الجانب العراقي وبغياب التغذيه من الجانب الايراني بسبب وجود السده الايرانيه الفاصله على طول الحدود الدوليه الممتدة عبر هور الحويزه. أثنا عشر سيناريو أقترحت كخطوه اولى لغرض انعاش وديمومة الهور بالكامل. ولعدم امكانية السيطره على مغذيات من الجانب الايراني اضافة لانحسار تصاريفها موخرا لذلك كان من الضروري دراسة الجزء الشمالي من هور الحويزه كخطوه بديله لضمان توفير كميات كافيه من المياه لغرض المحافظه على انعاش وديمومة الهور في ظل التحديات الراهنه. استخدم نموذج الاستتباع الهيدرولوجي لحساب الكميات المطلوبه لانعاش الهور بالكامل اضافه الى الكميات المطلوبه لانعاش الجزء الشمالي فقط. في هذا البحث ان كمية الاملاح الذائبه اعتمدت كمحدد لنوعية المياه وتم تحديد ثلاث محددات لقيمها وهي (2000,1750,1500) جزء بالمليون. أعد نموذج عددي ثنائي الابعاد باستخدام البرنامج الجاهز SMS (نظام نمذجة المياه السطحيه) حيث استخدم RMA2، RMA4 لدراسه حركه ونوعية المياه. ولتحسين نوعية المياه داخل هور الحويزه وفقا للمحددات نوعية المياه اضافه الى التحديات الراهنه. درسنا امكانية تحويل جزء من مياه نهر دجله والمخصصه لشط العرب ومن ثم اطلاق نفس الكميه الى نهر دجله من خلال منفذ الكساره ، حيث لوحظ تحسن كبير في نوعية مياه هور الحويزه كمحصلة خلط 25% او 50% من مياه نهر دجله والمخصصه لشط العرب. لوحظ من خلال الدراسه ان استعاده الهور وديمومته بأكمله لايمكن ان يتحقق في ظل الظروف الحاليه حيث محدودية مغذيات الهور (من الجانب العراقي) وكذلك انحسار التغذيه من الجانب الايراني. كما اتضح ان السيناريو الافضل كان بكمية مياه مطلوبه هي 3650 مليون متر مكعب لكل سنه والذي يقابل مساحة قدرها 338 كيلومتر مربع و منسوب سطح الماء يساوي 3 متر فوق مستوى سطح البحر كذلك تبين ان ناظم الكساره الحالي غير قادر على امرار التصاريف المطلوبه عند المناسيب المياه الواطئة لتحسين نوعية المياه وفقا للمحددات القياسيه المطلوبه.

الكلمات الرئيسية: هور الحويزه، الاستتباع الهيدرولوجي، التصريف، كمية الاملاح الذائبه ، نمذجه المياه السطحيه.

1. INTRODUCTION

Al-Huweizah Marsh is the largest marsh in Iraq with total area of 2060km^2 of it 1360km^2 within Iraq, **Al-Thamiry, 2009**. It is located at the east side of Tigris River at Mayssan and Al-Basrah Governorates, extending from AsSanna'f Marsh outfall down to the south to the outlet of AsSwaib River. Iran has constructed a dike along the Iran-Iraq border; this dike contains seven hydraulic structures, **Fig. 1**, extending from the northern of the Ghzayla bridge, in Mayssan Governorate, down to outlet Southern at AsSwaib, in Al-Basrah Governorate, at level 6 meters above mean sea level (*m.a.m.s.l.*), and a width 10*m* from top. It led to the separation of the marsh into two marshes and to prevent the flow of water from Iranian side, Al-Azim Marsh, to the Iraqi part of Al-Huweizah Marsh. As a result, the environmental and hydrological consequences of these changes are great, **CRIMW, 2012**.

The main problem that faces improvement the ecosystem in any Iraqi marshland is the absence of scientific management and the limited discharges of Iraqi feeders. In order to reduce the environmental impact of the Iranian dike on the Iraqi part of Al-Huweizah Marsh, Iraq has recently started constructing a dike, parallel to the Iranian dike and about 250*m* apart, in order to achieve proper water management system that will be built on a scientific basis and to ensure security of workers in Iraqi marsh, and this will contribute significantly to knowledge of the circumstances of this region in terms of social, environmental and hydrological. The

construction of this dike will prevent the inflow of Iranian drainage water into Iraqi part but the water resources deficit must be compensate from Iraqi feeders.

2. PREVIOUS STUDIES

Studies on the marshes are divided into two parts; the first is concerning on the hydrological studies while the second is focused on environmental studies. One of the hydrological study that prepared by, **Ministry of Environment, et al., 2006**. With main objective of studying the current and future water resources requirements in the marshlands area by using a set of numerical tools capable of providing valid presentation of the hydrodynamic phenomena in the marsh. This study included many Iraqi marshes, Abu Zirig marsh, the Central Marshes and Al-Huweizah Marsh. The scope of this work included identification of typical annual hydrological cycles for the marshes (inflow, outflows, evaporation, storage and water surface elevation variation) and provided a first set of circulation models was which prepared using the software's (flow-2d) and RMA2 to identify and analysis the development of the marshes re-flooding and point out which amount of water necessary to obtain the flooding extensions related to the investigated scenarios; more over the results variation during time were studied, in terms of water depth and of flooded area extension. The general scope of the modeling process is the identification of the best management way for water necessary for the wetlands, minimizing the inflow volumes and the evaporated volumes, keeping the water variation level necessary for the biological development. **Yousef, 2006**, prepared a study with main objectives were to over viewing the monitoring field data of Al-Huweizah Marsh concerning hydraulic and water quality aspects. The research used RMA2 model to calculate depth, averaged velocity gradients, water depths and surface water elevations for Al-Huweizah marsh according to date of measurements. From the comparison between the surface water area of the marsh before and after drying, it has been found that the surface water area is reduced to 28% of its area before drying 1976.

Al-Thamiry, 2009, prepared a study on Al-Huweizah Marsh. This study included hydrological and environmental influences on the Iraqi part resulting from the constructing of the Iranian separation dike through hydrological routing for two cases, case one; in the absence of Iranian dike and case two; the existence of the dike. The main results of the comparison showed that there is no contribution from Al-Karkheh River into the Iraqi part of the marsh during dry years; while the contribution of this river will be 36% and 31% from its inflow into the marsh during wet and normal years respectively.

In the environmental field, **Shaimaa, 2008**, studied the effect of Al-Huweizah Marsh boundary configuration on the velocity patterns and water quality distribution. This study has been achieved by using a two dimensional depth-average hydrodynamic model and a two dimensional water quality transport model. These models were built using RMA2 and RMA4 models under surface water modeling system package. This model has been applied on three hypothetical scenarios. Selection of these scenarios are mainly based on the marsh boundary configuration and the results of the hydrological and routing carried out by CRIM. Results of this study show that the construction of the earth dike along the Iraq-Iran boundary line causes variation in the direction of water flow in all portions of the marsh and also it has an influence on the variation of water quality for all parameters within the marsh.

Al Khafaji, 2013, prepared a study on Al-Huweizah Marsh which includes two cases, case one: without existence of the Iranian dikes and case two: with the Iranian dikes. The electrical conductivity, EC, value was adopted to be the indicator for the water salinity within the marsh. A steady two-dimensional water quality model was implemented by using the RMA2 and RMA4

software within the SMS computer package to estimate the seasonal distribution of the EC values within the marsh during the wet, normal and dry water years, the main results of this study showed that the estimated distribution patterns of EC values with the existence of the Iranian dikes, Case2,deteriora water salinity within most of the Iraqi part of the marsh during the four seasons of the wet, normal and dry water years.

3. AL-HUWEIZAH MARSH FEEDERS

Fig. 2, shows a schematic diagram of the main water resources of Al-Huweizah Marsh which can be classified into two types depending on the existence of water control structures. The first, controlled feeders, are Al-Musharrah, and Al-Kahla'a Rivers which are sharing the same intake located north of Al Amarah Barrage on Tigris River and controlled by a head regulators located upstream of each river. The second, uncontrolled feeders, are Al Karkheh River and AsSanna'f Marsh, which is feeding by AtTeeb, Dwayreach, Kmait Rivers, the surface runoff of AShama'ashir area and the drain water of Sa'ad River irrigation project.

The main discharge outlets of Al-Huweizah Marsh are Al-Kassara and AsSwaib Rivers. Al-Kassara River water is discharged to Tigris River through two sets of pipes. These pipes will be replaced by a control structure with a design discharge of 125m^3/sec. AsSwaib River flows from the southern part of Al-Huweizah Marsh and directly outfalls in Shatt Al-Arab River with an average flow capacity of 600 m^3/sec. A control structure with a design discharge of 200 m^3/sec has been designed to control the outflow of this river into Shatt Al-Arab River, **Ministry of Water Resources, el. at 2007**.

4. TOPOGRAPHY OF AL-HUWEIZAH MARSH

Different estimations of Al-Huweizah Marsh area may be found in literature. According to the study that carried out by **Ministry of Water Resources, 2003**. The estimated area of Al-Huweizah Marsh is about 1500km^2 including AsSanna'f Marsh area. During the autumn season, the marsh reaches its minimum area, about 650km^2. Only the deep parts of the marsh remains forming water ponds such as Um Al-Na'aj, and Al-Azim. These water ponds are connected to each other by water paths that pass through dense areas of weeds, reeds, and other water bushes types which make the movement within the marsh so difficult, **CRIM, 2008.**

CRIM, 2006, developed a complete topographical map for Al-Huweizah Marsh, **Fig. 3,** using the topographical survey which has been carried out for the Iraqi part of the Al-Huweizah Marsh, using the ultra sonic device and the topographical map of the Iranian part of the marsh which is presented in the Azadegan Environmental Baseline Studies, **UNEP, IRAN, 2004.**

5. AREA AND STORAGE ELEVATION CURVES

Depending on the achieved DEM of the marsh and using Arc-view GIS software assuming that the water surface profile is horizontal within the marsh (hypothetical case), the area and storage elevation curves for the Iraqi part (total marsh) of the marsh were obtained by **CRIM, 2008**. In the present study, according to the same above assumptions, the area and storage elevation curves for north part of the marsh are computed and presented in **Figs. 4** and **5**.

6. CONSUMPTION DISCHARGES FOR IRRIGATION FROM IRAQI FEEDERS

Marsh feeders are flow several kilometers before they reach the marsh boundary. Along these rivers, there are many intakes for irrigation purposes for the nearby farms. The monthly required water for irrigation was calculated according to the difference between the diverted discharges

through Al-Musharrah and Al-Kahla’a regulators and that reach the marsh through feeders and their tributaries. The estimated irrigation requirement will help decision maker to identify the required discharges at the inlets of Al-Musharrah and Al-Kahla'a regulators so as to ensure the marsh share of water, **Table 1**. It must be noticed that the actual feeder of the marsh during the last years is Al-Kahla'a River only since the whole water within Al-Musharrah River was used for irrigation, **Figs. 6** and **7**.

7. HYDROLOGICAL ROUTING OF AL-HUWEIZAH MARSH

The hydrological routing of Al-Huweizah Marsh was carried based on the mass conservation law and has the form of a mass balance equation, that is:

$$dV_m / dt = I - O - ET_o * A \qquad (1)$$

V_m is the volume of water within the marsh (*cubic meters*); t, I, O, A and ET_o represent the time (*sec*), inflow, outflow (m^3/s), area (m^2) and evapo-transpiration (*m/sec*), respectively.
Since Al-Huweizah Marsh lies within a region of high ET_o and according to the above equation, ET_o will be the key factor affecting the required water to maintain the marsh area and the water quality deterioration. To minimize the losses due to ET_o, a suggestion is made to minimize the marsh area to a value that keeps continuous lake during the period of high ET_o and to be increased up during the period of low ET_o. This suggestion simulates the natural fluctuation in the marsh area that was occurred before. Twelve scenarios of the total Iraqi Marsh boundary are suggested as the first step for the water management of the Iraqi marsh. But, since the Iranian feeders are uncontrolled feeders it must be study the absence of Iranian water, so the northern part of Al-Huweizah Marsh were taken as another alternative that will ensure the reasonable amount of water to maintain a permanent marsh, especially with the present challenges.

8. AL-HUWEIZAH MARSH WATER QUALITY

In this research, TDS is water quality parameter that was used as a measure of the salinity of the water. The effects of human activities on water quality are both widespread and varied and in the degree to which they disrupt the ecosystem and restrict water use. Pollution of water by human faces, for example, is attributable to only one source, but the reasons for this type of pollution, its impacts on water quality and the necessary remedial or preventive measures are varied. The marsh feeders, AsSanna'f Marsh (which is a seasonal marsh), Al-Karkheh River, Al- Musharrah River and Al-Kahla’a River, can be classified into three types depending on the existence of water control structures on these feeders; the locations of these control structures and the way of controlling the discharges of these feeders. These types are: uncontrolled feeders (AsSanna'f Marsh), controlled Iranian feeders (Al- Karkheh River) and controlled Iraqi feeders (Al-Musharrah and Al-Kahla’a Rivers).
Historically, the salinity was less than 700 mg/l, **Abbas, 2006**. But the water quality of the marsh varies with time. This variation depends on the source of water and whether the water passes urban area. Except the dissolved Oxygen, DO, the electrical conductivity, EC (or TDS), all other water quality parameters are about or within the acceptable limits for drinking water standards. The maximum recorded EC at Al Musharrah River, Al Ma’eel channel, Um AtToos River, Al Husa'chi River, Al-Kassara River, and AsSwaib River is slightly higher than the acceptable limit. While the maximum recorded EC at AsSanna'f Marsh outfall , AtTeeb River, Dwayreach River, Kmait River, and Sa'ad Drain let stations was 9000 μs/cm and it is higher than the acceptable

limit in most of the measurements, **CRIM, 2006**. Available information on Karkheh River water quality is restricted to the chemical elements such as total dissolved salts (TDS), pH, Electrical conductivity, anions and cat ions for the main stations. According to the available information, the salt content of the river water is mainly composed of sodium chloride followed by calcium sulfate and calcium carbonate. During the low flow periods, Sodium Chloride very clearly dominates other than salts while during the high flow periods; the composition is almost uniform, **UNEP, 2004**. The balance of the ecological system of the Al-Huweizah Marsh has a large effect on the balance of the overall ecological system because of the large area, location, variety of feeding sources and variety of ecological and biological systems of this marsh.

9. WATER QUALITY MODEL

The mass conservation law also applied to TDS, that is:

$$C_m*dV_m/dt+V_m*dC_m/dt = C_i * I – C_m*O+C_m * ET_o * A \quad (2)$$

Where C_m= Concentration of the marsh, *ppm*, C_i = Concentration of the feeder's marsh, *ppm*, V_m= Storage, m^3, I and O= Inflow and Outflow, m^3/s, $ET_{o=}$ Evapotranspiration, *m/s*, A= Area of marsh, m^2. In this study, TDS is water quality parameter that was used as a measure of the salinity of the water. TDS fairly indicates the level at which salinity problem is likely to occur. The TDS is an indicator to presence of calcium, magnesium, potassium, sodium, bicarbonates, chlorides and sulfates salts. Water quality of the northern part of Al-Huweizah Marsh was studied with the six adopted scenarios and the total dissolved solids TDS was limited to be below 1500, 1750 and 2000 *ppm* within the marsh. In order to improving water quality in the marsh, we studied diverting some of Tigris River water, which is one of Shatt-Al-Arab feeders, into the marsh and releasing this amount into Tigris River through Al-Kassara control structure into Shatt-Al-Arab. Additional 25% of Tigris River is to be diverted into the marsh when the value of the TDS of Tigris River at Qalat Saleh is greater than 1000 *ppm* and about 50% of Tigris River water when the value of the TDS of Tigris River at Qalat Saleh less or equal to1000 *ppm*.

10. THE SIMULATION MODELS

The Surface Water Modeling System, SMS, RMA2 is a two-dimensional, finite element hydrodynamic modeling code that supports subcritical flow analysis. It computes a finite element solution of the depth-integrated equations of fluid mass and momentum conservation in two horizontal directions. Friction is calculated with the Manning's formula, and eddy viscosity coefficients are used to define turbulence characteristics, **Donnell, 2004 a**. RMA2 model was used to compute the water surface elevation and velocity variation over Al-Huweizah Marsh. The Surface Water Modeling System, SMS, RMA4, is a companion model to RMA2, is a finite element water quality transport numerical model. RMA4 is applied to represent the transport of a contaminant, salinity intrusion in a system. RMA4 was used to investigate the water quality inside Al-Huweizah Marsh.

11. BOUNDARY CONDITIONS SIMULATION

There are two hydraulic models the first is of the Iranian side no feeding and the second for the Iranian side feeding. The downstream boundary conditions for the both models are the same which are Al-Kassara Rivers while the difference in the upstream boundary conditions is the feeding water that enters the marsh from Al-Karkheh Rivers. The reason of the difference is the

existence of the presumed Iranian dike that will prevent the incoming water from the river from entering the Iraqi part of the marsh when the water levels within the Iranian part of the marsh is lower than 6*m.a.m.s.l* and then the water will spill over this dike when the water level exceeds 6*m.a.m.s.l.* Al-Huweizah marsh has five inlets: Al-Karkheh River, AzZubair River, Um Al-Toos River, Al-Husa'chi River and AsSanna'f Marsh and Al-Musharrah River were treated as a one source point, since Al-Musharrah River flows into AsSanna'f Marsh before AsSanna'f Marsh feed the Al-Huweizah Marsh as shown in **Figs. 8** and **9**.

12. RESTORATION THE WHOLE AND NORTHERN PART OFAL-HUWEIZAH MARSH

Table 2, shows a comparison between the mean annual volume required to restore the whole area and the northern part of Al-Huweizah marsh according to the studied scenarios. The table reveals that the percentage mean annual volume ratio between the required volume to restore the northern marsh and the whole marsh is about 58%.

13. RESTORATION THE NORTHERN PART WITH AND WITHOUT IRANIANS FEEDERS

Table 3, shows the comparison between the mean annual volume that required to restore the northern part of Al-Huweizah Marsh due to the adopted scenarios including and excluding Iranians feeders. It is clear that the absence of Iranian feeders reduces the water resources of the marsh by about 1000*MCM*, (in normal year).

14. WATER QUALITY ANALYSIS OF NORTHERN PART WITHOUT IRANIAN FEEDERS

Table 4, presents inflow and outflow for restoration of the northern part of Al-Huweizah Marsh in all scenarios. The results of these scenarios are used as a first run for the water quality study and then the inflows and outflows are corrected according to water quality requirements**. Table 5,** shows the amount of the inflow and outflow required discharges for northern marsh area due to hydrological and environmental model for two consecutive years, namely, in the years 2009-2010 and 2010-2011, for limit 1500 *ppm*.

15. AL-KASSARA STRUCTURE OUTLET

According to water quality model of the northern part of Al-Huweizah Marsh in the presence of Al-Kassara structure had no flexibility to pass the large outflow values at the low level of water due to the absence of feeding from the Iranian side therefore the value of TDS cannot be improved. To solve this problem, an additional outlet structure is needed to give the required flexibility to discharge higher flow rates than in the present condition. **Fig. 10** shows comparison between TDS, if the downstream control structure is only Al-Kassara structure or an alternative structure for the first scenario when the maximum allowable TDS is 1500*ppm*. It can be noticed significant improvement in TDS due to the alternative structure when it compared with that of the existing of Al-Kassara structure. The main reason is that Al-Kassara structure currently cannot passed the outflow required to achieve the water quality accordance to required determinants. As an example, it is noticed from the **Fig. 10** at September, the concentration of TDS was 8808*ppm* with Al-Kassara structure while it was 1499*ppm* at the same month in the case of alternative structure, where the percentage mean annual TDS ratio (improvement ratio) was 83%.

16. AL-HUWEIZAH MARSH BEFORE AND AFTER MIXING WITH ADDITIONAL SHARE

Significant water quality improvement in the marsh was noticed as a result of mixing additional share of the water allocated of Shatt Al-Arab. **Figs. 11, 12, 13, 14, 15** and **16**, show the monthly variation of TDS in Al-Huweizah Marsh and Shatt Al-Arab before and after mixing with additional share of Shatt Al-Arab for limit 1500 ppm. **Table 6** presents the percentage ratio of mean annual TDS among the suggested scenarios for the northern part of Al-Huweizah Marsh. The percentage annual TDS ratio (TDS improvement ratio) is used in comparison between the different scenarios, **Table 6**. When the maximum allowable TDS in the marsh is 1500*ppm*, the TDS of the marsh before mixing is 1492*ppm* and after mixing is 1353*ppm*, the improvement ratio (percentage mean annual TDS ratio) in TDS of the marsh is 9% and the percentage of deterioration in TDS of Tigris River after mixing is 24% in the first scenario. In other scenarios the improvement ratio in the marsh after mixing is approximately 8% and the percentage of deterioration in TDS of Tigris River after mixing is 23%.

17. SEASONAL DISTRIBUTION OF TDS IN THE MARSH WITHOUT IRANIAN FEEDING

A larger area of the marsh has a good quality during Summer, but it will be worst during Winter with or without mixing. It is to be noticed that the east part of the marsh near the Iraq-Iran international boundary is almost stagnant. The contribution of the extra water (with mixing) will lower the upper limit of TDS in the marsh while the TDS distribution is same**, Figs. 17** and **18**.

18. SEASONAL DISTRIBUTION OF TDS IN THE MARSH WITH IRANIAN FEEDING

The water quality of the marsh with the feeding from Iranian side is very bad in spite of good mixing process, so it is necessary to avoid the Iranian side feeding by complete the construction of the Iraqi separation dike along the boundary to prevent the deterioration within the marsh area, **Fig. 19**.

19. CONCLUSION

The hydrological routing was carried out based on marsh operation, which minimizes the evaporation from the marsh, and with different scenarios of inflow and outflow discharges. The variation of the marsh area, water level, inflow and outflow discharges, water volume, and the water quality within the marsh were specified for each scenario. Based on the hydrological routing analysis, a mathematical water quality models was used to study the variation of the water quality within the marsh. The following conclusions were extracted:

1. Restoration of the whole marsh cannot be achieved since the required annual volume of water is 1384 million cubic meters which is very difficult to be supplied according to the current circumstances of Al-Huweizah Marsh feeders. Whereas, the northern part restoration need 62% of that required for the whole marsh area.
2. The current Al-Kassara control structure fail to pass the required outflow in order to satisfy the required water quality limitations within the marsh area.
3. Significant water quality improvement in the marsh was noticed as a result of mixing additional share of the water allocated of Shatt Al-Arab.
4. Restoration of Al-Huweizah marsh according to the hydrologic and environment considerations is required 3650 million cubic meters from Iraqi feeders which are more than 4

times of that for the hydrological requirements only. This amount of water is sufficient to preserve the concentration of water contaminants within the acceptable determinants.

5. When the maximum allowable of TDS in the marsh water is equal to 1500*ppm* (whether with or without extra inflow) it is noticed that TDS in 5th scenario is similar to that of the 2nd, 3rd and 4th scenarios.

6. It is clear that the absence of Iranian feeders reduces the water resources of the marsh by about 1000 million cubic meters (in normal year).

0. REFERENCES

- Abbas, S. F., 2006, *Application of Hydrodynamic Model in Abu Zirig Marshland*, M. Sc., Thesis, University of Mustansiriya.

- Al Khafaji, M. S., 2013. *Effect of the Iranian Separation Dikes on the Water Salinity Patterns Within Al-Huweizah Marsh* Journal of Engineering, College of Engineering . University of Baghdad. Baghdad/Iraq. No.1, Vol.19, p35-51.

- Al Thamiry, H. A., 2009. *Hydrological Damage of Iranian Separation Dike on the Iraqi Part of Al-Huweizah Marsh*, The 6th Engineering Conference/ College of Engineering / Baghdad University (5-7 April 2009) Vol. V, p 112-126.

- CRIM (Center for the Restoration of Iraqi Marshlands), 2006. *Study the Rehabilitation of Al-Huweizah Marsh Ecological System* Vol.1 to Vol.7.

- CRIM, 2008. *Study The Hydrological And Ecological Effect For The Construction Of An Earth Dyke By The Iranian Administration To Separate The Part Of Al Huweizah Marsh Which Is Located Within The Iranian Territories*.

- CRIM, 2012. *Report about Dike Construction Along the Iraq-Iran Border in Al-Huweizah Marsh.*, Unpublished, (Arabic).

- Donnell, B. P., 2004. (a), User Guide to WES-RMA2 Version 4.5, "*Water Ways Experiment Station, Costal and Hydraulics Laboratory*", California, Davis, U.S.A.

- Ministry of Environment, Ministry of Water Resources, Ministry of Municipalities and Public Works Iraq and Italian Ministry for the environment and Territory and the Free Iraq Foundation , 2006. *New Eden Master Plan for Integrated Water Resources Management in the Marshlands Area*" Italy, Iraqi.

- Ministry of Water Resources, Ministry of Environment, Municipalities and Public Works Iraq and Italian Ministry for the Environment, Land and Sea, 2007. *The New Eden Project - Master Plan for Integrated Water Resources Management in the Marshlands Area*; Outlet of Al-Huweizah Marsh Along Al-Kassara River & AsSwaib River, technical Report, phase II.

- Nicholson, E. and P .Clark (Eds), 2002. *The Iraqi Marshlands: A Human and Environmental Study* The AMAR Appeal International Charitable foundation.

- Partow, H., 2001, *The Mesopotamian Marshlands: Demise of an Ecosystem* Report United Nations Environmental Program.
  Available online at.
  (http://earthobservatory.nasa.gov/Newsroom/NewImages/Images/meso2.pdf).

- Shaimaa, A., 2008. *Effect of Al Huweizah Marsh Boundary Configuration on the Velocity Patterns and Water Quality Distribution*. M. Sc. Dissertation. Collage of Engineering. University of Baghdad.

- *UNEP, 2003. Environment in Iraq:* UNEP Progress Report, UNEP. Geneva, Switzerland.

- *UNEP, 2004. Azadegan Environmental Baseline Studies.* The Natural Environment, Iran.

- *Yousef, S. S., 2006. Application of Steady Flow Model for Analysis of the Flow in Al-Huweizah Marsh. M. Sc.* Thesis-Building and Construction Engineering Dept., University of Technology.

Figure 1. Hydraulic structures in Iranian dike at the coordinate in UTM (N=3474521.24891*m*, E =755381.586716 m), **during 5-12-2012**.

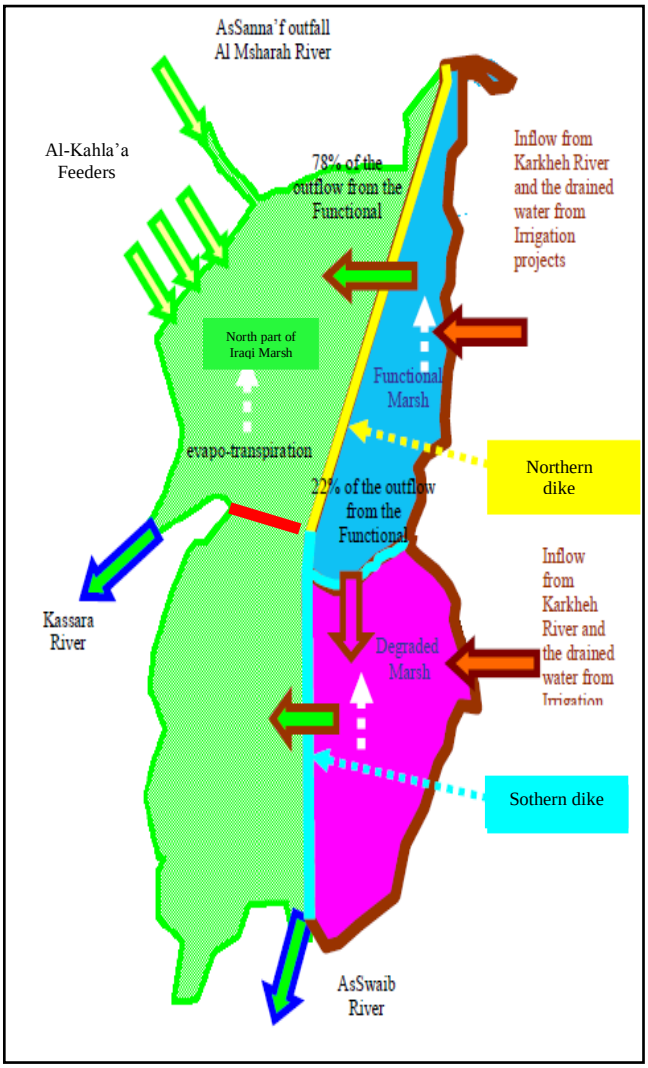

Figure 2. Schematic diagram for the hydrological interference, ***CRIM, 2008***.

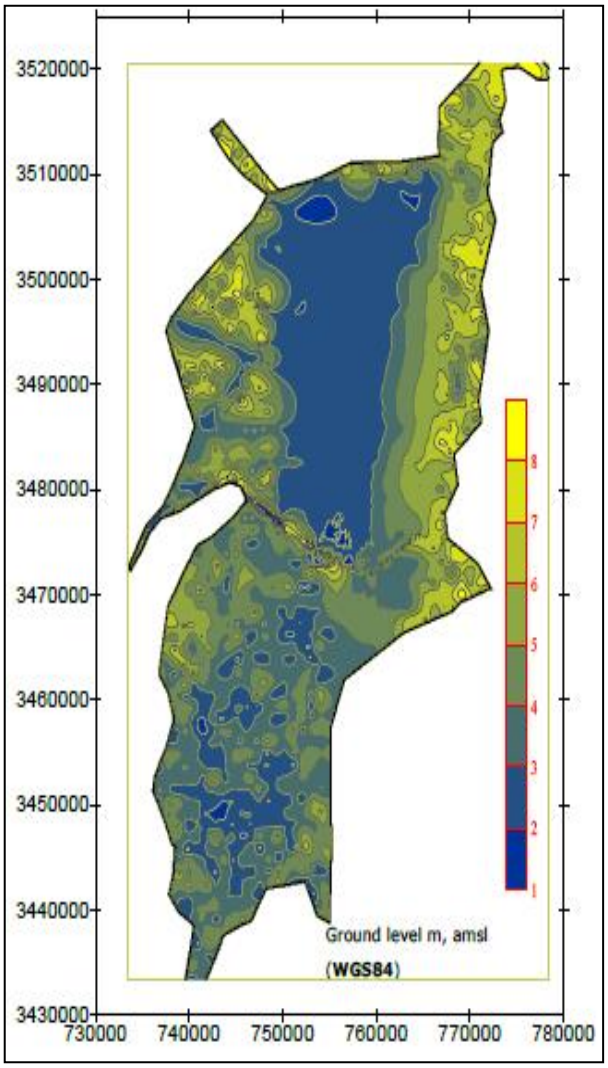

Figure 3. Digital elevation model (DEM) of Al-Huweizah Marsh, ***CRIM, 2006***.

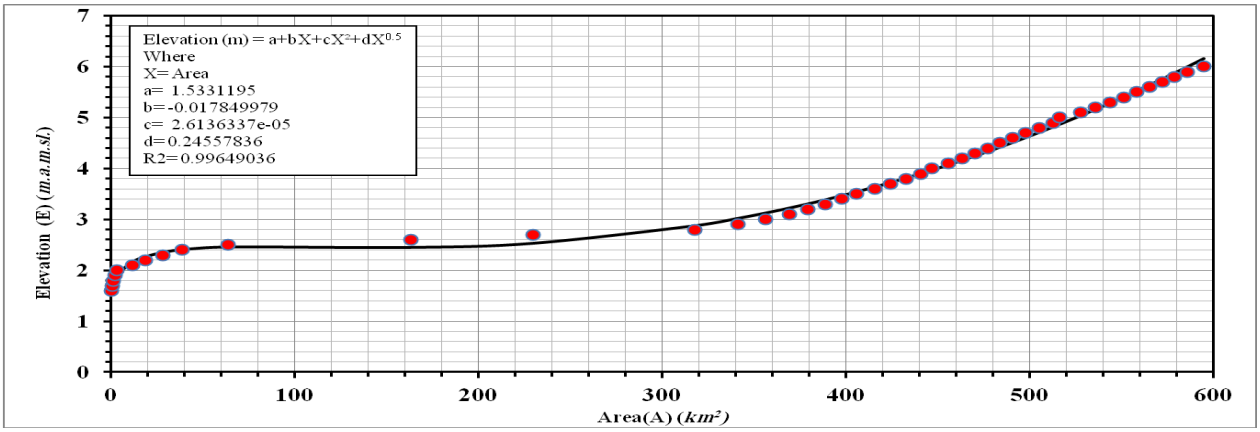

Figure 4. Area-elevation curve of the north Iraqi part of Al-Huweizah Marsh.

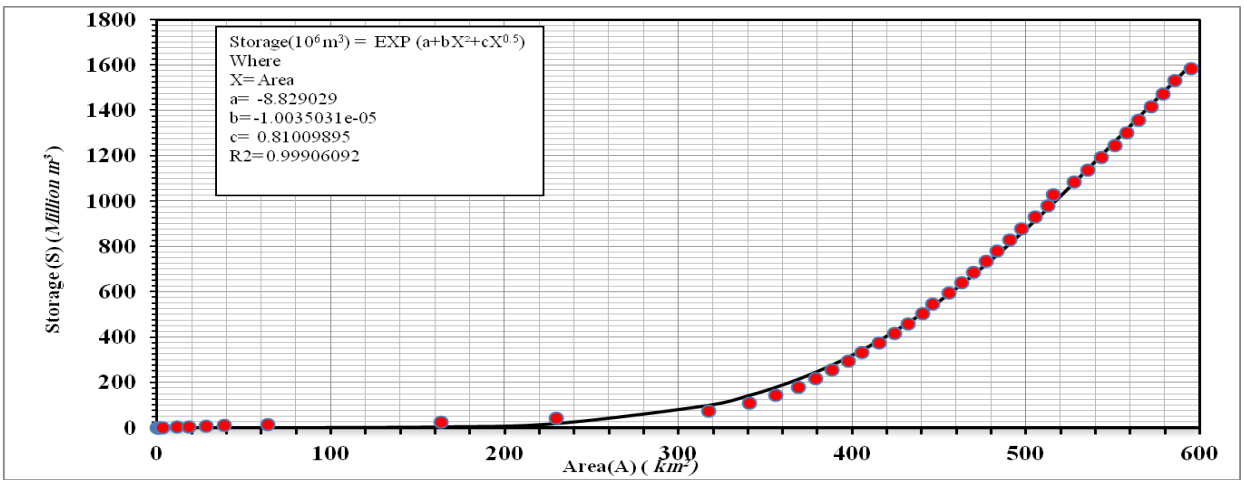

Figure 5. Area-storage curve of the north Iraqi part of Al-Huweizah Marsh

Table 1. Monthly average water consumption in m^3/sec along Al-Musharrah and Al-Kahla'a Rivers.

	Month	Al-Kahla'a River			Al-Musharrah River		
		River inflow	Total consumption	Marsh inflow	River inflow	Total consumption	Marsh inflow
2009 - 2010	Oct	28.52	9.77	18.75	6.42	6.42	0
	Nov	22.37	10.37	120	4.43	4.43	0
	Dec	28.64	9.14	19.50	6.04	6.04	0
	Jan	22.74	9.99	12.75	5.26	5.26	0
	Feb	17.68	4.93	12.75	6.64	6.64	0
	Mar	17.67	6.86	10.81	5.90	5.90	0
	Apr	21.10	4.32	16.78	7.80	7.80	0
	May	29.23	9.46	19.77	7.19	7.19	0
	Jun	22.63	9.08	13.55	5.30	5.30	0
	Jul	17.89	5.61	12.28	4.04	4.04	0
	Aug	19.58	8.23	11.35	6.04	6.04	0
	Sep	20.07	8.52	11.55	6.40	6.40	0

Figure 6. Al Jdeda regulator on Al-Musharrah River at the coordinate in UTM (N=3525693m, E =722787m), ***during5/ 1/2012***.

Figure 7. Al Alah regulator on Al-Musharrah River at the coordinate in UTM(N=3525151m, E =711674m), ***during 5/ 1/2012***

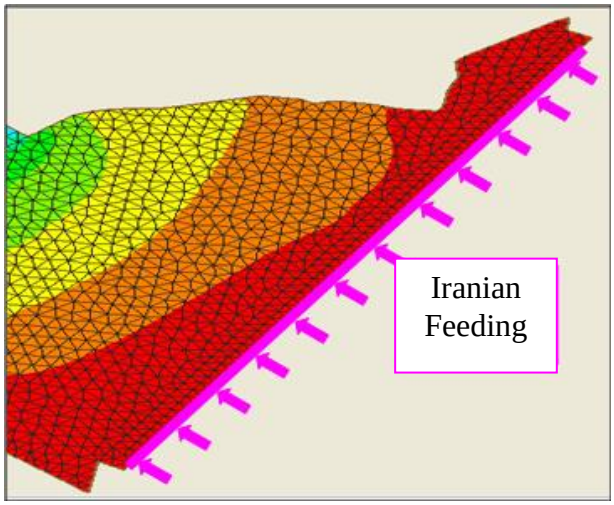

Figure 8. The inflow from Iranian part into the Iraqi part of the marsh.

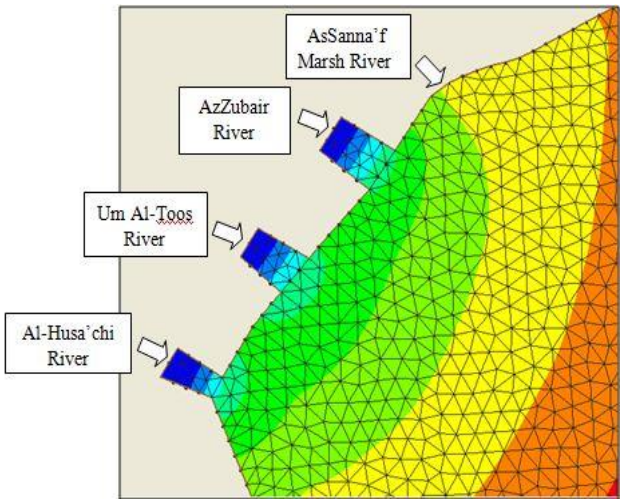

Figure 9. Iraqi feeders of Al-Huweizah Marsh.

Table 2. Comparison of the required means annual volumes of water in MCM for restoration of the whole and northern part of Al-Huweizah marsh area.

Scenario	1	2	3	4	5	6	7	8	9	10	11
Northern Marsh	857	1076	1105	1155	1181	1179	1591	1615	1659	1674	1655
Whole Marsh	1384	1797	1839	1912	1948	1944	2871	2904	2960	2966	2913

Table 3. Comparison the mean annual volumes of water in MCM for the suggested scenarios with and without Iranians feeders.

Scenario	1	2	3	4	5	6
Including Iranian Feeders	1842	2060	2089	2139	2162	2146
Excluding Iranian Feeders	857	1076	1105	1155	1181	1179

Table 4. Net required monthly inflow (I), outflow (O)and annual volume in MCM for two consecutive years for northern part.

			Discharge, m^3/s													
			Oct	**Nov**	**Dec**	**Jan**	**Feb**	**Mar**	**Apr**	**May**	**Jun**	**Jul**	**Aug**	**Sep**	**Mean Annual**	**Volume**
S-1	**I**	1st year	22	13	7	7	11	16	26	35	49	53	49	36	27	857
		2nd year	22	13	7	7	11	16	26	35	49	53	49	36	27	857
	O	1st year	0	0	0	0	0	0	0	0	0	0	0	0	0	0
		2nd year	0	0	0	0	0	0	0	0	0	0	0	0	0	0
S-2	**I**	1st year	51	44	42	20	0	0	0	35	49	53	49	36	32	1007
		2nd year	54	57	65	33	0	0	0	35	49	53	49	36	36	1144
	O	1st year	0	0	0	31	42	24	5	0	0	0	0	0	8	262
		2nd year	0	0	0	31	42	24	4	0	0	0	0	0	8	260
S-3	**I**	1st year	40	47	45	22	0	0	14	35	49	53	49	36	33	1036
		2nd year	39	59	71	38	0	0	14	35	49	53	49	36	37	1175
	O	1st year	0	0	0	37	49	27	3	0	0	0	0	0	10	298
		2nd year	0	0	0	37	49	27	3	0	0	0	0	0	10	298
S-4	**I**	1st year	25	36	60	31	0	9	26	35	49	53	49	36	34	1088
		2nd year	22	39	88	53	0	9	26	35	49	53	49	36	38	1222
	O	1st year	0	0	0	57	68	17	0	0	0	0	0	0	12	361
		2nd year	0	0	0	57	68	17	0	0	0	0	0	0	12	361
S-5	**I**	1st year	25	15	56	54	6	16	26	35	49	53	49	36	35	1117
		2nd year	22	13	71	92	6	16	26	35	49	53	49	36	39	1245
	O	1st year	0	0	0	104	51	0	0	0	0	0	0	0	13	401
		2nd year	0	0	0	104	51	0	0	0	0	0	0	0	13	401
S-6	**I**	1st year	25	15	9	97	11	16	26	35	49	53	49	36	35	1118
		2nd year	22	13	7	150	11	16	26	35	49	53	49	36	39	1240
	O	1st year	0	0	0	162	0	0	0	0	0	0	0	0	14	435
		2nd year	0	0	0	162	0	0	0	0	0	0	0	0	14	434

Table 5. Net required monthly inflow (I), outflow (O) and annual volume in MCM for two consecutive years for northern part, (maximum allowable TDS in the marsh is 1500ppm).

			Discharge, m^3/s													
			Oct	**Nov**	**Dec**	**Jan**	**Feb**	**Mar**	**Apr**	**May**	**Jun**	**Jul**	**Aug**	**Sep**	**Mean annual**	**Volume**
S-1	**I**	1st year	22	116	28	30	39	69	106	137	188	226	195	139	108	3412
		2nd year	89	69	33	47	69	159	156	142	182	210	184	135	123	3887
	O	1st year	0	103	21	23	29	53	80	102	139	173	146	103	81	2560
		2nd year	67	56	26	40	59	143	130	107	133	157	135	99	96	3036
S-2	**I**	1st year	51	44	42	20	50	80	111	137	188	229	194	140	107	3385
		2nd year	96	77	65	33	76	185	164	139	182	212	182	135	129	4075
	O	1st year	0	0	0	31	92	104	114	102	139	176	145	104	84	2641
		2nd year	43	21	0	31	118	210	168	104	133	159	133	99	101	3194
S-3	**I**	1st year	40	47	45	22	49	75	111	140	187	226	196	140	107	3369
		2nd year	89	75	71	38	57	181	159	144	182	211	183	135	127	4014
	O	1st year	0	0	0	37	98	102	100	105	138	173	147	104	84	2634
		2nd year	49	16	0	37	106	209	148	109	133	158	134	99	100	3143
S-4	**I**	1st year	25	36	66	31	31	81	106	138	187	228	194	140	105	3337
		2nd year	90	67	88	53	0	202	156	140	182	213	181	135	126	3991
	O	1st year	0	0	6	57	99	89	80	103	138	175	145	104	83	2615
		2nd year	68	27	0	57	68	210	130	105	133	160	132	99	99	3134
S-5	**I**	1st year	25	43	70	54	28	66	106	140	187	225	197	141	107	3386
		2nd year	88	68	73	92	6	200	156	140	182	213	181	135	128	4062
	O	1st year	0	28	14	104	73	50	80	105	138	172	148	105	85	2675
		2nd year	66	55	2	104	51	184	130	105	133	160	132	99	102	3221
S-6	**I**	1st year	25	39	48	97	11	74	106	137	187	229	193	140	107	3406
		2nd year	92	68	35	150	11	181	156	141	182	212	182	135	129	4088
	O	1st year	0	24	40	162	0	58	80	102	138	176	144	104	86	2728
		2nd year	70	55	27	162	0	165	130	106	133	159	133	99	103	3284

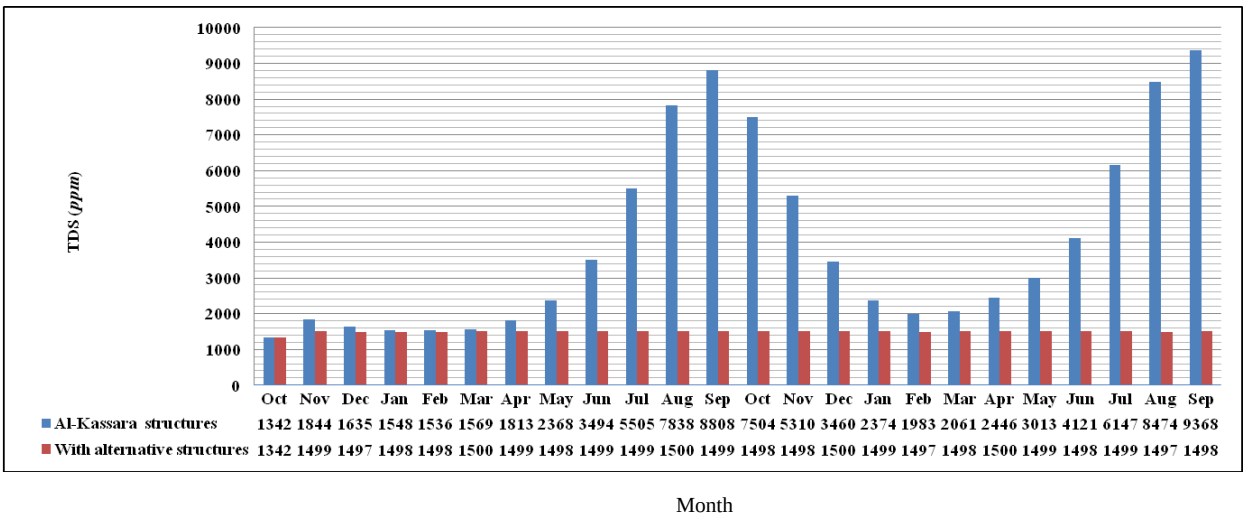

Figure 10. Monthly variation of TDS within the marsh with and without Al-Kassara structure.

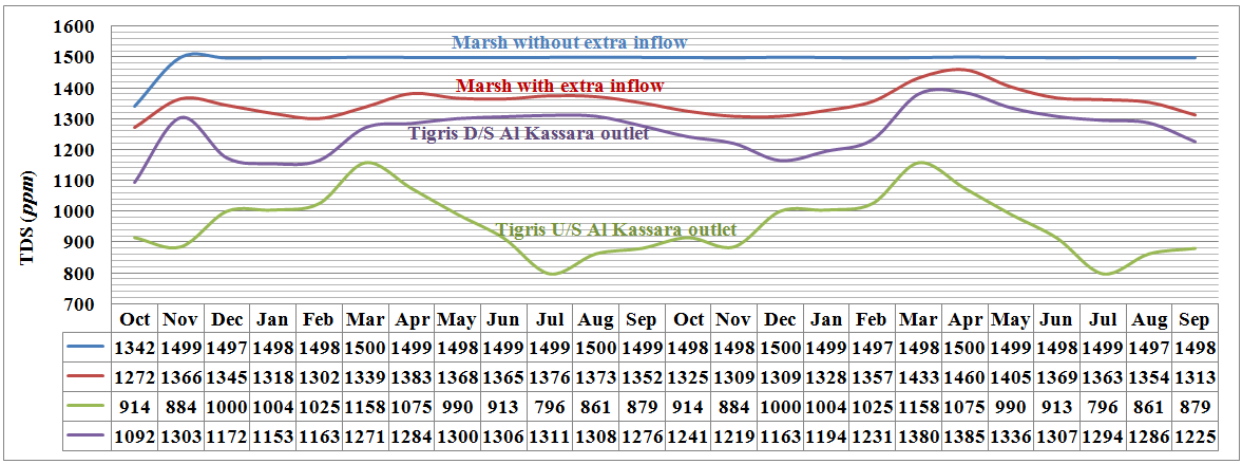

	Oct	Nov	Dec	Jan	Feb	Mar	Apr	May	Jun	Jul	Aug	Sep	Oct	Nov	Dec	Jan	Feb	Mar	Apr	May	Jun	Jul	Aug	Sep
Marsh without extra inflow	1342	1499	1497	1498	1498	1500	1499	1498	1499	1499	1500	1499	1498	1498	1500	1499	1497	1498	1500	1499	1498	1499	1497	1498
Marsh with extra inflow	1272	1366	1345	1318	1302	1339	1383	1368	1365	1376	1373	1352	1325	1309	1309	1328	1357	1433	1460	1405	1369	1363	1354	1313
Tigris U/S Al Kassara outlet	914	884	1000	1004	1025	1158	1075	990	913	796	861	879	914	884	1000	1004	1025	1158	1075	990	913	796	861	879
Tigris D/S Al Kassara outlet	1092	1303	1172	1153	1163	1271	1284	1300	1306	1311	1308	1276	1241	1219	1163	1194	1231	1380	1385	1336	1307	1294	1286	1225

Figure 11. Monthly variation of TDS in Al-Huweizah Marsh and Tigris River for the 1st scenario, (maximum TDS in the marsh is below 1500ppm).

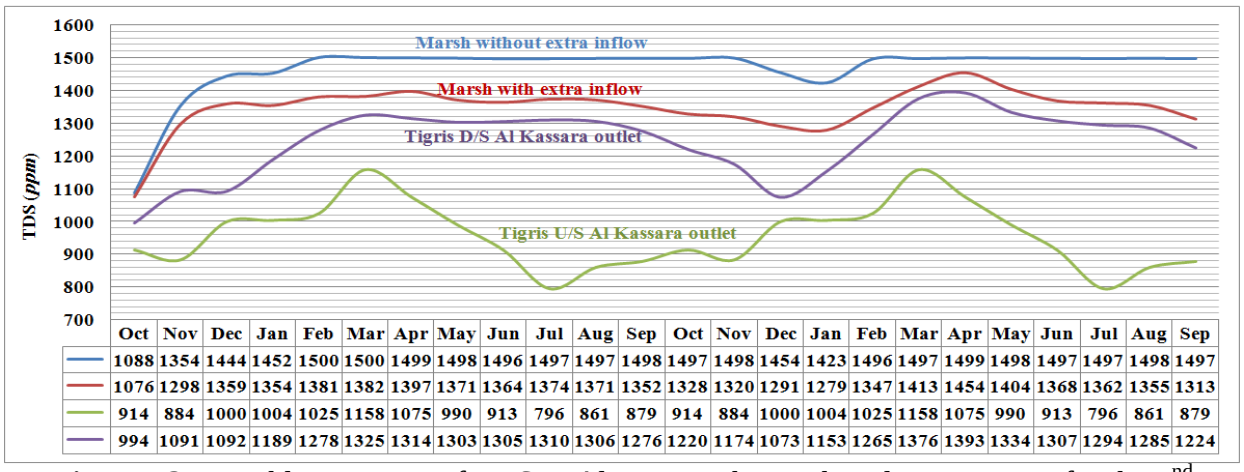

	Oct	Nov	Dec	Jan	Feb	Mar	Apr	May	Jun	Jul	Aug	Sep	Oct	Nov	Dec	Jan	Feb	Mar	Apr	May	Jun	Jul	Aug	Sep
Marsh without extra inflow	1088	1354	1444	1452	1500	1500	1499	1498	1496	1497	1497	1498	1497	1498	1454	1423	1496	1497	1499	1498	1497	1497	1498	1497
Marsh with extra inflow	1076	1298	1359	1354	1381	1382	1397	1371	1364	1374	1371	1352	1328	1320	1291	1279	1347	1413	1454	1404	1368	1362	1355	1313
Tigris U/S Al Kassara outlet	914	884	1000	1004	1025	1158	1075	990	913	796	861	879	914	884	1000	1004	1025	1158	1075	990	913	796	861	879
Tigris D/S Al Kassara outlet	994	1091	1092	1189	1278	1325	1314	1303	1305	1310	1306	1276	1220	1174	1073	1153	1265	1376	1393	1334	1307	1294	1285	1224

Figure 12. Monthly variation of TDS in Al-Huweizah Marsh and Tigris River for the 2nd scenario, (maximum TDS in the marsh is below 1500ppm).

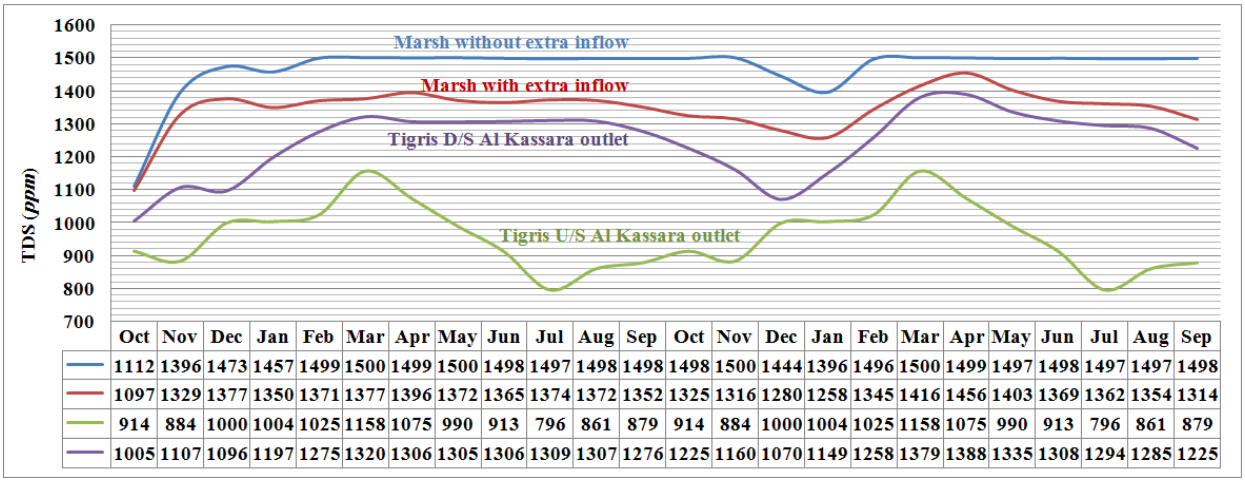

	Oct	Nov	Dec	Jan	Feb	Mar	Apr	May	Jun	Jul	Aug	Sep	Oct	Nov	Dec	Jan	Feb	Mar	Apr	May	Jun	Jul	Aug	Sep
Marsh without extra inflow	1112	1396	1473	1457	1499	1500	1499	1500	1498	1497	1498	1498	1498	1500	1444	1396	1496	1500	1499	1497	1498	1497	1497	1498
Marsh with extra inflow	1097	1329	1377	1350	1371	1377	1396	1372	1365	1374	1372	1352	1325	1316	1280	1258	1345	1416	1456	1403	1369	1362	1354	1314
Tigris U/S Al Kassara outlet	914	884	1000	1004	1025	1158	1075	990	913	796	861	879	914	884	1000	1004	1025	1158	1075	990	913	796	861	879
Tigris D/S Al Kassara outlet	1005	1107	1096	1197	1275	1320	1306	1305	1306	1309	1307	1276	1225	1160	1070	1149	1258	1379	1388	1335	1308	1294	1285	1225

Figure 13. Monthly variation of TDS in Al-Huweizah Marsh and Tigris River for the 3rd scenario, (maximum TDS in the marsh is below 1500ppm).

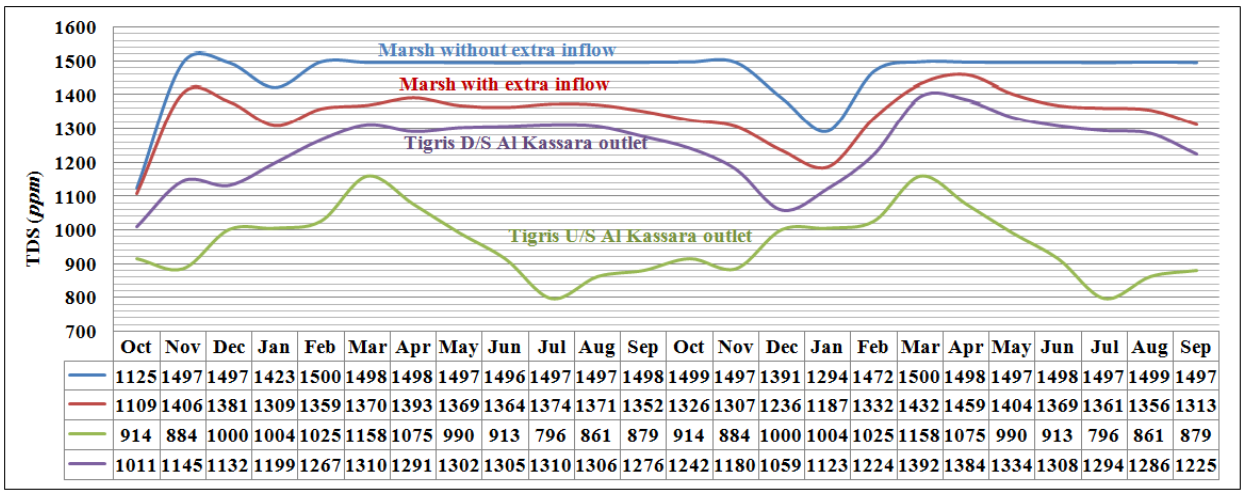

	Oct	Nov	Dec	Jan	Feb	Mar	Apr	May	Jun	Jul	Aug	Sep	Oct	Nov	Dec	Jan	Feb	Mar	Apr	May	Jun	Jul	Aug	Sep
Marsh without extra inflow	1125	1497	1497	1423	1500	1498	1498	1497	1496	1497	1497	1498	1499	1497	1391	1294	1472	1500	1498	1497	1498	1497	1499	1497
Marsh with extra inflow	1109	1406	1381	1309	1359	1370	1393	1369	1364	1374	1371	1352	1326	1307	1236	1187	1332	1432	1459	1404	1369	1361	1356	1313
Tigris U/S Al Kassara outlet	914	884	1000	1004	1025	1158	1075	990	913	796	861	879	914	884	1000	1004	1025	1158	1075	990	913	796	861	879
Tigris D/S Al Kassara outlet	1011	1145	1132	1199	1267	1310	1291	1302	1305	1310	1306	1276	1242	1180	1059	1123	1224	1392	1384	1334	1308	1294	1286	1225

Figure 14. Monthly variation of TDS in Al-Huweizah Marsh and Tigris River for the 4th scenario, (maximum TDS in the marsh is below 1500ppm).

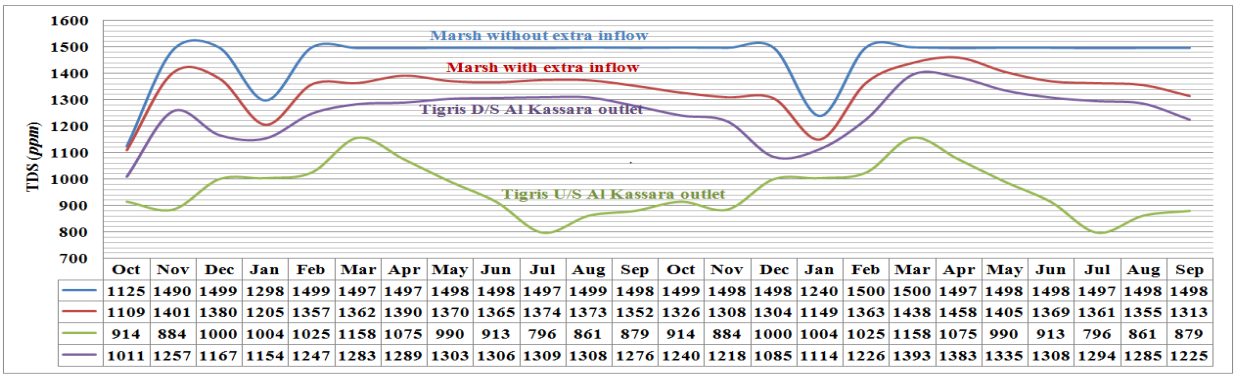

	Oct	Nov	Dec	Jan	Feb	Mar	Apr	May	Jun	Jul	Aug	Sep	Oct	Nov	Dec	Jan	Feb	Mar	Apr	May	Jun	Jul	Aug	Sep
Marsh without extra inflow	1125	1490	1499	1298	1499	1497	1497	1498	1498	1497	1499	1498	1499	1498	1498	1240	1500	1500	1497	1498	1498	1497	1498	1498
Marsh with extra inflow	1109	1401	1380	1205	1357	1362	1390	1370	1365	1374	1373	1352	1326	1308	1304	1149	1363	1438	1458	1405	1369	1361	1355	1313
Tigris U/S Al Kassara outlet	914	884	1000	1004	1025	1158	1075	990	913	796	861	879	914	884	1000	1004	1025	1158	1075	990	913	796	861	879
Tigris D/S Al Kassara outlet	1011	1257	1167	1154	1247	1283	1289	1303	1306	1309	1308	1276	1240	1218	1085	1114	1226	1393	1383	1335	1308	1294	1285	1225

Figure 15. Monthly variation of TDS in Al-Huweizah Marsh and Tigris River for the 5th scenario, (maximum TDS in the marsh is below 1500ppm).

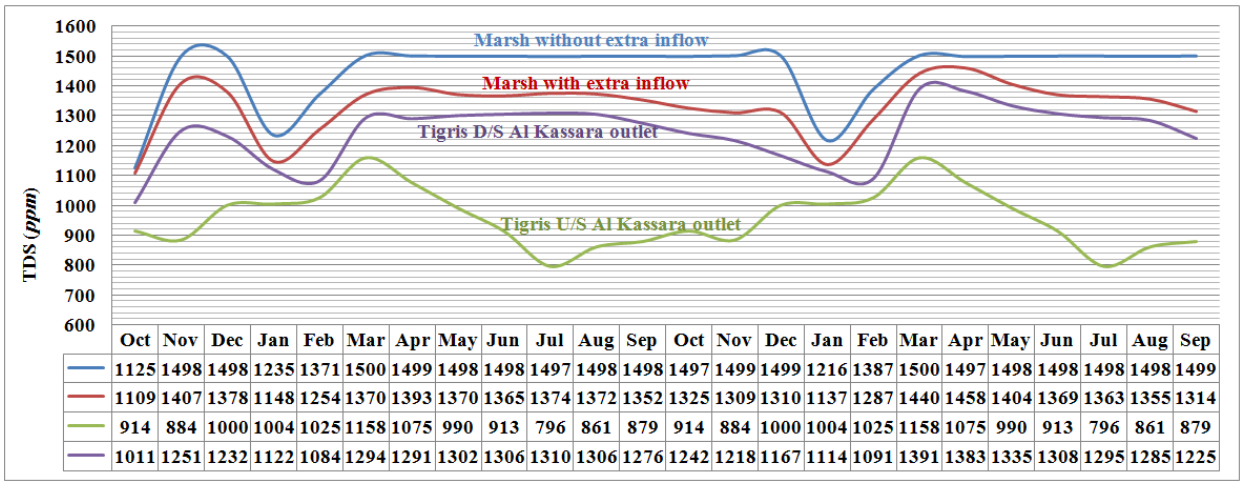

Figure 16. Monthly variation of TDS in Al-Huweizah Marsh and Tigris River for the 6th scenario, (maximum TDS in the marsh is below 1500ppm).

Table 6. Variation of TDS for Al-Huweizah Marsh before and after mixing with a share of Tigris River water (allocated to Shatt Al-Arab) for two consecutive years.

Maximum allowable TDS in *ppm*	Scenarios	Al-Huweizah Marsh			Tigris River		
		TDS, *ppm*		Percentage of improvement	TDS, *ppm*		Percentage of deterioration
		without extra inflow	with extra inflow		Before mixing	after mixing	
1500	S-1	1492	1353	9	958	1258	24
	S-2	1466	1346	8	958	1245	23
	S-3	1469	1347	8	958	1245	23
	S-4	1465	1343	8	958	1246	23
	S-5	1463	1341	8	958	1251	23
	S-6	1450	1332	8	958	1243	23
1750	S-1	1731	1483	14	958	1341	29
	S-2	1664	1464	12	958	1323	28
	S-3	1664	1462	12	958	1322	28
	S-4	1654	1455	12	958	1322	28
	S-5	1663	1460	12	958	1325	28
	S-6	1660	1456	12	958	1319	27
2000	S-1	1962	1596	19	958	1409	32
	S-2	1852	1561	16	958	1385	31
	S-3	1849	1558	16	958	1385	31
	S-4	1835	1547	16	958	1384	31
	S-5	1847	1554	16	958	1387	31
	S-6	1855	1556	16	958	1379	31

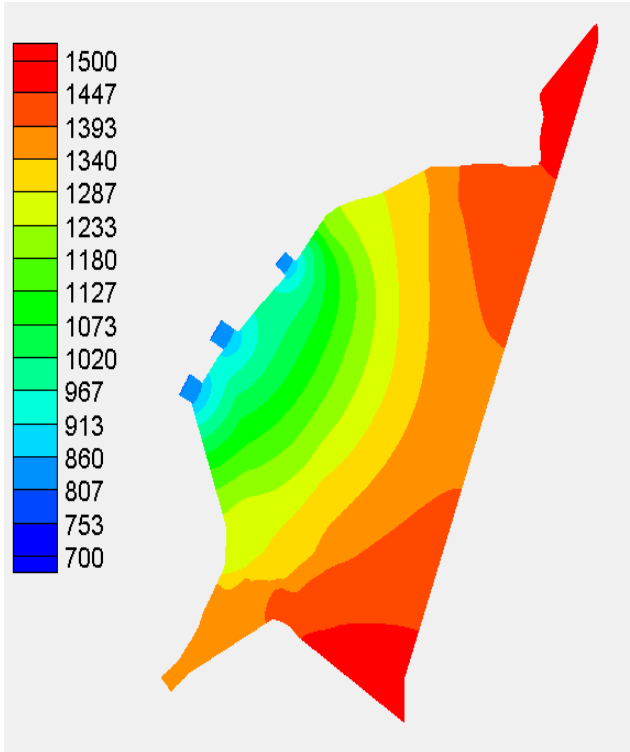

a. Autumn

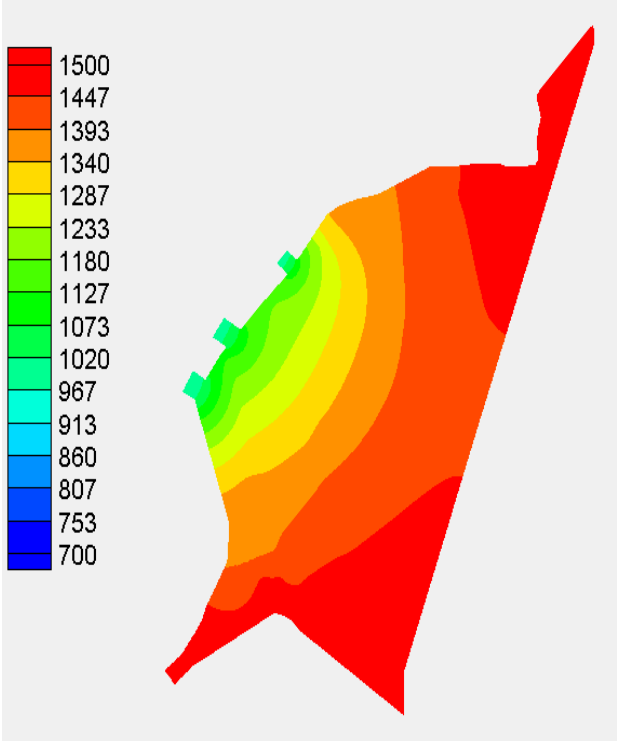

b. Winter

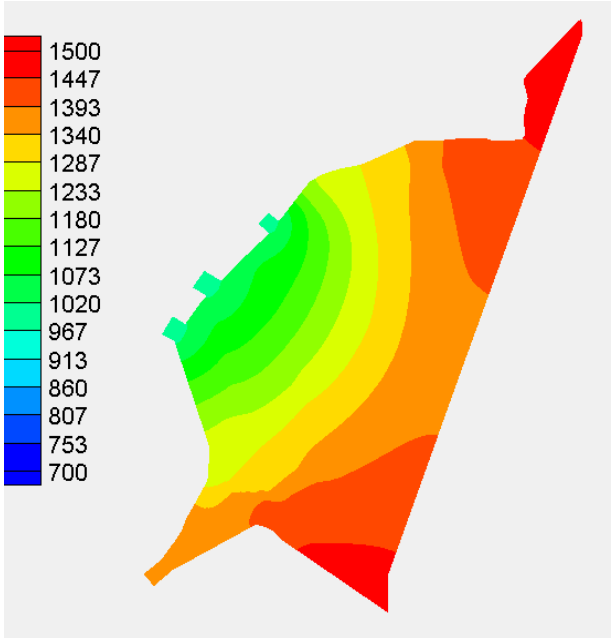

c. Spring

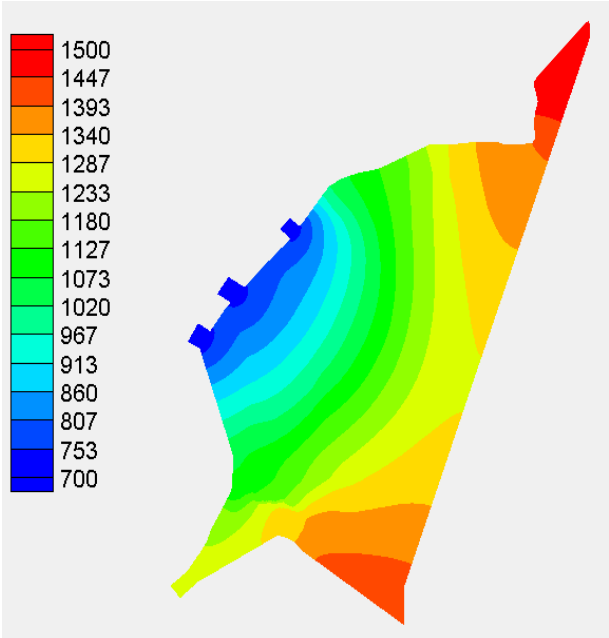

d. Summer

Figure 17. Seasonal TDS distribution within the marsh for 1st scenario without mixing with additional share.

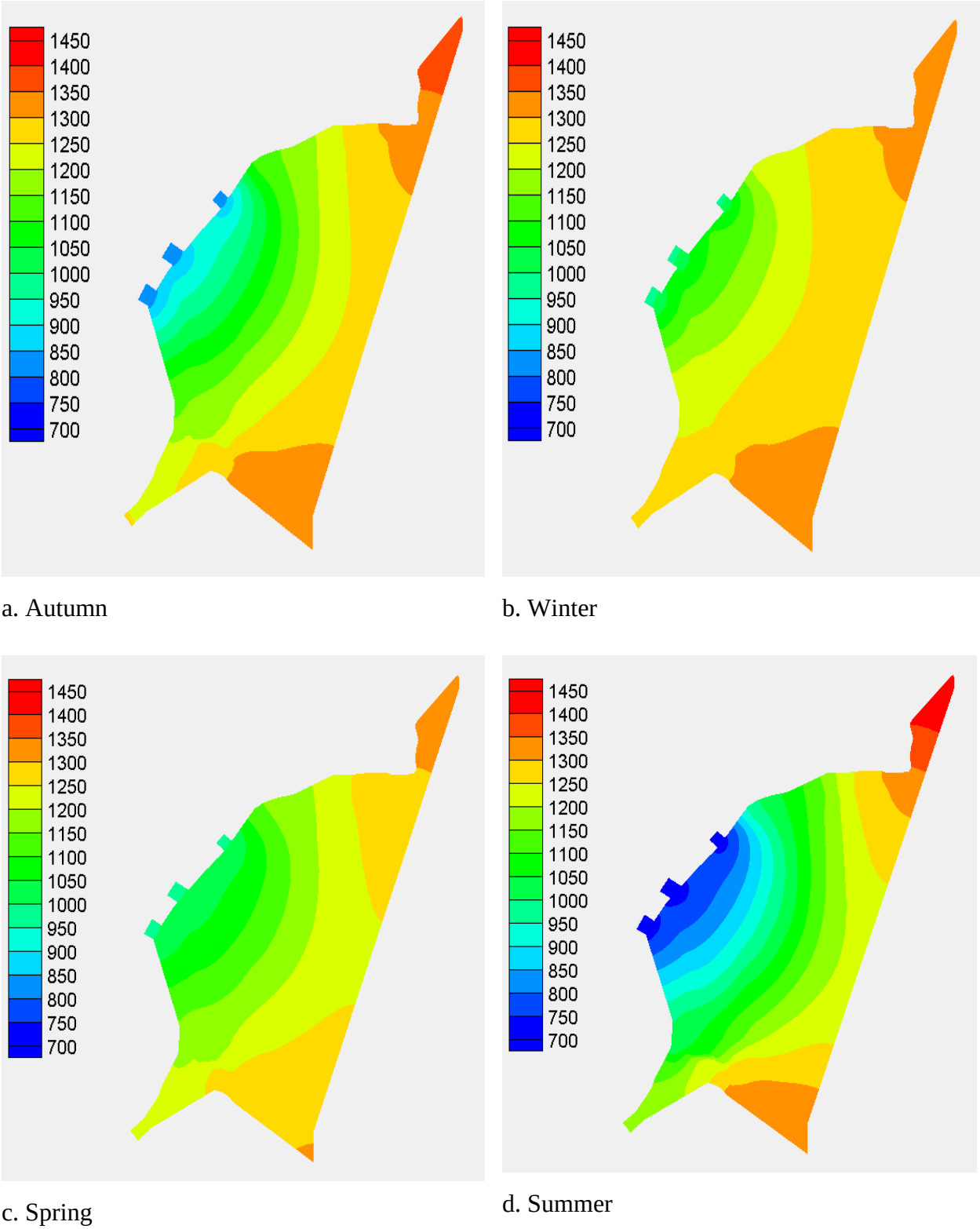

a. Autumn

b. Winter

c. Spring

d. Summer

Figure 18. Seasonal TDS distribution within the marsh for the 1st scenario with mixing with additional share.

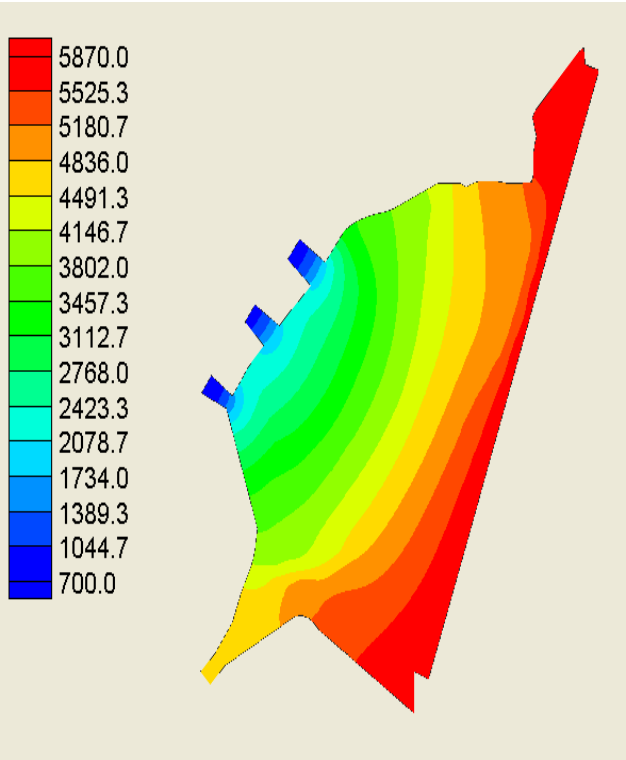

a. Autumn

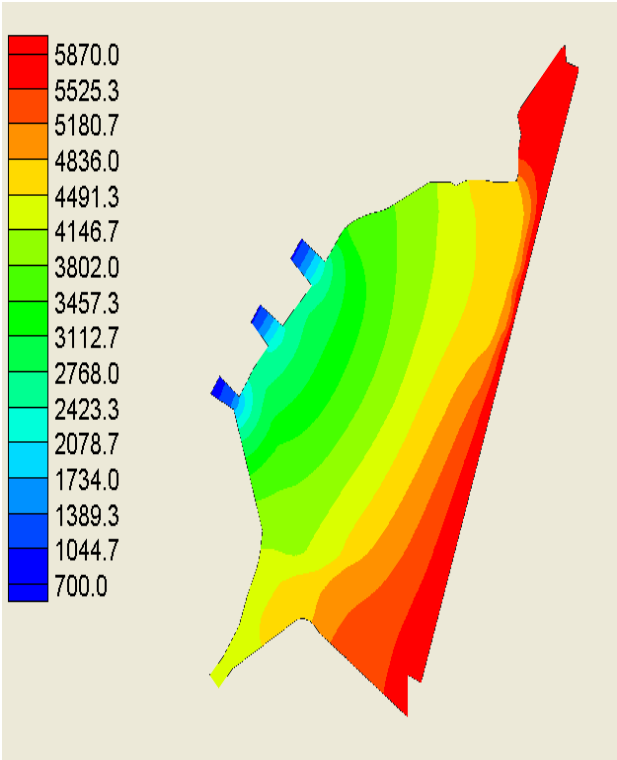

b. Winter

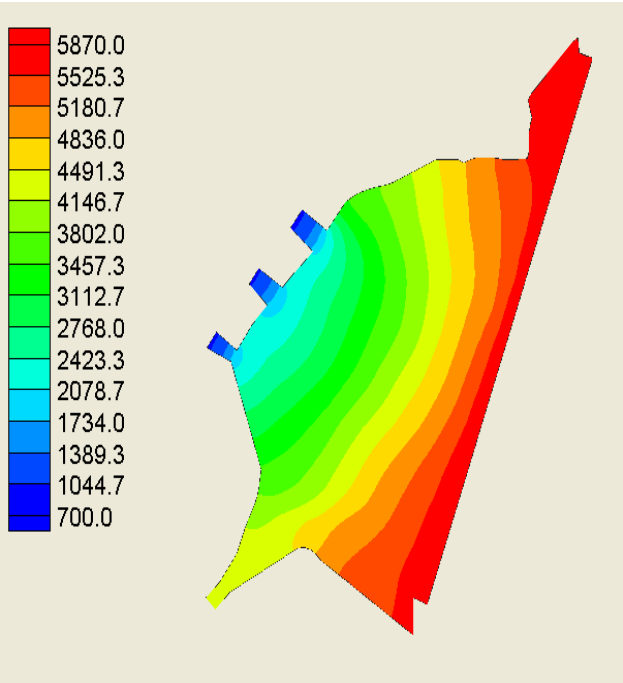

c. Spring

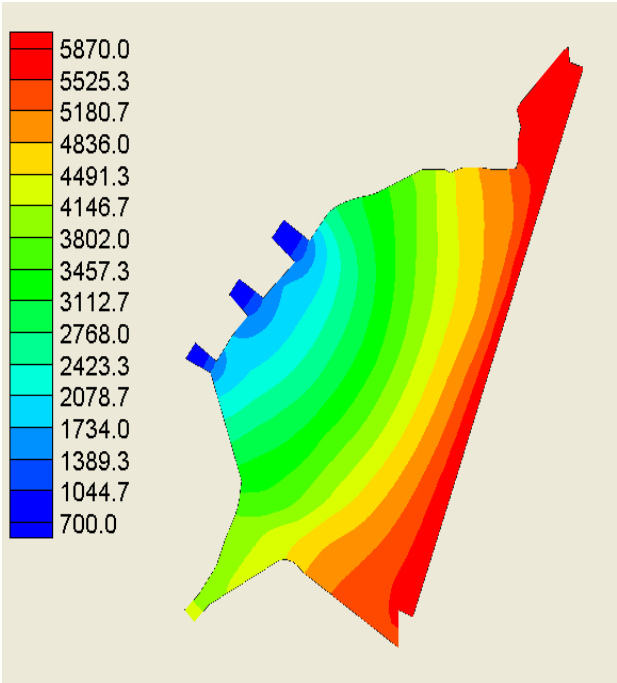

d. Summer

Figure 19. Seasonal TDS distribution within the marsh area with Iranian feeders for the 1st scenario without maxing with additional share.

Aeroelastic Flutter of Subsonic Aircraft Wing Section with Control Surface

Dr. Hatem Rahim Wasmi
Assistant Professor
College of Engineering - University of Baghdad
E-mail : hatemrwa@coeng.uobaghdad.edu.iq

Dr. Ali Abdul Mohsin Hasan
Assistant Professor
College of Engineering - University of University
E-mail dralicit@coeng.uobaghdad.edu.iq

Waleed Jasim Mhaimeed
Assistant Lecture
Al-Khwarizmi College of Engineering- University of Baghdad
E-mail waleed_jmm@kecbu.uobaghdad.edu.iq

ABSTRACT

Aeroelastic flutter in aircraft mechanisms is unavoidable, essentially in the wing and control surface. In this work a three degree-of-freedom aeroelastic wing section with trailing edge flap is modeled numerically and theoretically. FLUENT code based on the steady finite volume is used for the prediction of the steady aerodynamic characteristics (lift, drag, pitching moment, velocity, and pressure distribution) as well as the Duhamel formulation is used to model the aerodynamic loads theoretically. The system response (pitch, flap pitch and plunge) was determined by integration the governing equations using MATLAB with a standard Runge–Kutta algorithm in conjunction with Henon's method. The results are compared with previous experimental data. The results show that the aerodynamic loads and wing-flap system response are increased when increasing the flow speed. On the other hand the aeroelastic response led up to limit cycle oscillation when the flow equals or more than flutter speed.

Key word: aeroelastic, wing, control surface, aerodynamic

المرونة الهوائية لرفرفة مقطع جناح طائرة مع اسطح السيطرة في سرعة دون سرعة الصوت

د. حاتم رحيم وسمي
استاذ مساعد
كلية الهندسة-جامعة بغداد

د. علي عبدالمحسن حسن
استاذ مساعد
كلية الهندسة-جامعة بغداد

وليد جاسم محيميد
مدرس مساعد
كلية الهندسة الخوارزمي-جامعة بغداد

الخلاصة

الرفرفة في نظام المائع-هيكل لا يمكن تجنبها في ميكانيكيا الطائرات خاصة في الجناح واسطح السيطرة. نموذج جناح مع قلاب خلفي بثلاث درجات حرية تم تمثيله عدديا و نظريا. تم استخدام برنامج FLUENT لغرض حساب الخواص الايروديناميكية بالاضافة الى استخدام صيغة دوهامل لتمثيل الاحمال الايروديناميكية نظريا. تم تحديد الاستجابة الديناميكية لنظام جناح-قلاب من خلال استخدام الماتلاب (MATLAB) و التكامل بطريقة Runge-Kutta وتم مقارنة النتائج مع تجارب عملية سابقة. بينت النتائج ان الاحمال الايروديناميكية والاستجابة الديناميكية للجناح-قلاب تزداد بزيادة سرعة التدفق ومن ناحية اخرى فان استجابة المائع-هيكل تؤدي الى حالة محدد من التذبذب الدوري المستمر عندما تكون سرعة التدفق مساوية او اكثر من سرعة الرفرفة.

الكلمات الرئيسية: هيكل - مائع, الجناح, اسطح السيطرة, ايروداينمك .

1. INTRODUCTION

Aeroelasticity can be defined as the science which studies the mutual interaction between aerodynamic, elastic of structure and inertial forces. The analysis of dynamic characteristics of either complex or simple structures is quite developed nowadays as far as numerical and experimental methods are concerned. Hence, it is correct to state that reliability in aeroelastic calculations is strongly dependent on the correct evaluation of the aerodynamic operator, **Marques** and **Azevedo, 2007**.

Flutter is one of the most representative topics of aeroelasticity. Flutter is a complex phenomenon where structural modes are simultaneously coupled and excited by aerodynamic loads. In a more formal way, flutter is the condition where an aircraft component exhibits a self-sustained oscillatory behaviour at speeds higher than the critical one, **Wright, 1991**. With recent advances in CPU speeds, current research has turned toward the application of computational • fluid dynamics (CFD) models to the solution of these aeroelastic problems. By the use of an unsteady Euler or Navier–Stokes CFD algorithm coupled with a structural dynamics solver, the complete aeroelastic response of the structure can be predicted. However, the major limitation in applying such a CFD solution is the computational time required to run a full aeroelastic simulation due to the high dimensionality of even the simplest geometry, **Cowan et al, 2001.**

A three degree-of-freedom aeroelastic airfoil section with control surface free play were modeled theoretically as a system of piecewise linear state-space models. They were investigated by **Conner et al., 1997and Liu et al., 2001.** The wing flutter calculated by integrated computational fluid dynamics (CFD) and computational structural dynamics (CSD) method. The coupled CFD–CSD method simulates the aeroelastic system directly on the time domain to determine the stability of the aeroelastic system. Computational fluid dynamics (CFD) solver technique for modeling unsteady aerodynamic forces used in time-domain aeroelastic analysis. The system identification as was predicted by **Cowan et al., 2001. Tricky, 2002.** It could accurately model the unsteady aerodynamic forces for complex aerospace structures of practical interest**. They** presented the effects of a free play structural nonlinearity on an aeroelastic in the three-degree-of-freedom airfoil model. **Dowell et al., 2003** analyzed the effective of leading and trialing edges control surfaces on the airfoil. He used a simple control strategy, then used a combination of leading-and trailing-edge control surface rotations to maintain lift and roll effectiveness and to minimize control surface rotations. **Le Maître et al., 2003,** investigated numerically the aeroelastic flutter derivative of a two-dimensional airfoil by means of Navier–Stokes simulation solver employed influence matrix techniques to determine the exact boundary conditions and a conformal mapping of the physical space. **Ardelean et al., 2006,** designed a new piezoelectric actuator which meets the requirements for trailing edge flap actuation in both stroke and force to study the aeroelastic control of wings with trailing-edge control surfaces. Wind tunnel experiments showed that air flow has a little influence on flap deflection, suggesting good actuation authority. **Marqui et al., 2006,** investigated the flutter parameters for two-degree-of-freedom flexible mounting rigid wings tests with in wind tunnel. The plunging and pitching flutter obtained with this experimental system was described as the combination of structural bending and torsion vibration modes. **Marques and Azevedo, 2007,** used the unsteady computational fluid dynamics tool to calculate the aerodynamic operator for aeroelastic analysis of lifting surfaces in the transonic regime. The flow problem was modeled by the two-dimensional Euler equations using the finite volume method applied in an unstructured grid context. The state-dependent Riccati equation method was derived for aeroelastic response and flutter suppression with control surface free play and Theodorsen theory for aerodynamics of

airfoil section with trialing edge flap were studies by **Li et al., 2010. Ghommem et al., 2012**, studied the response of aeroelastic system consisting of a plunging and pitching rigid airfoil, supported by nonlinear translational and torsional springs, used a three-dimensional code based on the unsteady vortex lattice method to predict the unsteady aerodynamic loads for coupled model of the wing flow interaction. **Vasconcellos et al., 2012,** used a different representations (discontinuous, polynomial and hyperbolic tangent) for control surface freeplay nonlinearity in a three degree of freedom aeroelastic system. **Abdelkefi et al., 2013,** investigated analytically and experimentally the dynamics of an aeroelastic system consisting of two degrees of freedom airfoil section supported by a linear spring in the plunge degree of freedom and a nonlinear spring in the pitch degree of freedom and as well the aerodynamic loads was represented by the quasi-steady and an unsteady formulations. **Saxena** and **Agrawal, 2013** used FLUENT software to study the flow separation over airfoil at different angle of attacks. **Kim** and **Chang, 2014,** studied the effect of a low Reynolds number on the aerodynamic characteristics of a pitching NACA0012 airfoil. The result showed that the phase angle, at which boundary-layer events occurred, was in an inverse proportion to the increase in Reynolds number.

The goals of the present work can be summarized as follow**:**

(a)- A CFD tool is applied with structured two-dimensional meshes around airfoil with control surface to obtain the aerodynamic characteristics at different freestream speed, angles of attack and flap angles.

(b) Predict the flutter speed of the three degrees-of-freedom airfoil section with trialing edge flap.

(c) Investigate the aeroelastic response of plunging, pitching and flap pitching for the airfoil with control surface at freestream speed under, equal and above flutter speeds. The aerodynamic loads are approximated using the Duhamel formulation.

The validity of flutter speed prediction and aeroelastic response are determined through comparison with the experiments of **Conner et al., 1997.** Good agreement was determined.

2. COMPUTATIONAL FLUID DYNAMICS (CFD)

Computational fluid dynamics is a subject that has played an extremely important role in recent studies of aerodynamics. The possibility of numerically treating a broad range of phenomena which occur in flows over bodies of practically any geometry has numerous advantages over experimental determinations, such as greater flexibility together with time and financial resource savings. However, obtaining more reliable numerical results for a growing number of situations has been one of the major recent challenges in many science fields **Marques** and **Azevedo, 2007.** The simulation of the flow was carried out by running ANSYS FLUENT software which based on the solution of the Navier-Stokes equations using the finite-volume method under the same value of the response of airfoil for Angle Of Attack (AOA) and flap pitching angles.

The grid generator ANSYS FLUENT CFD is used to mesh the domain. **Fig.1** presents the airfoil element domain. To increase the grid points at the surface of the wall, skewed mesh should be avoided.

3. AEROELASTIC MODEL

The aeroelastic system modeled of three degrees-of-freedom, two dimension NACA 0012 wing section, constrained to move with degrees of freedom, namely the plunge (h), pitch (α), and control surface angle (β) motions, as shown in **Fig. 2.** The elastic axis is located at distance *ab*

from the mid chord. The mass center of wing section is located at distance $x_\alpha b$ from the elastic axis. Both distances are positive when measured towards the airfoil flap. The cb and $x_\beta b$ distances are the distance from the hinge line of the flap and distance from the mass center of the flap to the mid chord respectively.

The non-dimensional aeroelastic equation of motion for the airfoil with trailing edge control surface are given by **Li et al., 2010.**

$$r_\alpha^2\ddot{\alpha} + \left[r_\beta^2 + (c-a)x_\beta\right]\ddot{\beta} + x_\alpha\ddot{h} + r_\alpha^2\omega_\alpha^2 F(\alpha) = \frac{M_\alpha}{(mb^2)} \qquad (1-a)$$

$$\left[r_\beta^2 + (c-a)x_\beta\right]\ddot{\alpha} + r_\beta^2\ddot{\beta} + x_\beta\ddot{h} + r_\beta^2\omega_\beta^2 G(\beta) = \frac{M_\beta}{(mb^2)} \qquad (1-b)$$

$$x_\alpha\ddot{\alpha} + x_\beta\ddot{\beta} + \left(\frac{m_t}{m}\right)\ddot{h} + \omega_h^2 h = \frac{L}{(mb)} \qquad (1-c)$$

Where

$$x_\alpha = \frac{S_\alpha}{m_w b}, \qquad x_\beta = \frac{S_\beta}{m_w b}, \qquad r_\alpha^2 = \frac{I_\alpha}{m_w b^2}, \qquad r_\beta^2 = \frac{I_\beta}{m_w b^2}$$

The matrix of structural damping is created in this model according to **Conner et al., 1997**, the natural frequency $\omega_i = \sqrt{\lambda_i}$, where λ_i is eigenvalue and the eigenvector matrix are obtained from the left-hand side structure components of equations (1-a, 1-b and 1-c). Then the system modal mass matrix $\boldsymbol{M_{mod}} = \boldsymbol{\Lambda^T M_s \Lambda}$ and the modal damping matrix $\boldsymbol{B_{mod}}$ can be calculated as

$$\mathbf{B_{mod}} = \begin{bmatrix} 2m_\alpha\omega_\alpha\varsigma_\alpha & 0 & 0 \\ 0 & 2m_\beta\omega_\beta\varsigma_\beta & 0 \\ 0 & 0 & 2m_h\omega_h\varsigma_h \end{bmatrix} \qquad (2)$$

Where m_α, m_β *and* m_h are the values at the diagonal entries of $\boldsymbol{M_{mod}}$ and $\varsigma_\alpha, \varsigma_\beta$ *and* ς_h are the measured damping ratios. The structure damping matrix can be determined as
$\boldsymbol{B_s} = (\boldsymbol{\Lambda^T})^{-1}\boldsymbol{B_{mod}}(\boldsymbol{\Lambda})^{-1}$.

The Theodorsen approach is used to model the unsteady aerodynamic force and moments L, M_α *and* M_β in incompressible flow were calculated and written as by Theodorsen, 1935**.**

$$M_\alpha = -\rho b^2\left\{\pi\,(1/(2-a))Ub\dot{\alpha} + \pi b^2(1/(8+a^2))\ddot{\alpha} + (T_4+T_{10})U^2\beta + (T_1 - T_8 - (c-a)T_4 + (1/2)T_{11})Ub\dot{\beta} - [T_7 + (c-a)T_1]b^2\ddot{\beta} - a\pi b\ddot{h}\right\} + 2\rho U b^2\pi((a+1)/2)C(k)\left(U\alpha + \dot{h} + b(1/(2-a))\dot{\alpha} + 1/\pi T_{10}U\beta + b(1/2\pi)\,T_{11}\dot{\beta}\right) \qquad (3)$$

$$M_\beta = -\rho b^2\{\left(-2T_9 - T_1 + T_4((a-1)/2)\right)Ub\dot{\alpha} + 2T_{13}b^2\ddot{\alpha} + (1/\pi)U^2\beta(T_5 - T_4T_{10}) - \left((1/2\pi)\right)Ub\dot{\beta}T_4T_{11} - (1/\pi)T_3b^2\ddot{\beta} - T_1b\ddot{h}\} \times \rho Ub^2T_{12}C(k)\left(U\alpha + \dot{h} + b(1/(2-a)\dot{\alpha} + 1/\pi T_{10}U\beta + b((1/2\pi))T_{11}\dot{\beta}\right) \quad (4)$$

$$L = -\rho b^2\left(U\pi\dot{\alpha} + \pi\ddot{h} - \pi ba\ddot{\alpha} - UT_4\dot{\beta} - T_1b\ddot{\beta}\right) - 2\pi\rho UbC(k)\left(U\alpha + \dot{h} + b(1/(2-a))\dot{\alpha} + 1/\pi T_{10}U\beta + b(1/2\pi)T_{11}\dot{\beta}\right) \quad (5)$$

Where the T functions are given in Appendix A

The aerodynamic force and moment in Eqs. (3)-(5) are dependent on reduced frequency *k*. so Eqs. (1-a) - (1-c) are restricted to simple harmonic oscillation. Aerodynamics in Eq. (3)–(5) is dependent on Theodorsen's function, *C(k)*, where *k* is the non-dimensional reduced frequency of harmonic oscillation. So the aerodynamics is restricted to simple harmonic motion. In order to simulate arbitrary motion of the airfoil, the loading associated with Theodorsen's function *C(k)f(t)* is replaced by the Duhamel formulation in the time domain and written as, **Li et al., 2010.**

$$L_c = C(k)f(t) = f(0)\emptyset(\tau) + \int_0^\tau \frac{\partial f(\sigma)}{\partial\sigma}\phi(\tau-\sigma)d\sigma \quad (6)$$

Where

$$f(t) = U\alpha + \dot{h} + b\left(\frac{1}{2-a}\right)\dot{\alpha} + 1/\pi T_{10}U\,\beta + b\left(\frac{1}{2\pi}\right)T_{11}\dot{\beta} \quad (7)$$

and $\phi(\tau)$ is Wagner function. In this work, convenient approximation of Sears is used as

$$\phi(\tau) \approx c_0 - c_1e^{-c_2\tau} - c_3e^{-c_4\tau} \quad (8)$$

the coefficient in equation (8) are $c_1 = 0.165,\ c_2 = 0.0455,\ c_3 = 0.335\ and\ c_4 = 0.3$. in order to simplify the Theodorsen function, rewrite the Duhamel integral using integration by parts ,

$$L_c = f(\tau)\phi(0) + \int_0^\tau f(\sigma)\frac{\partial\phi(\tau-\sigma)}{\partial\sigma}\,d\sigma \quad (9)$$

And following the state space method proposed by **Li et al., 2010**.

$$L_c = (c_0 - c_1 - c_3)f(t) + c_2c_4(c_1 + c_3)\bar{x} + (c_1c_2 + c_3c_4)\dot{\bar{x}} \quad (10)$$

With the introduction of two augmented variables $x_{a1} = \bar{x},\ x_{a2} = \dot{\bar{x}}$, Eq. (1) can be product as

$$(\mathbf{M_s} - \mathbf{M_{NC}})\ddot{\mathbf{x}} + \left(\mathbf{B_s} - \mathbf{B_{NC}} - \frac{\mathbf{1}}{\mathbf{2RS_2}}\right)\dot{\mathbf{x}} + \left(\mathbf{K_s} - \mathbf{K_{NC}} - \frac{\mathbf{1}}{\mathbf{2RS_1}}\right)\mathbf{x} - \mathbf{RS_3x_a} = \mathbf{0} \quad (11)$$

Where $x = [\alpha \quad \beta \quad h/b]^T$ and $x_a = [x_{a1} \quad x_{a2}]^T$.
In the state space form, this equation is written as

$$\dot{\mathbf{X}} = \mathbf{A}(\mathbf{X})\mathbf{X} \tag{12}$$

The solution Algorithm and definition of the matrices in Eqs. (11) and (12) are presented in Appendix B.

4. RESULTS AND DISCUSSIONS

4.1 Aerodynamic Results

Once the meshes are generated, the next step will be simulations. There were more than 70 cases run in ANSYS/Fluent which different AOA from -6 to 6 degree with step 2 degrees as well as the same pitch angle differential with all AOA step and different freestream velocities. These simulations yielded solutions to the two dimensional flow fields around the airfoil with trailing edge flap.

The lift and drag forces at (4) degrees angle of attack (α) as well as various flap pitching angles (β) are analyzed with increasing velocity and it is cleared that lift force increases when velocity is increased as well decreasing of flap pitching angle as shown in **Fig. 3- a and Fig. 3- b. These figures** show that the drag forces were affected slightly with values of (β) while they increased with increasing the velocity. Pitching moments are greatly influenced with (β) as well increased with velocity as shown in **Fig. 3-c** which showed when (β = 2°) that the pitching moment was increased but decreased when velocity more than 15 m/s.

The simulations were run with limit of responses of varying angles of attack from (-6 to +6 degree step 2) and flap angles from (-6 to +6 degree step 2) at velocity equals to (25 m/s) for the analytical calculated flutter. The AOA and flap angle variation play important role in the lift generation as well as the effect of drag and pitching moments. For maximization of the lift in the aircraft wings, the trialing edge flap angle should be down, while the AOA must be increasing as verified in **Fig. 4-which** shows increasing of lift force with decreasing the flap angle (down) while AOA increased. **Fig. 4-b** shows that the increasing of drag force was happened when the AOA was increased-decreased. Flap angles as well as the result observed that the increment of drag force with swing of airfoil more than variation of flap angle, nevertheless the behavior of the ratio of lift-drag asymptotic to lift force demeanor as shown in **Fig. 4-c**. Finally **Fig. 4-d** illustrates the effect of AOA and flap angle changing to the pitching moment. They were important factors were affecting to airfoil swing result, and that shows that the flap angle was significantly affected to the pitching moment.

Pressure contours at different velocities variations are shown in **Fig. 5**. It can be seen that the pressure increased when the freestream velocity increased with values of 5 to 30 step 5 m/s at zero flap angle and 4 degree AOA. At the same time, pressure contours around the airfoil also was varied. For maximization of the lift in the aircraft wings, the pressure should be low at the upper surface of the wings and high at the bottom surface of the wing. **Fig. 6** shows the pressure distribution around the airfoils at zero flap angle, calculated flutter velocity and swing AOA up/down were zero value. Results show that the pressure on the lower surface of the airfoil is high and the pressure over the upper surface is low only at positive AOA and vice versa which produces inverse lift generation.

Fig. 7 clarifies the dynamic pressure contour at flutter velocity, zero AOA and swing flap angle which affect to the pressure contour even at zero AOA and symmetric airfoil. The velocity distribution around airfoil was affected by the swing of AOA and flap angle. **Fig. 8** displays the velocity contour at swing of AOA and flap angle. It is clear that the maximum velocity was 31 m/s when AOA and flap angles at the same sign i.e. all up or down because it is a case of symmetry. On the other hand when the angles reverse, the maximum velocity was 34 m/s and this is asymmetry case.

4.2 Aeroelastic Response Results

The prediction of flutter speed was obtained by using the results of Eq.(11) where the flutter speed is the value of speed corresponding to the speed at zero real part of one or more eigenvalues which determined to be 25 m/s and compared with **Conner et al 1997** which was (20.6 m/s experimentally and 23.9 m/s analytically).The parameters used in the mathematical models were taken from **Conner et al 1997** and listed as follows: a = -0.5, b = 0.127 m, c = 0.5, s = 0.52 m, $m_T = 1.2895\ kg,\ I_\alpha = 0.01347\ kgm^2, I_\beta = 0.0003264 kgm^2, x_\alpha = 0.434, x_\beta = 0.01996, k_h = 2818.8\ N/m, S_\alpha = 0.08587\ kg\ m, S_\beta = 0.00395\ kg\ m, \rho = 1.225\ kg/m^3, \varsigma_1 = 0.01626, \varsigma_2 = 0.0115\ and\ \varsigma_3 = 0.0113$. The variations of the real parts with wind speed are shown in **Fig 9. Fig. 10** shows the comparison between present work and experimental **Conner et al 1997** for the response of pitch angle at wind speed 6.75 m/s.

Using MATLAB with fourth order Runge-Kutta method has been used for numerical integration with a time step of (0.001) to solve the state-space Eq. (12). Time histories of plunge response were shown in **Fig. 11.** The response determined with wind speed under, equal and above flutter speed. The limit cycle oscillation of plunge amplitude is similar to harmonic motion with speed under and equal flutter speed as well with above flutter speed but the peak value was irregulars peak value with the complete cycle. This may be due to the relatively high unstable values of the plunge displacement.

Pitch angle response converges with time at velocity 20 m/s which less than flutter speed as shown in **Fig. 12** which also shows the limit cycle oscillation continue at the same peak value (4 degree) and this happens at flutter velocity because the damping is zero at this speed where the value of pitching angle reached to (7.4 degree) at 30 m/s wind speed.

Fig. 13 presents the response of flap pitching angle at degree with time at velocity 20 m/s, 25 m/s and 30 m/s it can be noted that the time histories was increased in the peak value and limit cycle oscillation to be irregulars at wind speed above flutter speed value. The rates versus displacement of plunge, pitching and flap pitching are shown in **Figs. 14, 15 and 16** respectively at calculated flutter speed. It can be shown that the behavior and values are symmetry about stable zone which zero value as that the harmonically response which Theodorsen assumptions.

5. CONCLUSION

The objective of this study is to investigate the aeroelastic modeling and flutter analysis of a three degrees-of-freedom airfoil section with trialing edge flap. The steady CFD solution was used to present the aerodynamic characteristics with different freestream speeds, AOA and flap angle, which showed that affect on the aerodynamic forces and moment especially flap angle factor as shown from the pressure distribution and velocity distribution diagrams. Using a standard state-space approximation to Theodorsen aerodynamics for two-dimensional incompressible flow to the fourth order Runge-Kutta numerical integration of a piecewise linear

system to predict the aeroelastic response and flutter behavior which verified with previous experimental work. For experimental test of wing flutter response at velocity over flutter speed was difficult because the risk of model shattering, theoretical investigation discuss the limit cycle oscillation which irregulars response behavior at over flutter speed. The study compared this irregular response with harmonically time histories which obtained at velocity under and equal flutter speeds.

REFERENCES.

- Abdelkefi, A., Vasconcellos, R., Nayfeh, A. H. and Hajj, M. R., 2013, *An analytical and Experimental Investigation into Limit-Cycle Oscillations of An Aeroelastic System*, Nonlinear Dynamics Journal, Vol. 71, PP.159–173.

- Ardelean, E. V., Mark A. M., Cole, D. G and Clark, R. L. 2006 *Active Flutter Control with V-Stack Piezoelectric Flap Actuator* Journal of Aircraft Vol. 43, No. 2 PP. 482-486.

- Balaguru, I., Sendhilkumar, S. 20013 *Numerical and Experimental Investigation on Aerodynamic Characteristics of SMA Actuated Smart Wing Model* International Journal of Engineering and Technology (IJET) Vol. 5, No. 5, PP. 3813-3818.

- Bohbot, J., Garnier, J., Toumit, S. and Darracq, D. 2001 *Computation of the Flutter Boundary of an Airfoil with a Parallel Navier-Stokes Solver,* American Institute of Aeronautics and Astronautics 39th Aerospace Sciences Meeting & Exhibit (AIAA 2001-0572).

- Conner, M. D., Tang, D. M., Dowell, E. H and Virgin, L. N., 1997, *Nonlinear Behavior of A Typical Airfoil Section with Control Surface Freeplay :* A Numerical and Experimental Study, Journal of Fluids and Structures Vol. 11 , PP. 89 – 109.

- Cowan, T. J, Arena, A. S., Jr. and Gupta, K. K 2001, *Accelerating Computational Fluid Dynamics Based Aeroelastic Predictions Using System Identification*, Journal of Aircraft Vol. 38, No. 1, PP. 81-87.

- Dong-HaKima, and Jo-WonChang, 2014, *Low-Reynolds-number Effect on the Aerodynamic Characteristics of a Pitching NACA0012 Airfoil*, Aerospace Science and Technology Vol. 32, PP. 162–168.

- Dowell, E. H., Bliss, D. B. and Clark, R. L 2003, *Aeroelastic Wing with Leading- and Trailing-Edge Control Surfaces,* Journal of Aircraft Vol. 40, No. 3, PP. 559-565.

- Edwards , J . W ., Ashley , H . & Breakwell , J . V . 1979, *Unsteady Aerodynamic Modeling For Arbitrary Motions* . *AIAA Journal* **17 ,** 365 – 374 .

- Fazelzadeh, S. A. and Kalantari, H. A. 2009, *Bending-Torsional Flutter of Wings with an Attached Mass Subjected to a Follower Force*, Journal of Sound and Vibration Vol. 323 PP. 148–162.

- Ghommema, M., Abdelkefi, A., Nuhait,A. O. and .Hajj, M. R. 2012, *Aeroelastic Analysis and Nonlinear Dynamics of an Elastically Mounted Wing*, Journal of Sound and Vibration Vol. 331, PP. 5774–5787.

- Le Maître, O. P., Scanlan, R. H. and Knio, O. M., 2003, *Estimation of the Flutter Derivatives of an NACA Airfoil by Means of Navier–Stokes Simulation*, Journal of Fluids and Structures, Vol. 17, PP. 1-28.

- Li, D., Guo, S., and Xiang, J. 2010, *Aeroelastic Dynamic Response and Control of an Airfoil Section with Control Surface Nonlinearities*, Journal of Sound and Vibration Vol. 329, PP. 4756–4771.

- Liu, F., Cai, J., Zhu, Y., Tsai, H. M. and Wong, A. S 2001 *Calculation of Wing Flutter by a Coupled Fluid-Structure Method*, Journal of Aircraft Vol. 38, No. 2, PP 334-342.

- Marques, A. N and Azevedo, J. L 2007, *Application of CFD-Based Unsteady Forces for Efficient Aeroelastic Stability Analyses*, Journal of Aircraft Vol. 44, No. 5, PP. 1499-1512.

- Marqui, C. D., Rebolho, C. D., Belo E. D. and Marques F. D, 2006, *Identification of Flutter Parameters for a Wing Model*, J. of the Braz. Soc. of Mech. Sci. & Eng Vol. XXVIII, No. 3, PP. 339-346.

- McNamara, J. J. and Friedmann, P. P. 2007, *Flutter-Boundary Identification for Time-Domain Computational Aeroelasticity*, AIAA Journal Vol. 45, No. 7, PP. 1546-1555.

- Parker, G. H., Maple, R. C., and Beran, P. S., 2007, *Computational Aeroelastic Analysis of Store-Induced Limit-Cycle Oscillation*, Journal of Aircraft Vol. 44, No. 1 PP. 48-59.

- Platanitis, G., and Strganac,T. W., 2004, *Control of a Nonlinear Wing Section Using Leading- and Trailing-Edge Surfaces*, Journal of Guidance, Control, and Dynamics Vol. 27, No. 1, PP. 52-58.

- PrabhakaraRao, P. and Sampath.V., 2014, *CFD Analysis on Airfoil at High Angles of Attack*, International Journal of Engineering Research Vol. 3, No.7, PP. 430-434.

- Rajakumar, S., Ravindran., D., 2010, *Computational Fluid Dynamics of Wind turbine Blade at Various Angles of Attack and Low Reynolds Number*, International Journal of Engineering Science and Technology Vol. 2, No 11, PP. 6474-6484.

- Saxena, G. and Agrawal, M., 2013, *Aerodynamic Analysis of NACA 4412 Airfoil Using CFD*, International Journal of Emerging Trends in Engineering and Development Vol.4, No. 4, PP. 416-423.

- Srivastava, R and Reddy, T. S. 1997 *Forced Response Analysis Using a Two-Dimensional Multistage Euler Aeroelastic Solver*, Journal of Aircraft Vol. 34, No. 1, PP. 114-119.

- Theodorsen, T., 1935, *General Theory of Aerodynamic Instability and The Mechanism of Flutter*, NACA Report 496.

- Trickeyl, S. T., Virgina, N. and Dowell, E. 2002, *The Stability of Limit-Cycle Oscillations in a Nonlinear Aeroelastic System* ,Proceedings: Mathematical, Physical and Engineering Sciences, Vol. 458, No. 2025. PP. 2203-2226.

- Vasconcellos, R., Abdelkefi, A, Marques, F. D and Hajj, M. R. 2012, *Representation and Analysis of Control Surface Freeplay Nonlinearity*, Journal of Fluids and Structures Vol. 31, PP. 79–91.

- Woodgate, M. A., Badcock, K. J., Rampurawala, A. M., Richards, B. E. and Nardini, D. 2005, *Aeroelastic Calculations for the Hawk Aircraft Using the Euler Equations*, Journal of Aircraft Vol. 42, No. 4,PP. 1005-1012.

- Wright, J.R., 1991, "*Introduction to Flutter of Winged Aircraft*", von Karman Institute for Fluid Dynamics, Lecture series 01: Elementary Flutter Analysis.

NOMENCLATURE

AOA	angle of attack, degree
a	non-dimensional distance from airfoil mid-chord to elastic axis
b	airfoil semi-chord
Pa	Pascal, N/m^2
s	wing span, m
C(k)	generalized Theodorsen function
CPU	central processor unit
c	non-dimensional distance from airfoil mid-chord to the control surface hinge line
c_i	coefficients of Wagner's function
h	plunge displacement, m
k	reduced frequency
L	aerodynamic lift
M_α, M_β	aerodynamic moment of wing-aileron and of aileron
m	mass of wing-aileron (per unit span), kg/m
m_t	total mass of wing-aileron and support blocks (per unit span), kg/m
r_α	radius of gyration of wing-aileron
r_β	reduced radius of gyration of aileron
t	time, sec
U	free stream velocity, m/s
$\boldsymbol{X}_a$	vector of augmented variables
x_α	non-dimensional distance from airfoil elastic axis to center of mass

x_β non-dimensional distance from aileron hinge line to center of mass
α pitch angle about the elastic axis, degree
β aileron displacement about the hinge line, degree
ρ density of air, kg/m^3
ς damping ratio
τ time delay
ω uncoupled natural frequency, rad/s

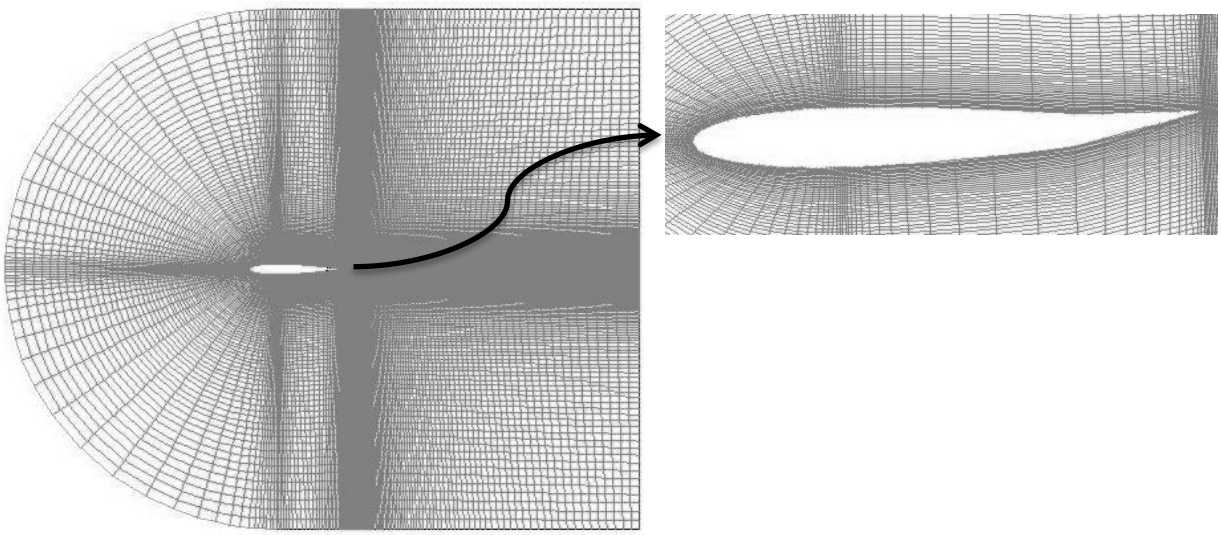

Figure1. Airfoil domain mesh.

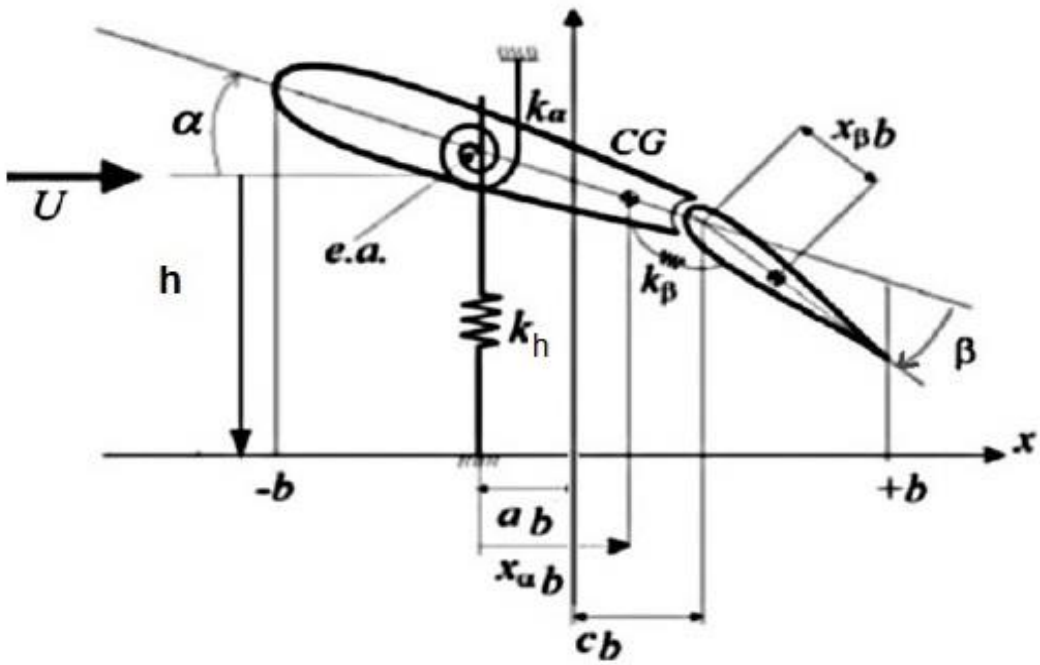

Figure 2. Schematic of airfoil section with trialing edge flap.

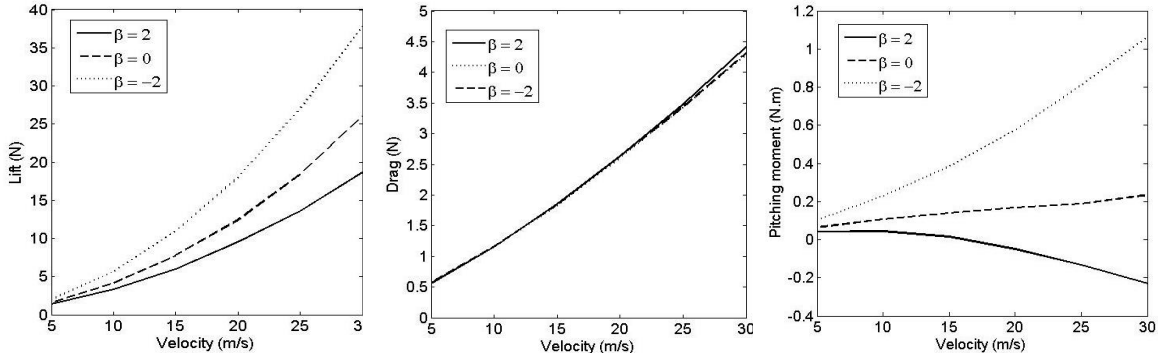

(a) (b) (c)

Figure 3. Variations of (a) the lift forces, (b) the drag forces and (c) the pitching moment as function of freestream velocity for various flap pitching angle (β).

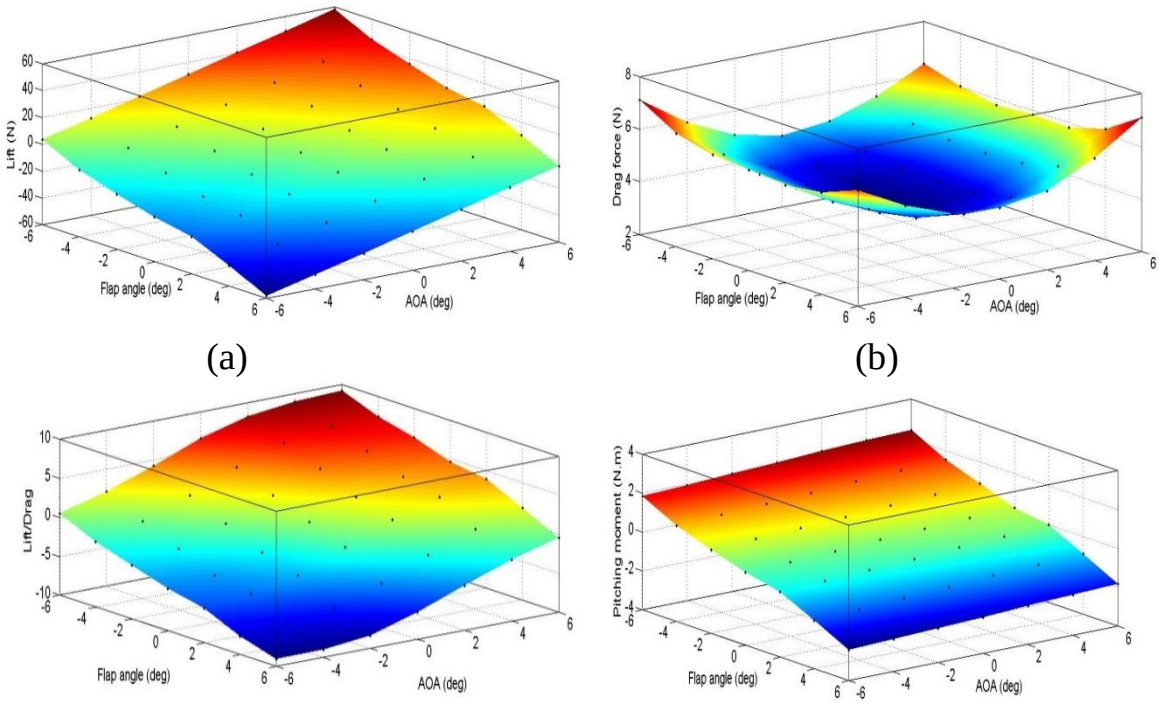

(a) (b)

(c) (d)

Figure 4. Effect of increasing –decreasing of angle of attack and flap angle to the (a) lift force (b) drag force (c) lift/drag ratio and (d) pitching moment.

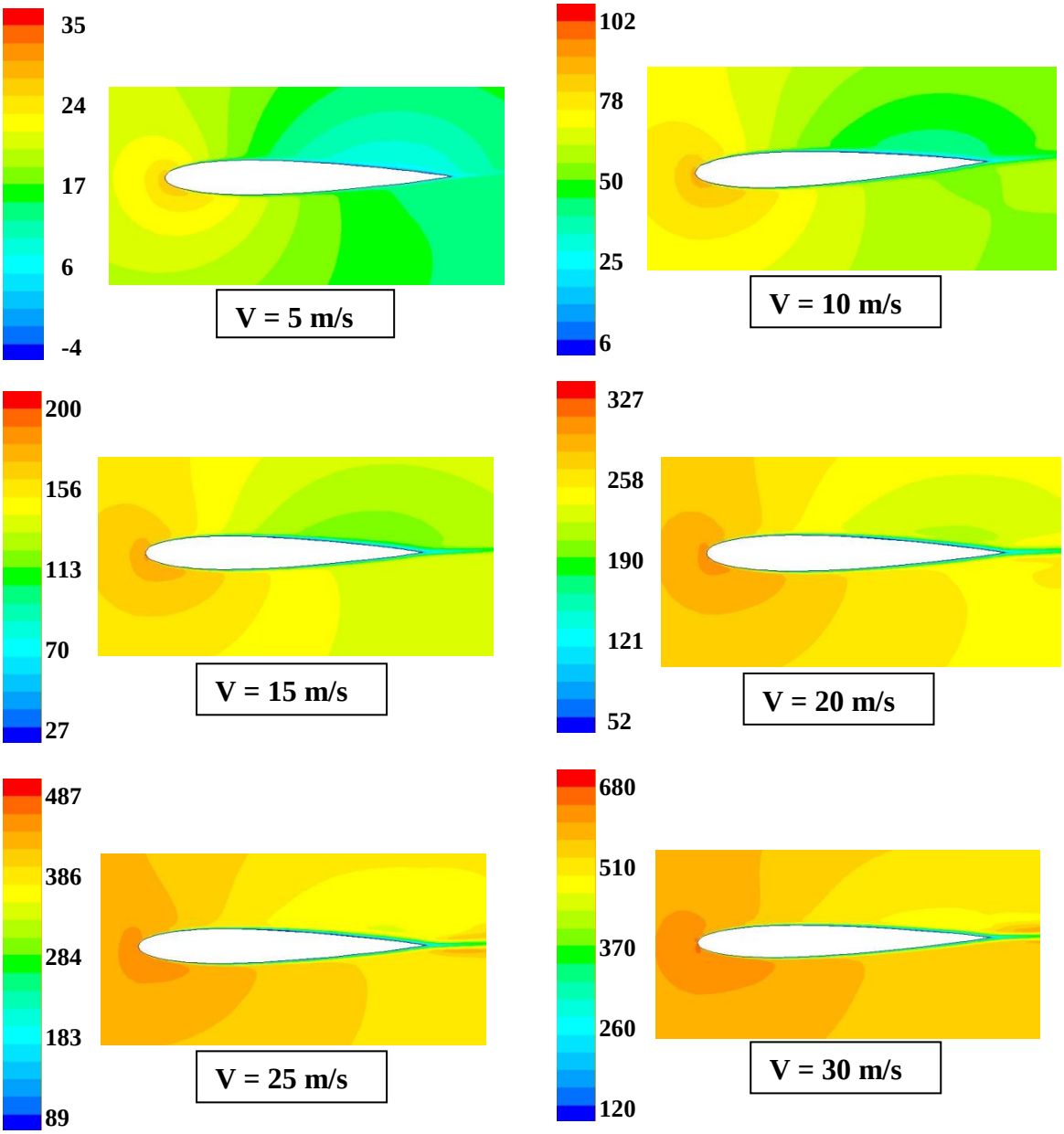

Figure 5. Contours of total pressure (Pa) around the airfoil at different free stream velocity, zero flap angle and 4 degree AOA.

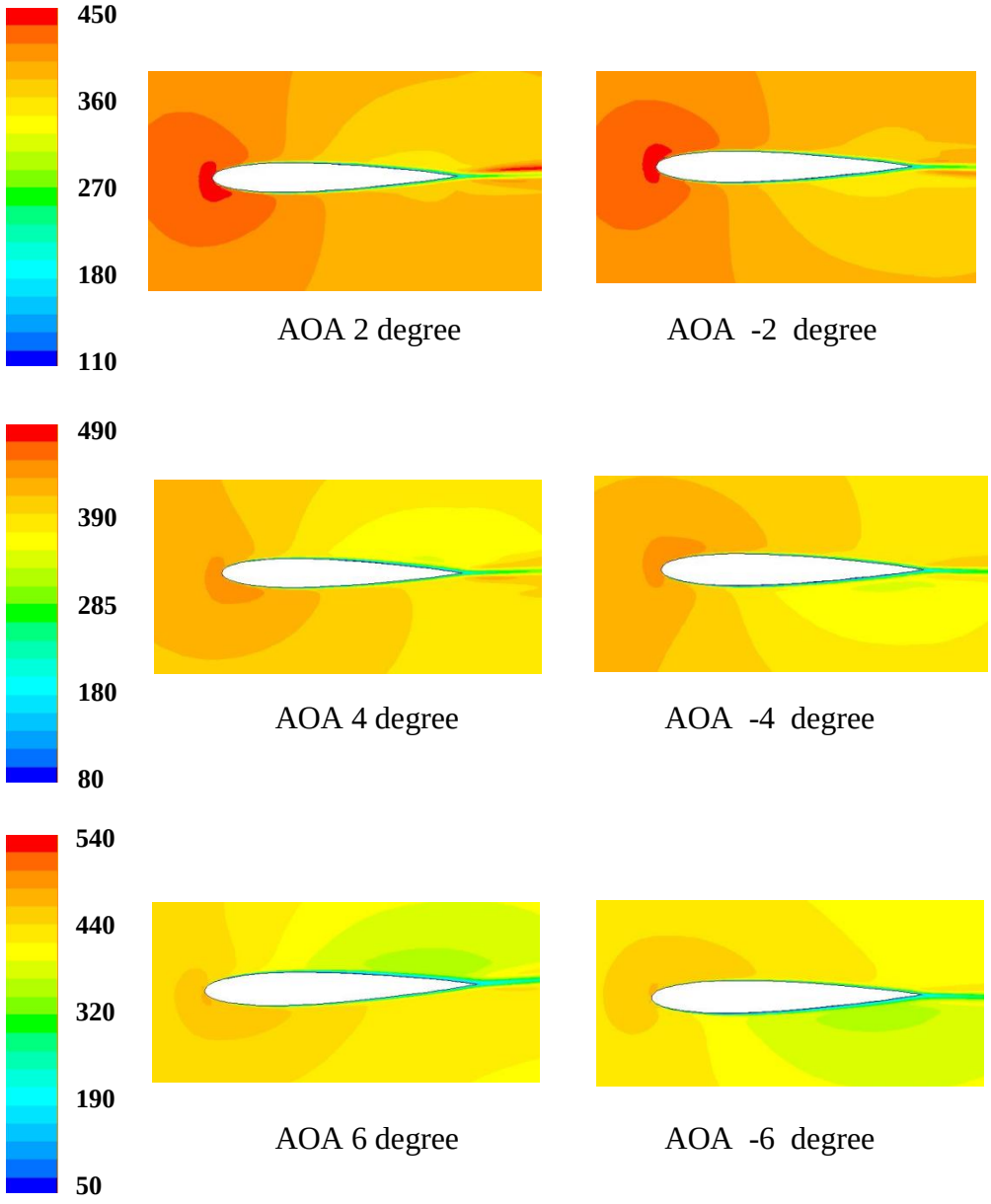

Figure 6. Contours of total pressure (Pa) around the airfoil at different AOA, zero flap angle and 25 m/s air speed.

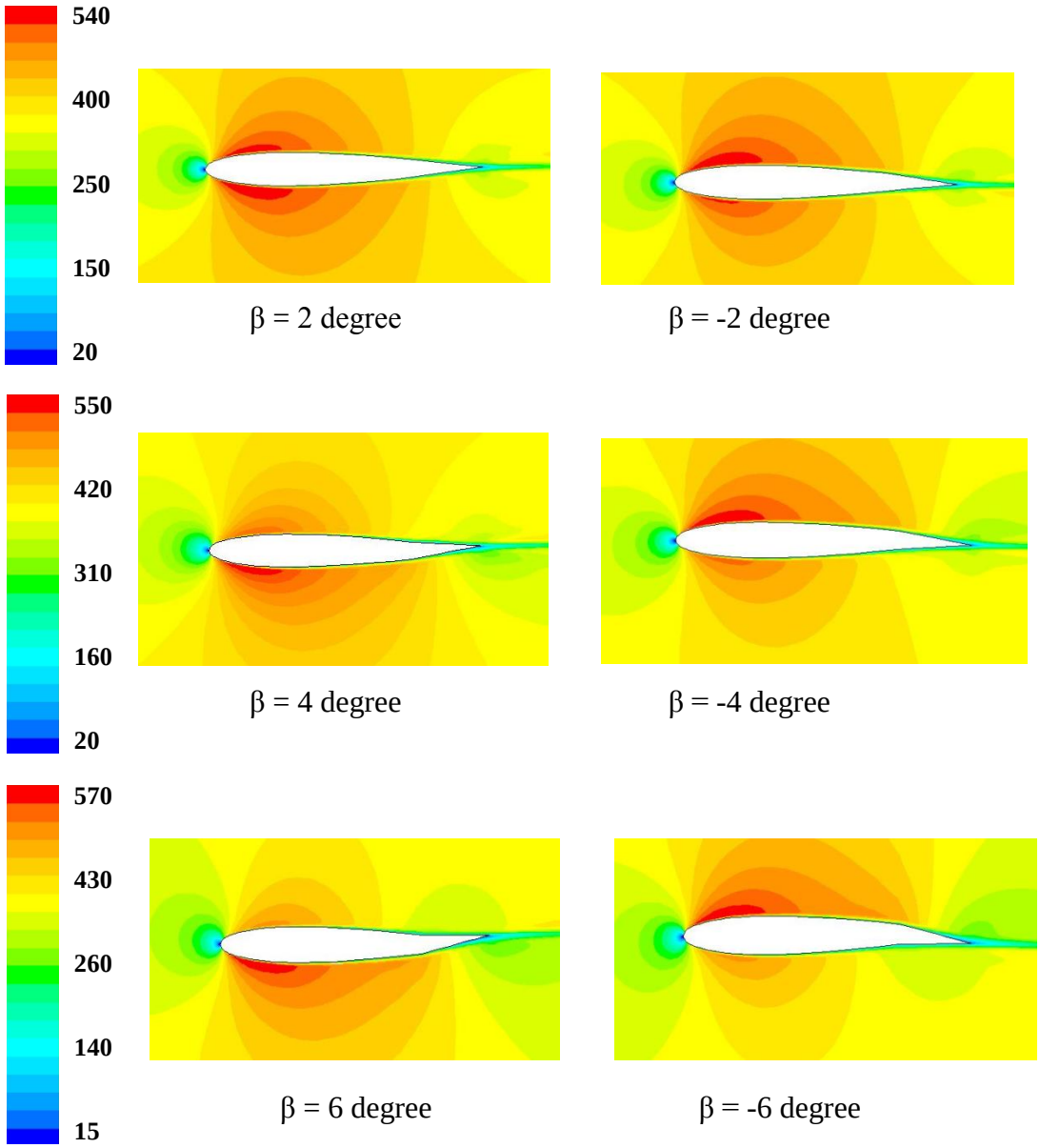

Figure 7. Dynamic pressure (Pa) around the airfoil at different flap angle, zero AOA and 25 m/s air speed.

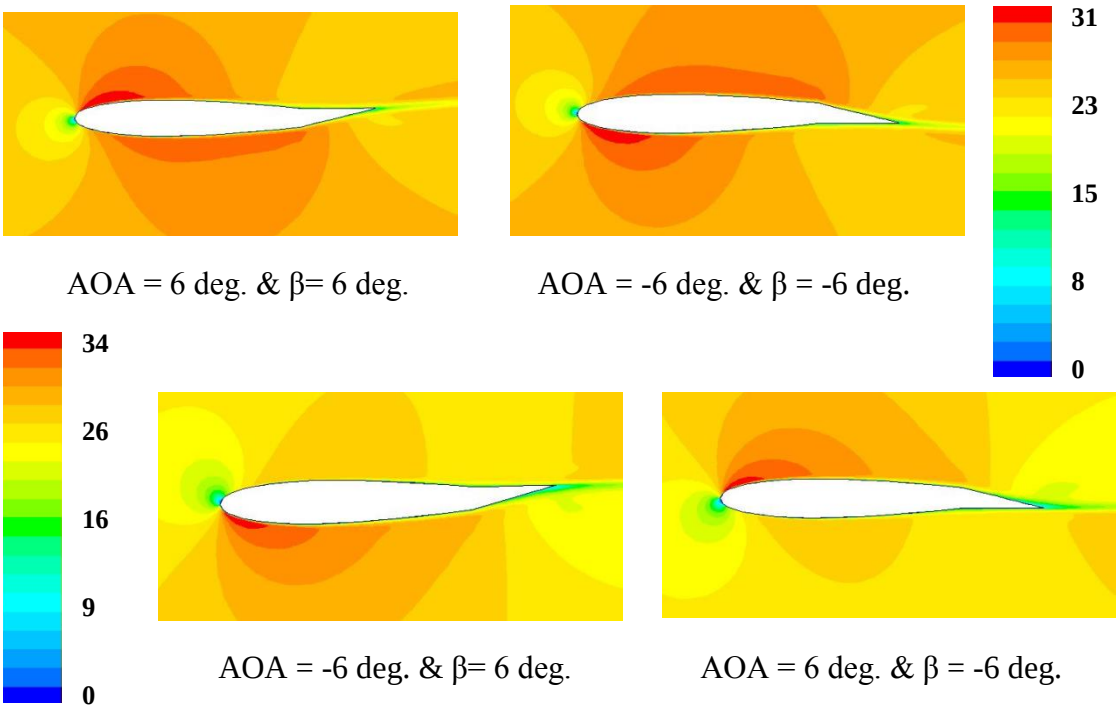

Figure 8. Velocity (m/s) distribution around the airfoil at fluttering profile for V=25.

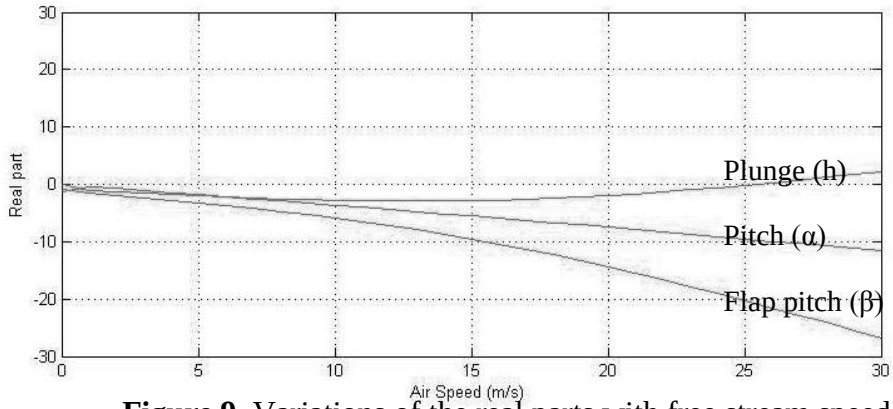

Figure 9. Variations of the real parts with free stream speed.

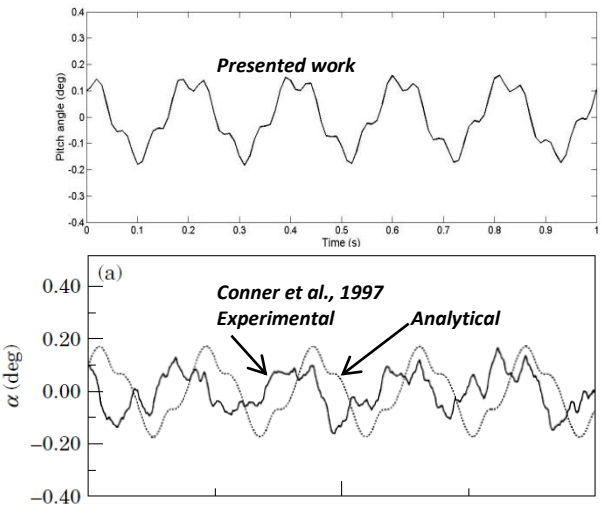

Figure 10. Pitch time histories for the low frequency limit-cycle at $U = 0.27\ U_f$.

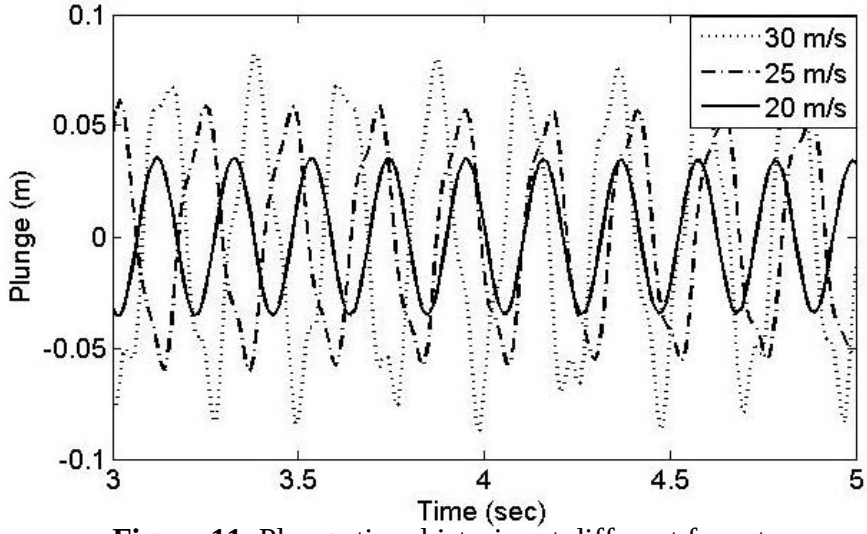

Figure 11. Plunge time histories at different free stream.

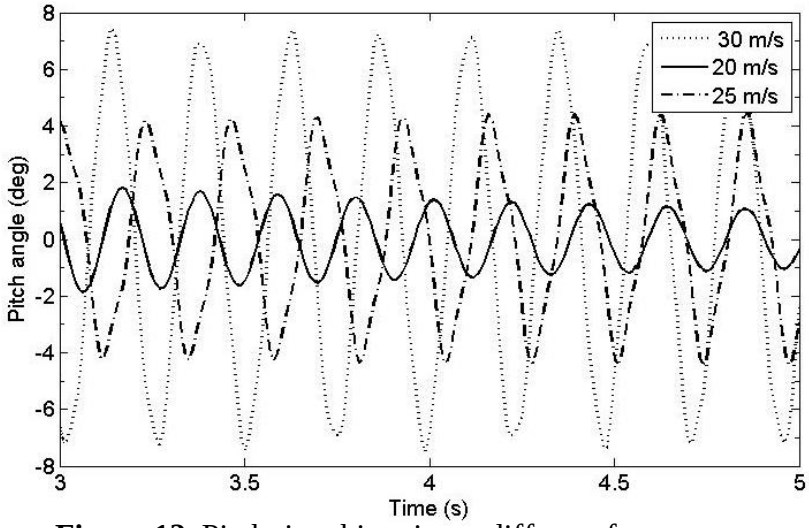

Figure 12. Pitch time histories at different free stream.

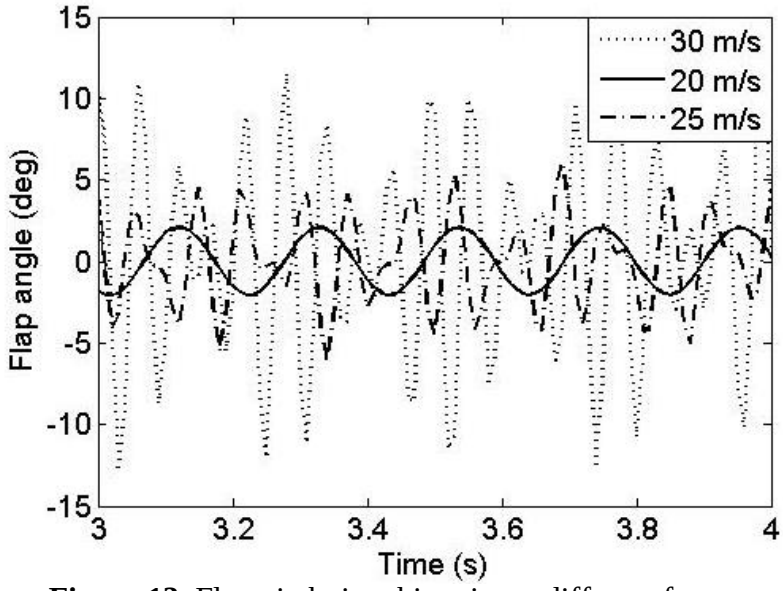

Figure 13. Flap pitch time histories at different free stream.

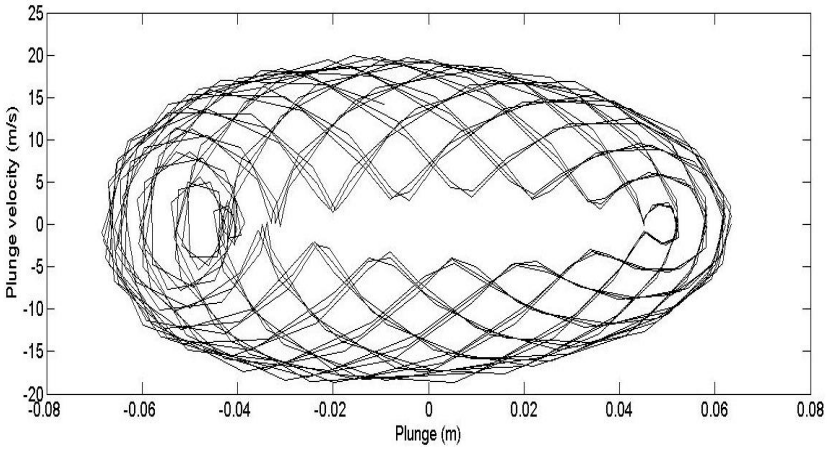

Figure 14. Phase portraits of plunge at flutter speed.

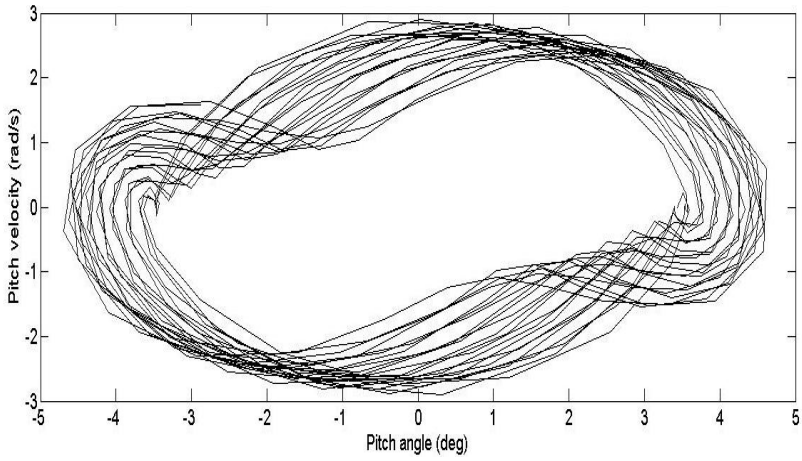

Figure 15. Phase portraits of pitch at flutter speed.

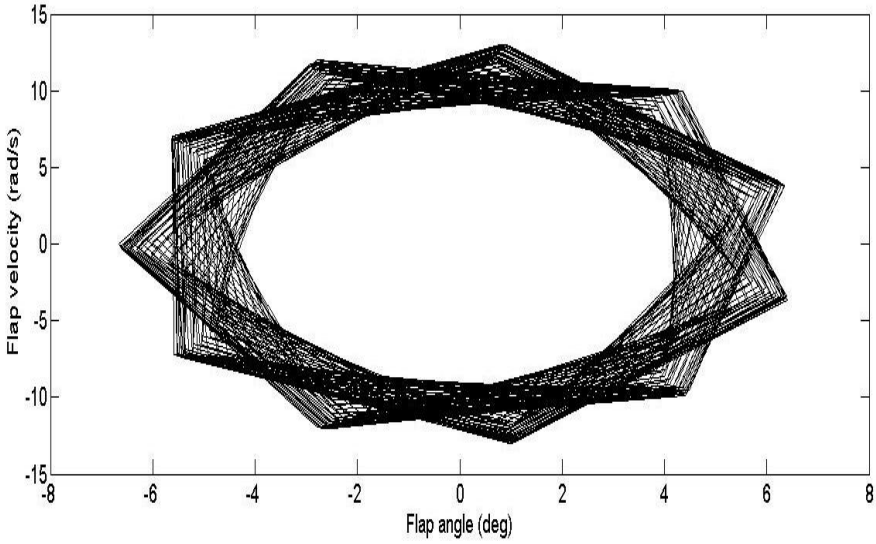

Figure 16. Phase portraits of flap pitch at flutter speed.

APPENDIX A. Theodorsen Constant in Eqs. (3)-(5)

$$T_1 = -\frac{1}{3}\sqrt{1-c^2}(2+c^2) + \cos^{-1} c$$

$$T_3 = -\left(\frac{1}{8}\right)c(1-c^2)(5c^2+4) + \frac{1}{4}(7+2c^2)\sqrt{1-c^2}\cos^{-1} c - \left(\frac{1}{8}+c^2\right)(\cos^{-1} c)^2$$

$$T_4 = c\sqrt{1-c^2} - \cos^{-1} c$$

$$T_5 = -(1-c^2) + 2c\sqrt{1-c^2}\cos^{-1} c - (\cos^{-1} c)^2$$

$$T_7 = \left(\frac{1}{8}\right)c(7+2c^2) - \left(\frac{1}{8}+c^2\right)\cos^{-1} c$$

$$T_8 = -\left(\frac{1}{3}\right)(1+2c^2)\sqrt{1-c^2} + c\cos^{-1} c$$

$$T_9 = \frac{1}{2}\left[\frac{1}{3}\left(\sqrt{1-c^2}\right)^3 + aT_4\right]$$

$$T_{10} = \sqrt{1-c^2} + \cos^{-1} c$$

$$T_{11} = (\cos^{-1} c)(1-2c) + \sqrt{1-c^2}(2-c)$$

$$T_{12} = \sqrt{1-c^2}(2+c) - (\cos^{-1} c)(2c+1)$$

$$T_{13} = \frac{1}{2}[-T_7 - (c-a)T_1]$$

APPENDIX B. Definitions of Matrices in Eqs. (11)-(12)

$$\mathbf{M}_s = \begin{bmatrix} r_\alpha^2 & r_\beta^2 + (c-a)x_\beta & x_\beta \\ r_\beta^2 + (c-a)x_\beta & r_\beta^2 & x_\beta \\ x_\alpha & x_\beta & M_t/M \end{bmatrix}$$

$$\mathbf{B}_t = (\mathbf{\Lambda}^T)^{-1}\begin{bmatrix} 2m_\alpha\omega_\alpha\varsigma_\alpha & 0 & 0 \\ 0 & 2m_\beta\omega_\beta\varsigma_\beta & 0 \\ 0 & 0 & 2m_h\omega_h\varsigma_h \end{bmatrix}\mathbf{\Lambda}^{-1}$$

$$\mathbf{K}_s = \begin{bmatrix} r_\alpha^2\omega_\alpha^2 & 0 & 0 \\ 0 & r_\beta^2\omega_\beta^2 & 0 \\ 0 & 0 & \omega_h^2 \end{bmatrix}$$

$$\mathbf{M}_{\mathrm{NC}} = -\frac{\rho}{m}\begin{bmatrix} \pi b^2\left(\frac{1}{8}+a^2\right) & -(T_7+(c-a)T_1)b^2 & -\pi a b^2 \\ 2T_{13}b^2 & -T_3 b^2/\pi & -T_1 b^2 \\ -\pi a b^2 & -T_1 b^2 & \pi b^2 \end{bmatrix}$$

$$\mathbf{B}_{\mathrm{NC}} = -\frac{\rho}{m}\begin{bmatrix} \pi\left(\frac{1}{2}-a\right)Ub & (T_1-T_8-(c-a)T_4+T_{11}/2)Ub & 0 \\ \left(-2T_9-T_1+T_4\left(a-\frac{1}{2}\right)\right)Ub & -T_4T_{11}Ub/(2\pi) & 0 \\ \pi Ub & -UT_4 b & 0 \end{bmatrix}$$

$$\mathbf{K}_{\mathrm{NC}} = -\frac{\rho}{m}\begin{bmatrix} 0 & (T_4+T_{10})U^2 & 0 \\ 0 & (T_5-T_4T_{10})U^2/\pi & 0 \\ 0 & 0 & 0 \end{bmatrix}$$

$$\mathbf{R} = [2\pi\rho U\left(a+\frac{1}{2}\right)/m \quad -\rho U T_{12}/m \quad -2\pi\rho U/m]^T$$

$$\mathbf{S}_1 = [U \quad T_{10}U/\pi \quad 0]$$

$$\mathbf{S}_2 = \left[b\left(\frac{1}{2}-a\right) \quad bT_{11}/2\pi \quad b\right]$$

$$\mathbf{S}_3 = [c_2c_4(c_1+c_3)U^2/b \quad (c_1c_2+c_3c_4)U]$$

$$\mathbf{A} = \begin{bmatrix} 0 & \mathbf{I}_{3\times3} & 0 \\ -\mathbf{M}_t^{-1}\mathbf{K}_t & -\mathbf{M}_t^{-1}\mathbf{B}_t & \mathbf{M}_t^{-1}\mathbf{D} \\ \mathbf{E}_1 & \mathbf{E}_2 & \mathbf{F} \end{bmatrix}$$

$$\mathbf{M}_{\mathrm{t}} = \mathbf{M}_{\mathrm{s}} - \mathbf{M}_{\mathrm{NC}},$$

$$\mathbf{B}_{\mathrm{t}} = \mathbf{B}_{\mathrm{s}} - \mathbf{B}_{\mathrm{NC}} - 1/2\mathbf{R}\mathbf{S}_2,$$

$$\mathbf{K}_{\mathrm{t}} = \mathbf{K}_{\mathrm{s}} - \mathbf{K}_{\mathrm{NC}} - 1/2\mathbf{R}\mathbf{S}_1, \quad \mathbf{D} = \mathbf{R}\mathbf{S}_3$$

$$\mathbf{E}_1 = \begin{bmatrix} 0 & 0 & 0 \\ U/b & UT_{10}/(\pi b) & 0 \end{bmatrix},$$

$$\mathbf{E}_2 = \begin{bmatrix} 0 & 0 & 0 \\ (1/2-a) & T_{11}/(2\pi) & 1 \end{bmatrix},$$

$$\mathbf{F} = \begin{bmatrix} 0 & 1 \\ -c_2c_4U^2/b & -(c_2+c_4)U/b \end{bmatrix}$$

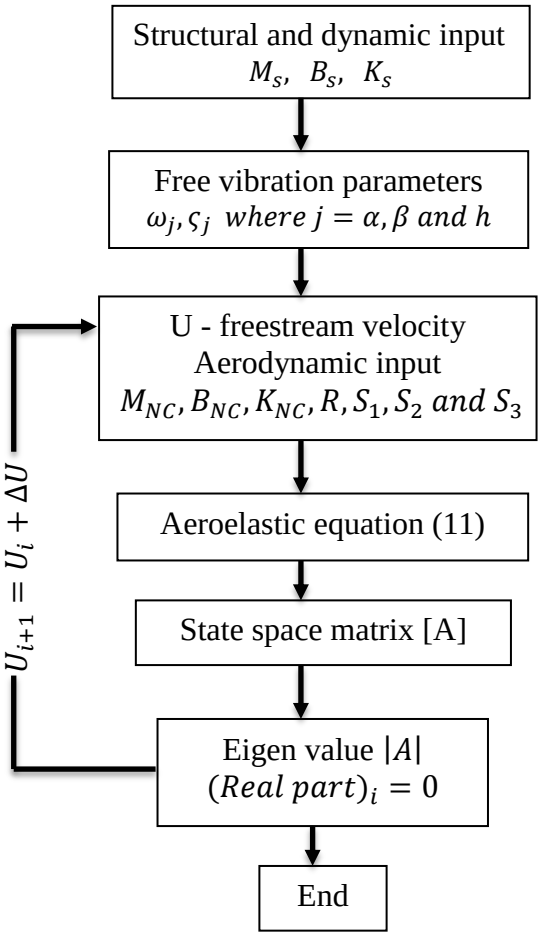

Solution Algorithm to find flutter speed

Modeling and Control of Fuel Cell Using Artificial Neural Networks

Dr. Hayder Sabah. Abad Al-Amir
Lecturer
Mechanical Department
Institution of Technology
hayder286@yahoo.com

Dr. Hayder Abed Dahd
Lecturer
Mechanical Engineering Department
University of Technology
hayder_abed2002@yahoo.com

Eiman Ali Eh. Sheet
Lecturer
Energy and Renewable Energies Technology Center
University of Technology
Eman_sheet@yahoo.co.uk

ABSTRACT

This paper includes an experimental study of hydrogen mass flow rate and inlet hydrogen pressure effect on the fuel cell performance. Depending on the experimental results, a model of fuel cell based on artificial neural networks is proposed. A back propagation learning rule with the log-sigmoid activation function is adopted to construct neural networks model. Experimental data resulting from 36 fuel cell tests are used as a learning data. The hydrogen mass flow rate, applied load and inlet hydrogen pressure are inputs to fuel cell model, while the current and voltage are outputs. Proposed model could successfully predict the fuel cell performance in good agreement with actual data. This work is extended to developed fuel cell feedback control system using PID controller to stabilize the fuel cell voltage. Particle swarm optimization technique is used to tune the PID controller gains. The voltage error and hydrogen flow rate are input and the actuator of the PID controller respectively. Simulation results showed that using PID controller with proposed model of fuel cell can successfully improve system performance in tracking output voltage under different operating conditions.

Key words: fuel cell, hydrogen fuel, renewable energy, artificial neural networks, PID , Particle swarm optimization

النمذجة والسيطرة لخلية وقود باستخدام الشبكات العصبية الاصطناعية

د.حيدر صباح عبد الامير
مدرس
قسم المكائن- والمعدات- معهد التكنولوجيا -بغداد

د.حيدر عبد ضهد
مدرس
قسم الهندسة الميكانيكية-الجامعة التكنولوجية

ايمان علي احسان شيت
مدرس
مركز تكنولوجيا الطاقة والطاقات المتجددة- الجامعة التكنولوجية

الخلاصة

تتضمن هذه الورقة دراسة عملية لتاثير معدل كتلة تدفق الهيدروجين و ضغطه على أداء خلية الوقود. بالاعتماد على النتائج التجريبية، تم اقتراح نموذجا لخلية الوقود مبنيةعلى أساس الشبكات العصبية الاصطناعية. طريقة الانتشار الخلفي مع دالة التفعيل من النوع (log-sigmoid) اعتمدت لانشاء نموذج الشبكة العصبية. استخدمت البيانات التجريبية الناتجة من 36 اختبار لخلية الوقود كبيانات للتعلم. معدل تدفق كتلة الهيدروجين و الحمل المطبق و ضغط الهيدروجين اخذت كمدخلات لنموذج الخلية، في حين أن التيارالكهربائي والجهد الكهربائي اصبحت المخرجات. النموذج المقترح تمكن من التنبئ بنجاح بأداء خلية الوقود مع حصول توافق جيد مع البيانات الفعلية. هذا العمل تم توسيعه ليشمل تطوير نظام سيطرة لخلية الوقود باستخدام المتحكم التناسبي التفاضلي التكاملي لتحقيق الاستقرار في جهد الخلية . استخدمت تقنية أمثلية حشد الجسيمات لحساب البارمترات المثالية للمسيطر التناسبي التكاملي التفاضلي. الخطأ الجهد ومعدل تدفق الهيدروجين هما الادخال و المشغل للمتحكم على التوالي. أظهرت نتائج المحاكاة أن استخدام جهاز تحكم مع النموذج المقترح لخلية الوقود امكنه تحسين أداء المنظومة في تتبع انتاج الجهد الكهربائي المطلوب في ظل ظروف التشغيل المختلفة .

1. INTRODUCTION

The fuel cell is a device that converts chemical energy into electrical energy and is more efficient than the internal combustion engine in fuel conversion to twice or three times the energy ,**Ferng et al. 2004**. The electrochemical cell uses to produce electrical energy continuously through the supply of oxygen and hydrogen ,**Kordesch, 1996.** For a hydrogen/oxygen fuel cell the inputs are hydrogen (fuel) and oxygen (oxidant) and the outputs are dc power, heat, and water. In general, the hydrogen is oxidized to protons moving through the electrolyte to the anode, as well as to electrons moving from outside the cell to the anode where they will meet with oxygen is reduced to water takeaways. There are various types of fuel cells developed and used over the years and can be classified either as types of fuel and oxidizer or as electrolyte type or working temperature of the cell or by mechanism of reactants entry to the cell, but the most common type of classification common is the classification cell according to the type of electrolyte used. These types of fuel cells could produce electrical power ranging from mille watts to megawatts. It could be used in a structure of portable electronic equipment, vehicles, residential or in distributed power systems ,**Mann, 2004.**When pure hydrogen is utilized no pollutants are produced, and the hydrogen itself could be generate from water using renewable energy sources such that the system is environmentally benign. Practically hydrogen was the best fuel for most applications. In addition to hydrogen several fuel cells could also use carbon monoxide and natural gas as a fuel. In these fuel cells, carbon monoxide reacts with water generating hydrogen and carbon dioxide, and natural gas reacts with water producing hydrogen and carbon monoxide, the hydrogen that generated is then used as the actual fuel.

For the purpose of study and improve the performance of fuel cell , many different mathematical models were proposed to speculation the behavior of voltage change with discharge current of a fuel cell. Recently, theoretical modeling and programming simulation have been developed for understanding better the fuel cell itself. Artificial neural network model has been provided useful and reasonably accurate input–output relations because of its excellent multi-dimensional mapping capability.

The neural networks architectures have been used for power analysis of fuel cell are multilayer feed forward network, radial biased function network, generalized regression neural network and adaptive neuro fuzzy interface systems ,**Mohanraj, 2015**.

K. Mammar et al. applied artificial neural networks for creating the optimal model of proton exchange membrane (PEM) fuel cell. The ANN network had an input layer with three inputs: partial pressures of hydrogen, partial of oxygen and cell operating current, one hidden layer with 10 neurons and an output layer with one outputs of fuel cell voltage. They create fuzzy logic controllers to control active power of proton exchange membrane fuel cell (PEMFC). Their results assured the high performance capability of the neural network to control power generation.

B. Grondin et al.,**Mammar, 2012**. have been used A mechanistic and an artificial neural network (ANN) model to depict all internal phenomena in a single-cell for PEM fuel cell .They illuminate the benefits and drawbacks of the two different models using statistical error criteria. In S. Rakhtala et al. ,**Grondin,2014**. work, a neural network model was used as control algorithm of the fuel cell voltage to improve fuel cell performance. Air pressure was the control signal applied to the system and fuel cell voltage was the output .The system behavior has been tested under random current variations and compared to the fuel cell nonlinear dynamic model. J. Zamora1 et al. **Rakhtala, 2011**. presented the modeling of a PEM fuel cell system, by ANNs. The selected ANN structure was validated for the transient state, during the start up of the

system, and in steady state. The training strategy and the ANN topology were tested with a large number of parameters and network structures, to obtain high precision results.
The primary purpose of this research is to build a model for fuel cell using neural networks. The objective of this model is to estimate fuel cell power depend on training data: hydrogen mass flow rate, hydrogen pressure, applied load, current and voltage. The training data are collected from real tests measurements.

The automatic control of the fuel cell is very important case to improve the performance of it. The present work is widened to investigate the performance of the fuel cell control system using neural networks model and PID controller.
The proportional integral derivative (PID) controller is widely used in the industry because of its simple structure and robust performance within a wide range of operating conditions ,**C.Kao, 2006**. Unfortunately, it has been difficult to correctly adjust the gains of PID controllers because many industrial systems have complex physics phenomena such as: high orders; time delays; and nonlinearities.
In this paper a particle swarm optimization (PSO) technique is used to tune the parameters of the PID controller for fuel cell.

2. FUEL CELL PERFORMANCE

2.1 Electrochemistry

In a fuel cell, there is no combustion processes because reaction takes place between fuel and oxygen at low temperature and the products of reaction were electric current, heat and water. Furthermore, they are environmentally friendly ,**Parsons, 2000**.

In PEMFC type fuel cell, hydrogen flow over the anode pole where it was decomposed into electrons and protons (hydrogen ions). The hydrogen ions pass through the polymer electrolyte membrane which considers the center of the cell ,**Larminie, 2012**. Then with the oxygen at the cathode, the hydrogen ion reacts with oxygen to generate water. Electrons created at the anode cannot pass through the membrane; therefore they flow through an external electric circuit from the anode to the cathode. In fact, the electrochemical reactions and the physical procedures, which occur at the cell poles, are very complex reactions. At the anode, hydrogen gas must spread through the winding paths to meet the platinum particles, where the platinum dismantle molecule of hydrogen to two atoms of hydrogen (H) and only then can the hydrogen atom to disintegrate into a proton and an electron , the proton will pass through the membrane towards the cathode and passes the electron through the outer circuit. This process is going through several stages before it reaches its end .In fact, platinum is the only currently known catalyst capable of shorthand to conduct this reaction at low temperature. **Fig1.** represent a diagram illustrating the structure and operation of PEMFC type fuel cell,

2.2 Efficiency

The important parameter has been used to measure energy conversion in fuel cells is fuel cell efficiency which represents the ratio between the actual voltage produced in the fuel cell to the maximum ideal voltage of fuel cell ,**Kordesch, 1996**.
The calculation of ideal voltage which could be produced from fuel cell can be made by carrying out the process of energy balance between the initial state of the reactions in the chemical reaction in the cell $\left(H_2 + \frac{1}{2}O_2\right)$ and the final state of reaction product H_2O.
The balance process has been representing by a Gibbs free energy. The maximum ideal voltage of the cell (ΔE) at constant pressure and temperature is ,**Kordesch, 1996**.

$$\Delta E = \Delta G / nf \quad (1)$$

$$\Delta G = \Delta H - T\Delta S \quad (2)$$

where:

ΔG is the deference in Gibbs free energy
n is the number of moles of electrons
f is Faraday constant
ΔH is the deference in enthalpy
T is the cell temperature
ΔS is the deference in entropy

The thermal efficiency of fuel cells can be representing as the ratio between the useful electrical energy to the heat that is generated from fuel, that is, enthalpy of formation. Therefore, the fuel cell maximum efficiency in the ideal state can be defined as the ratio between Gibbs free energy to the enthalpy of formation, that is,

$$\text{Efficiency} = \frac{\Delta G}{\Delta H} \quad (3)$$

The generated voltage is less than ideal voltage because of irreversible losses. There are three types of irreversible losses which working on reduce the performance of the cell. These losses are activation polarization, Ohmicpolarization, and concentration polarization ,**Mann, 2000 and Larminie, 2000.**

There are several types of fuel cells which were developed and used during the last few years. They are classified depending on the type of fuel and oxidant or type of electrolyte or cell operation temperature or the reactants entering method to the cell, however, the common classification is that of type of electrolyte used in the cell. The proton exchange membrane fuel cell (PEMFC) is the most used for many reasons, the most important reason is it operates at relatively medium temperature and the solid membrane it uses. Those reasons make this type of fuel cells appropriate for various applications, especially in cars and other means of transport, mobiles, computers and household appliances. The most important advantages are high energy density and fast startup as well as simple structure and safety in operation fuel cell ,**Youssef, 2010.**

3. EXPERIMENTAL SETUP

The fuel cell unit is supplied with a stack of proton exchange membrane fuel cell (PEMFC) with a rated power of 100 W. The stack is composed of 24 cells with the shape of channeled plate that allows the air flow through the membrane. The membrane facilitates the hydrogen flow, generating the electrons release. There are separating plates which conduct electricity, allowing thus such electrons flow, between each pair of cell. The schematic of the experimental setup and a photograph of the fuel cell unit are shown in **Fig 2.**

Cells are self- humidifying and do not require any type of external humidification. The stack has an integrated fan able to provide the required air for the good operation and maintenance of the operation temperature.

Hydrogen storage represents one of the essential points regarding the hydrogen economy. For that purpose, a canister of metal hydride (300L) is included. Internal pressure of the device is 8 bar at a room temperature of 20-25°C. It has discharge pressure of 15-20 bar, for that reason the fuel cell unite also includes two pressure regulators. One of them is for it's the installation in the H2 cylinder in order to regulator the outlet pressure at 30 bar. The other is placed at the outlet of the metal hydride canister in order to regulate the inlet pressure to the stack in a range of 0.4 – 0.5 bar. In additional, the unit includes two solenoid valves. One of them is located before the stack. It controls the hydrogen inlet and when the unit is switched off, the valve is closed to avoid any possible hydrogen leakage. This valve is automatically closed when the temperature of the stack exceeds 65 ^{o} C. The other valve is placed at the stack outlet. It purges outside the excess of water and hydrogen for a correct operation.

Hydrogen storage represents one of the essential points regarding the hydrogen economy. For that purpose, a canister of metal hydride (300L) is included. Internal pressure of the device is 8 bar at a room temperature of 20-25°C. It has discharge pressure of 15-20 bar, for that reason the fuel cell unite also includes two pressure regulators. One of them is for it's the installation in the H2 cylinder in order to regulator the outlet pressure at 30 bar. The other is placed at the outlet of the metal hydride canister in order to regulate the inlet pressure to the stack in a range of 0.4 – 0.5 bar. In additional, the unit includes two solenoid valves. One of them is located before the stack. It controls the hydrogen inlet and when the unit is switched off, the valve is closed to avoid any possible hydrogen leakage. This valve is automatically closed when the temperature of the stack exceeds 65 ^{o} C. The other valve is placed at the stack outlet. It purges outside the excess of water and hydrogen for a correct operation.

The unit also has load regulation system. It enables the study of the generated electrical energy, the representation of the characteristic operation curves and their comparison with theoretical curve. It included a variable power, which enables to vary the generated current.

The whole electrical circuit of the stack is protected by a short circuit unit in case over current (12A) and low voltage shut down (12V). In the event of one of these problems, the hydrogen inlet solenoid valve is automatically closed.

Lastly, and as a result of the danger in the use of hydrogen, include a hydrogen leak detector with a detection range from 0 to 2% Vol.

4. EXPERIMENTAL RESULTS

Figures (3), (4) and (5) show the effect of hydrogen flow rate and inlet pressure on fuel cell performance parameters. The current density-voltage relationship for a fuel cell and operating conditions (concentration, flow rate, pressure, temperature, and relative humidity) is a function of kinetic (activation), ohmic, and mass transfer resistances. The current density vs. voltage curve, shown in figure 3 at different inlet pressure, the figure is called as the polarization curve. Deviations between the ideal equilibrium voltage and the polarization curve provide a measure of fuel cell efficiency. These results give a good agreement with published results **, Ferng, 2004, Rowe , 2001.**

Electrical energy is gained from a fuel cell when a current is drawn, but the actual cell voltage has been lowered from its equilibrium voltage because of irreversible losses due to several reasons. Several factors give the irreversible losses in a practical fuel cell. The losses, which were generally called polarization, formed primarily from activation polarization, ohmic polarization, and gas concentration polarization. The activation loss is the first of these polarizations, Performance loss due to slow reaction kinetics at either/both the cathode and anode surfaces is called activation polarization. Activation polarization is related to the

activation energy barrier between reacting species and it is primarily a function of temperature, pressure, concentration, and electrode properties. The reactions can also play a role in activation polarization. Kinetic resistance rules the low current density portion of the polarization curve, where deviations from equilibrium were small. At these conditions, reactants were plentiful (no mass transfer limitations) and the current was so small that ohmic (iR) losses were negligible.

Performance loss resulting from resistance to the flow of current in the electrolyte and through the electrodes is called ohmic polarization, the ohmic polarization change with the current increase. Ohmic polarization is present using Ohm's Law (V=iR), where i is current density (mA/cm^2) and R is resistance ($W\text{-}cm^2$), and command in the linear part of the current density-voltage curve as shown in figure 4. The concentration losses happen significantly at all range of current density [Chou, 2003].

Concentration polarization has been happen when a reactant is interacting on the surface of the electrode cause a concentration gradient between the gas and the surface. Concentration polarization has been affected by concentration and flow rate of the reactants, the temperature of fuel cell temperature, and the structure of the gas diffusion layer and catalyst properties ,**Mann, 2000.**

Numbers of processes have been caused the formation of the concentration polarization. These are (1) diffusion difficulties of the gas phase in the electrode pores, (2) solution formation of reactants into the electrolyte, (3) dissolution formation of products out of the system ,**Chou, 2003.**

In **Fig 3.** it can be seen that the increase of operating inlet pressure leads to decrease of losses, which mean high voltage output. An increase in operating pressure has several positive effects on fuel cell performance. The partial pressures of reactant gases, solubility, and mass transfer rates are higher at higher pressures. The electrolyte loss by evaporation is reduced at higher operating pressures. The system efficiency is increased by the increase in pressure.

This is evident from **Fig4.** where can be observed decrease cell efficiency with the increase in operating pressure. As can be observed decrease in efficiency with increasing hydrogen flow rate so that the maximum efficiency of the cell was at low current densities and high voltage due to increased losses with increasing current density as described in **Fig4.** In fact, as the current density is decreased, the active cell area must be increased to obtain the desired amount of power.

The variation of power with current density is shown in **Fig5.** Where power increased with current density increase, it is normal and seems logical to design the cell to operate at the maximum power that peaks at a higher current density. However, operation at the higher power will mean operation at lower cell voltages or lower cell efficiency. Setting the operating point at the peak power density may cause instability in power control because the system will have a tendency to oscillate between higher and lower current densities around the peak. It is normal practice to operate the cell at a point towards the left side of the power peak and at a point that yields a compromise between low operating cost (low current density) and low capital cost (high current density).

4. Fuel cell modeling

A fully connected feed forward multi-layer configuration using back propagation learning algorithm was implemented to model the fuel cell. This type of ANN has a strong ability to express complex non-linear mapping and has already found wide ranging applications ,**Khandekar, 2002**.

The structure of this type of ANN usually consists of an input layer, hidden layer (one or more) and an output layer. Each layer has some nodes representing artificial neurons. Each node connected to the nodes of its preceding layer through adaptable weights ,**Latha, 2010**. Individual neurons have limited ability of calculation and expression but when they connect with each other, the whole network achieves ability to model complex functions. A network accepts an input vector and generates a response in the form of an output vector as shown in **Fig6.**
The concept of learning of neural networks related to finding the values of weights such that the error condition was minimized. The error is the difference between the actual output vector to the estimated output vector by neural networks and the resulting error back propagates to alter the connecting weights in the direction of reducing the error. This process does running many times until the error reaches to the lowest possible value. Then the network holds the weights constant and becomes a valid model for prediction. ,**Latha, 2010**.

In this work, the pressure, mass flow rate and generated power are considered as inputs to the network. The current and voltage are network output. In present work, ten nodes in hidden layer are adopted. Mean squared error concept has been used to express about the error incurred during the learning as shown in equation (4)

$$Error = \frac{1}{2}\sum_{1}^{m}(V_{act} - V_{est})^2 + (I_{act} - I_{est})^2 \qquad (4)$$

where m is the number of patterns V_{act} is actual voltage, V_{est} is estimated voltage by neural networks model, I_{act} is actual current, and I_{est} is estimated current by neural networks model. The algorithm of the neural networks for fuel cell model is carried out using MATLAB version 2012.

A training set of 36 patterns is used with a learning rate of 0.1. After 12 epochs, the output of the neural network is approximated to the actual output (voltage and current) as shown in figure (7). The error is equal to 7.4 e^{-6} for excellent learning of fuel cell model as shown in **Fig8.**

5. PID CONTROLLER

The presented PID Controller in this work has been consisted of classic PID controller, direct closed-loop control of controlled objects and particle swarm optimization (PSO) technique to find PID controller parameters k_p, k_i; and k_d to reach optimization of control performance index according to system operating condition as shown in **Fig9.** The plant is fuel cell model based on neural network which is described in previous section.

In PSO algorithm, the system has been initialized with particles of random solutions, which , and each potential solution has been also assigned a randomized velocity. Each particle adjusts its trajectory towards its best solution (fitness) that is achieved so far. This value is called *pbest.* Each particle also modifies its trajectory towards the best previous position attained by any member of its neighborhood. This value is called *gbest.* Each particle moves in the search space with an adaptive velocity .
The particles have been evaluated using a fitness function to see how close they are to the optimal solution .

$$V_{i,n}^{m+1} = V_{i,n}^{m} + c_1 rand_1 (pbest_{i,n}^{m} - x_{i,n}^{m}) + c_2 rand_2 (gbest_{n}^{m} - x_{i,n}^{m}) \qquad (5)$$

$$x_{i,n}^{m+1} = x_{i,n}^{m} + V_{i,n}^{m+1} \quad (6)$$

where

$V_{i,n}^{m}$ is the velocity of the ith particle at m^{th} iteration.

$x_{i,n}^{m}$ is the position of the ith particle at m^{th} iteration.

I is number of particles.

n is the dimension of particle.

c_1 and c_2 are the acceleration constants with positive values equal to 1.17.

$rand_1$ and $rand_2$ are random numbers between 0 and 1.

$pbest_i$ is best previous weight of ith particle.

$gbest_n$ is best particle among all the particle in the population.

In present analysis, $\Delta K_n^{m+1} = V_{i,n}^{m+1}$, $\Delta K_n^{m} = V_{i,n}^{m}$ and $K_n^{m} = x_{i,n}^{m}$,where K are the parameters K_p, K_i and K_d of the PID controller. The mean square error function is chosen as criterion for estimating the model performance as equation (7)

$$E = \frac{1}{p}\sum_{j=1}^{p}(V_{ref}(m+1)^{j} - V_{out}(m+1)^{j})^{2} \quad (7)$$

where p is number of samples, V_{ref} is desired voltage and V_{out} is fuel cell output voltage.

6. Simulations Results

In this section, the performance of proposed fuel cell model with PID which its parameters have been tuned by PSO is tested .The task of present controller assumes the fuel cell must give desired voltage when the load has been applied on it. This means the time history responses of fuel cell voltage under different working condition have been tested using suggested PID controller as shown in **Fig10**. It can be seen from this figure, the suggested PID controller is able to make the fuel cell gives the desired voltage (18 volt) at short time not exceed 1sec depending on the operating pressure and load. The pressure changes 0.4, 0.45 and 0.5 bar , while the load (power) is applied at values of 50,80,and 100 W. The responses seem smoothly and without over shoot. These results show the voltage output reaches the desired value quickly as applied power decreases.

Fig 11. show the time history responses of hydrogen mass flow rate. it can be seen from this figure, the controller give more mass flow when the pressure decreases .Also, when the applied load increases from 50 to 100 W the mass increases by 29% ,42% and 73% at pressure 0.4,0.45 and 0.5 bar respectively.

7. CONCLUSIONS

The performance of the fuel cell is studied experimentally. The experimental results appear that the polarization curve is identical with the theoretical polarization curve of fuel cell where the three types of losses are clear and showed the same behavior known of the cell. The hydrogen inlet pressure increased has a significant effect on the performance of fuel cell where the losses are decreased when the inlet pressure increase. The fuel cell efficiency decrease with the increase the operating pressure and hydrogen flow rate. The maximum efficiency of the cell was at low current densities and high voltage.

The operating point the fuel cell must be selected so that the power output greater as possible, taking into consideration both of the cell voltage and efficiency were their being inversely proportionate with the power output.

A fuel cell model based on artificial neural networks with back propagation algorithm is successfully trained, validated and used for prediction the performance of fuel cell under different working conditions. The using of neural networks to model complicated physical systems is very good choice because it deals with the input –output data of the systems regardless of the composition source.

Also, in this paper, PID controller with PSO technique for tuning its gains is used to control output voltage of fuel cell under different pressure and applied load. Present controller can offer good performance with fast response and without overshoot. This response reflects the fuel cell speed access to the required operating conditions, and this feature is one of the most important features that are characterized by fuel cells for mechanical engines.

Finally, the increase in pressure may decrease the controller power and the Consumption of hydrogen.

Also, in this paper, PID controller with PSO technique for tuning its gains is used to control output voltage of fuel cell under different pressure and applied load. Present controller can offer good performance with fast response and without overshoot. This response reflects the fuel cell speed access to the required operating conditions, and this feature is one of the most important features that are characterized by fuel cells for mechanical engines.

Finally, the increase in pressure may decrease the controller power and the Consumption of hydrogen.

REFERENCES

- Ferng, Y.M.,Tzang, Y.C., Pei, B.S., Sun, C.C., Su, A., *Analytical and experimental investigations of a proton exchange membrane fuel cell*,International Journal of Hydrogen Energy, 29,2004,381-391.

- Rowe, A., Li, X., *Mathematical modeling of proton exchange membrane fuel cells*, Journal of Power Sources, 102, 2001, 82-88.

- K. Kordesch, G. Simader, *Fuel Cells and TheirApplications*, VCH, 1996

- Mann, R.F., Amphlett, J.C., Hooper, M.A.I., Jensen, H.M., Peppley, B.A., *Development and appli-cation of a generalized steady-state electrochemical model for a PEM fuel cell*, Journal of Power Sources, 86, 2000, 173-179.

- M. Mohanraj, S. Jayaraj, C. Muraleedharan *Applications of artificial neural networks for thermal analysis of heatexchangers - A review* International Journal of Thermal Sciences 90 (2015) 150-172.

- K. Mammar and A. Chaker *Neural Network-Based Modeling of PEM fuel cell and Controller Synthesis of a stand-alone system for residential application*, IJCSI International Journal of Computer Science Issues, Vol. 9, Issue 6, No 1, November 2012

- B. Grondin, S. Roche, and Carole Lebreton *Mechanistic Model versus Artificial Neural Network Model of a Single-Cell PEMFC*, Engineering, 2014, 6, 418-426 ,Published

Online July 2014 in SciRes. http:// www.scirp.org/ journal/ eng http://dx.doi.org/10.4236/ eng.2014.68044

- S. Rakhtala, R. Ghaderi , and A. Ranjbar *Proton exchange membrane fuel cell voltage-tracking using artificial neural network*s, Journal of Zhejiang University-SCIENCE C (Computers & Electronics),Vol.4, 2011.

- J. Zamora1, J.J. San Martín2,. V. Aperribay2,and P. Eguía1, *Neural Network Based Model for a PEM Fuel Cell System*, International Conference on Renewable Energies and Power Quality ,Valencia (Spain), 15th to 17th April, 2009.

- C.Kao , C. Chuang and R. Fung, *The self-tuning PID control in a slider–crank mechanism system by applying particle swarm optimization approach*, Mechatronics, Vol. 16 ,2006.

- EG&G Services Parsons, Inc., ScienceApplications International Corporation, "Fuel Cell Handbook Fifth Edition", National Energy Technology Laboratory, October 2000.

- J. Larminie, and A. Dicks, *Fuel Cell SystemsExplained*, John Wiley and Sons, November 2000.

- M. ELSayedYoussef ,MoatazH.Khalil , Khairia E.AL-NAdi *Neural Network Modeling for Proton Exchange Membrane Fuel Cell (PEMFC)* Advances in Information Sciences and Service Sciences. Volume 2, Number 2, June 2010.

- ShaoduanOu, Luke E.K. Achenie, *A hybrid neural network model for PEM fuel cells*, Journal of Power Sources, 140, 2005, 319–330.

- Maher A.R. Sadiq Al-Baghdadi, Haro-un A.K. Shahad Al-Janabi, *Parametric and optimization study of a PEM fuel cell performance using three dimen-sional computational fluid dynamics model*,Renewable Energy 32 ,2007, 1077–1101

- Won-Yong Lee, Gu-Gon Park, Tae-Hyun Yang, Young-Gi Yoon, Chang-Soo Kim , *Empirical modeling of polymer electrolyte membrane fuel cell performance using artificial neural networks*, International Journal of Hydrogen Energy ,29 ,2004, 961 – 966.

- S. Khandekar, X. Cui and M. Groll, *Thermal performance modeling pulsating heat pipes by artificial neural networks*,Proceedings of 12th International Heat Pipe Conference, pp. 215-219, Moscow, Russia, 2002.

- Latha, K. Vijaya Kumar Reddy, J. Chandra SekharaRao and A. V. Sita Rama Raju, *Performance analysis on modeling of loop heat pipes using artificial neural networks*,Indian Journal of Science and Technology Vol. 3 ,No. 4 ,2010.

- S.M.GirirajKumar, D.Jayaraj and A.R.Kishan , *PSO based Tuning of a PID Controller for a High Performance Drilling Machine* International Journal of Computer Applications Volume 1 – No. 19, 2010.

- S. Talukder 2011, *Mathematical Modeling and Applications of Particle Swarm Optimization*, Master's Thesis Submitted to the School of Engineering at Blekinge Institute of Technology.
- J -Chou Lin, H. R. Kunz, J. M. Fenton and S. S. Fenton 2003, *The Fuel Cell – An Ideal Chemical Engineering*,Proceedings of the 2003 American Society for Engineering Education Annual Conference & Exposition.

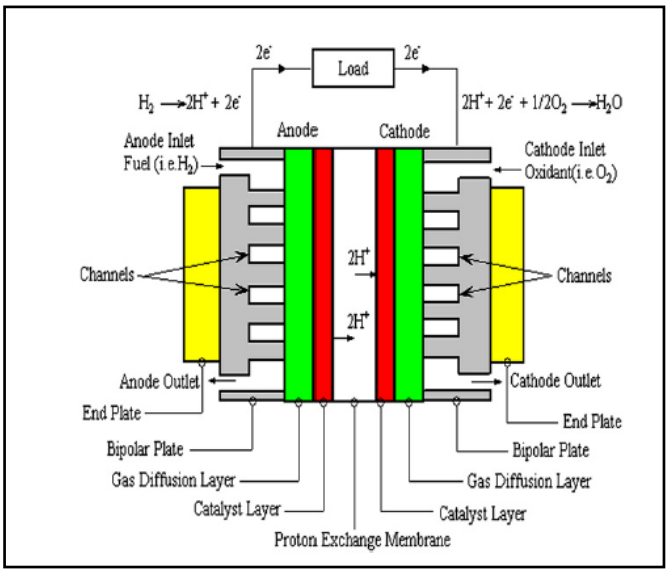

Figure (1) Operating scheme of a PEMFC [13]

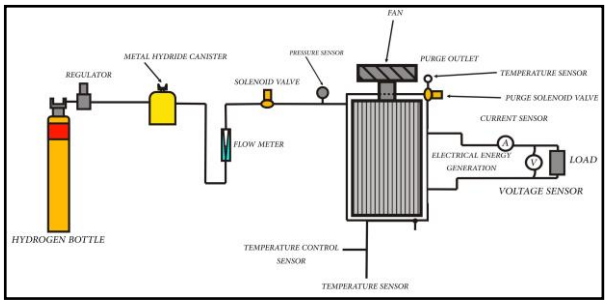

(a)

(b)

Figure 2. Schematic diagram and photograph of fuel cell experimental setup.

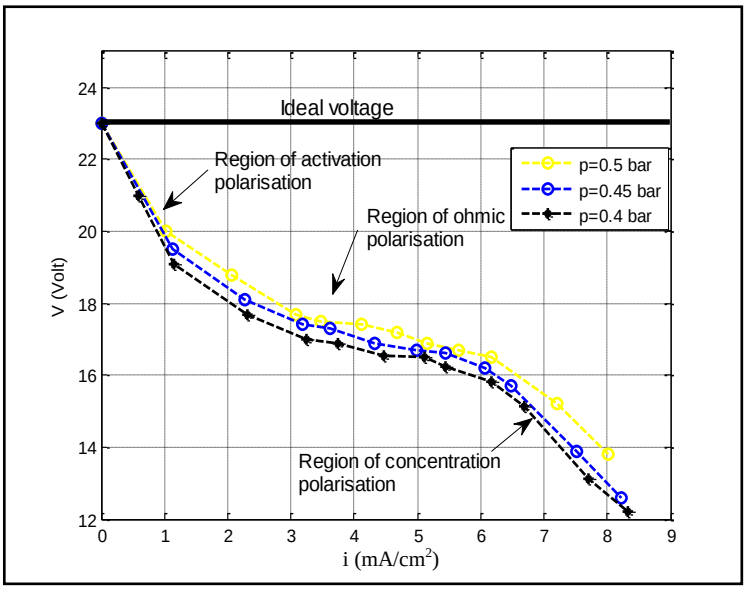

Figure 3. Experimental results of the polarization curve at different inlet hydrogen pressure

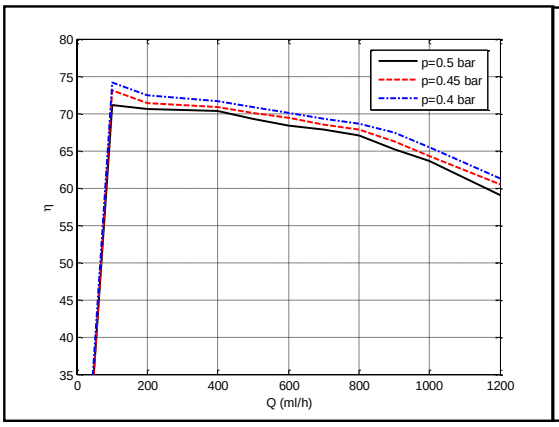

Figure (4) Variation of fuel cell efficiency with hydrogen flow rate at different inlet hydrogen pressure

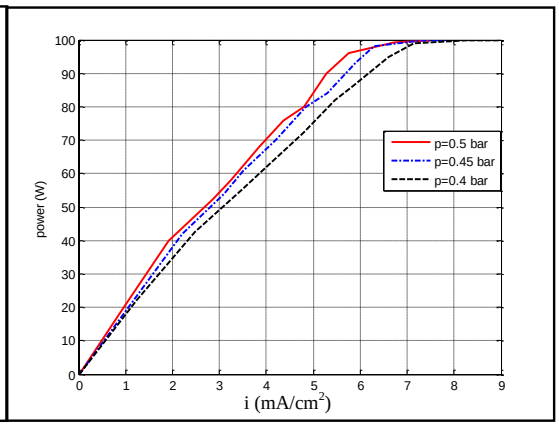

Figure (5) Output power relation with current density at different inlet hydrogen pressure

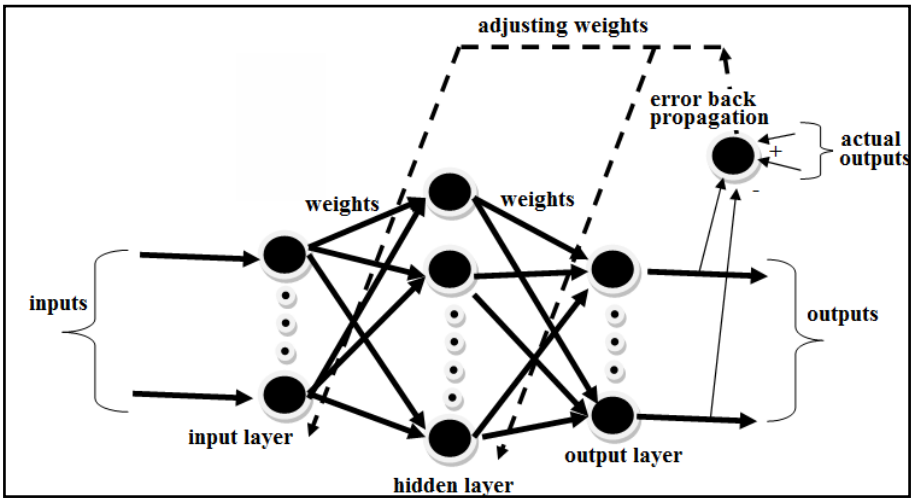

Figure 6. Neural networks structure

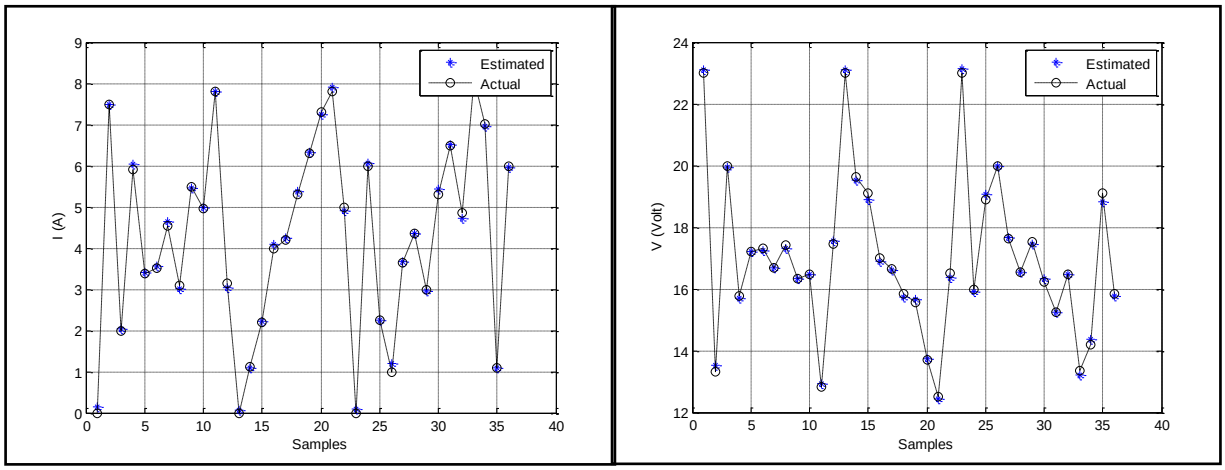

(a) (b)

Figure 7.Current and voltage; estimated by neural networks model vs. actual data

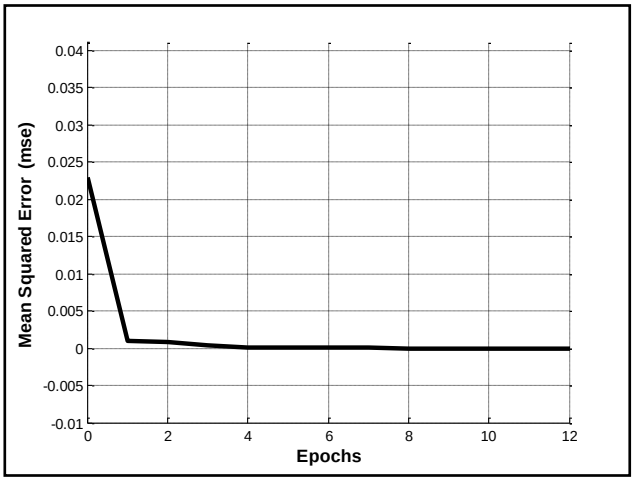

Figure 8. Mean square error vs. epoch

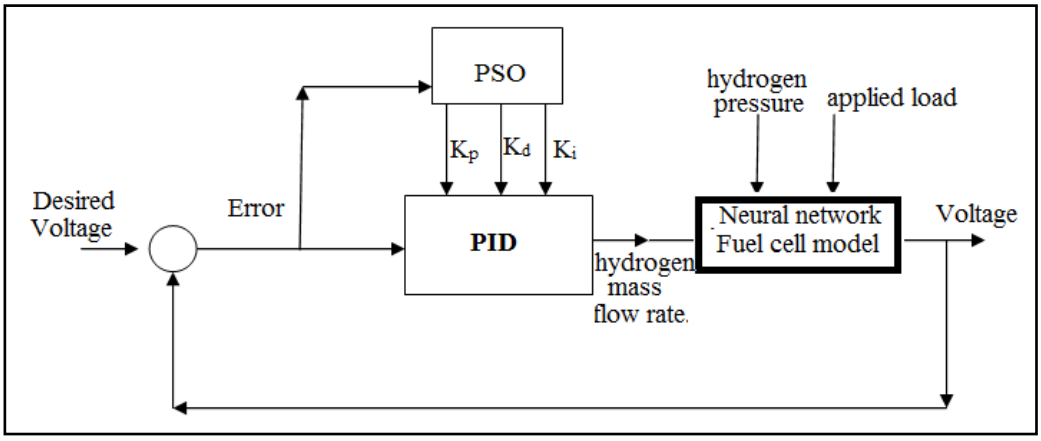

Figure (9) PID controller structure

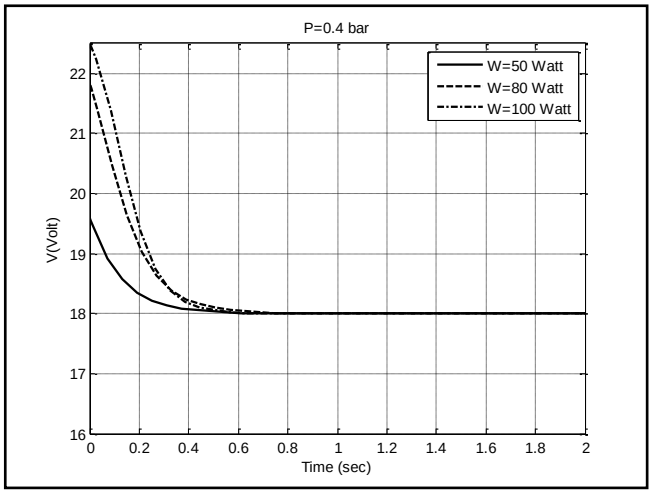

(a)

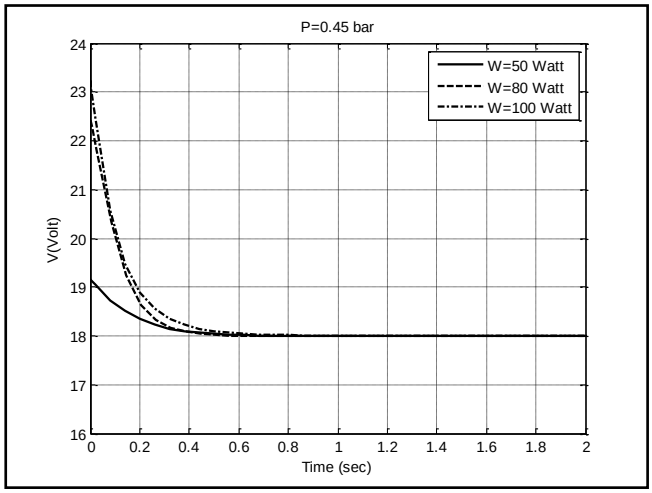

(b)

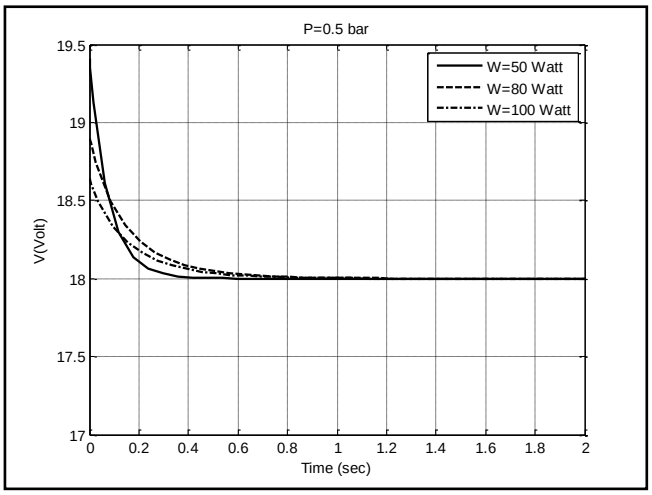

(c)

Figure 10. Time history response of voltage output of fuel cell at different operating conditions

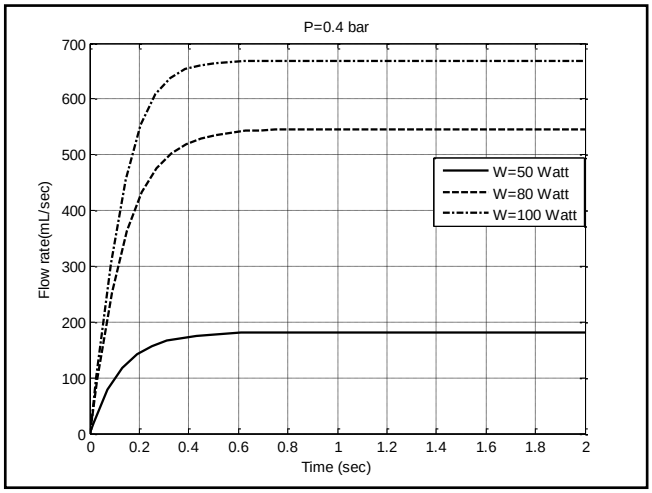

(a)

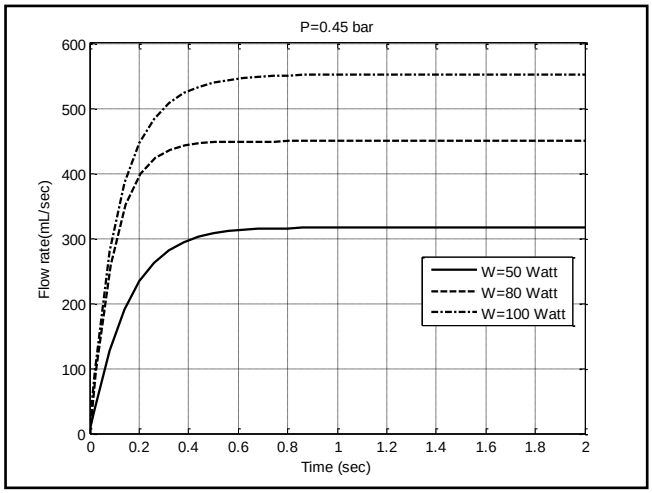

(b)

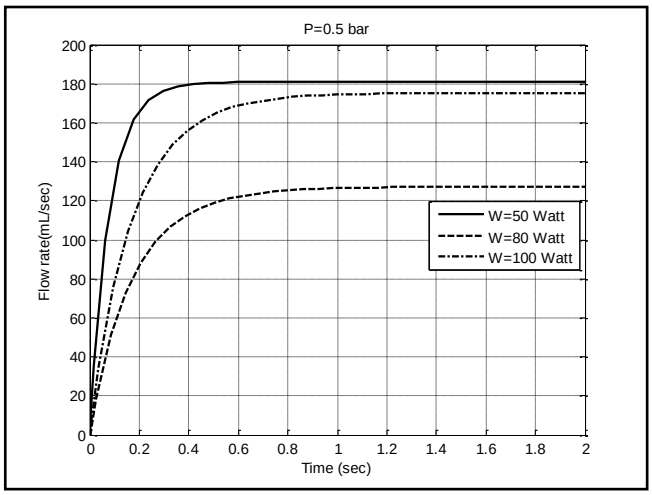

(c)

Figure 11. Time history response of hydrogen flow rate of fuel cell at different operating conditions

Strengthening of Reinforced Concrete T- Section Beams Using External Post-Tensioning Technique

Dr. AbdulMuttalib Issa Said
Professor
University of Baghdad-College of Engineering
abdmusawi@yahoo.com

Dr. Ali Hussein Ali Al-Ahmed
Lecturer
University of Baghdad-College of Engineering
ali_hussein_alahmed@yahoo.co.uk

Dhafer Mohsin Al-Fendawy
M.Sc Student
University of Baghdad-College of Engineering
dhaferhafdh@yahoo.com

ABSTRACT

This research is carried out to investigate the externally post-tensioning technique for strengthening RC beams. In this research, four T-section RC beams having the same dimensions and material properties were casted and tested up to failure by applying two mid-third concentrated loads. Three of these beams are strengthened by using external tendons, while the remaining beam is kept without strengthening as a control beam. Two external strands of 12 mm diameter were fixed at each side of the web of the strengthened beams and located at depth of 200 mm from top fiber of the section (d_{ps}). So that the depth of strands to overall depth of the section ratio ($d_{ps}/h=0.8$). For each strengthened beams, the strands have been tensioned by using a hydraulic jack with constant stress of 600 MPa. The main parameter conducting in this research is the strengthening length ratio (L_s/L) which is equal to the length of strengthening region (L_s) divided to the length of beam (L), these ratios are 0.83, 0.67 and 0.50. The experimental results showed that this technique for strengthening is efficient for reducing cracks width and increasing first cracking, service cracking and ultimate load capacities. The percentage increasing in first crack loads were 100%, 133% and 167%, for service crack loads (0.3 mm) were 63%, 75% and 88% and for ultimate loads were 78%, 89% and 67% for strengthening length ratios 0.83, 0.67 and 0.50 respectiviely as compared with the control beam.

Key words: post-tensioning, externally, strengthening, T- section, strands.

تقوية العتبات الخرسانية المسلحة ذات مقطع على شكل حرف (T) باستخدام تقنية الشد اللاحق الخارجي

د. عبد المطلب عيسى سعيد
استاذ
جامعة بغداد-كلية الهنسة

د. علي حسين علي أل احمد
مدرس
جامعة بغداد-كلية الهنسة

ظافر محسن حسن الفنداوي
طالب ماجستير
جامعة بغداد-كلية الهنسة

الخلاصـــة

في هذا البحث تم التحري عمليا عن التقوية لعتبات خرسانية مسلحة من خلال استخدام تقنية الشد الاحق المثبت خارج المقطع الخرساني. حيث تم صب وفحص اربعة عتبات خرسانية ذات مقطع على شكل حرف T بالانكليزية لحد الفشل وذلك بتسليط قوتين مركزتين عند نقطتي الثلث الوسطي للعتب حيث صممت هذه العتبات بنفس الابعاد و المواصفات. ثلاثة عتبات تم تقويتها باستعمال جدائل فولاذية خارجية بينما تركت العتبة الرابعة بدون تقوية كعتب مرجعي للمقارنة. تم استعمال جدائل فولاذية بواقع جديلة واحدة قطر 12 ملم ثبتت في كل جانب من جدع العتب المقوى حيث تم تثبيت هذه الجدائل بعمق 200 ملم من اعلى مقطع العتب حيث ان نسبة عمق الجدائل الى العمق الكلي للمقطع تساوي الى 0.8. تم شد هذه الجدائل باستخدام مضخه هيدروليكية للسيطرة على اجهاد الشد والذي هو ثابت لجميع العتبات بمقدار 600 ميكاباسكال. ان هذا البحث يهدف الى تقوية جزء من طول العتب حيث تم اعتماد نسبة الطول المقواة وهي 0.83, 0.67 و 0.5 حيث تمثل هذه الارقام نسبة الجزء الذي تم تقويته بالنسبة للطول الكلي للعتب. اظهرت النتائج كفاءة هذه التقنية في تقليل عرض التشققات وزيادة في مقاومة العتب للاحمال المسلطة. حيث ان بنقصان نسبة الطول المقواة ازدادت نسب حمل التشقق الاول بمقدار 100% و 133% و 167% وحمل الشق الخدمي (0.3 ملم) بمقدار 63% و 75% و 88% والحمل الاقصى بمقدار 78% و 89% و 67% عن العتب المرجعي لنسب الطول المقواة 0.83, 0.67 و 0.5 على التوالي.

الكلمات الرئيسية: الاجهاد المسبق ;خارجي; التقوية; مقطع على شكل حرف T ; جدائل الحديد

1. INTRODUCTION

The repairing and strengthening of deteriorated and substandard structures has become one of the important challenges confronting civil engineering worldwide. There is a significant and growing need for the strengthening of RC structures. In other hand, the decision to rehabilitate or replace a structure depends upon its importance, the severity of the damage**,** the availability of resources, and the economic factors. While replacement of a structure is generally costly and time consuming, strengthening techniques that make efficient use of labor and economic resources provide attractive alternatives to new construction. Rehabilitation can extend the life of a structure, or if a building or a bridge is to be replaced, temporary repairs can return a critical structure to service until a replacement is operational**, Balbool, 2009**. External post-tensioning technique is considered one of the most powerful techniques that have been used for strengthening concrete structures because of ease of installation of the strands and reduced or no interruptions to the regular function of the structures. The advantage recorded previously, that the tendons were placed on the web of concrete beams; on the contrary the analysis and design of the strengthened members were more complicated**, Tan, and Ng, 1997**.

This study will be spot-light on the behavior of externally prestressed RC T-beams. External tendons are not bonded to the concrete, are free to move between the deviator, and have a nearly constant stress along their lengths. In the present study, the effect of the strengthening length ratio (L_s/L) which is equal to the length of strengthened region (L_s) divided to the length of beam (L) will be conducted. Stresses increment for rebars and strain in concrete at critical section also, the first crack, service and ultimate load capacities are also adopted in this study.

2. OBJECTIVES

The main objective of this study is:

1. Predicting the first cracking, service and ultimate load capacities of RC T-beams strengthened by using external prestressed tendons that subjected to short-term loading. In addition, determine the percentage increasing in these load capacities as compared with beam without strengthening.
2. Ability of installation of externally strands at a distance from supports with governed the purpose of strengthening.
3. Estimating the optimum position to fix the external strands without effected on the behavior of strengthened member.

3. LITERATURE REVIEW

Cooke, et al., 1981. conducted an experimental investigation to study the effect of (L/d_{ps}) ratio and the amount of prestressing steel on the stress at ultimate stage in unbonded tendons. They tested nine simply supported fully prestressed one-way slabs with unbonded tendons. The slabs were divided into three groups with varying (L/d_{ps}) ratio. Each group had a varying amount of prestressing steel.

Yaginuma, and Kitada, 1988. tested three series of unbounded partially prestressed concrete beams. All beams were strengthened using straight tendons covering whole length of the beams. Two (L/d_{ps}) ratios of 18 and 32 were taken into account. They concluded that the stresses in prestressed strands increased as decreasing (L/d_{ps}) ratio.

Harajli, and Kanj, 1992. tested 16 RC beams. These beams were externally strengthened using steel tendons along the beams and subjected to cyclic fatigue loading. They concluded that using a straight horizontal profile is less effective in increasing the flexural capacity than a deviated profile due to reduction in depth of the straight strands throughout loading.

Tan, and Ng, 1997. tested six T-section RC beams, each of 3.3 m in length. The beams were externally strengthened with external strands along the span. They used straight and draped tendons for comparison. They concluded that, the beams with draped tendons showed wider spread of cracks, greater tendon stress increase and greater ductility compared with beams of straight tendons.

Tan, et al., 2001. conducted two series of simply supported T section-RC beams, one strengthened with external steel tendons and the other with carbon FRP tendons. They concluded that the exterior tendons anchored at inter-span locations could efficiently enhanced beams capacity.

Ng, 2003. tested seven T-section RC beams strengthened with external tendons with constant strand depth of 200 mm. It concluded that the span to depth ratio has insignificant effect on the tendon stress at ultimate stage in externally prestressed beams. Also he proposed a modified bond reduction coefficient for evaluation the flexural strength of externally prestressed beams based on strain compatibility and force equilibrium.

Sivaleepunth, et al., 2005. conducted an experimental investigation on RC beams with external tendons by varying the geometry of loading whether it is one-point loading or two-point loading. A comparison has been done of the experimental results with the results of prediction equations recommended by ACI 318M-99 and AASHTO LRFD design codes. It is found that all beams have similar behavior and first cracks observed in the midle of beams.. Also, it is found that the flexural cracks occurred at approximately 50% of the ultimate load.

4. MATERAILS USED FOR CASTING BEAMS

4.1 Concrete

The ingredients of concrete are: cement, fine aggregate, coarse aggregate and mixing water. An ordinary strength concrete mix was prepared using Portland cement (Type IV). For all beams, the cylindrical compressive strength of concrete (f_c') was 30 MPa at 28 days.

4.1.1 Cement

Sulphate resistance Portland cement from Karbala city company plant popular name (Lafarge Bridge) is used throughout this investigation. All quantity of cement was tested chemically and physically. The properties conform to the **Iraqi Specifications No. 5, 1984.** for Portland cement and British standard, this test was conduct with the help of laboratory of southern cement company.

4.1.2 Fine aggregate

Natural sand from Al-Akhaidher quarries in Karbala city has been used for concrete mixes. The fine aggregate has (4.75mm) maximum size with rounded-shape particles and smooth texture with fineness modulus of (2.84). The sand has been washed and cleaned with water several times and conform to the **Iraqi specification No.45, 1984**.

4.1.3 Coarse aggregate

Crushed gravel from Al-Sudor region whith maximum size of 15 mm has been used throughout this research. The crushed river coarse aggregate was washed. The specific gravity and absorption were (2.66) and (0.66%) respectively and conform to the **Iraqi specification No.45, 1984**.

Slump test is the direct method which it gives measure to workability for concrete mix. So that, in the present study the slump is taken 75 to 100 mm that make the mix medium

workability. The curing of concrete is achieved normally by spray water for 28 days with covered the beams with roughness clothes.

4.2 Steel Rebars

Three sizes of deformed bars have been utilities in the present study which their diameters are: ϕ8 mm, ϕ10 mm and ϕ10 mm with yield stresses (f_y) of 530, 559, and 615 MPa respectively conform to **ASTM standard A615**.

4.3 Stress-Relived Strands

conform to **ASTM standard A416**. These strands of ϕ12 mm in diameter were made from seven wires by twisting six of them around one wire which is slightly larger than them. The ultimate strength and the modulus of elasticity were 1860 MPa and 190000 MPa respectively.

5. EXPERIMENTAL WORK

5.1 General

The experimental work is based on casting and testing up to failure four T section-RC beams having the same dimensions and internal reinforcement. Three of these beams have been strengthened by using external tendons (strands), while the remaining beam is kept without strengthening as a control beam. The primary effect is the length of the strengthening region (L_s). Where part of the span is strengthened to enhance the flexural behavior of simply supported T section-RC beams.

5.2 Specimens

All specimens were reinforced concrete with T-section having dimensions as: *hf =75 mm, bf=350 mm,* b_w*= 150 mm* and *h=250 mm*. The total length of the specimens is 3200 mm and the effected length (***L***) is 3000 mm. These beams were internally reinforced by 2ϕ12 mm as bottom reinforcement (tensile reinforcement), 4ϕ10 as top reinforcement (compressive reinforcement) and ϕ8 mm@100 mm as stirrups (shear reinforcement). All four beams were subjected to two mid-third concentrated loads up to failure. Fig. 1 shows the full details and setup of the tested beams.

Two external strands of diameter 12 mm (cross-sectional area of 98 mm^2) have been fixed at each side of the web of the strengthening beams and located at eccentricity (***e***) of 100 mm from center of gravity of the section, ***C.G.C,*** (or depth of strands=200 mm from top fiber of the section, d_{ps}) with one deviator at mid-span so that the depth of strands to overall depth of the section ratio ($d_{ps}/h=0.8$). A special anchorage system has been achieved to fix these external tendons with the web of the strengthened beams.

The main parameter conducting in this research is the strengthening length ratio (L_s/L) which is equal to the length of strengthening region (L_s) divided to the length of beam (***L***). In this research the strengthening ratios were 0.83, 0.67 and 0.50.

The tested beams is remarked as AT-0, AT-1, AT-2 and AT-3. AT-0 is the control beam and the three beams (AT-1, AT-2, and AT-3) are strengthened beams. The remark at the end of symbol of the beams refers to the strengthening region (L_s), where number (1,2and 3) refers to (2500,2000, and 1500) mm (L_s) respectively as shown in Fig. 2. Also, Table 1 illustrates the properties of the strengthened beams.

5.3 Anchorage System

Two plates with dimensions of 200 by 200mm and thickness of 10 mm have been bent to form an angle-shape section with unequal legs of 120 mm and 80 mm. These angle-shapes were then welded back to back together and with additional stiffeners to form a shape that able to resist any expected deformation when subjected to load as shown in Fig. 3. The mechanical transfer system has been attached by drilling four holes in the web of beams at distances according to strengthened length (L_s) required for each strengthened beam and then fixed with bolts.

5.4 Deviator

To reduce second order effect, one deviator was used at mid span for all strengthened beams. This deviator was fabricated from a plate of 6 mm thickness surrounding beam web in the bottom and welded to perpendicular stiffener plates on both sides as shown in Fig. 4.

5.5 Jacking Process

The maximum initial post-tensioning prestressed stress was 600 MPa. To control the stress of strands, a balance device has been used as shown in Fig. 5 to insure distributed load neutrally and avoided laterally deformation.

5.6 Mesuring Devices

In the present study, device equipments are provided such as hydraulic jack for post-tensioning requirements, universal testing machine for applying load, strain tools measurement, crack width tool, and dial gauge for recording central deflection.

6. EXPERIMENTAL RESULTS

All beams were tested up to failure by applying two mid-third point load with load division of 7 kN. This test is carried out using a universal testing machine with full capacity of 200 ton.

6.1 Crack Pattern

The first cracks for beam **AT-0** (control beam) propagated at load 21 kN, spread and distributed along the span. Seven to eight cracks at each side beyond the center line of the beam were appeared, their length were ranged between (67 to 171) mm. The cracks within the zone of pure bending moment were longer than the cracks outside this zone. However, as the load increased, the cracks moderately propagated upward to the flange through few steps after first cracking load. Increasing load caused cracks progressed upward rapidly and significantly until they reached their final length which ranged between (190 to 220) mm at ultimate load of 63 kN. It is worth to mention that at load 56 kN, the crack width was 0.3 mm. So that according to **ACI committee R224-07**, this load is considered as a service load. Fig. 6 shows the crack pattern at three stages of loading, first crack, service and ultimate stages of loading.

For strengthened beam **AT-1** ($L_s/L=0.83$) at load step 42 kN, only five short cracks were appeared at each side beyond the center line of the beam within the pure bending moment zone with length ranged between (47 to 99) mm. These cracks were very small in length. Accordingly, as load increased, the cracks were progressed and increased in length upward to compression zone with generated new cracks outside the pure bending moment zone. The service load was 91 kN which corresponding to crack width of 0.3 mm. These cracks were progressed continously till they reached their final length which ranged between (97 to 148) mm. The ultimate load at this stage was 112 kN. Fig. 7 shows the crack pattern generated in this beam.

For strengthened beam **AT-2** ($L_s/L=0.67$), Eight cracks were appeared at load step 49 kN. These cracks were spread and distributed within the pure bending moment zone, their length was

ranged between (68-138) mm. Increasing load caused a slightly increasing in crack width and length. The service load was 98 kN with increasing the crack width to 0.3 mm at this load. The ultimate load was 119 kN and the cracks reached their final length as shown in Fig 8. From this figure, it could be noted that inclined cracks were created outside the strengthening region and beyond the anchorage system.

For strengthened beam **AT-3** ***($L_s/L=0.50$)***, only two cracks at each side of the beam were noticed at load 42 kN outside the strengthening region with very small width. Thereby, when the load increased up to 56 kN, the cracks length had increased outside the strengthened region with generating new cracks within the strengthening zone their length ranged between (108 to 115) mm. As the load increased, the cracks were increased and directed toward the compression flange till failure at load 105 kN. It is worth to mention that at this load the crack width was 0.3 mm, so that this load is also considered as service load. This cracks pattern is similar the result of further study, ***Tan, and Ng, 1997***. Fig. 9 shows the stages of loading for this beam.

Fig. 10 shows all tested beams after failure. Also, the results obtained from these four tested beams could be summerised as illustrated in Table 2. From this table, It can be noticed that the percentage increasing in first crack loads were 100%, 133% and 167%, for service loads were 63%, 75% and 88% and for ultimate loads were 78%, 89% and 67% for strengthening ratios 0.83, 0.67 and 0.50 respectively as compared with the control beam.

The load-cracks width curve for all tested beams is shown in Fig. 11. It could be noticed from this figure that, when reducing the strengthening ratio (***L_s/L***), the width of cracks at same level of load is reduced, due to increase the stiffness of the member within the strengthening zone.

6.2 Failure Mode

When a concrete member has a low steel ratio, that mean steel yielding before concrete crushing. In this research, all tested beams were designed with low steel ratio. The failure mode was predicted by measuring concrete strains at mid-span section of beams according to readings obtained from demec points throgout loadings. While, stresses in the ordinary reinforcement were calculated as strains at steel level (***d_s***) multiplied by steel modulus of elasticity but no greater than yield stress. Forgoing, the test focused on the member when failed only by yielding steel or crushing concrete. The control beam was failed by yielding of bottom steel but the stresses of concrete at top fiber was less than the ultimate strain. Generally, strengthened beams by external tendons have been enhanced slightly the strains in concrete and stresses in ordinary steel as compared with control beam at the same level of load. As decreasing ***(L_s/L)*** ratios from 0.83 to 0.5, the strains in concrete and the stresses in steel rebars were decreased at the same level of load as shown in Figs. (12 and 13) respectively. From Fig. (13) it could be noticed that the stresses in steel rebars for strengthened beams at transfer stage of loading having a negative signs. This is because the cambering effect due to strands tensioning.

6.3 Curvature

The results viewed with decreasing the strengthening length ratio from 0.83 to 0.5, the curvature is reduced as compared with the control beam due to increase the stiffness of beams due to strands effect. Fig. 14 shows the moment-curvature responses at mid-span section for tested beams. For strengthened beams, the curvature values at early stages of loading having approximately constant values this behavior might be due to constant moment within strengthened region. Also, it is clear form this figure that at transfer stage when strands have been tensioned, the curvature values have negative sign due to camber effect. The curvature is

depends on concrete top and bottom extreme strains fiber recorded throughout the test. Eq. (1) is used for uncracked section. While, Eq. (2) is used for cracked section.

$$\emptyset_i = \frac{\varepsilon_{cbi} - \varepsilon_{cti}}{h} \quad (1)$$

$$\emptyset_i = \frac{\varepsilon_{cdi}}{d} \quad (2)$$

Where ϕ_i is the curvature at load step *i*.

ε_{cbi} is the bottom extreme strain fiber of concerete at load step *i*.

ε_{cti} is the top extreme strain fiber of concerete at load step *i*.

ε_{cdi} is the concrete strain at depth *d* above the neutral axis at load step *i*.

6.4 Load-Deflection Response

Central deflection has been recorded for each beam during the test by using dial gage located at mid-span of beam. The load-deflection responses for the strengthened beams were significantly stiffer than the control beam because of greater flexural rigidity (***EI***) for strengthened beam than control beam. Decreasing (***L_s/L***) ratio from 0.83 to 0.5 caused increasing in deflection within the inter range of loading, because the value of (***EI***) decreased as decreasing strengthening ratio. Fig. 15 shows the load-mid span deflection cuvers for tested beams.

The **ACI Code 318M-11**, limits the maximum permissible deflections to ***L/180*** (***Ds2***)***, or L/360*** (***Ds1***) for immediate deflection due to live load. The first limitation is for members which are not likely to be damaged by large deflection. While, the second limitation is for members which are likely to be damaged by large deflection.

6.5 Stresses of Strands

Strain in strands is determined by measuring the displacement between two demec points dividing by the distance between them. On the other hand, stresses in the strands within the elastic range are calculated by Eq. (3). Increments of strands stresses above initial stress (600MPa) are shown in Fig. 16. Increment stresses in strengthening beams are approximately similar this is because of constant (***d_{ps} /h***) ratio which equal to 0.8. Increment strand stresses measured experimentally by applying Eq. (3) and predicated analytically by applying Equation (18-4) of the **ACI Code 318M-11** are presented in Table (3).

$$\Delta f_{ps} = \Delta \varepsilon_{ps} \times E_{ps} \quad (3)$$

Where Δf_{ps} is the increment of strand stress

$\Delta \varepsilon_{ps}$ is the increment of strand strain

E_{ps} is the modulus of elasticity of the strand

7. CONCLUSIONS

1. Generally, using external strands technique for strengthening RC beams is effecient to increase beams capacities.
2. Decreasing strengthening length ratio affected on delaying the appearance of first cracks.
3. Decreasing strengthening length ratio lead to increasing first cracks load, service cracks load and ultimate loads. The percentage increasing in first crack loads were 100%, 133% and 167%, for service loads were 63%, 75% and 88% and for ultimate loads were 78%, 89% and 67% for strengthening ratios 0.83, 0.67 and 0.50 respectively as compared with the control beam.

4. Strengthened beams by external tendons would enhanced slightly the strains in concrete and stresses in ordinary steel as compared with control beam. As decreasing (L_s/L) ratios from 0.83 to 0.5, the strains in concrete and the stresses in steel rebars were decreased at the same level of load.
5. The results viewed with decreasing the strengthening length ratio from 0.83 to 0.5, the curvature is reduced as compared with the control beam due to increase the stiffness of beams due to strands effect.
6. Increments of strands stresses above the initial stress is approximately similar for all strengthened beams due to constant (d_{ps}/h) ratio.

REFRENCES

- ACI Committee 224, 2007, *Causes, Evaluation, and Repair of Cracks in Concrete Structures (ACI 224.1R-07)*, American Concrete Institute, Detroit.
- ACI Committee 318, 2008, *Building Code Requirements for Reinforced Concrete and Commentary (ACI 318M-08 and ACI 318RM-08)*, American Concrete Institute, Detroit.
- ASTM Designation A416/A416M-06, 2006, *Standard Specification for Steel Strand, Uncoated Seven-Wire for Prestressed Concrete*, Annual Book of ASTM Standards, American Society for Testing and Materials, Philadelphia, Pennsylvania, vol. 1.03.
- ASTM Designation A615/A615M-01b, 2001, *Standard Specifications for Deformed and Plain Billet-Steel Bars for Concrete Reinforcement*, Annual Book of ASTM Standards, American Society for Testing and Materials, Philadelphia, Pennsylvania, vol. 1.04.
- Balbool, A. N. A., 2009, *Prestressed Fiber Reinforced Polymer (FRP) For Strengthening of Concrete Members*, University of Baghdad, College of Engineering, Civil Engineering Department
- Cooke, N., Park, R., and Yong, P., 1981, *Flexural Strength of Prestressed Concrete Members with Un-bonded Tendons*, PCI Journal, Vol. 26, No. 6, PP. 52-81.
- Harajli, M.H., and Kanj, M., 1992, *Service Load Deflection of Concrete Members Prestressed with Unbonded Tendons*, Journal of Structural Engineering, ASCE, Vol. 118, No. 9, PP.2569-2588.
- Iraqi Specification No. 5, *Portland Cement*, Baghdad, 1984
- Iraqi Specification No. 45, *Natural Sources for Gravel That is Used in Concrete and Construction*", Baghdad, 1984
- Ng. C. K., 2003, Tendon Stress and Flexural Strength of Externally Prestressed Beams, ACI Structural Journal, Vol. 100, No. 5, PP. 644–653.

- Sivaleepunth, C., Niwa, J., Tamura, S., and Hamada, Y., 2005, Flexural Behavior of Externally Prestressed Concrete Beams by Considering Loading Application, Technical Paper, Vol.27, No.2, PP. 553-558.

- Tan, K.H., and Ng, C. K., 1997, *Effects of Deviators and Tendon Configuration on Behavior of Externally Prestressed Beams*, ACI Structural Journal, Vol. 94, No. 1, PP. 13–22.

- Tan, K.H., Ng, C. K., and Al-Farooq, M. A., 2001, *Behavior of Simple-Span Reinforced Concrete Beams Locally Strengthened with External Tendons*, ACI Structural Journal, Vol. 98, No. 2, PP. 174-183.

- Yaginuma, Y., and Kitada, Y., 1988, *Influence of Span on Behavior of Partially Prestressed Concrete Beams with External Cables*, Transactions of the Japan Concrete Institute, Vol. 10, PP. 409-416.

NOMENCLATURE

d_s depth of ordinary reinforcement from top fiber of the section
d_{ps} depth of strand from top fiber of the section
EI flexural rigidity
E_{ps} modulus of elasticity of the strand
f_c' cylindrical compressive strength of concrete
f_y yield stress of steel reinforcement
h overall depth of the section
L length of beam
L_s length of strengthened region
RC reinforced concrete
Δf_{ps} increment of strand stress
$\Delta \varepsilon_{ps}$ increment of strand strain
ε_{cbi} bottom extreme strain fiber of concerete at load step i.
ε_{cdi} concrete strain at depth d above the neutral axis at load step i.
ε_{cti} top extreme strain fiber of concerete at load step i.
ϕ_i curvature at load step i.

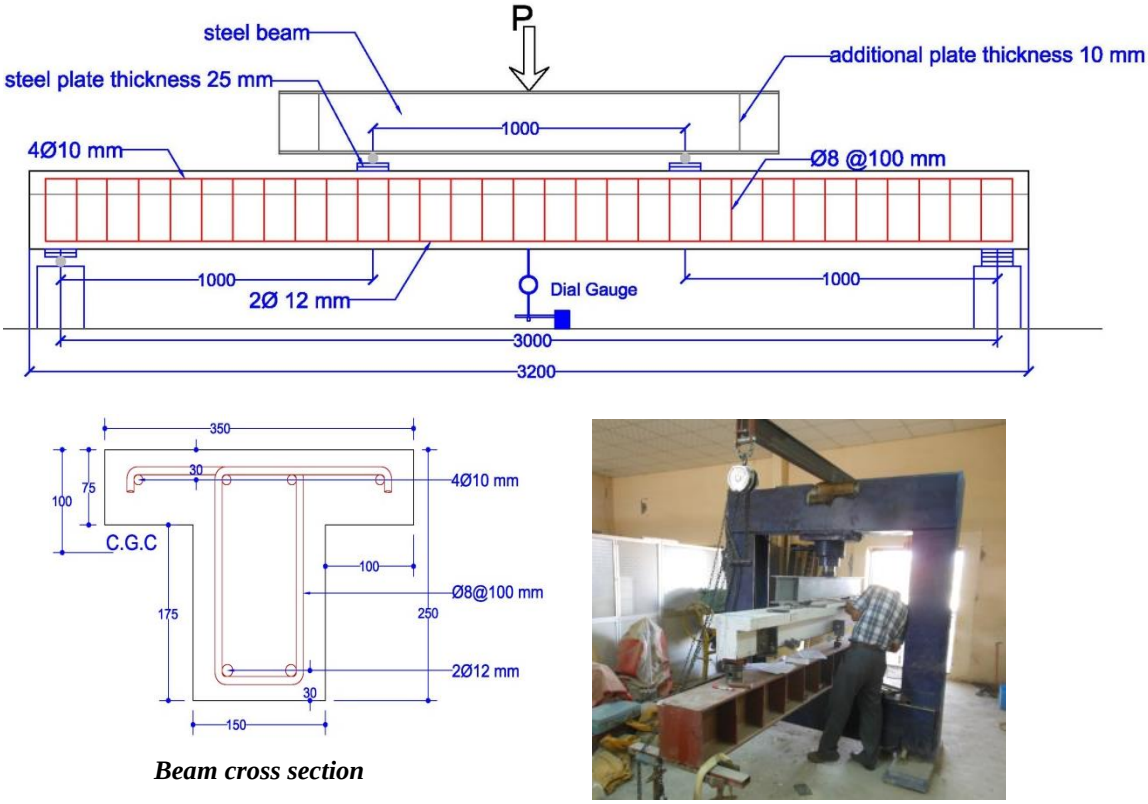

Beam cross section

Figure 1. Layout and setup of typical tested beam (all dimensions are in mm).

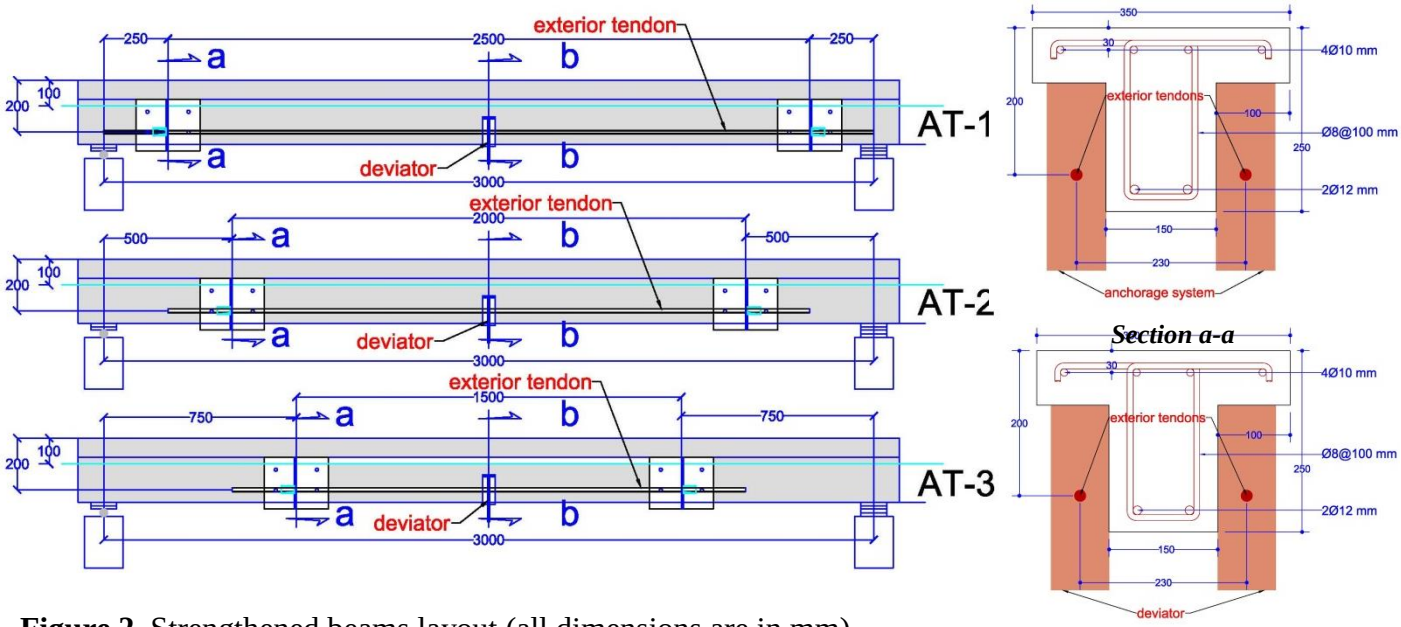

Figure 2. Strengthened beams layout (all dimensions are in mm).

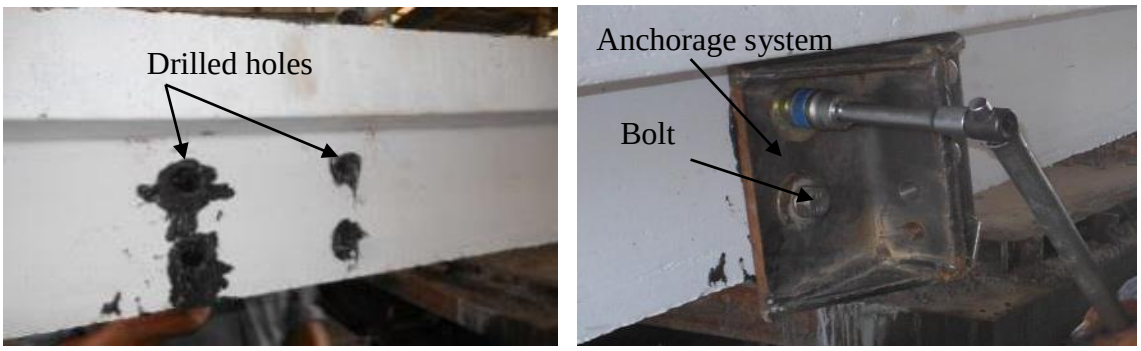

Figure 3. Operation used to fix the anchorage system.

Figure 4. Deviator.

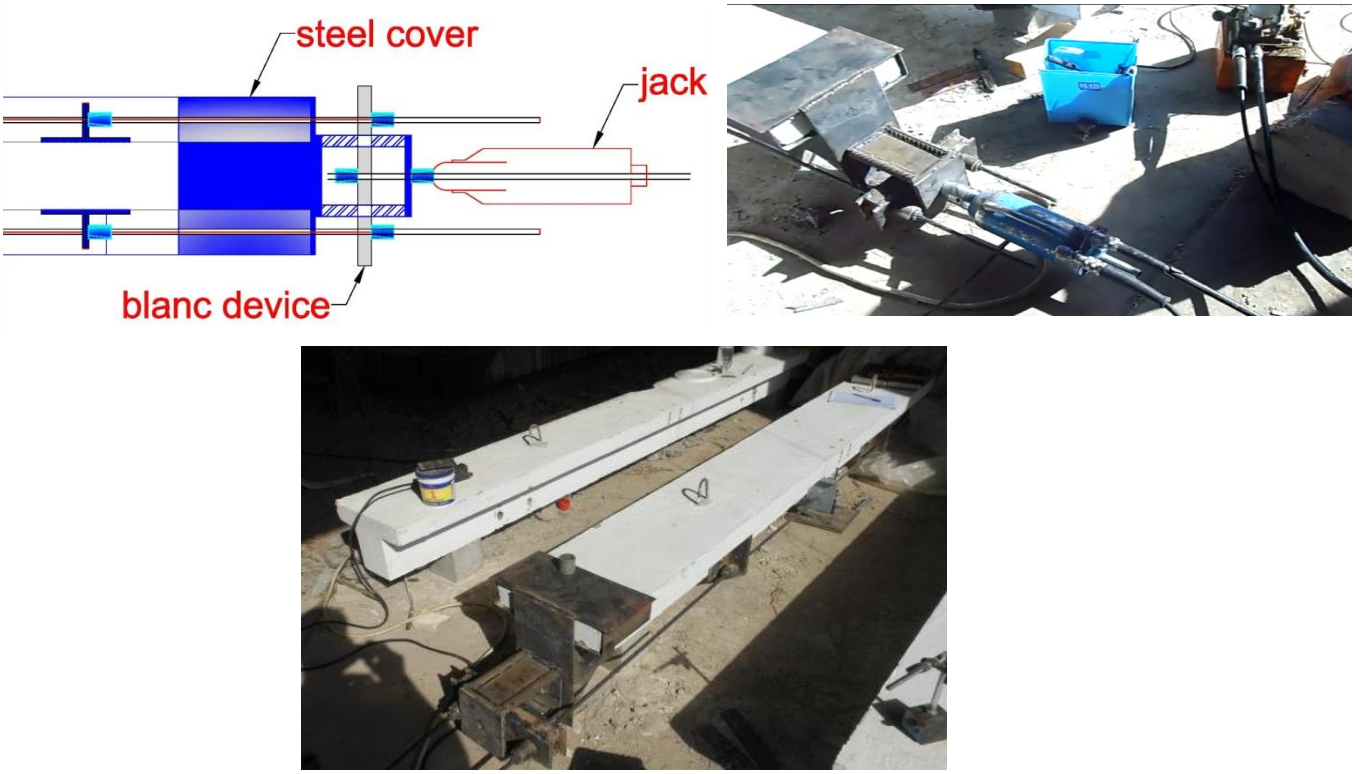

Figure 5. Jacking prosses to balance the force.

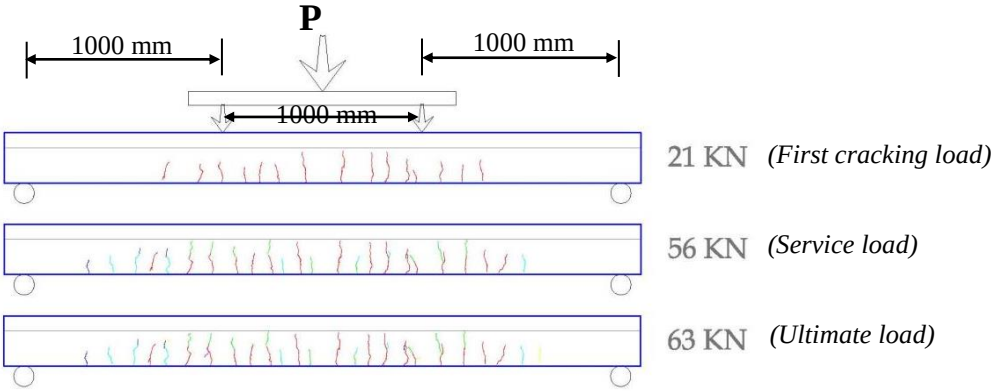

Figure 6. Cracks pattern for beam AT-0 (control beam).

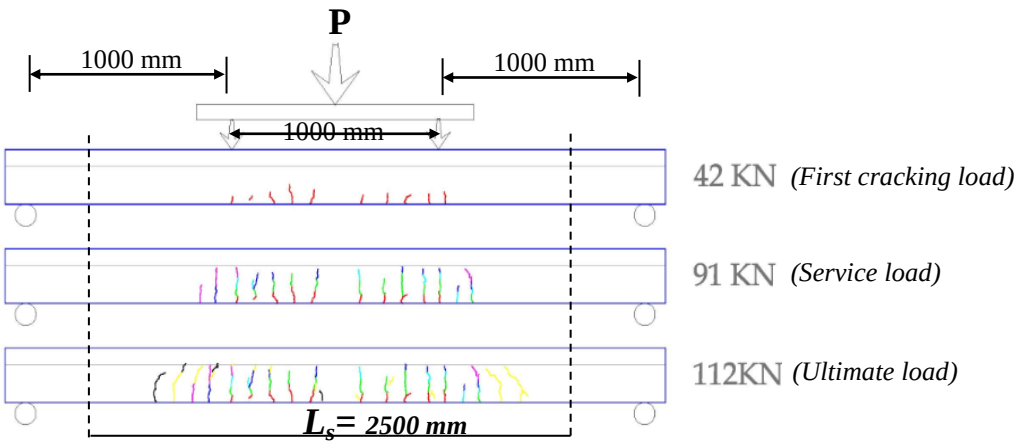

Figure 7. Cracks pattern for strengthened beam AT-1 (L_s/L=0.83).

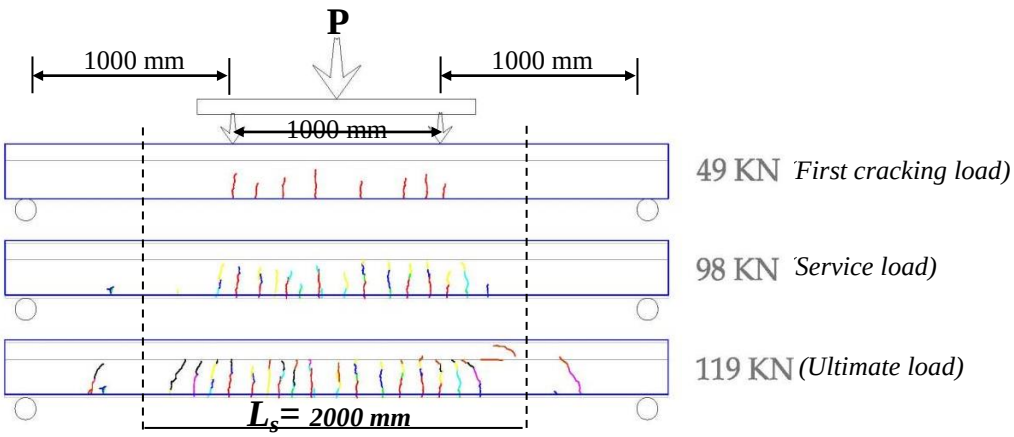

Figure 8. Cracks pattern for strengthened beam AT-2 (L_s/L=0.67).

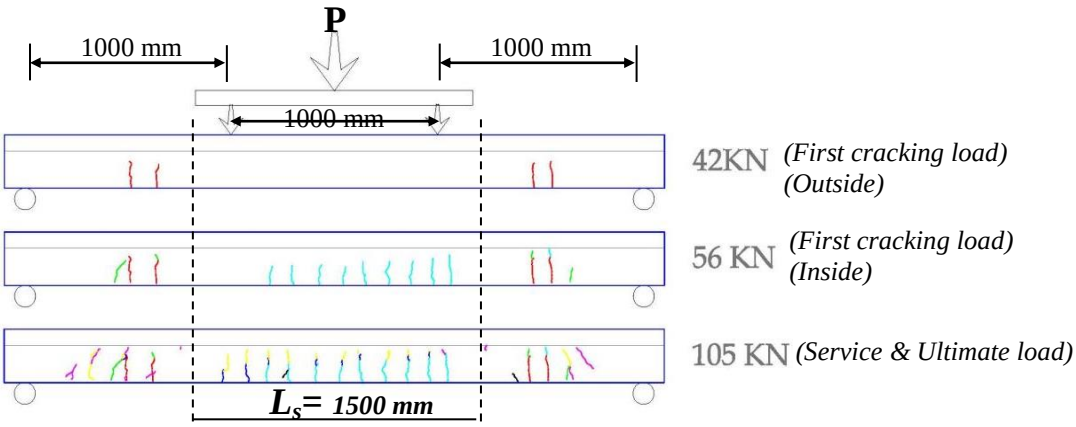

Figure 9. Cracks pattern for strengthened beam AT-3 (L_s/L=0.50).

Figure 10. Tested beams after failure.

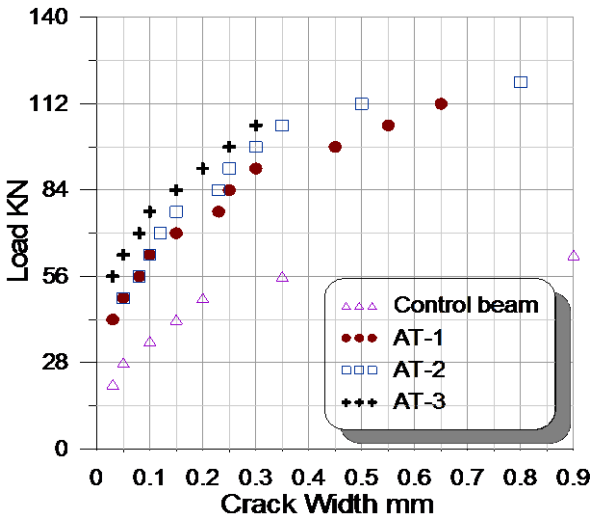

Figure 11. Load-cracks width curves for tested beams.

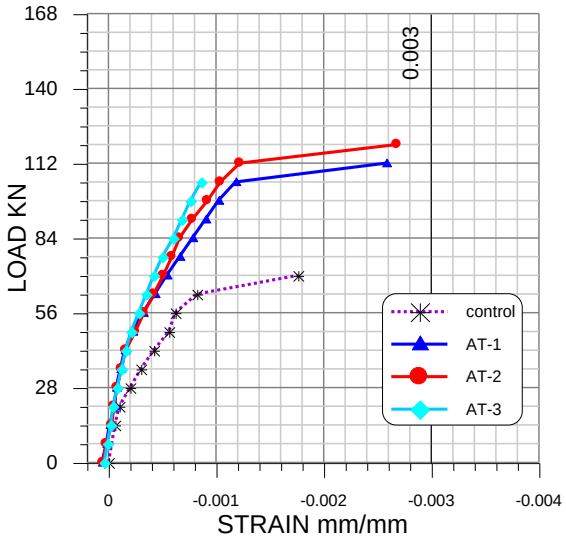

Figure 12. Strain at top fiber of concrete at mid-span section of tested beams.

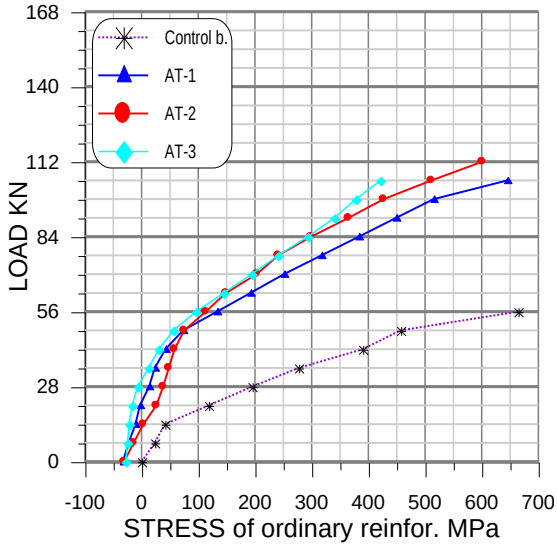

Figure 13. Stresss of ordinary steel rebars of tested beams.

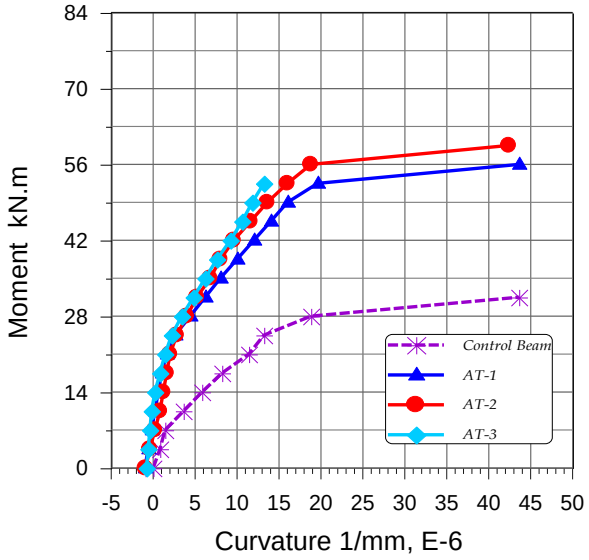

Figure 14. Moment- curvature responses for tested beams.

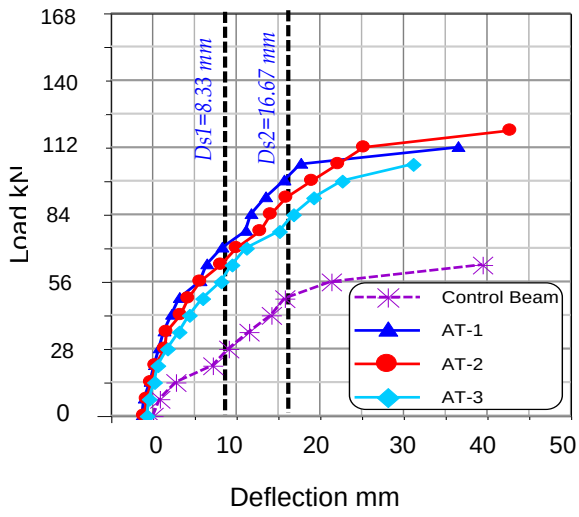

Figure 15. Load- mid span deflection responses for tested beams.

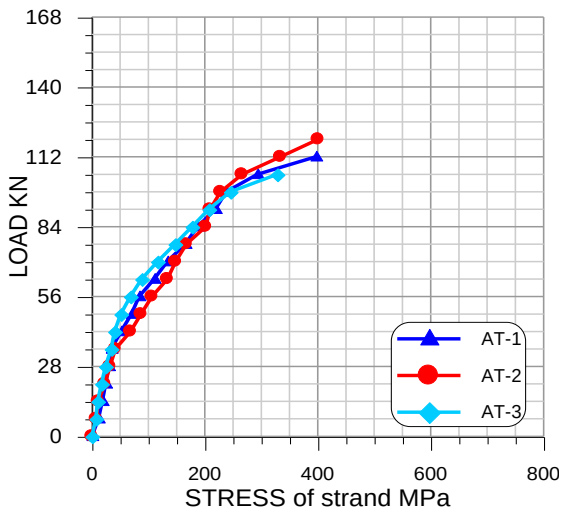

Figure 16. Increment stress in the strands above initial stress.

Table 1. Properties of the strengthened beams.

Beam designation	*Strengthening length (L_s) mm*	*(L_s/L) Ratio*	*Configuration of strand*	*Depth of strand (d_{ps}) mm*	*(d_{ps}/h) Ratio*
AT-0	Control Beam				
AT-1	2500	0.83	Straight	200	0.8
AT-2	2000	0.67	Straight	200	0.8
AT-3	1500	0.50	Straight	200	0.8

Table 2. Properties of the strengthened beams.

Beam designation	*First crack load (P_{cr}) kN*		*Service crack load (P_s)* kN*	*Ultimate load (P_u) kN*	*% Increasing in first cracking load*		*% Increasing in service cracking load*	*% Increasing in ultimate load*
Control beam	21		56	63	-		-	-
AT-1	42		91	112	100		63	78
AT-2	49		98	119	133		75	89
AT-3	42 Out	56 In	105	105	100 Out	167 In	88	67

$$\% \text{ Increasing} = \frac{P(strengthened) - P(control)}{P(control)} \times 100$$

*Crack width=0.3 mm

Table 3. Stresses in strands

Beam designation	*(L_s/L) Ratio*	*Δfps Y MPa*	*Δfps U MPa*	*fps Y MPa*	*fps U MPa*	*fps MPa ACI Code Eq. (18-4)*
				fps=Δfps+fpe		
AT-1	0.83	293	397	893	997	786
AT-2	0.67	334	401	934	1001	
AT-3	0.50	328		928		

Y,U the value of stress increment in yield and ultimate stages.
fpe =600 MPa

Modified Grid Clustering Technique to Predict Heat Transfer Coefficient in a Duct of Arbitrary Cross Section Area

AbdulKareem Abbas Khudhair
Lecturer
Mechanical Engineerig Deparemement / U.O.T.
E-mail: karimmosawi@yahoo .com

ABSTRACT

A simple straightforward mathematical method has been developed to cluster grid nodes on a boundary segment of an arbitrary geometry that can be fitted by a relevant polynomial. The method of solution is accomplished in two steps. At the first step, the length of the boundary segment is evaluated by using the mean value theorem, then grids are clustered as desired, using relevant linear clustering functions. At the second step, as the coordinates cell nodes have been computed and the incremental distance between each two nodes has been evaluated, the original coordinate of each node is then computed utilizing the same fitted polynomial with the mean value theorem but reversibly.

The method is utilized to predict Nusselt number distribution in a hybrid cross section area duct, non-circular non-rectangular, for laminar incompressible flow under Uniform Wall Temperature condition. The results have been compared with the published data and the agreement has been found very well.

Key words: heat transfer, grid generation, clustering.

طريقة مطورة لتنضيد العقد لغرض التنبؤ بمعامل انتقال الحرارة على طول مجرى ذو مقطع مساحة اعتباطي

عبد الكريم عباس خضير
مدرس
قسم الهندسة الميكانيكية / الجامعة التكنولوجية

الخلاصة

تم تطوير طريقة رياضية مباشرة لتنضيد العقد على قطعة حد منحنية ذات شكل اعتباطي بشرط انه يمكن تمثيل قطعة الحد هذه باستعمال متطابقة متعددة الحدود مناسبة. تتكون طريقة الحل بشكل عام من مرحلتين. الأولى تتمثل بتحويل قطعة الحد هذه الى قطعة مستقيم وايجاد طولها باستخدام نظرية متوسط القيمة. ثم نقوم بتوزيع العقد على قطعة المستقيم باستخدام طرق التنضيد الملائمة. وتتمثل المرحلة الثانية بإرجاع المستقيم الى أصله كقطعة خط منحني بعد ان تمت معرفة احداثيات العقد والمسافات بينها بالاستفادة من متطابقة متعددة الحدود نفسها ونظرية متوسط القيمة ولكن بشكل معكوس.

استخدمت الطريقة لإيجاد توزيع عدد نسلت على طول مجرى ذو مقطع هجين غير دائري وغير مستطيل لجريان طباقي غير انضغاطي وتمت مقارنة النتائج مع البيانات المنشورة وكان التطابق جيد جدا.

1. NTRODUCTION

For computational fluid dynamics problems, grid clustering in regions of high gradients of variables is of vital importance. It is obvious that one of the most regions of high gradients is at the vicinity of wall.

For a straight-line boundary segment such as rectangular cross section duct inlet, room walls …etc., the clustering is straightforward and linear clustering functions are available in many related CFD books. For example Robert in 1971 proposed a family of general stretching transformations, **Tannehill, et al., 1997**, represented a set of linear clustering functions. Some of these clustering functions are adapted here.

Usually grids clustering are made along a straight line (along one Cartesian axis) by adapting one of the linear cluster function. For curved segment, nodes have a variable x, y coordinates and these cluster function are not applicable directly.

Generally, and especially for strongly curved segments, it is not convenient to approximate the curved boundary as a straight line. For example when solving for flow around an airfoil, airfoil cannot be approximate as a rectangular.

Now days, the majority of CFD researchers are using a commercial CFD package to generate grids externally and internally for curved geometries and solving for flow variables. The body fitted coordinate system is the default coordinates system used to describe such geometries.

But for researchers who are interest in programming the governing equations rather using a commercial CFD package will face a real problem in clustering for such curved segments.

A simple procedure is suggested, developed and presented here to cluster grids along boundary segment of an arbitrary geometry. The method is utilized to predict Nusselt number distribution along a duct of hybrid cross section area for laminar incompressible flow under uniform wall temperature condition. The cross section area is quadrilateral which consists of two straight segments and two curved segments. The results were compared with the published data.

2. MATHEMATICAL REPRESENTATION.

The following stretching function is preferable in s-direction for a straight line, **Tannehill, et al., 1997**, which clusters grids towards segment ends:

$$\eta = \alpha + (1-\alpha) * \ln \frac{\{\beta + [s(2\alpha+1)/L] - 2\alpha\}}{\{\beta - [s(2\alpha+1)/L] + 2\alpha\}} / \ln[(\beta+1)/(\beta-1)] \qquad (1)$$

Eq. (1) describes the clustering in the computation domain. It must be inverted in order to express (s) as a function of (η) in the physical domain, as:

$$\frac{(\eta-\alpha)}{(1-\alpha)} ln[(\beta+1)/(\beta-1)] = ln \frac{\{\beta + [s(2\alpha+1)/L] - 2\alpha\}}{\{\beta - [s(2\alpha+1)/L] + 2\alpha\}}$$

$$[(\beta+1)/(\beta-1)]^{\frac{(\eta-\alpha)}{(1-\alpha)}} = \{\beta + [s(2\alpha+1)/L] - 2\alpha\}/\{\beta - [s(2\alpha+1)/L] + 2\alpha\}$$

let $A = [(\beta+1)/(\beta-1)]^{\frac{(\eta-\alpha)}{(1-\alpha)}}$ (2)

$A\{\beta - [s(2\alpha+1)/L] + 2\alpha\} = \{\beta + [s(2\alpha+1)/L] - 2\alpha\}$

$A(\beta+2\alpha) - (\beta-2\alpha) = (A+1)[s(2\alpha+1)/L]$

$$s = L\frac{A(\beta+2\alpha)-(\beta-2\alpha)}{(A+1)(2\alpha+1)} \quad (3)$$

The stretching parameter (β) has a numeric value which is slightly above unity, $\beta = 1.01\ to\ 1.2$ and it controls the grids refining intensity. (η) in Eq. (3) is a counter from ($1\ to\ NJ$). (NJ) is the number of grids along the segment in η-direction. (L) is the length of this straightened segment. Then (s) represent the incremental distance between two successive grids along η-direction.

In this transformation, the clustering parameter (α) is a numeric constant, which is chosen to refine grids near segment ends. If ($\alpha = 0$), grids will be refined near segment end where (J $= N$J) and if ($\alpha = 1$), grids will be refined near segment end where (J $= 1$), see **Fig. 1**.

For two-dimensional flow between two parallel plates, grids need to be clustered equally near solid boundaries so the clustering parameter is usually taken to be ($\alpha = 0.5$), and Eq. (2) becomes:

$$s = L\frac{A(\beta+1)-(\beta-1)}{2(A+1)} \quad (4)$$

Eq. (4) is used to cluster grids along (η -coordinate). For the computation domain, usually $\Delta\eta$ has a numeric value of unity, but in the physical domain $\Delta\eta = s$.

For a straight-line segment, Eq. (4) is applied directly. But For curved segment, the linear clustering cannot be applied directly. So a mathematical manipulation to the curved segment should be executed. The segment is first straightened mathematically and its exact length is computed, and then Eq. (4) is applied.

According to mean value theorem, **George,** and **Ross, 1998**, which states" if $y = f(x)$ is continuous at each point of [a, b] and differentiable at each point of [a, b], then there is at least one tangent (g) between (a) and (b) for which, see **Fig. 2**.

$$\frac{f(x_2)-f(x_1)}{x_2-x_1} = \acute{f}(g) \quad (5)$$

The curved segment (PQ) is approximated by a straight line, which length equals $\sqrt{(\Delta x)_j^2 + (\Delta y)_j^2}$, so the overall length of the curved segment (ab) is;

$$L \cong \sum_{J=1}^{n} \sqrt{(\Delta x)_J^2 + (\Delta y)_J^2} \quad (6)$$

$$L = \lim_{n\to\infty} \sum_{J=1}^{n} \sqrt{(\Delta x)_j^2 + (\Delta y)_J^2} \qquad (7)$$

The slope of line (PQ) is approximate by;

$$\acute{f}(g) = \Delta y / \Delta x \qquad (8)$$

$$\Delta y = \Delta x \, \acute{f}(g) \qquad (9)$$

Then Eq. (7) becomes: -

$$L = \lim_{n\to\infty} \sum_{J=1}^{n} \sqrt{(\Delta x)_j^2 + \left(\Delta x \, \acute{f}(g)\right)_J^2}$$

Then;

$$L = \int_a^b \sqrt{1 + \left(\acute{f}(g)\right)_J^2} \, dx \qquad (10)$$

The segment end points $a(x, y)$ and $b(x, y)$ are prescribed in advance while segment equation, $y = f(x)$, either known or a relevant, simple polynomial is fitted to the curved boundary segment.

Segment length (L) is evaluated from Eq. (10) and the number of grids is decided then Eq. (4) is used to cluster grids along the straightened boundary. The incremental distance, (s), distribution is computed.

Substitute each incremental distance length and the starting point (x) value, starting from point $(a(x, y))$ as input data, in the solution of Eq. (10). Then the value of (x) for each ending point is evaluated, since this equation has the (x) variable only. The $(NJ - 2)$ number of linear Equations are solved by (Do …. ENDDO) loop.

The calculated value of (x) is then substituted into segment equation $(y = f(x))$ to determine the (y) value for the corresponding point. The final result is a desirable well-clustered curved segment.

To demonstrate the beneficial of the method, let consider a common example which is simple and popular. For a circular arc shape segment of constant radius (R), the arc is described by the following special polynomial equation:

$$x^2 + y^2 = R^2 \qquad (11)$$

$$y = (R^2 - x^2)^{1/2}$$

$$\acute{y} = 0.5(R^2 - x^2)^{-0.5}(-2x)$$

$$\acute{y} = -x/\sqrt{R^2 - x^2} \qquad (12)$$

Substitute for the slope ($\acute{f}(g)$) from Eq. (12) in to Eq. (10) , then the length (L) becomes;

$$L = \int_a^b \sqrt{1 + \left(-x/\sqrt{R^2 - x^2}\right)^2}\, dx \qquad (13)$$

$$= \int_a^b \left(\frac{R^2}{(R^2 - x^2)}\right)^{0.5} dx$$

$$= R \int_a^b \frac{1}{(R^2 - x^2)^{0.5}}\, dx \qquad (14)$$

.

To interpret from Cartesian to polar coordinate system, precede as;

$$x = R\cos\theta$$

$$dx = -R\sin\theta\, d\theta$$

$$R^2 - x^2 = R^2 - R^2\cos^2\theta$$

$$R^2 - x^2 = R^2(1 - \cos^2\theta)$$

$$= R^2\sin^2\theta \qquad (15)$$

Substitute from Eq. (15) into Eq. (13) gives;

$$L = R\int_{\theta_a}^{\theta_b} \frac{-R\sin\theta\, d\theta}{(R^2\sin^2\theta)^{0.5}}$$

$$= -R\int_{\theta_b}^{\theta_b} d\theta$$

$$L = R(\theta_b - \theta_a)$$

$$= R\left(\theta_{J=NJ} - \theta_{\mathrm{J}=1}\right) \qquad (16)$$

Eq. (16) is well-known, **George,** and **Ross, 1998**. (θ_a) is the starting angle of the arc in radius at ($J = 1$) and (θ_b) is the ending angle of the arc in radius at ($J = NJ$). These two ends angle are prescribed in advance.

Substituting the value of arc length (L) from Eq. (16) into Eq. (4), then the length of sub-division segment (s_J) is evaluated directly. Rearrange Eq. (16) to compute the end segment angle (θ_J) in terms of the start sub-division segment angle (θ_{J-1}) and it length (s_J), as;

$$\theta_J = \theta_{J-1} - \frac{s_J}{R} \qquad (17)$$

Now all nodes angle, $\theta_1, \theta_2, \theta_£, \ldots\ \theta_{NJ}$, are computed and ($R$) is constant then, the value of (x) and (y) for each node are evaluated directly as:

$$x_J = R\cos\theta_J \ ;\ y_J = R\sin\theta_J \qquad (18)$$

At this stage grids are distributed externally along the boundaries nicely and as needed. The internally grid distribution is accomplished by using the TTM Poisson type method, **Thompson, et al., 1985**. The TTM method, named due to (Thompson, Thames, and Mastin), with an essential contribution from (Thomas, and Middlecoff), **Thomas, 1980**, **Thomas, et al., 1982**. The TTM method is the corner stone of grid generation techniques now days, **Thompson, 2000**. **Fig. 6** shows two types of internally grid generation depending on the external grids distribution.

The details of the TTM method for internally grid generation is prescribed by **Khudhair, 2003.**

3. HEAT TRANSFER APPROACH.

To demonstrate the validity of the method, a convective heat transfer coefficient was evaluated in a duct of non-circular and non-rectangular cross section as shown in **Fig. 3**.

Unfortunately neither the Cartesian nor the cylindrical coordinate system is a proper choice for such cross section. The body fitted coordinate system is convenient system. So the fluid governing equations will be first written in a Cartesian coordinate system and then transferred to a body fitted coordinate system.

The governing equations in Cartesian coordinate system for steady, incompressible, three-dimensional laminar flow with constant specific heats are, **Tannehill, et al., 1997**:

$$\nabla.\left(\rho\vec{\boldsymbol{V}}\right) = 0 \qquad (18)$$

$$\nabla.\left(\rho u\vec{\boldsymbol{V}}\right) = -\frac{\partial p}{\partial x} + \nabla.(\mu\nabla.u) + S_{Mx} \qquad (19a)$$

$$\nabla.\left(\rho v\vec{\boldsymbol{V}}\right) = -\frac{\partial p}{\partial y} + \nabla.(\mu\nabla.v) + S_{My} \qquad (19b)$$

$$\nabla.\left(\rho w\vec{\boldsymbol{V}}\right) = -\frac{\partial p}{\partial z} + \nabla.(\mu\nabla.w) + S_{Mz} \qquad (19c)$$

$$\nabla.\left(\rho T\vec{\boldsymbol{V}}\right) = \nabla.(\mu\nabla.T) + S_T \qquad (20)$$

These governing equations are in Cartesian coordinate system, which is not convenient to solve for a flow inside a duct with arbitrary cross section area. Also the polar coordinate is not convenient for a cross section area as shown by **Fig. 5**. The body fitted coordinate system is the convenient choice. Details of transformation to body fitted coordinate system and discretization for continuity, momentum and energy equations are presented in details by **Khudhair, 2003, 2013**.

From **Fig. 4**, the increase or decrease of heat within the control is equal to the heat gained or lost by convection through duct wall, i.e.

$$\delta Q_{C.V.} = \delta Q_{conv} \qquad (21)$$

$$\dot{m} c_p dT = h_j P dx \left(T_w - T_{f,j}\right) \qquad (22)$$

Since T_w is constant, then;

$$dT = d\left(T_w - T_{f,j}\right)$$

and Eq. (22) becomes:

$$h_j = -\frac{\dot{m} c_p dT}{P dx \left(T_w - T_{f,j}\right)}$$

$$h_j = \frac{\dot{m} c_p}{A_s} \ln \frac{\left(T_w - T_{f,j+1}\right)}{\left(T_w - T_{f,j}\right)} \qquad (23)$$

or simply;

$$\dot{m} c_p \Delta T = h_j A_s \left(T_w - T_{f,j}\right)$$

$$h_j = \frac{\dot{m} c_p \left(T_{f,j+1} - T_{f,j}\right)}{A_s \left(T_w - T_{f,j}\right)} \qquad (24)$$

Eqs. (23) and (24) for local heat transfer coefficient have been programed and solved and they have given ave an identical results. T_f represents the local fluid mean temperature within the control volume between two successive sections.

The local bulk temperature T_b, which is the fluid average temperature at each duct section, is evaluated from the conservation of energy. At each cross section, J, the number of cells equals $(NI - 1) \times (NK - 1)$.

$$\dot{m}_j c_p T_{b,j} = \sum \dot{m}_{i,j,k} c_p T_{i,j,k}$$

$$= \sum \rho c_p \left(V_{i,j,k} A_{i,j,k} T_{i,j,k} \right) \qquad (25)$$

For the duct under consideration, the cross section area and sectional mean velocity are constant, then.

$$\therefore T_{b,j} = \frac{\sum \left(V_{i,j,k} A_{i,j,k} T_{i,j,k} \right)}{V_m A_C} \qquad (26)$$

The variables $V_{i,j,k}$ and $T_{i,j,k}$ are the output data from the flow governing equation after the solution is converged while $A_{i,j,k}$ is computed from tensor mathematic during grid generation stage.

The local Nusselt number is then evaluated as;

$$Nu_j = \frac{h_j D_j}{k} \qquad (27)$$

D_j is a length scale which is usually taken as the hydraulic diameter. For the case under consideration the hydraulic diameter is constant.

$$D_j = \frac{4A_{cross}}{P} \qquad (28)$$

The average convective heat transfer coefficient depends on the average bulk temperature, which can be interpreted as;

$$T_{b,mean} \sum \dot{m}_j c_p = \sum \dot{m}_j c_p T_{b,j} \qquad (29)$$

Heat transfer coefficient or Nusselt number are usually plotted along the duct length, x, in terms of the inverse Graetz number which is a non-dimensional number.

$$Graetz\ number, Gr = Re\ Pr \frac{D_j}{x} \qquad (30)$$

Where Reynolds and Prandtl numbers are define as

$$Re = \frac{\rho V_m D_j}{\mu} \quad ; \quad Pr = \frac{\nu}{\alpha} = \frac{c_p \mu}{k} \qquad (31)$$

4. DUCT GEOMETRY.

Firstly, the duct geometry has been drawn programmatically using FORTRAN 90 code. **Fig. 5** shows the duct cross section area, which represents a quadrilateral entry. It consists of two straight walls and two curved walls. Number of grids chosen is $(15 \times 15 \times 501)$. The pipe cross section geometry is not convenient neither for Cartesian coordinate system nor for polar coordinate system and the body fitted coordinate system is the best choice. Grids are

distributed automatically as desire directly from Eq. (4) for the straight walls while for the curved walls the grids are distributed entirely following the prescribed procedure as follow:

1. Compute arc length of curved walls from Eq. (16), as $\theta_1$and θ_{NJ} are known.
2. Cluster grids along the segment ab and cd as desire using Eq. (4).
3. The output of Eq. (4) is the interval distance (s_J) between each two successive nodes, which represent the interval arc length.
4. Recalculate (θ) distribution, starting from ($J = 2$) to ($J = NJ - 1$), from Eq. (17).
5. Finding grid node coordinates from Eq. (18).
6. Internally grid generating using the TTM method.

5. INPUT DATA.

The working fluid is air with the specifications, which was considered at ($325\ K$), presented in **Table (1)**.

6. CODE CONSTRUCTION.

All the related equations have been programed using a FORTRAN 90 programing language. The corestone of the code was developed earlierby **Khudhair, 2003**, and it is modified later to handle the heat transfer problem and the forementioned modification.

7. SOLUTION PROCEDURE.

The solution procedure is illustrated in the provided flow chart, **Chart. (1)**.

8. RESULT AND DISCUSSION.

Fig. 7 shows the local Nusselt number distribution along the proposed duct with cluster and uniform grid distribution. The result were compared with the data presented by **Holman, 2010**. Clustering is important at region of high gradient. At the developing entrance region the agreement between predicted with cluster and comparator data is excellent over that uniform grid distribution. At the developed region where temperature and velocity distribution profile is settled, the advantage of clustered over uniform grid generation is vanished and both distribution are in a good agreement with the comparator data.

Fig. 8 shows the average Nusselt number distribution. The agreement between predicted result with **Holman, 2010,** and the empirical formula proposed by Hausen is very good with $+6.7\%$ and -4.3% error for uniform and clustered grids respectively, except at the very beginning of entry which may interpreted to the assumed uniform velocity profile at entry. The Hausen empirical relation for fully developed laminar flow for circular tubes at constant wall temperature, presented by **Holman, 2010,** which based on hydraulic diameter, is:

$$\overline{Nu} = 3.66 + \frac{0.0668(d/L)RePr}{1 + 0.04(d/L)RePr^{2/3}}$$

Uniform grid distribution gives fair agreement especially at developing region where high gradients are expected.

9. CONCLUSION.

Distribution grid nodes along a curved wall segment is important for thermo-problems. The described method is a mathematical dependent and well programed. Distribution grids along straight wall segment is straight forward. And can be find in many CFD books.

Grid clustering near wall is of vital importance for internal flows in confined conducts or external flows over plates where high gradients are exist. But uniform grid distribution works well when these gradients moderated. At the fully developed region where variables profile is constant, uniform distribution performs better since the cell skewness is greatly reduced.

The proposed technique predicted Nusselt number distribution very well in such conductor with a non-rectangular, non-circular cross section area. As expected the value of Nusselt number at entry has the maximum value where velocity and temperature gradients are high and these values fall down temperature profile settled.

At the end of the duct the predicted average Nusselt number value for clustered grid distribution equals (4.134) with error value of (-4.3%) when compare with Hausen predicted method. While for uniform grid distribution the average Nusselt number value at duct end is (3.698) with error value of ($+6.68$).

The technique presented here is aimed for those who are interest in programming their problem rather using commercial CFD package.

REFERENCES.

- Al-Dabagh, A. M., Al-Musawi, A. A. and Salam, A. Q., 2012, *Experimental and numerical study of enhancement heat transfer in twisted tubes heat exchangers*, Special Issue of Engineering and Development Journal, ISSN 1813-7822, pp 194-215.

- George B. T., and Ross, L. F.,1998, Calculus and Analytic Geometry, 9th ed, Addison-Wesly Publishing Company.

- Holman J.P., 2010, Heat transfer, 10th ed, The McGraw-Hill companies, Inc.

- Khudhair, A. A. 2013, Twist Parameter Influence on Heat Transfer Coefficient Augmentation for Square Twisted Tube, Engineering & Technology Journal, Vol. 31, part A, No. 9, pp 1802-1819.

- Khudhair, A. A., 2003, Computational Fluid Dynamics with Particular Reference to Centrifugal Pump Impellers. Ph .D. thesis. Mechanical Engineering Department, University of technology.

- Mohammed, A. A., Mohammed, B. A., and Muhee, R. J., 2014, Heat Transfer Enhancement in a Tube Fitted with Nozzle-Turbulators, Perforated Nozzle Turbulators with Different hole shap, Enginnering and Technology, Vol. 32, Part A, No. 10, pp 2514-2527.

- Tannehill, J. C., Anderson, D. A., and Pletcher, R. H., 1997, Computational Fluid Mechanics and Heat Transfer, 2nd editin, Hemisphere publishing corporation, Taylor & Francis group, New York.

- Thomas, P. D. and Middlecoff, J. F., 1980, Direct control of the grid point distribution in meshes generated by elliptic equations, AIAA J., vol. 18, no. 06, pp. 652-656.

- Thomas, P. D., 1982, Composite three-dimensional grid generated by elliptic systems. AIAA J., vol. 20, no. 09, pp. 1195-1202.

- Thompson, J. F., 2000, A Rreflection on Grid Generation in the 90's; Trends, Needs and Influences, Mississippi State University, Mississippi State, MS 39762 USA. Joe Thompson, joe @ erc.msstate.edu.

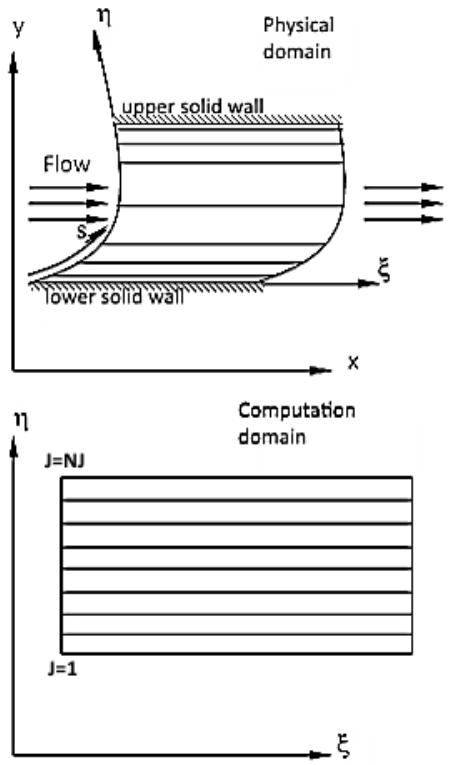

Figure 1. Pysical and computation domain

- Thompson, J. F., Warsi, Z. U. A., and Mastin, c. W., 1985, Numerical grid generation, foundations and applications, Elsevier Science Publishing Co., Inc.

NOMENCLATURE

Ac	cross section.	m^2	k	condictivity.	$W/m.°C$
As	surface area.	m^2	L	segment length.	m
c_p	specific heat.	$kJ/kg.°C$	$\dot{m}$	mass flow rate.	kg/m^3
D	hydraulic diameter.	m	Nu	nusselt number.	
H	heat transfer coefficient.	$W/m^2.°C$	P	perimeter.	m

p	pressure.	N/m^2
Pr	prandtl number.	
R	arc radius.	m
Re	reynolds number.	
s	incremental distance.	m
S_M	source term.	N/m^3
S_T	source term.	$kg.°C/s$
T	temperature.	°C or K
u	velocity components.	m/s
v	velocity components.	m/s
V	velocity.	m/s
$\vec{V}$	velocity vector.	m/s
w	velocity components.	m/s
X	cartesian coord. system.	
Y	cartesian coord. system.	
Z	cartesian coord. system.	
α	clustering parameter.	
β	streching parameter.	
η	coord. along boundary.	
θ	angle.	radian
μ	dynamic viscosity.	$kg/m.s$
ν	kinematic viscosity.	m^2/s

Table 1. Inlet air specifications, input data and duct size

Air density, ρ	$1.088\ kg/m^3$
Specific heat, c_p	$1007.4\ J/kg.K$
Dynamic viscosity, μ	$1.96 \times 10^{-5}\ kg/m.s$
Air condictivity, k	$0.028\ W/m.K$
Prandtl number	0.705
Inlet air temperature	25 °C
Wall temperature	50 °C
Bulk velocity	$0.4184\ m/s$
Reynolds number	1000
Cross section height	$3.536\ cm$
Cross section width	$5.0\ cm$
Duct length	$600\ cm$

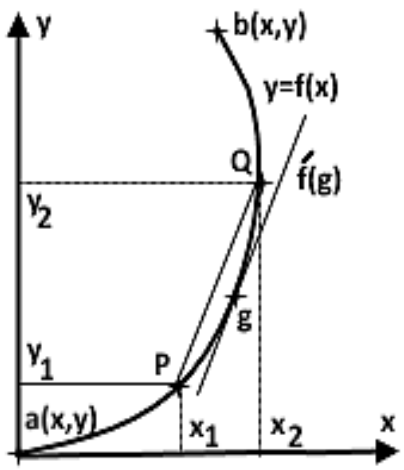

Figure 2. Mean value theorm

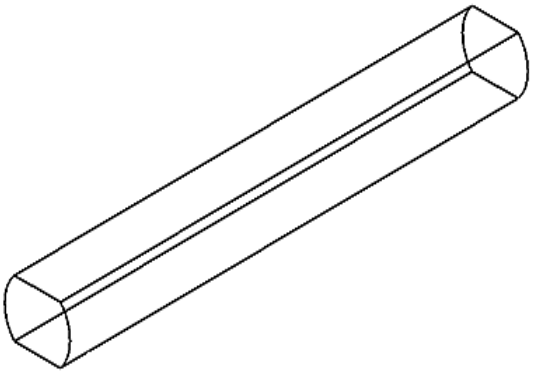

Figure 3. Non-circular and non-rectangualar cross section duct.

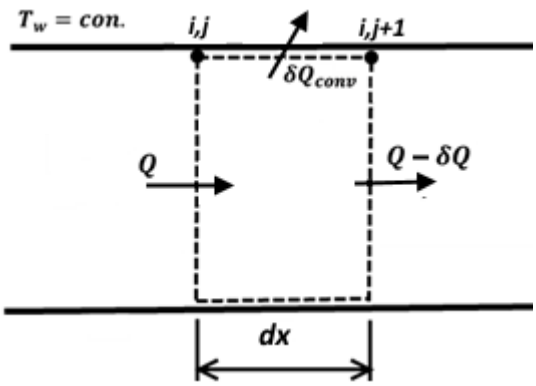

Figure 4. Control volume inside the duct

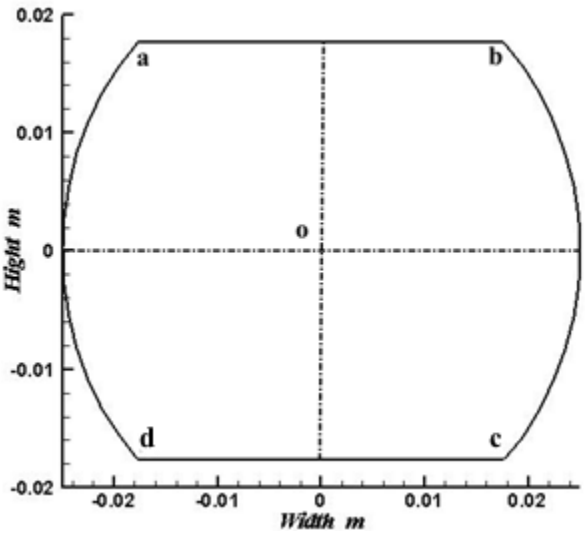

Figure 5. Duct cross section area

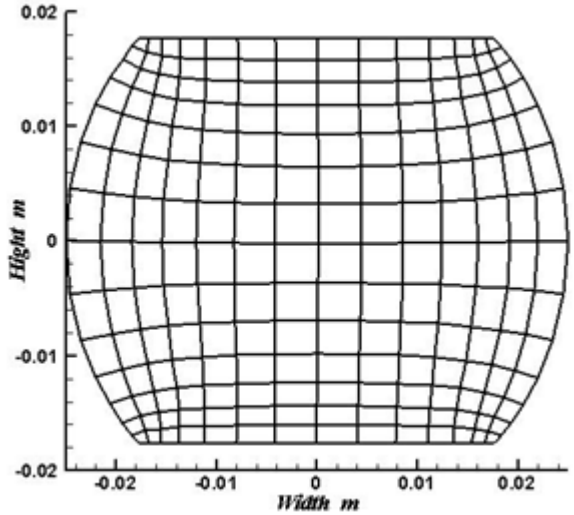

Figure 6a. Modify grid clustering

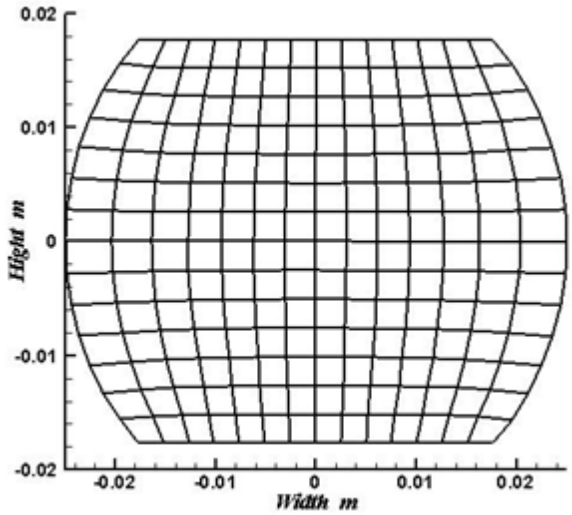

Figure 6b. Uniform grid Clustering

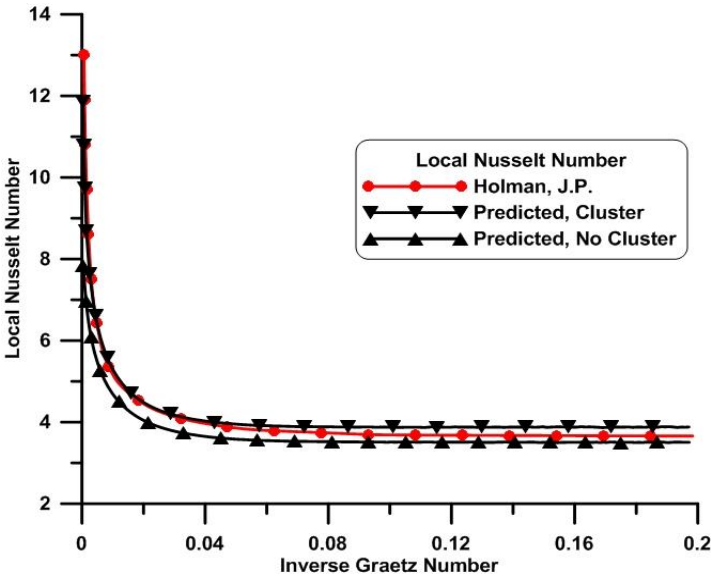

Figure 7. Local Nusselt number distribution

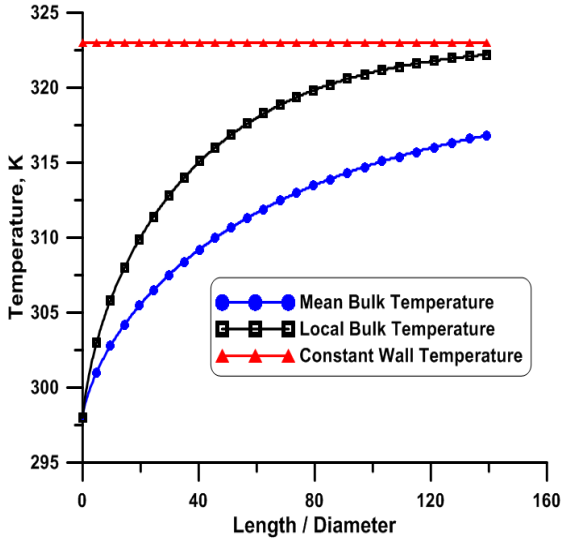

Figure 10. Bulk temperature

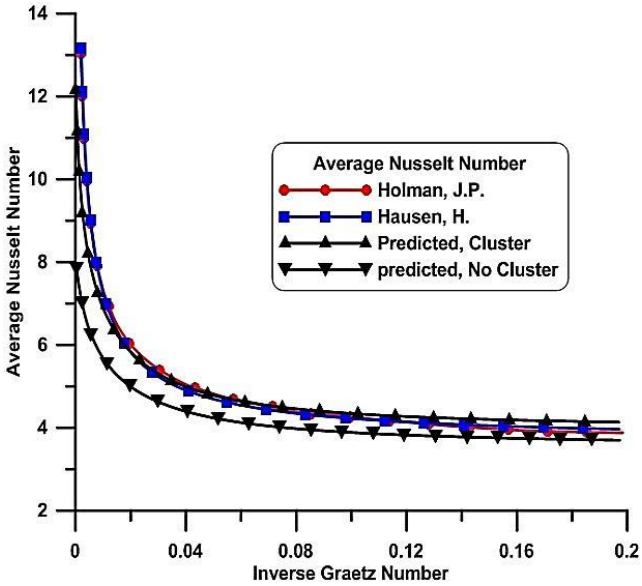

Figure 8. Average Nusselt number distribution

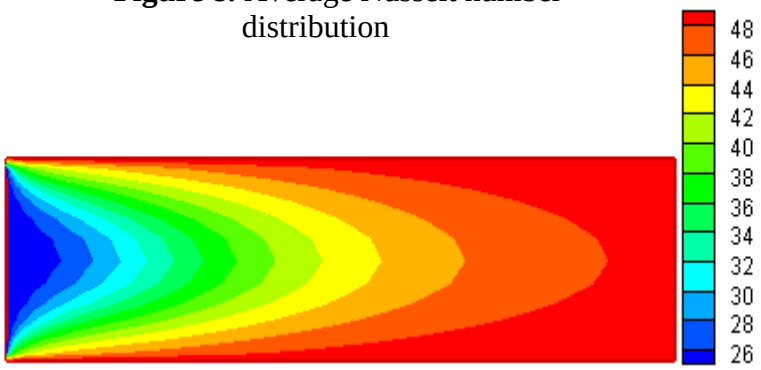

Figure 9. Temperature contors at longitudinal mid-section.

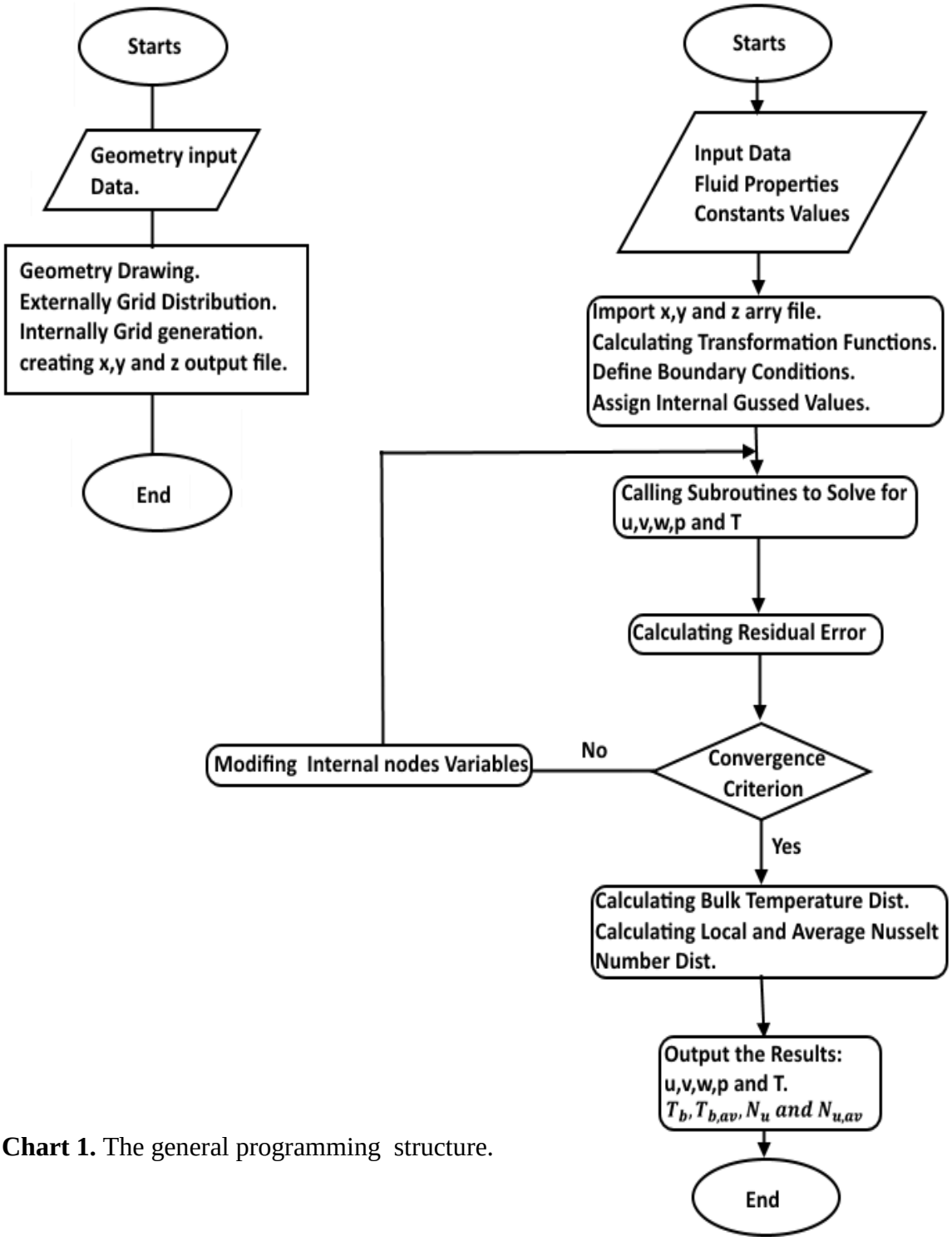

Chart 1. The general programming structure.

المحددات الحضارية والبيئية للمكان في عمارة العتبات الإسلامية المقدسة في العراق

(العتبة الكاظمية المقدسة –حالة دراسية)

الأستاذ الدكتورة صبا جبار نعمة الخفاجي
قسم هندسة العمارة–كلية الهندسة–جامعة بغداد

المهندس مهدي سهيل مهدي الكليدار
قسم هندسة العمارة–كلية الهندسة–جامعة بغداد

مستخلص البحث

عمارة العتبات الإسلامية نمط بنائي معماري إسلامي منتشر في ربوع العالم الإسلامي، ويحمل هذا النمط ميزات وخصوصيات معمارية تميزه عن باقي أنماط العمارة الإسلامية بحكم خصوصية وظيفته كمرقد لشخصية إسلامية مهمة تحمله الكثير من الجوانب الرمزية والاعتبارية ضمن التكوين المعماري. تطور نمط عمارة العتبات الإسلامية من مراقد بسيطة ثم اخذت بالاتساع مع تطور الزمن، وقد تطورت بعضها لتصبح نواة لنشوء مدن كبرى في العديد من ارجاء العالم الإسلامي.

برزت المشكلة البحثية: "**عدم كفاية المعرفة حول أهمية المكان وتأثير محدداته الحضارية والبيئية على عمارة العتبات الإسلامية المقدسة في العراق من حيث الأنماط والتطور الزمني**". ويفترض البحث بأن: "عمارة العتبات الإسلامية المقدسة في العراق بصفتها صروحا معمارية مهمة ومتميزة ولها أثرها الواضح على البنية العمرانية والتخطيطية في العديد من مدن العراق المهمة، فضلا عن ابعادها المعنوية والعقائدية وأثرها على المجتمع، فأنها قد تطورت بأنماطها وتخطيطها عبر الزمن وفقا للحاجات والمتطلبات الظرفية، الا ان عامل المكان كان له الدور الأساس في تشكيل كتلها وفضاءاتها ومعالجاتها الشكلية إضافة الى دور الدين الإسلامي الاساسي" كما ان توفر المعرفة حول العوامل المكانية التي انتجت العمارة العراقية، يوفر صورة متكاملة حول أصل المعالجات والتكوينات المعمارية ومنابعها المكانية الاصلية التي جاءت منها. مما يوسم عمارة العتبات الإسلامية المقدسة في العراق بمميزاتها وصفاتها التكوينية والتفصيلية الاصيلة.

الكلمات الرئيسية: عمارة إسلامية، عوامل المكان، السياحة الدينية، المراقد، العتبات المقدسة، الكاظمية.

Civilizations and Environmental Particulars of Place in Islamic Holy Thresholds in Iraq

(Alkadhumain Holy Threshold as a case study)

Prof. Dr. Saba J. Neamah Al-Khafaji
Department of architecture-College of Engineering-University of Baghdad
Saba.jabar@yahoo.com

Mahdi Suhail Mahdi Alkilidar
Department of architecture-College of Engineering-University of Baghdad
Alkilidar2020@yahoo.com

ABSTRACT

Islamic shrines architecture is one of the Islamic Architectural building types. It is called (Thresholds); (Atabat) in Arabic. Thoroughbred throughout the Islamic world from the east to west. In addition, it carries the style features and peculiarities of uniqueness from the rest of the types of Islamic architecture. By virtue of the particularity of its function as tomb for important person in Islamic history. Islamic shrines architecture has grown and evolved in started from the small shrines, and then taken to widen with the evolution of time in line with the value of the event and the rituals associated with it. Some of them to became centers of large cities of the largest in many parts of the Islamic world.

The research problem represented is the insufficiency of information about what roles influences and factors of place (cultural and environmental) in the formation of patterns and relationships space holy Islamic shrines architecture in Iraq. In addition, what the role-played by the inherited urban civilization Iraqi both sides physical & moral support and integration with the concepts and spirit of the Islamic religion, and its rules in construction of architecture. Moreover, presumably Holy Islamic shrines architecture in Iraq are to be studied and its impact on the urban structure and planning in many cities

of Iraq mission. In addition to the dimensions of the moral and doctrinal and their impact on society, they have evolved modes of planning over time according to the needs and requirements circumstantial, but the factor of place had a role the basis for the formation of masses and spaces. In addition to the formal role of the Islamic religion and the nature of religious practice in which they are, and the availability of spatial knowledge about the factors that produced the Iraqi architecture, provides a comprehensive picture about the origin of processors and architectural configurations and their source of origin from which it came. Which branded the Islamic holy shrines in Iraq equipped and versatile textural characteristics and detailed thoroughbreds.

Keywords: Islamic Architecture, Place factors, Islamic tourism, Shrines, Holy Thresholds, Al-Kadhimiyeh.

1- المقدمة

نشأت وتطورت العمارة العربية الإسلامية ضمن محيط مكاني بيئي وحضاري غني وخصب بمؤثراته وعوامله، وقد كان لتلك العوامل الدور البارز في صياغة بعض العناصر المعمارية التي ارتبطت فيما بعد بالعمارة الإسلامية وأصبحت بمرور الوقت تمثل الصورة النمطية لها. ولم يقتصر التأثير المكاني على الشكل الخارجي والعناصر المعمارية وحسب، بل تعداه ليؤثر على النمط المعماري والمعالجات البنائية والانشائية فيها مدفوعا من مؤثرات الموروث الحضاري.

وقد تنوعت أنماط العمارة الإسلامية في وظائفها واستخداماتها واتسع نطاق تلك الاستخدامات مع اتساع وامتداد الدولة الإسلامية، فلم يعد يقتصر في انشاء المباني العامة على المساجد، اذ قد ظهرت المدارس والمستشفيات والقصور والمساجد الجامعة والمراقد التي تضم قبور لشخصيات مهمة والربط (جمع رباط) والتكايا وغيرها، وقد تنوعت في مساقطها الافقية وخصائصها التزيينية بحسب وظيفتها ولكنها اتحدت في الخصائص العامة لها التي نبعت من المبادئ العامة للعقيدة الإسلامية والمفاهيم المعمارية المستقاة منها.

اكتسبت عمارة المراقد الإسلامية دورا مهما وبارزا من ضمن الأنماط العمرانية والانشائية الإسلامية، وجانب اكتسابها لتلك الأهمية نبع من كونها تحمل جوانبا دينية وجوانب رمزية تذكارية، وهذين الجانبين مكملان لبعضهما.

وقد وجد لعوامل المكان ومؤثراته اثرا واضحا على عمارة المراقد الدينية الإسلامية من ناحية الطراز ومواد الانهاء والعناصر المعمارية حالها كحال الأنماط العمرانية الإسلامية الأخرى، ويتجلى ذلك في التنوع في الصياغات وتوظيف المواد والعناصر المعمارية في ابنيتها من منطقة لأخرى ومن إقليم إسلامي لأخر.

لقد اتسع مفهوم التأثير المكاني ليشمل جميع ما يتعلق بالمكان من النواحي الحضارية والنواحي البيئية ولم يعد هذا المفهوم مقتصرا على جانب دون الاخر وكما سيتم بيانه لاحقا.

1-1 تأثير عامل المكان الحضاري والبيئي على العمارة الاسلامية.

يلعب عامل المكان الأثر البالغ في العمارة بالرغم من وجود جوانب أخرى ظرفية ومتغيرة كجانب الدين والمعتقد والتطورات التقنية والتكنلوجية، ولكن يبقى تأثير هذا العامل هو الأكثر وضوحا وتأثيرا على العمارة. اذ ان أثره يتعدى كونه اثرا مرحليا وانيا ظرفيا بل هو أثر ممتد وينعكس على طبيعة الافراد النفسية وبالتالي النواحي الاجتماعية للمجتمع ككل. وان طباع أي شعب من الشعوب وسلوكياته وتصرفاته لا بد وان تكون نابعة بالأساس من خصائص المكان وبيئته الطبيعية.

ان مفهوم الأثر لعامل المكان في مجال العمارة والعمران يقسمها الى قسمين: الأول يمثل الأثر الطبيعي وتشمل العاملين الجغرافي والمناخي وكل ما له علاقة بخصائص الموقع، والثاني الأثر الحضاري ويشمل كل ما يتعلق بالجوانب الدينية والاجتماعية والثقافية وحتى الجوانب السياسية والاقتصادية، وهذين العاملين مرتبطين مع بعضهما البعض بروابط وصلات وثيقة، والى ذلك يشير ابن خلدون الى الاختلافات التي تنشأ بين سكان الأقاليم المختلفة في الجانب المادي كالخلقة والهيئة الجسمانية والجانب المعنوي من

ناحية الطباع والتصرفات والسلوكيات انما تؤشر الى ظاهرة الارتباط بين سلوكيات البشر والبيئة الجغرافية المحيطة بهم.[1] كما ان " لكل امة عقلية خاصة بها كما ان لكل امة نفسية تميزها عن نفسيات الأمم الأخرى وشخصية تمثل تلك الامة وملامح تكون غالبة على أكثر افرادها تجعلها سمة لتلك الامة تميزها عن سمات الأمم الأخرى تبعا لبيئتها وطبيعة محيطها". (جواد علي، 1993م، ج1، ص35). وتؤكد الدكتورة كريستين نصار في كتابها الانسان والتأريخ على ان الطبيعة الجغرافية والبيئة الطبيعية تجد لها انعكاسات على ثقافة وديانة واخلاق وطبائع اية امة من الأمم، وان ما يميز شعبا او امة عن غيرها ويساهم في إعطائها شخصية جماعية خاصة ووحدة عضوية اجتماعية وقومية هو اتحاد هذا الشعب الوثيق بالبيئة الجغرافية التي يعيش فيها. (نصار، 1991م، ص33). والقول المشهور بأن الدين يظهر في خلفية كتب الجغرافيا، ونفهم الجغرافيا من قرأتنا للكتب الدينية يعكس مدى تأثير المكان ومعطياته على مزاج الشعوب وتأريخها وثقافتها وسلوكياتها الدينية والاجتماعية. (Park, 2004, p.3). ويشير الآثاري العراقي عبد الأمير الحمداني الى دور البيئة الطبيعية في توحيد أفكار المجتمعات البشرية بقوله "تساهم وحدة البيئة الطبيعية في توحيد المرتكزات والبنى الاجتماعية للتجمعات البشرية على الرغم من الاختلاف فيما بينها في المسارات التأريخية والمعتقدات الدينية والأصول العرقية، وهو ما يفسر إمكانية وجود روابط وصلات في الظواهر والممارسات الاجتماعية في مجتمعين مختلفين زمنيا وعرقيا او حتى في حالة وجود انقطاع ثقافي بينهما شريطة ان يكون هذين المجتمعين يشتركان في بيئة طبيعية واحدة". (الحمداني، مجلة الكوفة، عدد4، 2013م، ص145).

وإذا كان هذا الأثر البالغ للجغرافيا والبيئة الطبيعية على طبيعة المجتمع فمن الطبيعي ان يكون لهما الأثر على العمارة ومخرجاتها باعتبارها مخرج من مخرجات المجتمع ومعبرة عن حاجاته وتطلعاته وحضارته. اذ أن للعمارة القدرة على إظهار قيم المجتمع والإرث الحضاري وتشكيل الحياة اليومية وذلك من خلال الترميز الحضاري. فلها القدرة على إظهار الحياة اليومية وتجسيد الوضع الآني الذي يشكل جزء من التواصل الحضاري، الامر الذي لا يتحقق مع باقي الفنون وذلك لعدم ارتباطها بحياة الإنسان بصورة يومية ومستمرة. لذلك تعتبر العمارة هي أم الفنون لعلاقتها الوثيقة بالإنسان واحتياجاته وتطلعاته. لقد نظر معماريو الحداثة الى العمارة نظرة نفعية تعبر عن حاجات معاصرة وتلبي متطلباتها من دون ان يأخذوا بنظر الاعتبار المنظور الحضاري وظروف الطبيعة ومحدداتها بوصفها عوامل مهمة لتشكيل العمارة. فالعمارة مضمون أكبر يشمل إضافة الى الجوانب النفعية والجمالية جوانب حضارية، وعلى حد تعبير (Huyghe) بأن العمارة جزء من عملية النشوء والارتقاء الكلي للأفكار والتقاليد الحضارية والإنسانية، وان انتاج العمارة يرجع الى عاملين أساسيين هما:

أ. العوامل الناتجة عن عالم الواقع The World of reality: وهي التي تتعلق بالبيئة الفيزيائية والمواد البنائية والمناخ والطبوغرافية والبيئة الطبيعية بشكل عام.

ب. العوامل الناتجة من التفاعل Interaction: وترتبط بالمجتمع والدين والعادات الاجتماعية والحضارية والسياسة بصورة عامة. (جنان عبد الوهاب، 2002م، ص140).

ولذا فان روح المكان (بكل عوامله ومقوماته المادية والمعنوية) تمثل الجوهر الثابت في العمارة، وبحسب (Schulz) فان هناك ظواهر طبيعية واصطناعية تتكرر بأشكال مختلفة ولكن بعلاقات ثابته مما يفترض وحدة الأجواء، وتقابلها صفة تعرف المكان وتكسبه هويته تسمى "روح المكان" او Genius Loci، وهو يدعو الى فهم العمارة وروحيتها من خلال النظر الى علاقتها الوجودية بالمكان وارتباطها به. (ينار جدو، 1993م، ص67).

ومن كل ما تقدم يدرك بأن لعامل المكان الأثر الذي لا يمكن انكاره على اية عمارة بأعتباره يمثل عامل الثبات في مقابل متغيرات الزمان. وهي تتمثل بجانبين هما: العامل المكاني الحضاري والعامل المكاني البيئي.

2-1 خصائص العمارة الإسلامية وعوامل المكان.

1 (راجع مقدمة ابن خلدون، المقدمة الخامسة في اختلاف أحوال العمران في الخصب والجوع وما ينشأ عن ذلك من الآثار في أبدان البشر وأخلاقهم).

حدد الإسلام مهمة أساسية وجوهرية لوجود الانسان على الأرض ومن اجلها خلق، وهي مهمة الخلافة في الأرض كما ورد في الآية رقم 30 من سورة البقرة:﴿ وإذ قال ربك للملائكة إني جاعل في الأرض خليفة ﴾. والخلافة في الأرض تعني التعمير فيها تعميرا معنويا بترقي الانسان في سلم الإنسانية فردا ومجتمعا، وتعميرا ماديا بأستثمار المقدرات الكونية والانتفاع بها. ووفقا لمنهج محدد هو منهج العبادة الذي جاء به الهدي الديني قرأنا وسنة. (النجار، 2010م، ص148). لذا فأن الإسلام لم يقتصر على المظهر المادي للبناء، وانما يقدم اضاءات حول الغاية المرتبطة بإشعاع تعاليم الإسلام في المحيط العمراني وفي تكامل المبنى وتوافقه مع بيئته المحيطة به واستفادته من مقدراتها واقتصاده فيها بالقدر الذي يوفر احتياجاته ويحقق اكتفاءه، كما ونظر الى جانب الموروث العمراني في البلاد بنظرة فاحصة فأستفاد من التجارب والخبرات وحقق التنوع في إطار وحدة المفاهيم.

ان ما يميز خصوصية التوجه الإسلامي في الفن عامة والعمارة خاصة هو الاتي:

أ. مراعاة المبادئ الإسلامية في تصميم المبنى وتتمثل تلك المبادئ باستقراء المفاهيم والتعاليم القرآنية والأحاديث النبوية الشريفة والروايات المتواترة عن الائمة والصالحين، ومبادئ الاخلاق وحسن الجوار وكف الأذى بجميع صوره وعدم الاسراف والاتزان والتجريد والخروج من حدود العالم المادي المحدود الضيق الى عوالم لا متناهيه من التفكر والتي دعى اليها الإسلام كمبادئ أساسية في الممارسة الحياتية اليومية وكذلك في انشاء المباني.

ب. التجاوب مع البيئة جاء من خلال توظيف المواد المتوفرة محليا والحلول المناخية التي تحقق الراحة لمستخدمي المبنى والاقتصاد في الكلف. والتواضع وعدم الاسراف في قوله تعالى:﴿ وكلوا واشربوا ولا تسرفوا ﴾. (الأعراف، اية31). وقوله تعالى في وصف المؤمنين:﴿ والذين هم عن اللغو معرضون ﴾. (المؤمنون، اية3). والحفاظ والتوازن مع البيئة والمحيط في قوله تعالى:﴿ ولا تفسدوا في الأرض بعد إصلاحها ﴾. (الأعراف، اية56). وقوله تعالى:﴿ وأحسن كما أحسن الله اليك ولا تبغ الفساد في الأرض ﴾. (القصص، اية77). في قوله تعالى:﴿ والذين إذا أنفقوا لم يسرفوا ولم يقتروا وكانوا بين ذلك قواما ﴾. (الفرقان، اية67). (وزيري، 2008م، ص9 وما يليها). كما ان التعبير البيئي أصبح ميزة من ميزات عمارة الإسلام، فبفعل شدة الحرارة والمناخ الصحراوي في معظم انحاء العالم الإسلامي أصبحت العمارة الإسلامية تتجه نحو الداخل وتقلل قدر الإمكان مساحة السطوح المعرضة للتأثيرات الخارجية، بالإضافة الى ان طبيعة البيئة الصحراوية ساعدت في دفع الفن الإسلامي الى ان يسلك الجانب التجريدي، ففي الصحراء لا وجود للجمال "بمعناه الغربي الكلاسيكي"، فلا توجد أشجار ولا طيور ولا ماء، والجمال في الصحراء مجرد غير محسوس، واصبح فن الزخرفة الإسلامي فنا ثنائي البعد وممتد بدون حد كالصحراء الممتدة وهو جانب بيئي يضاف الى الموانع الفقهية. (القحطاني، 2009م، ص51).

ج. عدم ربط الفن والعمارة بجانب عقائدي او فكرة دينية وكراهية الإسلام للتصوير التجسيمي والنحت. دفع هذا المعماريين المسلمين الى التحرر من قيود الطبيعة والبحث في جوانب جمالية أخرى كالعلاقات الفضائية والكتلية والتجريد التي أبدعوا فيها واتقنوها، وهو ما لم يصل اليه الفن في اوربا الا في عصر النهضة في إيطاليا خلال القرن الخامس عشر. (زكي محمد حسن، 1984م، ص ل).

د. ان تأثر الفن الإسلامي بفنون الحضارات التي سبقته والتي احتواها الإسلام كان تأثرا خلاقا. (عكاشة، 1994م، ص32). اذ ان الإسلام لم يقتبس العناصر والتكوينات المعمارية وينقلها مباشرة وانما أعاد صهرها وترتيبها بما يلائم العقيدة والتوجه الإسلامي وبما يتلاءم أيضا مع البيئة الطبيعية والمناخية المحيطة به.

ويشير الباحث (ضياء الدين سردار) الى القيم التي حكمت البيئة العمرانية الإسلامية والتي تؤكد تمسك العمارة الإسلامية بعوامل المكان ومعطياته وارتباطها به ويحصرها بالمفردات التالية: (المعموري، 2005م، ص108).

1. الإحساس بالبيئة (environmental sensation): فالإحساس بالبيئة يتضمن احترام مصادر الطبيعة ومكوناتها بجميع اشكالها (المناخ، طبوغرافيا الأرض، الاستجابة لعوامل الطبيعة بجميع صورها والتعامل معها، الاستفادة من المواد المتوفرة محليا).

2. التكامل التشكلي (Morphological integration): ومن مظاهره الاحتفاظ بمفاهيم التدرج بين العام والخاص، والتكامل الفضائي استنادا لمتغيرات الحجم والمقياس، والتي تعطي الشعور بالاستمرارية اللامتناهية، والعمارة الإسلامية تحقق التكامل من خلال البحث عن الوظيفية، والمعنى والرمز، والظل والضوء، والماء والحركة، باعتبارها تمثل أجزاء مهمة من الكل، وتحقق تكامل الكل مع الأجزاء، وضمن علاقة توافقية توصف بالوحدة في التنوع (unity in variety).
3. الوضوح الرمزي (Symbolic clarity): ويتمثل باحترام الماضي والتراث والحضارة، فالمضامين الإسلامية الأساسية يمكن تطبيقها في كل زمان ومكان من العالم الإسلامي ويبقى بعد ذلك البحث عن الذات المحلية بما يتناسب مع القيم التراثية والبيئة المحلية والخلفية الحضارية والثقافية التي تتغير مع تغير المكان والزمان وتؤكد على خصوصية المكان.

ويشير الدكتور يحيى وزيري الى ان العمارة الإسلامية شكلتها وانضجتها روافد عدة؛ دينية وحضارية ومناخية، وهذه الروافد في مجملها تمثل الرؤية الأكثر شمولا لمفهوم البيئة والذي لا يجب ان يقتصر على العوامل المناخية فقط، ولكن يتعداه ليشمل البيئة الدينية والاجتماعية والثقافية أيضا. (وزيري، 2004م، ص24).

ان الدين الإسلامي حاول تحقيق التوافق والانسجام ما بين الأعراف والطرز المحلية في الفن والعمران وما بين مبادئه، فلم يجد ضيرا في استخدام عناصر وتكوينات معمارية موروثة وموجودة إذا ما حققت مفاهيم الإسلام وتوافقت معها، كما ان المسلمين حاولوا تكييف وتحوير بعض العناصر بالشكل الذي يمكنهم من استخدامها في التوافق مع مفاهيم الإسلام.

3-1 العمارة الإسلامية في العراق.

مع دخول العراق في الإسلام بعد الفتح العربي الإسلامي عام (632 بعد الميلاد)، ومع اتساع نطاق الفتوحات الإسلامية احتك المسلمون بحضارات عظيمة كانت سائدة ولها انماطها وطرزها واساليبها المعمارية والفنية التي استفاد منها المسلمون وكيفوها بصورة تتوافق مع المبادئ والتعاليم الإسلامية وتحتفظ في الوقت ذاته بخصوصياتها المكانية والمعالجات البيئية، الامر الذي أدى الى أنتاج عمارة إسلامية لها خصائصها المكانية المتنوعة مع الاحتفاظ بوشائج ارتباطها مع تعاليم الدين الحنيف. وفي العراق فقد اخذت العمارة العربية الاسلامية كثيرا بالأساليب المعمارية الممتدة جذورها الى الحضارة الاشورية. (زكي محمد حسن، 1984م، ص ي).

يبدو أن الفتح الاسلامي للعراق كان نقطة تحول ثقافية، ولكن التغيير "بحسب الباحث عبد الأمير الحمداني" كان بطيئا وانصب على التغيير العقلي دون ان يمس الأعراف والثقافة المادية، ومثلما ورثت المسيحية الامبراطوريتين اليونانية والرومانية فقد ورث الإسلام ثقافة منطقة غرب اسيا والشرق الأدنى القديم. فالإسلام لم يلغ الثقافة العراقية القديمة بل أصبحت الحضارة الإسلامية استمرارا وبناء لثقافة أقدم. (الحمداني، مجلة الكوفة، عدد4، 2013م، ص149). ويلتمس الباحث ذلك في رصد أوجه الشبه بين المجتمع العراقي بعد الإسلام في الأرياف والاهوار وبين المجتمعات العراقية القديمة التي عاشت في البيئة نفسها سواء كان في مجال الثقافة المادية المتضمنة طرق الري والزراعة ووسائط النقل وطرق الصيد وبناء القوارب وبيوت القصب وطرائق البناء واساليبه، او في الفعاليات والأنشطة الثقافية. كما وتناولت دراسة (عبد الوهاب حميد رشيد) الموسومة: "حضارة وادي الرافدين "ميزوبوتاميا"، والصادرة عن دار المدى عام 2004م. ثلاث جوانب شكلت الحياة الفكرية والاجتماعية في منطقة جنوب وادي الرافدين ولا تزال رواسبها مترسخة في فكر وذهنية أبناء العراق وهي: (العقيدة الدينية وما يتعلق بها من نظرة الانسان لوجوده وعلاقته بالكون المحيط به، والحياة الاجتماعية وطبيعتها، والأفكار الفلسفية)، ويشير المؤلف في مقدمة كتابه الى ان فهم الماضي فهما موضوعيا ونقديا يسهل معرفة الحاضر والتخطيط للمستقبل، حيث ان المعتقدات والممارسات الدينية والاجتماعية للعراقيين القدماء لاتزال تعيش معنا في افكارنا ومعتقداتنا وممارساتنا. (عبد الوهاب رشيد، 2004م، ص11). وترى الدكتورة (كريستين نصار) في كتابها الانسان والتأريخ، والصادر عن جروس برس عام 1991م، حول الدين والتدين فهي تميز ما بين العاطفة الدينية وتعتبرها طابع وراثي وعنصر أساسي وثابت، ويتلقى الفرد تلك العاطفة بشكل عادات وتقاليد منذ مولدهم وينشئون على ممارستها والتطبع بها، وهي تعبر عن تراكمات ماضية أصبحت تشكل تراثا من الإباء والاجداد يصعب على الفرد التنازل عنه، وبين العقائد والممارسات والشعائر الدينية والتي تعبر عن مظاهر خارجية للعاطفة الدينية وهي متغيرة لكونها عناصر مكتسبة اجتماعية وثقافية ووليدة لبيئتها بكل متغيراتها. (نصار،

1991م، ص55). ويشير الباحث في الفن والعمارة الإسلامية الدكتور عفيف بهنسي في كتابه "جمالية الفن العربي" الى ان جوهر الديانات السماوية قام على أرضية خصبة من المواقف الفكرية التي تبناها العرب منذ بدء التأريخ، والتي نبعت كنتيجة حتمية للتأمل الذي كان يمارسه العراقيون عندما كانت السماء الصافية أكثر أيام السنة تجذبهم اليها فيرقبون الكواكب والنجوم ويستطلعون المستقبل والغامض، فالعالم السماوي كان صبوتهم ولم يكن العالم الأرضي الا عرضا زائلا كما اكدت ذلك جميع الديانات السماوية. (بهنسي، 1979م، ص45-46). وينطلق من هذا المفهوم الى اعتبار ان الإسلام كان في جانب منه حركة بعث لبعض القيم والأفكار والعقائد التي تعاقبت على الأرض العربية. (نفس المصدر السابق، ص46). وهذا يدل على عمق الترابط بين الدين والطبيعة المكانية، والذي قد يعزى الى وحدة البيئة والطبيعة والاصل العرقي كعوامل مكانية منتجة للمعتقد بحسب (النظرة العلمانية) او الى انتشار التعاليم الابراهيمية الحنيفية بين شعوب تلك المناطق ولكنها حرفت بمرور الزمن واخذت سبلا مختلفة بحسب (النظرة الدينية). (الحاج قاسم، 2007م، ص106).

وبأعتبار ان العمارة اهم مظهر للحضارة، فلا بد انها تأثرت بالعوامل التي افرزتها استمراريتها المكانية من الثبات وان تغيرت من ناحية المعطيات الزمانية الظرفية بحكم تغير طبيعة العبادات والمعتقدات. ان الأصل الحضاري العراقي للعمارة الإسلامية ظل راسخا وواضحا في الاثار التي خلفتها عمارة العصر العباسي في العراق والتي تحمل اثارا واضحة من العمارة العراقية قبل الاسلام. شكل (1-1).

2- عمارة المراقد الإسلامية في العراق.

تكاد لا تخلو منطقة من العراق من مرقد او مقام إسلامي مقدس او تذكاري. فعلى ارضه عاش الانبياء والاولياء والعلماء وعليها ماتوا وسجل تأريخهم مرورهم بهذه الارض واقامتهم فيها. وعند التجوال من شمال العراق الى جنوبه كثيرا ما يصادف وجود مقامات ومزارات ومراقد لأولياء صالحين كانت سببا في النمو والتوسع الحضري في تلك المناطق بتأثير وجود ذلك المقام او ذاك فيها. وكثيرا ما نمت وتوسعت مدن فيه واصبحت مترامية الاطراف بسبب وجود مرقد او مزار يتعاهده الناس بالزيارة.

2-1 دوافع اقامة المراقد والعتبات الاسلامية.

تقسم المراقد الإسلامية الى نوعين اساسين وهما **المراقد المقدسة الدينية والمراقد التذكارية غير المقدسة**. وأن ما يفرق بينهما هو المبدأ الاساس الذي تم انشاءها بموجبه، فاذا كان من دفن فيها من الاشخاص لهم ارتباط بالعقيدة الاسلامية، فأن اثارهم المادية وعلى رأسها مراقدهم تحاط بهالة من القدسية والمداومة على الاهتمام بها ورعايتها وتجديدها وتطويرها وتعاهد زيارتها. اما النوع الثاني فهو المراقد التذكارية كمرقد الجندي المجهول او المراقد المشادة على قبور الملوك والامراء او بعض الادباء والشعراء، وتكون ذات طابع تذكاري رمزي، وقد تشاد لكون هؤلاء الاشخاص كان لهم أثر في رقي المجتمع من خلال مساهماتهم الحضارية والإنسانية، فتبنى على اضرحتهم الشواهد التي تعكس اهميتهم ومنزلتهم في نظر مجتمعهم في تلك المرحلة، ويستمر الاهتمام بها نتيجة لما قد تحمله من جوانب اعتبارية او معمارية وفنية فتجري العادة لزيارتها والتمتع بها بعيدا عن اي جانب من الجوانب الاعتقادية. من هنا يدرك بأن هنالك ثلاث دوافع اساسية لأنشاء المراقد الاسلامية، الدافع الديني والدافع السياسي والدافع الاجتماعي. وتتكامل هذه الدوافع في الكثير من الاحيان مع بعضها البعض بروابط قوية، وهي كما يأتي:

أ. **الدافع الديني لأنشاء المراقد الإسلامية.**

يعد الدافع الديني من أبرز الدوافع واكثرها تأثيرا على انشاء المراقد الإسلامية وضمان استمرار بقاءها وعمارتها على مر الاجيال. فاكتساب القدسية بالنسبة لمرقد ليس امرا متاحا لجميع المراقد المشيدة، وانما لأشخاص محددين كان لهم أثر عقائدي او موقف ديني. لذا نجد ان مراقدهم تحاط بهالة من القدسية والاحترام من قبل اتباعهم ومحبيهم. ولا يقتصر الامر في ذلك على ديانة او طائفة دون اخرى بل تشترك جميعها بالاهتمام بها بوصفها جزءا من الثقافة الروحية والعقائدية للإنسان. (الكرملي، كتاب الكتروني، ص18). ان المرقد الإسلامي المقدس هو مكان الرجوع إلى الله والتعبد بالاعتبار من سيرة السلف فهو تجسيد للذكريات

التي تهدى إلى الأجيال ليعتبر بها الإنسان، فمنه يطالع الزائر تاريخ سيرة المزور العلمية والسياسية ودوره المهم في تحقيق المنفعة العامة والمتوارثة للمجتمع. (حيدر ناجي، 2010، ص27).

ب. **الدافع السياسي لأنشاء المراقد الإسلامية.**

تجسد العمارة رمزا لقوة الدولة وتوجهاتها السياسية في أي مرحلة من مراحل التأريخ، وتتمثل هذه الرمزية في عدد من المدلولات المعمارية التي يحمل بعضها مضمونا حضاريا، وبعضها الاخر مضمونا سلطويا سياسيا، ويجمع البعض الاخر بين المدلولات مجتمعة.[2] وبما ان المراقد تمثل جزءا مهما من انماط المباني الإسلامية، لذا يكون لهذا الدافع اهميته البالغة بوصفه عامل مهم في تشييد العديد من المراقد والاهتمام بها. اذ كان الهدف من الاهتمام والتشييد لبعض المراقد في ان يحمل فضلا عما يحمله من الجوانب العقائدية جوانبا سياسية تهدف لتوطيد الحكم لسلطة او اظهار اهميتها، لذا كان في الاهتمام والبذل على بعض المراقد المقدسة للأولياء الصالحين من قبل بعض الملوك والامراء هدفا الغرض منه استمالة الرعية واجتذاب عواطف العامة، فأظهار الاهتمام بتلك المراقد له دور في تكوين قاعدة شعبية بالغة الاهمية بالنسبة للحكام. (عكاشة, 1994م، ص146). بالإضافة الى ذلك فقد شيد الملوك والحكام وعلى مر العصور الاسلامية مراقد فخمة لهم ولعوائلهم، فالكثير من المراقد انشأت لدفن سلاطين او امراء.

ج. **الدافع الاجتماعي لأنشاء المراقد الإسلامية.**

ان الغريزة البشرية والدافع النفسي بالشعور بالارتباط ما بين الناس والرغبة في استمرار هذا التواشج العاطفي حتى بعد الموت، ولدت لدى الناس الرغبة في تخليد ذكرى الموتى، وتتعزز هذه الرغبة إذا كان لدى الاشخاص المتوفين مكانة مرموقة او كانت لديهم انجازات ومساهمات حضارية. وفي حالة كون هؤلاء الاشخاص المتوفين يمثلون رموزا من الناحية العقائدية، كأن يكونوا اولياء وما الى ذلك تكتسب القدسية بعدا اخر في تمجيد وتعظيم شأنهم ويكون ذلك جزءا لا يتجزأ من التدين. كما ان" للمراقد المقدسة حيويتها في المجتمع العراقي تحديدا، فهي تحكي سير المدن والقصبات ولا تقتصر تلك المراقد على الديانة الإسلامية فقط فكل الديانات في العراق لها مراقدها التي تبجلها وتحترمها ". (مازن لطيف واخرون، 2013م، ص266). ومن المعلوم ايضا ان التدين له جوانب اجتماعية ونفسية لها دورها في بعث الطمأنينة والتفاؤل وتقديم حلول لما يواجهه الانسان من مشاكل واخطار في حياته. (الوردي، 2010م، ص257). وتصف المستشرقة الليدي درور زيارتها لمرقد ابي حنيفة (رض) في بغداد واطلاعها على طبيعة طقوس وشعائر الزيارة فيه، بأن الناس يتبركون بزيارة ضريحه ويزوروه كثيرون، انهم يعتقدون بخوارق صاحب الضريح، وصاحب المذهب الحنفي الإسلامي، وانه لا يزال معنيا بأتباعه عناية الاب بأبنائه". (الليدي درور، 2008م، ص135). وهذا يعكس التداخل ما بين الدافعين الديني والاجتماعي، فلا يقل دور الدافع الاجتماعي أهمية عن دور الدافع الديني في العناية بتشييد المراقد وملازمة الاهتمام بها ورعايتها.

2-2 اهمية المراقد الإسلامية وأثرها.

يمثل جانب الأهمية للمراقد الإسلامية ما يعطيها قابليتها للاستمرار في وجدان الناس، وتعاهد زيارتها والاقبال عليها، اذ انه يشكل عاملا أساسيا لدوام الحفاظ عليها بعد تشييدها، فقد يزول بعد فترة من الزمن الدافع الأساسي (سواء كان سياسي او ديني او اجتماعي) الذي كان وراء تشييدها الا انها تستمر في بقائها من خلال اجتماع جانب او عدة جوانب مما يأتي:

أ. **الاهمية الدينية والاجتماعية للمراقد الإسلامية.**

تلعب تلك الأهمية الدور الأساس في استمرار عمارة المرقد وتعاهدها بالزيارة من قبل الناس. اذ ان التدين هو السمة العامة التي تطغى على المجتمع المحيط بأماكن وجود مراقد مقدسة او مشاهد دينية. فنلاحظ أن قداسة المكان قد تنتقل إلى سكانه وتضفي عليهم اعتبارات خاصة بحكم قربهم من مشهد او مرقد لشخصية ذات سمات اعتبارية مهمة من الناحية

2 خالد عزب، الرمزية السياسية في العمارة.

العقائدية لدين او طائفة ما. (الموسوي، 1982م، ص93). كما إن وجود المراقد المقدسة في مختلف البقاع من الأرض كان له سبب مباشر في الاختلاط والتعارف بين شعوب واقوام مختلفة تجمعهم العقيدة من خلال القصد والزيارة لتلك المراقد من مختلف بقاع العالم.

كما قد أثبتت الوقائع التاريخية أن الدور الذي تضطلع فيه هذه المراقد له ميزاته الحسنة التي يشعر فيها الإنسان بالراحة والطمأنينة والأمان بوجوده الى جانبها. (حيدر ناجي، 2010م، ص28). اذ يورد الرحالة العربي ابن جبير رحلته عن دخوله الى مصر وزيارته لمشاهد الاولياء من اهل البيت (ع) فيها: **وشاهدنا من استلام الناس للقبر المبارك واحداقهم به وانكبابهم عليه وتمسحهم بالكسوة التي عليه، وطوافهم حوله مزدحمين باكين متوسلين الى الله سبحانه وتعالى ببركة التربة المقدسة ومتضرعين ما يذيب الاكباد ويصدع الجماد، والامر فيه أعظم، ومرأى الحال اهول.** ثم يردف ابن جبير بقوله: **نفعنا الله ببركة ذلك المشهد الكريم.** (رحلة ابن جبير، في وصفه لمشهد الحسين (ع) في القاهرة، كتاب الكتروني).

ب. الاهمية الثقافية للمراقد الإسلامية.

تلعب المراقد دورا هاما في تنشيط حركة الثقافة من خلال نشر المعارف والعلوم من خلال الاختلاط والتبادل المباشر للمعرفة. وخصوصا خلال مواسم الزيارة والتبادل الثقافي والحضاري الذي ينتج عنه دورا بارزا في التصاهر بين الثقافات وتنشيط عملية الانتقال المعرفي من مكان لأخر. بالإضافة الى الحلقات الدراسية التي كانت تعقد في تلك المزارات والتي كانت تتناول العلوم بمختلف صنوفها. وقد تلحق المدارس العلمية بأبنية المزارات او انها تشاد قريبة منها مستفيدة من العبق الروحي الذي تستمده من السيرة العطرة للأولياء الصالحين وكذا بالتواصل مع الحضارات الاخرى دورا بارزا في عملية نشر المعرفة.

زار الرحالة العربي ابن بطوطة مدينة النجف الاشرف عام 726 هجري، ووصف المدينة ومشهد الامام (ع) فيها وكان مما جاء بكلامه "**ويدخل من باب الحضرة الى مدرسة عظيمة يسكنها الطلبة والصوفية ومن تلك المدرسة يدخل الى باب القبة وعلى بابها الحجاب والنقباء**". (ابن بطوطة، 1987م، ص193). وهذا يشير الى الدور التي قامت به المشاهد الشريفة في تكوين نوى جمعت الطلبة والمريدين للتعلم والتثقف. كما انه يدل على نشاط الحركة العلمية والثقافية في المدن بتأثير تواجد المراقد المقدسة فيها.

ج. الاهمية المعمارية والفنية للمراقد الإسلامية.

نظرا للأهمية التي اولاها الإسلام للمراقد وانشاءها وعمارتها، والذي ظهر جليا بالعناية البالغة بعمارتها ونقوشها. فقد أصبحت بعضها اية من آيات الجمال والذوق المعماري بعد أن سخرت لها جميع الامكانيات الهندسية والفنية، ودرست الجوانب التي تظهر الجمالية والصرحية والفخامة بصورة متقنة مما حولها الى اعاجيب معمارية وهندسية، استحقت بأن تكون سجلا يدون مجمل ما وصل اليه عصرها في فن الريازة والبناء. يصف ابن خلكان في كتابه وفيات الاعيان عمارة المشهد الكاظمي بقوله: وقبره – ويعني قبر موسى بن جعفر(ع)–هناك مشهور يزار، وعليه مشهد عظيم فيه قناديل الذهب والفضة وانواع الآلات والفرش ما لا يحد. (ال ياسين، 1967م، ص45). كما وتصفه الليدي درور بقولها: وأنك لترى القباب المغشاة بالذهب المطروق والمنائر المستقيمة النحيفة وكأنها زهور السوسن والابواب المزينة بالقاشاني (الاجر المزجج) البديع وصحون الجامع الجميلة. (الليدي درور، 2008م، ص94). وبالإضافة لذلك فأن المراقد الاسلامية تمثل في اغلب المدن التي تكون فيها النواة الحضرية لنشوء ونمو المدينة والمرجع التخطيطي لها.

د. الاهمية الاقتصادية والسياحية للمراقد الإسلامية.

ان للمراقد اهميتها الاقتصادية والسياحية وخصوصا في مجال السياحة الدينية التي هي أحد أنواع السياحة المهمة إن لم تكن أكثرها نمواً، والسياحة الدينية هي أداة للتواصل الحضاري والثقافي بين شعوب العالم بسبب أنها وسيلة للتعارف بين المجتمعات والاطلاع على تقاليد وعاداتها ودراسة ثقافتها. فمثلا الزائر لتلك العتبات يحتاج بالإضافة الى الزيارة الى الفنادق

والمصارف والمكاتب السياحية والاسواق وغيرها وكل ذلك يلعب دورا في تنشيط وازدهار الاقتصاد لأي بلد. ولذا اعتبرت المراقد في المدن مورداً اقتصادياً ومالياً مهما من موارد المدن والفائدة تعم للبلد الذي فيه مدن المراقد المقدسة، حيث تنشط المنطقة اقتصادياً على مدار السنة ويشتد النشاط الاقتصادي في المناسبات والأعياد أو الزيارات المتعارف عليها للمراقد. (حيدر ناجي، 2010م، ص28). ومن جانب اخر نجد ان المراقد الإسلامية المقدسة تشد الناس باعتباراتها التأريخية وقيمتها الفنية والمعمارية كذلك. فالمراقد تمثل حلقة في سجل التأريخ البشري ومكانا جرت فيه تغيرات اثرت على المسيرة التأريخية لشعب من الشعوب. فكربلاء المقدسة او الكاظمية او النجف الاشرف او المدينة المنورة ليست مجرد مدن ولكنها أكثر من ذلك كونها بذكرها يستحضر سجلا كاملا من الاحداث ارتبطت بالوعي والمعرفة بتلك المدينة. والاثار والمراقد الموجودة فيها تجتذب السياح على مختلف انتماءاتهم الى الحضور والاطلاع عليها وفهم الجوانب التأريخية والمعمارية التي شيدت بموجبها.

2-3 أنماط عمارة المراقد الإسلامية.

تعد القبة الصليبية في سامراء ووفقا لأكثر المؤرخين لتأريخ العمارة الاسلامية من أولى المراقد الإسلامية التي عثر على اطلالها الاصلية، وقد شيدت كمدفن للخلفاء العباسيين (المنتصر بالله والمعتز بالله والمقتدر بالله)، وهي ذات تخطيط ذو سمة وظيفية محددة وذو نصبيه واضحة ومشيد **كضريح.**[3] (عكاشة، 1994م، ص143) و (الحديثي، 1974م، ص12). (ثويني، 2006م، ص545). شكل (2-1). تطور نمط بناء المراقد تبعا لعوامل عديدة ليتحول الى مباني فخمة تضم فضاءات متعددة ومداخل ضخمة ومبالغ بزخرفها وتزيينها، تزامن هذا التطور مع ظهور نمط جديد من عمارة المراقد المرفقة بأبنية المساجد والمدارس والبيمارستانات او في القصور، ان بناء المراقد في العصور الإسلامية المتأخرة وصل ذروته في دول المشرق الإسلامي (إيران والعراق) **فأصبحت تعبيريتها واضحة في الدلالة على وظيفتها الأساسية**، وتكونت ما يشبه الروضات المحيطة بالمراقد المقدسة. ويمكن ان تقسم المراقد الإسلامية معماريا الى ثلاثة أنماط أساسية هي:

2-3-1 نمط المراقد ذات الفضاء الواحد (البسيطة)

يعد النمط الاولي للمراقد الإسلامية. ويكون بهيئة مسقط افقي بسيط الشكل (مربع، دائرة، مضلع، نجمي) تعلوه قبة او سقيفة بسيطة، ويبنى بصورة منفردة تكوينيا بغض النظر عن وجود او عدم وجود مباني قد تكون الحقت به وقت انشاؤها او فيما بعد، فيظهر المرقد بشكل يماثل البرج يغطي المرقد ويدل على وجوده، وقد يأخذ شكلا نصبيا مرتفعا للدلالة والمبالغة على أهمية المدفون ومكانته، ويسمى بالميل. ابتدأت عمارة هذا النوع من المراقد منذ القرون الإسلامية الأولى واستمرت حتى نشوء الدولة العثمانية وما بعدها. **غالبا ما وظف هذا النمط من المراقد مع المراقد التذكارية ذات الطبيعة النصبية لقوة الدلالة والرمزية العالية وفي الاضرحة والمراقد الملكية الأولى.** واهم المراقد التي شيدت بهذا النوع هي مراقد السلاجقة الأولى في إيران والعراق.

2-3-2 نمط المراقد المركبة (المتعددة او الملحقة بفعاليات)

يؤشر ظهور هذا النوع من المراقد تزايد الاهتمام بها وبعمارتها وظهر نوعين أساسيين من المراقد المركبة هما:

1) **النوع الأول** لا يختلف عن المراقد البسيطة ولكنه محاط بفضاء إضافي حوله يسمى **الرواق**، ويكون المرقد ككل ذا شكل مركزي، وقد يكون مستوى المرقد اعلى من مستوى الرواق للسماح بالإنارة والتهوية الطبيعية، وقد تضاف المأذن او الاسوار الخارجية.

3 انظر كذلك (القصيري، 2008م، الفصل الثالث، كتاب الكتروني) وأيضا (Hoag, 1975, p.52).

2) **النوع الثاني** يكون بدمجها بأبنية ذات طبيعة نفعية دينية او دنيوية مثل المساجد او المدارس والبيمارستانات (المستشفيات) وغيرها فتكون بشكل مجمع متعدد الوظائف. وعادة ما يتبع المخطط ذو الفناء والاربع ايوانات، وتم اتباع ذلك الأسلوب في انشاء المراقد في محاولة لأضفاء الجانب الشرعي عليها لما ورد من النهي عن البناء على القبور وأصبحت القاعدة إضافة المراقد الى المدارس والمساجد والخانقات (التكايا) منذ العصر الايوبي في حكم مصر وبلاد الشام. (سعاد ماهر، مساجد مصر، ج1، ص27). وهناك سببا اخر ربما يكون الأهم وهو رغبة الحكام في استمرار تعاهد تلك المراقد وزيارتها واعمارها دفعهم لإضافة منشأت أخرى لها لتكون محط اهتمام الناس وزيارتهم كما وإنها تعمل بشكل محطة إعلامية للحكام وللترويج لهم.[4]

طور النوع الثاني من نمط المراقد المركبة ومهد لظهور النمط الثالث من عمارة المراقد وهو:

2-3-3 نمط الروضات (العتبات الإسلامية).

وتميز هذا النمط عن سابقيه بجرأة التعبير وقوته والصرحية، ويؤشر ظهوره في المشرق الإسلامي حصرا والممتد من العراق وحتى الهند، يدمج هذا النمط من عمارة المراقد ما بين ابنية المرقد والفضاءات الخارجية الحدائقية ضمن توليفه واحدة تتكامل عناصرها وتتفاعل في تكوين معماري واحد يضم بلاغة التعبير وجزالته في الإشارة لوظيفته ولأهمية من دفن فيه. واهم امثلتها عمارة لمراقد خلال الممالك الإسلامية الهندية الأخيرة والعمارة الصفوية والعمارة القاجارية.

2-4 أثر العوامل المكانية على عمارة المراقد الإسلامية.

يمكن ان يتضح دور الأثر الذي من خلال الجوانب التالية:

أ. **النمط المعماري:** لعبت وظيفة المرقد دورا أساسيا في التحكم بطبيعة خصائص نمطه المعماري، اذ غلبت عليه المركزية والتناظر والمحورية وتمركز الكتلة حول بؤرة رئيسية تجتمع حولها جميع العناصر واليها تنتهي، وكان للمفاهيم الدينية الإسلامية الدور البارز في تعزيز وإبراز قيم المركزية من خلال مبادئ الوحدانية والانتهاء الى نقطة مركزية محددة.

ان المراقد الإسلامية بشكلها المركزي اشتركت بخصائص تكوينية عامة اكسبتها جوانبها الفنية التي عرفت بها، وشكلت تلك الخصائص الملامح الجمالية والتعبيرية متكاملة مع العناصر الانشائية والزخرفية المكونة لها في خلطة متجانسة توصل الانطباع بالقدسية والاجلال والاحترام لدى المتلقي والمشاهد للمبنى. فهي ليست مباني وظيفية بحتة وانما هي مباني تلبي حاجات روحية وعليها ان تعكس تلك الحاجات من خلال تكوينها وتنظيمها. ويرى انتونيادس (Antoniades) بأن العمارة الإسلامية حالها حال العمارات ذات الوظيفة الأحادية (mono functional)، استخدمت الاشكال الهندسية البسيطة (المثلث والدائرة والمربع) الذي سهل لها تحقيق الانسجام بين شكل المبنى والحل الانشائي، بالإضافة الى خدمته للجوانب الرمزية والاعتبارية. وكان العنصر الأهم في تحقيق الجوانب الجمالية ليس الشكل الرئيسي ولكن الاشكال الثانوية التي تتكامل ضمن منظومة توافقية تناغمية لتحقيق الشكل الكلي للمبنى. ويتم تحقيق ذلك من خلال التناسب بين الكتلة والفراغ وبين وحدات القياس وبين احجام العناصر الانشائية وتغليفها وتجزئتها وتوزيعها، التي تماثل في تناغمها المقطوعة الموسيقية وما فيها من إيقاع وانسجام. (Antoniades, 1990, p.188). ومن اهم السمات التكوينية العامة لنمط المراقد الاسلامية:

1) **التناظر Symmetry**. ويعني التطابق على محور او أكثر في المبنى. وهو سريان التناغم والانسجام في العمل الفني نتيجة ما بين أجزاءه من تماثل وتناسب. (عكاشة، 1990م، ص452). وفي كل الأحوال يبقى التناظر عنصر مهم في ابنية المراقد لأنه يحقق جوانب التوازن والتماثل وتكون فيه ابعاد وانعكاسات نفسية وانطباعية فضلا عن ابعاده الجمالية

4 استنتاج الباحث من خلال الاطلاع على نماذج المراقد الإسلامية ومسار تطورها التأريخي.

نتيجة لما يولده من الإحساس بالتكافؤ والاقتصاد. (المالكي، 1997م، ص50). بالإضافة الى تأكيد التناظر على أهمية من دفن ومكانته وخصوصا في واجهات المدخل فيها.

2) **الوحدة. Unity** على مستوى التكوين المعماري ويتحقق من خلال التشكيل الموحد للعناصر العمرانية التي تنتظم لتكوين حالة بصرية التحاميه، والتكرار للعناصر كالفتحات والنتوءات والمواد وتكرار الانساق. (المعموري، 2005م، ص115). ولا يرتبط مفهوم الوحدة في العمارة الإسلامية بالجانب السلبي من الرتابة ولكنه يرتبط بالتنوع والاثراء الحسي من خلال الاستمرارية واللامتناهي والشد البصري وثنائية الوحدة والتنوع.

3) **التناسب[5] بين العناصر** سمة مميزة وشائعة في عمائر الحضارات المختلفة، ويعتبر التناسب خاصية واضحة للعمارة العربية الاسلامية، والتي تمثل منظومة تكوينية قابلة للتغيير والاضافة والتعديل، وذلك من خلال اعتمادها التكرار لوحدات معينة وفق قواعد ايقاعية مدروسة يحكمها نظام تناسبي دقيق. فالعمارة الاسلامية عمارة انفتاح الى الداخل (in ward looking) بصور عامة وعملية التوازن بين كتلة الضريح المقببة والفضاء المفتوح ضمن النسب الصحيحة تمثل النقطة الجوهرية الاهم في تحقيق التناسب الامثل.

ان الشكل المربع هو من أكثر الاشكال استخداما في العمارة الإسلامية وفي عمارة المراقد الإسلامية خصوصا كونه يحقق الاستقرار والتوازن ويؤكد على مركزية وجود الضريح، بالإضافة الى ارتباطه بالدين الإسلامي، اذ يرتبط رمزيا بشكل الكعبة المشرفة التي هي قبلة المسلمين وقد امتد تأثير هذا الشكل على عمارة الحضارات التي قامت في بلاد الرافدين وبلاد النيل وان مسقط المسجد الذي شيده الرسول (ص) في يثرب وغرف زوجاته كانت بشكل مربع. (كتانة، 2012م، ص34). وهذا يدل على أثر العقيدة الإسلامية والفطرة السليمة لدى المعمار المسلم والخبرة المتوارثة والثقافة العميقة بالنتاج المعماري والبيئة الطبيعية، بالإضافة الى تذوقه الذاتي للجمال الذي لعب دورا بارزا على مستوى التناغم والتناسب في التفاصيل الجزئية للعمارة الاسلامية.

ب. **العناصر المعمارية:** تمتاز العناصر المعمارية المستخدمة في ابنية المراقد الاسلامية بكونها تجمع الوظيفتين وهما:

1) إعطاء الشكل والهيئة المعمارية.
2) صدق التعبير والوضوح وتكامل الصورة ما بين المنشأ والشكل المعماري.

ولذا فقد جاءت المعالجات الشكلية على المنشأ بجعله متوائما مع الاهداف التكوينية والتعبيرية التي يراد تركها في ذهنية المتلقي للهيئة المعمارية للمبنى، وتم لهم بذلك تحقيق الرابطة بين العمارة والانشاء بصورة متناغمة، فغابت الحدود بين الهيكل والشكل، وأصبح المنشأ في العمارة الاسلامية كلا متكاملا بنسبه وابعاده وتراتبية عناصره وتوزيعها ومقاساتها مع الشكل المعماري والاهداف التعبيرية له.

كما أن المعمار العراقي وظف العناصر المعمارية الملائمة في المباني الدينية لأظهار أهمية الدين ومكانته بالإضافة الى ترسيخه لفكرة علو قامة الدين وسلطته على المجتمع من خلال العناصر المعمارية وتراكبها ضمن تكوينها الكلي المتكامل، وكذلك استفاد من إمكانات بيئته المحلية من المواد المتوفرة لديه في الانشاء والتزيين، وعندما تتطلب الامر اظهار الابهة والفخامة والاجلال لمبنى او صرح معين فأنه لم يبخل بأن يستورد له من البلدان المجاورة او التي وقعت تحت حكمه اجود أنواع المواد وافخرها، مما يدل على الخبرة والدراية لدى المعمار العراقي في التعامل مع المواد وتنسيقها ودمجها للوصول الى التوليفة الصحيحة وبما يتوائم أولا وأخيرا مع العوامل والمؤثرات المكانية (الحضارية والبيئية).

---

5 ويعرف فيتروفيوس التناسب بأنه "الجمال والدقة في المعايرة النسبية للأجزاء بعضها مع البعض الاخر، ويظهر ذلك عندما تكون اطوال او ارتفاعات أجزاء العمل مع عرضها وعرضها متناسبا مع طولها –أي بعبارة أخرى–عندما تنتظم الأجزاء بعضها مع بعض في كل موحد". (دوغزي، 2011م، ص15). وأشهر ما عرف منها هي مربع افلاطون والنسبة الذهبية والتي وضع أسسها الرياضية اقليدس (Euclid).

كما ان الدين الإسلامي استفاد من المؤثرات والعوامل المكانية ووظفها في خدمة الغرض الأساس فأوجد له قاعدة محلية بتبنيه للموروث الحضاري وبما يتوائم مع تعاليم الإسلام ولا يخرج عنها. وكذا الحال في جانب الفنون والعمارة والبناء، فالموروث الغني بالأنماط والأساليب العمرانية وجد له صداه الواضح في العمارة الإسلامية في العراق بعد الفتح الإسلامي، فالإسلام لم ينقض ما قبله وانما أكمل وحسن وطور، فأستفاد مما موجود من خبرات وكيفها لموائمة تعاليمه والعمل في نطاقه وضمن توجهاته. وهذا ما لمس عند المقارنة والتحليل للموروث وعمارة المراقد الإسلامية اذ ان هناك الكثير من نفحات العمارة العراقية الموروثة فيه.

ج. **المعالجات المعمارية:** اثرت العوامل الطبيعية والبيئية على المعالجات المعمارية والانشائية في المباني العراقية بصوة عامة والدينية منها على وجه الخصوص، مدفوعا بالرغبة في حفظ تلك المباني وزيادة مقاومتها للظروف المناخية والبيئية، وقد جاءت تلك المعالجات مكتملة مع الجوانب الرمزية والحسية في تلك المباني ومتكاملة مع الصورة الكلية للمبنى وتكوينه. وقد ظهرت تلك المعالجات بشكل:

1) التوجه الافقي في البناء وقلة الارتفاع.
2) كبر سمك الجدران في المباني العراقية واستخدام الجدران المزدوجة لزيادة إمكانية العزل الحراري والصوتي.
3) الانارة والتهوية في المباني العراقية تكون عن طريق الأبواب المطلة على فناءات مفتوحة.
4) مراعاة التوجيه مع القبلة بالإضافة الى الاخذ بالجوانب البيئية وحركة الشمس والرياح في التوجيه.

أن عامل المكان كان له الدور البارز في تشكيل العمارة العراقية بصورة عامة والدينية منها على وجه الخصوص قبل وبعد الإسلام، كما ان عمق التأثير المكاني يمتد أكثر من أي تأثير اخر على الأنماط والعناصر المعمارية. ان المعمار العراقي حاول تكييف العناصر والأساليب المعمارية وبما يتوفر لديه من مواد وتقنيات ظرفيه لتتوائم مع المتغيرات في الاعتقادات والأفكار وبما يحقق للعمارة جوانبها المكانية ويجعلها نابعة من مكانها ومن محيطها البيئي.

لذا يفترض البحث بأن " **عمارة العتبات الإسلامية المقدسة في العراق بصفتها صروحا معمارية مهمة ومتميزة ولها أثرها الواضح على البنية العمرانية والتخطيطية في العديد من مدن العراق المهمة، إضافة الى ابعادها المعنوية والعقائدية وأثرها على المجتمع، فأنها قد تطورت بأنماطها وتخطيطها عبر الزمن وفقا للمحددات المكانية (الحضارية والبيئية) التي وفرتها عمق الحضارة العريقة من موروث حضاري وعوامل مكانها البيئية والطبيعية بالإضافة الى تعاليم ومبادئ الدين الاسلامي، والتي كان لها الدور الأساس مجتمعة في تشكيلها وتخطيطها وعمارتها**".

3 مؤشرات المحددات والمؤثرات المكانية على عمارة العتبات الإسلامية المقدسة في العراق.

استكمالا لما تم تناوله، فقد برزت مجموعة من المؤشرات التي تحدد تأثير المكان ومحدداته على تطور عمارة العتبات الإسلامية المقدسة في العالم الإسلامي عامة وفي العراق خاصة كجزء مهم ومؤثر منه.

3-1 المحددات المكانية وأثرها على مباني العتبات الإسلامية المقدسة في العراق.

3-1-1 المحددات الحضارية لعمارة العتبات والمرتبطة بالجوانب الدينية والاجتماعية والثقافية.

مؤشرات المحددات المكانية (الحضارية والبيئية) المؤثرة على عمارة العتبات الاسلامية.				
المحددات الحضارية	**مؤشراتها**			
فعل الزيارة الى العتبات الاسلامية	التطهر	ويظهر بصورة جلية وواضحة في عمارة العتبات كجزء من مستلزمات القصد. ويؤكد عليه من خلال الإحاطة بالأسوار والبوابات كحاجز ما بين الديني والدنيوي.		
	تراتبية الزيارة والتعبد	التوجيه للمبنى الديني	وضع المبنى وتوجيهه يعطيه طابع هندسي ضمن محيط عضوي.	
			التركيز على اتجاه معين (القبلة) بالنسبة للمباني الإسلامية كمقصد عبادي.	
			مراعاة وقت الزوال وتحديده من خلال الظل بحيث تقابل البوابات الرئيسية الاتجاهات الأربعة تقريبا.	
		الدخول الى المبنى الديني	الاستئذان	ويظهر في تصميم البوابات وتسمياتها وضخامتها بالإضافة الى شكل الاسوار والاحاطة بالمبنى.
			التسليم	الدخول الى العتبة والتسليم على صاحبها ويكون في العادة من جهة الرأس والذي يكون بأتجاه القبلة في الاغلب.
			الصلاة	كأساس لقصد أي مبنى ديني هو الصلاة وما تتطلبه من احياز وفضاءات.
			التوديع	عند نهاية الزيارة وتكون جهة التوديع في الغالب من الجهة الغربية للعتبة.
الجوانب الاجتماعية والثقافية للعتبات الاسلامية	الارتباط النفسي والحسي مع المبنى	التسميات والرموز المستخدمة على جدران واسوار وبوابات العتبات.		
		طبيعة التكوين المعماري المتوازن والصرحية والتأكيد على التناظر والارتباط بالسماء.		
		العناصر المعمارية ذات الرمزية العالية.		
		المواد الانشائية والتزيينية المستخدمة في انشاء العتبات.		
	المنشأت ذات الطبيعة الخدمية والاجتماعية الملحقة بالعتبات المقدسة كالمكتبات والمساجد والمدارس الدينية والمتاحف وقاعات المؤتمرات وغيرها.			

3-1-2 المحددات الحضارية لعمارة العتبات والمرتبطة بجوانب الموروث العمراني والتخطيطي

الموروث الحضاري العمراني للمباني الدينية في العراق	أثر الموروث العمراني على النمط المعماري	الكلية في التصميم المعماري والتكامل بين الأجزاء لخلق الانطباع العام، حيث الأجزاء تعمل كمنظومات متكاملة مع التكوين العام.
		العلاقة بين الداخل والخارج، علاقة محكومة بالانغلاق نحو الخارج والانفتاح نحو الداخل.

			الفصل بين الخاص والعام، في التكوين المعماري تظهر الحدود واضحة بينهما.
			التكامل ما بين الكتلة والفراغ في التكوين المعماري، حيث وجود الفناء ويعادله الكتلة العمودية للمبنى الديني.
			التنظيم والتخطيط الهندسي الشكلي، حيث الاعتماد على نسب ثابتة في التصميم واعتماد الشكل المربع بشكل أساسي لما يوحيه من الاستقرار والسكون.
	الموروث العمراني في العناصر المعمارية	البوابات	الصرحية والبروز والوضوح ووقوعها مع المحاور الرئيسية.
		الاسوار	تكون بأسماك وارتفاعات عالية توفر العزل والخصوصية.
		الفناء (الصحن)	المنفتح بكليته الى السماء ويوازن تأثير الكتلة المرتفعة للمبنى ويوفر بيئة داخلية محاطة ومحمية.
		الاقواس والعقود	برمزيتها وارتباطها مع فكرة العلاقة بين الأرض والسماء.
		القبة	تقع عادة في مركز المبنى وتهيمن بكتلتها على كامل المبنى والفناء المفتوح.
		الجدران والدعامات	تمتاز بسمكها العالي وكونها مبنية من الاجر والجص وتكون بشكل بارز وخاسف.
		الايوان	ويمثل الجزء الامامي ويتقدم المدخل الرئيسي.
		المئذنة	وتمثل الشاخص العمودي للمبنى. وأبرز العناصر المؤشرة الى وجود المبنى الديني والرابط بين الأرض والسماء.
		السقف	العنصر الانشائي الأهم وعادة يكون بشكل اقبية وقباب واقواس.
		الاعمدة	عنصر انشائي يرفع في العادة الطارمات التي تتقدم مداخل المباني الدينية واستخدامه كعنصر تكميلي.
	الموروث العمراني في العناصر التزيينية	شباك الضريح	كعنصر تزييني مكمل للمراقد المقدسة ويرتكز في وسط المبنى وتحت القبة الرئيسية. ويرتبط بصريا وحركيا مع المحاور الأساسية.
		النوافذ	النوافذ تكون صغيرة وعلوية في العادة ولا تفتح بشكل مباشر الى الخارج.
		المقرنصات	تمثل عنصر يجمع ما بين الغرض الانشائي والجمالي وتعطي الإحساس بديناميكية الانتقال ما بين العنصر العمودي والافقي. تقع في مناطق: أسفل شرفات المأذن، اعلى الاواوين، التقاء الجدران بالسقف، التقاء العقود بالجدران، بين القبة وقاعدتها الاسطوانية.
	الموروث العمراني ومواد البناء	الطين	مادة البناء الأساسية ووظف بكافة اشكاله (المفخور والمجفف تحت الشمس) وكمادة رابطة.
		الجص	وظف كمادة رابطة وكمادة انهاء وتزيين.
		القار	وظف كمادة مانعة للرطوبة أسفل الجدران وكمادة رابطة.
		الخشب	استخدم بشكل روافد لدعم ثقل السقوف والفتحات بالإضافة الى استخدامه في عناصر التزيين والنقش.

		الحجر	يقتصر توظيفه في انهاء الارضيات ومناطق أسفل الجدران.
		المعادن	في العناصر التكميلية للأبواب والشبابيك والتزيين.
	الموروث العمراني وانماط التزيين	نمط التزيين الهندسي	
		نمط التزيين النباتي (التوريق)	
		نمط التزيين بالكتابات	
		نقش الارابيسك	

3-1-3 المحددات المكانية البيئية وأثرها على عمارة العتبات الاسلامية

ارتفاع درجات الحرارة والمناخ الصحراوي	جدران ذات سمك عالي.
	استخدام الخاسف والبارز في الجدران.
	قلة مساحة الفضاءات بالنسبة الى مساحة الهيكل الانشائي.
	توظيف الألوان الباردة على الواجهات.
	عدم الفتح المباشر الى الخارج.
التوجيه	مراعاة خط الزوال في التوجيه
	مراعاة ان ضبط المبنى مع الاتجاهات الاربعة

3-2 تطبيق مؤشرات الإطار النظري على العتبة الكاظمية المقدسة.

3-2-1 نبذة عن العتبة الكاظمية المقدسة.

تعتبر العتبة الكاظمية المقدسة من المعالم الحضارية والدينية الإسلامية المهمة في العراق والعالم، وأصبحت مدينة الكاظمية وبفضل وجود العتبة من المدن المهمة من النواحي التجارية والثقافية والاجتماعية، اذ أصبحت ملتقى للناس من كل حدب وصوب يتبادلون المعارف والعلوم والسلع والبضائع والخدمات، ويلتقون في مناسباتهم الاجتماعية والدينية وفي افراحهم واحزانهم. كان موقع مدينة الكاظمية أولا مقبرة انشاءها الخلفاء العباسيون في بداية عهدهم وسميت بمقبرة قريش، ومن ثم تطورت تدريجيا لتتحول الى مدينة ممتدة في الجزء الشمالي الغربي لمدينة بغداد.[6] الشكل (3-1).

3-2-2 مراحل عمارة العتبة الكاظمية المقدسة.

مرت العتبة الكاظمية المقدسة خلال تأريخها الممتد من نهاية القرن الثاني للهجرة والى العصر الحاضر بالعديد من الأدوار البنائية والعمرانية شهدت خلالها متغيرات متعددة وتوسعات ، تفاجئ الزائر الداخل اليها وبعد الفضاء التمهيدي للبوابات برحابة صحنها المفتوح نحو السماء والمطوق بالسور المرتفع، ويتوازن مشهد الصحن المفتوح مع مشهد القباب والمأذن السامقة في الارتفاع التي تعطي الشعور بالإجلال والرهبة والاحترام، مشاعر لا يمكن تلمسها الا عندما يقف الشخص ويختبر ذلك التكوين المتوازن

6 مقبرة قريش: تقع في ببغداد وهي مقبرة مشهورة ومحلة فيها خلق كثير وعليها سور بين الحربية ومقبرة احمد بن حنبل (رض) والحريم الطاهري وبينها وبين دجلة شوط فرس جيد وهي التي فيها قبر موسى الكاظم ... وكان اول من دفن فيها جعفر الاكبر بن المنصور الخليفة العباسي الثاني في سنة 150للهجرة، وكان المنصور اول من جعلها مقبرة لما ابتنى مدينته سنة 149 للهجرة. (الحموي, 1995م، ج5، ص163). كما أن زبيدة زوجة هارون الرشيد المتوفاة سنة 216 للهجرة وابنها الخليفة الأمين دفنا في هذه المقبرة ثم توالى الدفن فيها عبر العصور حتى احتوت على قبور كثيرة من الوزراء والأعيان والسادة والعلماء والأشراف. (النقدي, 2014م، ص77).

بنفسه، ويتكامل ذلك التكوين مع التزيينات والتحليات والنقوش التي تعمل معا في خلق الصورة الحسية والتعبيرية لذلك المشهد المقدس.

وان اهم ما يمكن رصده من دراسة مراحل الاعمار في العتبة ما يأتي:

1) ان تطور عمارة العتبة الكاظمية المقدسة واتساعها استجابة لعدة عوامل سياسية واقتصادية واجتماعية وثقافية وبيئية فرضتها كل مرحلة.
2) استخدام اعمار العتبة الكاظمية من قبل العديد من الدول التي توالت في حكمها للعراق لتحقيق جوانب الدعاية السياسية والدينية وكسب ود الناس من قبلهم.
3) الاكثار من استخدام المواد النفيسة والنادرة في عمارة العتبة المقدسة يظهر لما لهذا المرقد من أهمية في نفوس المسلمين على اختلاف قومياتهم وجنسياتهم ومذاهبهم.

3-3 تطبيق المؤشرات على العتبة الكاظمية المقدسة.

تطبيق المؤشرات على العتبة الكاظمية المقدسة

3-3-1 المحددات الحضارية لعمارة العتبات والمرتبطة بالجوانب الدينية والاجتماعية والثقافية

المحددات الحضارية		مؤشراتها		
	فعل الزيارة الى العتبات الاسلامية	التطهر		يتحقق مفهوم التطهر في العتبة الكاظمية المقدسة بأعتبار ان الوضوء جزء أساسي في أي عمل عبادي، بالإضافة الى وجوب التطهر لدخول العتبة. (الطوسي، التهذيب، ج6، باب 3).
		تراتبية الزيارة والتعبد	التوجيه للمبنى الديني	يتحقق، حيث ان مبنى العتبة هندسي ضمن محيط عضوي. شكل(3-2).
				انحراف عن التوجه نحو عين الكعبة، واصابة اتجاه المسجد الحرام في التوجيه. (الغريفي، 2009م، 72).
				يتحقق عنصر مراعاة وقت الزوال وتحديده من خلال الظل بحيث تقابل البوابات الرئيسية الاتجاهات الأربعة تقريبا.
			الدخول الى المبنى الديني	الاستئذان: يتحقق
				التسليم: يتحقق
				الصلاة: يتحقق من خلال وجود الجامع الصفوي
				التوديع: يتحقق
	الجوانب الاجتماعية والثقافية للعتبات الاسلامية	الارتباط النفسي والحسي مع المبنى		وظفت الأسماء (ك باب المراد وباب الرجاء وباب الرحمة) بالإضافة الى الآيات القرآنية الدالة على أهمية المرقد.
				تتحقق الصرحية والتناظر في التأكيد على أهمية المرقد. شكل(3-3).
				تتحقق
				يتحقق وباستخدام المواد النفيسة والمعادن والاحجار الكريمة كمؤشر على العناية والاحترام لصاحب القبر.
		يتحقق من خلال العديد من المنشأت ذات الطبيعة الخدمية والاجتماعية الملحقة.		

3-3-2 المحددات الحضارية لعمارة العتبات والمرتبطة بجوانب الموروث العمراني والتخطيطي

الموروث الحضاري العمراني للمباني الدينية في العراق	أثر الموروث العمراني على النمط المعماري	تتحقق	
		يتحقق	
		واضح الفصل بين العام والخاص في العتبة الكاظمية وخصوصا في مناطق الدخول حيث نجد الفضاء التمهيدي الذي يتقدم مداخل العتبة.	
		يتحقق	
		يتحقق. ويلاحظ في الشكل (3–4) والمعد من قبل الباحث توظيف نسبة المربع على مستوى المخطط الافقي والواجهات للعتبة الكاظمية المقدسة.	
	الموروث العمراني في العناصر المعمارية	البوابات	يتحقق
		الاسوار	يتحقق
		الفناء (الصحن)	يتحقق
		الاقواس والعقود	تتحقق
		القبة	تتحقق
		الجدران والدعامات	تتحقق
		الايوان	تتحقق
		المئذنة	يتحقق، وتوجد ثلاث أنواع ممن المأذن في العتبة الكاظمية المقدسة الرئيسية والثانوية ومئذنة الساعة.
		السقف	يتحقق
		الاعمدة	يتحقق كعنصر انشائي يسند ثقل الطارمات التي تتقدم واجهات الروضة وتعزز الصورة الجمالية والرمزية لها.
	العناصر التزيينية	شباك الضريح	يتحقق
		النوافذ	يتحقق
		المقرنصات	يتحقق
	الموروث العمراني ومواد البناء	الطين	مادة البناء الأساسية ووظف بكافة اشكاله (المفخور والمجفف تحت الشمس) وكمادة رابطة.
		الجص	وظف كمادة رابطة وكمادة انهاء وتزيين.
		القار	وظف كمادة مانعة للرطوبة أسفل الجدران وكمادة رابطة.
		الخشب	استخدم بشكل روافد لدعم ثقل السقوف والفتحات بالإضافة الى استخدامه في عناصر التزيين والنقش.
		الحجر	يقتصر توظيفه في انهاء الارضيات ومناطق أسفل الجدران.
		المعادن	في العناصر التكميلية للأبواب والشبابيك والتزيين.
	انماط التزيين	نمط التزيين الهندسي	
		نمط التزيين النباتي (التوريق)	
		نمط التزيين بالكتابات	
		نقش الارابيسك	

3-3-3 المحددات المكانية البيئية وأثرها على عمارة العتبات الاسلامية

ارتفاع درجات الحرارة والمناخ الصحراوي	يتحقق
	يتحقق
	يتحقق، حيث نجد بأن النسبة ما بين مساحة الهيكل الانشائي ومساحة الروضة تتعدى 33%. شكل (3-5)
	تحقق
	تتحقق
التوجيه	تتحقق ويشير الى ذلك العلامة حسين محفوظ بقوله: هنالك ميزة هندسية رائعة للعتبة الكاظمية المطهرة الا وهي كون اتجاه بناء العتبة يتفق من ناحية التوقيت مع حركة الشمس ودوران الأرض، فالشمس حين تصل الى حافة دكات اواوين طارمة صحن قريش (الجانب الغربي من الروضة) ففي ذلك إشارة مؤكدة الى دخول وقت الزوال وحلول منتصف النهار واذان الظهر، ومن الجدير بالذكر -يكمل محفوظ-ان العالم العربي بهاء الدين البهائي (متوفى 1301هجري) هو منشئ اغلب القضايا الهندسية في العتبات العراقية المقدسة. (مقابلة مع العلامة حسين محفوظ، المنبر، عدد15، 1429هـ). شكل (3-7).

3-4 نتائج تطبيق المؤشرات.

1. راعى المعمار العراقي المسلم ظروف بيئته المحلية في عمارة العتبة الكاظمية المقدسة. اذ وبالرغم من جميع المؤثرات الخارجية (بجميع جوانبها) استطاع ان ينتج عمارة اخذت بنظر الاعتبار الموروث الحضاري ودمجته بالمفاهيم الإسلامية والجوانب البيئية والمناخية.
2. أثرت المفاهيم الإسلامية على تصميم العتبة الكاظمية مندمجة مع مفاهيم موروثة ومعالجات بيئية من خلال:

أ. مركزية وجود العتبة ضمن نسيجها الحضري يعزز من الدور الذي تلعبه كنواة دينية وهذا يؤشر على أهمية التدين والعبادة في المجتمع ويؤكد عليها. كما ان هيمنة العتبة على خط الأفق في المدينة بأعتبارها الشاخص العمودي ضمن نسيج حضري ذا توجه افقي. ساعد في تعزيز مفهوم الظهور في عمارة العتبة وقوة المركز الديني وسيطرته.

ب. التوجه نحو الداخل. والذي يعزز من مفهوم الاحتواء أحد مفاهيم العمارة الإسلامية قلة التزيين في الواجهات الخارجية شبه المصمتة وعدم الفتح نحو الخارج.

ج. التوازن بين الكتلة والفراغ كمفهوم إسلامي ومفهوم عمراني موروث.

د. التجريد وروحية الابتعاد عن التصوير والتجسيم المباشر يعكس محاولة إيجاد خلود للعمارة بأبعادها عن عالم المادة والزمان والمكان.

3. أثر جانب الممارسة الدينية وطبيعة الزيارة وتراتبية طقوسها بحسب المرويات عن الائمة (ع) في الجانب التصميمي للعتبة الكاظمية المقدسة من الناحيتين المادية والمعنوية من خلال:

أ. الاهتمام بجهة القبلة بأعتبارها وجهة دخول الزائرين للمرقد.

ب.زيادة رسمانية ومهابة واجهة القبلة من خلال التركيز عليها بواسطة المأذن وارتفاع القبة.

ج. توجيه حركة الزائر من خلال المحاور البصرية المهمة والمؤثرة لبابي القبلة والمراد.

4. ويمكن ان يدرك من كل ما تقدم ما يأتي:

أ. ان جميع المنظومات الجزئية في مبنى العتبة الكاظمية المقدسة تفاعلت بكفاءة مع المنظومات الأخرى بشكل حققت معها وبمجملها الصورة متكاملة لشكل العتبة وهيئتها التعبيرية، فالمنظومة الانشائية تتفاعل مع المنظومة المعمارية وكذا المنظومة البيئية وكلها مجتمعة تصب في مصلحة الجانب التعبيري والفلسفة التصميمية. فعمارة العتبة الكاظمية المقدسة لا تتكون من جانب مادي مجرد ولا تبنى على وفق متطلبات بيئية او ظرفية بحته ومجردة، وانما هي سلسلة من الانفعالات والاحاسيس التي تنقل لنا الفكرة من وراء الجدران والحجر، وان فقدان هذا الرابط ما بين الجانبين المادي والمعنوي يفرغ العتبة من محتواها ويحولها الى مبنى كغيره من المباني الأخرى مجرد من العواطف.

ب. ان مبنى العتبة وفكرته لا تكتمل الا بوجوده ضمن نسيجه الحضري والذي للأسف الشديد قد انسلخ منه حقيقة ولا يزال العمل مستمر على إزالة ما تبقى من اثار لهذا النسيج الذي لا تكتمل صورة العتبة التعبيرية الا بوجوده ضمنها. فأي معنى يبقى للصحن بوجود فراغات شاسعة مفتوحة حول العتبة، واي هيمنة تبقى للمأذن والقباب بوجود مباني ترتفع الى ضعف ارتفاع تلك القباب والمأذن، واي مفاجأة بصرية تنتظر الزائر حين دخول لصحن مسقف ومحجوب عنه صورة القباب والمأذن بأرتفاعها وتفاعلها مع محيطها.

ان التطورات المعمارية التي مرت بها عمارة العتبة الكاظمية المقدسة ونموها التدريجي من مرحلة الى أخرى انما جاء نتيجة لتغيرات ظرفية وقتية ونمت مع الزمن بفعل التطورات التقنية في الانشاء واستخدام المواد وتنامي فعل الزيارة والاقبال الى المشهد ولكنها مع ذلك حافظت على اصالتها وميزاتها مع كل مرحلة من مراحل نموها من دون تشويه في نسبها الجمالية او في قواعد عمارتها وتخطيطها النابعة من اصول متينة خلفتها حضارة امتدت بجذورها وعمقها منذ فجر الخليقة. لذا فأن التوسع والنمو في عمارة العتبة في الوقت الحالي يجب ان يأخذ بنظر الاعتبار الجوانب التعبيرية والرمزية ولا يتناول العناصر والتشكيلات المعمارية بصورة فجة ومجردة ومادية بهيئتها بل يجب ان يفهم الروحية التي وضعتها في مكانها الذي هي فيه وهدف المعمار ويجب ان يتحسس النسب والعلاقات التكوينية التي تربط فيما ليتمكن من عكسها وتحقيقها في عمله ولكيلا يكون العمل مجرد تجميع لأشكال وعناصر مقتطعه من هنا وهناك من دون فهم روحيتها وهدف وجودها وعدم الانغماس في الجوانب المادية البحتة.

وهذا يثبت الفرضية البحثية حول دور وتأثير العوامل المكانية بشقيها الحضاري والبيئي على تكوين وبلورة عمارة العتبات الإسلامية المقدسة في العراق، بالإضافة الى الدور المحوري للفكر الإسلامي في الصياغة النهائية لعمارتها.

3-5 نظرة مستقبلية لمؤشرات الإطار النظري المستقبلية لعمارة العتبة الكاظمية المقدسة.

لا بد من الإشارة الى ان مشاريع التطوير والتحديث الجارية حاليا على عمارة العتبات الاسلامية المقدسة في العراق قد اثرت بدورها على بعض المؤشرات التي شهدت بعض التحولات، فهيمنة العتبة بأرتفاع مأذنها وقبابها على خط الأفق قد بدأ يفقد أهميته مقابل ارتفاعات الأبنية المجاورة ووجود الفضاء الحضري المهم والمؤثر والمتمثل بصحن العتبة قد بدأ يفقد دوره في مقابل فتح الشوارع والساحات المحيطة بالعتبة. كما ان انسلاخ العتبة عن النسيج الحضري المحيط بها بفعل عوامل الزمن وخطط التطوير والتحديث المستمر والذي أضاع العديد من الجوانب الفنية والاعتبارية للعتبة والمتكاملة مع نسيجها الحضري، كما وان العتبة وفي الوقت الراهن تشهد نقلة نوعية واسعة في مجال إضافة الكثير من المنشأت الخدمية الجديدة للعتبات المقدسة او احداث بعض التطويرات والتحسينات وكل ذلك نابع من الأسباب الاتية:

أ. تنامي فعل الزيارات المليونية على تلك المنشأت وكون المباني الحالية لا تلبي متطلبات ذلك الاتساع في فعل الزيارة مما استوجب إضافة الكثير من الفضاءات والابنية، كما يستوجب ذلك إيجاد الحلول لإيوائهم واطعامهم وضيافتهم وخصوصا في مواسم الزيارات الكبرى في المناسبات الدينية الرئيسية.

ب. ازدياد الاقبال على العتبات المقدسة استوجب استحداث الكثير من الأقسام الخدمية والإدارية التي تقوم على ادارتها ورعايتها والقيام بأعمال النظافة والصيانة الدورية فيها.

ج. اتساع نطاق التبادل الثقافي والمعرفي وتطور وسائل الاتصال وانتقال المعلومات وخصوصا مع الثورة الالكترونية الحالية وأساليب البث الحي والمرئي للمناسبات الدينية والذي تطلب إيجاد فضاءات إضافية لأغراض تنظيم تلك الوسائل وتهيئتها لمواكبة تلك التطورات.

د. ازدياد اعداد الوافدين الى تلك العتبات من مختلف دول وجنسيات العالم ورغبتهم في عقد المؤتمرات وإقامة الندوات وغيرها دفع الى الاتجاه نحو انشاء قاعات لاستقبالهم ولغرض إقامة تلك المحافل، كما تطلب الامر انشاء المتاحف والمعارض لغرض تعريفهم على تأريخ العتبات وما يوجد فيها.

من كل الأسباب السابقة يمكن ان يفهم بأن أي اعمال لتوسعة وتطوير العتبات الإسلامية المقدسة، أصبحت جزءا من واقع فرضته المتغيرات الحالية والمستقبلية، الامر الذي أصبح معه تحديد مؤشرات ثابته لعمارتها امرا لابد منه، كي لا تضيع مع موجة تلك المتغيرات المفاهيم الأساسية لعمارتها والتي تم تحديدها من خلال الدراسة.

4 الاستنتاجات.

1. ان المراقد كنمط بنائي إسلامي اصيل، له ميزاته الخاصة النابعة من طبيعة وظيفته كمكان يجمع ما بين الفعل العبادي والجانب التذكاري الذي يرسخ العلاقة مع رموز لأشخاص كان لهم الدور الفاعل في ترسيخ قيم الدين والشريعة في المجتمع الإسلامي، ولذا فقد اكتسب عمرانها جانبا من الأهمية والدور الفاعل في المجتمعات الإسلامية.
2. مرت عمارة المراقد الإسلامية المقدسة بعدد من المراحل التي مثلت تنامي الخبرة وأسلوب المعالجة والتخطيط وتطور تقنيات الإنتاج واتساع دائرة الاحتكاك بالحضارات، ودفع ذلك الى اقلمة المنتج المعماري مع خصوصيات كل منطقة مع ثبات وحدة المفهوم النابع من الإطار العام للدين الإسلامي.
3. مثلت النماذج الأولى للمراقد الإسلامية البذرة الأساسية لتطور عمارة العتبات الاسلامية، وترتكز على مخطط مركزي ومتناظر وملائم في شكله ليسقف بقبة تمثل في رمزيتها وتعبيريتها عن الشخص المدفون تحتها، وجعل الضريح في مركز هذا المبنى بأعتباره الهدف الأساس لتشييده. وهذه البذرة تنامت وتطورت الى اشكال ومخططات مختلفة ولكنها ضلت تدور حول هذا الفلك الأساسي المحدد في النقطتين أعلاه.
4. يظهر في العراق وكجزء من العالم الإسلامي الاهتمام البالغ بعمارة المراقد المقدسة، ووجودها منتشر في ربوعه من شماله لجنوبه وبمختلف انماطها الثلاثة البسيطة والمركبة والروضات (العتبات)، وهذا يبين ما تمثله المراقد المقدسة من أهمية دينية واجتماعية وثقافية بالنسبة للعراقيين، كما ان تعاهد زيارتها واقبال الناس عليها يدل على مكانتها الاعتبارية واهمية موقعها وعظم تأثيرها.
5. ان المراقد الإسلامية المقدسة في العراق قد مرت وحالها حال باقي أجزاء العالم الإسلامي بمراحل متعددة في الانشاء والتطوير والريازة، واختلفت تلك المراحل بحسب الأهمية التي تتعلق بصاحب المرقد ومدى الاقبال عليه، وتطور الامر ليصل الى تحول بعض تلك المراقد الى عتبات مثلت نواة لنمو مدن كبيرة ومهمة وأصبحت تلك العتبات مركزا للكثير من النشاطات الدينية والاجتماعية والثقافية، ومحطة لتلاقي الشعوب بالإضافة الى جذبها لاهتمام الدارسين والباحثين في الفن والعمارة وتطورها.
6. ان توظيف المعمار العراقي ما توفر له من مواد في البيئة المحيطة به في البناء والانشاء كالطين ومشتقاته والجص والقار وغيرها توافق مع جانبي المفاهيم العقائدية في التوافق والانسجام مع البيئة إضافة الى جانب الإيجابية البيئية التي تحققها تلك المواد من ناحية الحماية والعزل، ولذا استمر هذا المفهوم كسنة بنائية لدى العراقيين. ودفع توفر تلك المواد لديهم الى ابتكار

تقنيات جديدة في التعامل معها وتوظيف إمكاناتها الى حدودها القصوى. كما ان الظروف والاحوال البيئية والمناخية الصحراوية الحارة اغلب أوقات السنة أجبرت المعمار العراقي على التوجه بعمارته نحو الداخل مع تقليل مساحة الاسطح المعرضة للظروف الخارجية الى اقل حد ممكن.

7. ان تطبيق المؤشرات على عمارة العتبة الكاظمية المقدسة، اظهر ان مؤثرات عوامل المكان بشقيها الحضاري والبيئي قد ساهمت وبشكل بارز في تحقيق التكوين والتشكيل المعماري، واستطاعت تلك العوامل إزالة الحدود الزمانية الفاصلة وخلق الاستمرارية في التواصل الفكري والفني، وتفاعلت تلك العوامل مع المفاهيم الإسلامية بفاعلية وإيجابية في تشكيل ابنيتها.
8. من تتبع السير التأريخي لعمارة العتبة الكاظمية المقدسة، يلحظ بأنها قد مرت بالعديد من المراحل التكوينية (المورفولوجية) في عمارتها من مبنى بسيط ذا قبة منفردة محاط بالمساجد والمراقد الى تكوين معماري له استقلاليته التكوينية والفضائية. وبين هاتين المرحلتين مر بالعديد من المراحل في البناء والتطوير، ويلحظ بأن كل مرحلة قد اضافت الى عمارة العتبة شيئا من ميزاتها التي استمرت الى هذا اليوم. فبناء العتبة على رغم من كونه مر بمراحل الا انها رسخت قيم عمرانية وطرازيه فيه ثبتت في الذاكرة الجمعية وأصبح من غير الممكن التغاضي عنها واهمالها في مراحل الاعمار اللاحقة. لذا فمن غير الممكن اعتبار عمارة العتبة عمارة صدفة او انها نمت نموا مفاجئا او نشأت من الفراغ او ان تنسب الى جهة محددة نعتبرها بداية لها من غير وجود أسس رصينة وثابتة لتلك العمارة في مكانها، حفرتها ذاكرة أجيال متعددة من الخبرة الحسية والتعبيرية ومن التجارب العمرانية وخبرة أبناء بلد ذو حضارة عريقة.
9. ساهم الامتداد الافقي لنسيج مدينة الكاظمية القديمة في تعزيز حضور الشاخص العمودي المهم المتمثل بالعتبة والذي يتوسط مركزه ويهيمن عليه بأرتفاعه يحقق التوازن ما بين الافقي والعمودي. وهذا ما كان يلحظ في اغلب المدن العراقية قبل وبعد الإسلام حيث يكون المبنى الديني فيها هو نواة التجمع الحضري والذي يفرض هيمنته على صورة النسيج والمدينة.
10. ان لكل جزء مهمته التي تتكامل مع الأجزاء الأخرى في تحقيق التكامل للصورة التعبيرية والشعورية. فالسور بهيئته الخارجية المصمتة وتزيينه البسيط من الخارج والغنى التكويني من الداخل يحقق المفهوم الإسلامي في التوجه نحو الداخل، ومع وجود البوابات الصرحية البارزة والتي تتعارض في تزيينها ونقشها مع بساطته مؤشرة الى أهميتها وتاركة الانطباع بالرغبة في الدخول لولوج عالم اخر غير عالم الدنيا المادية ومؤشرا على مفهوم قرآني أكد على أهمية الباب وخصوصا إذا كان باب مبنى ديني في حط الذنوب وقضاء الحاجات في قوله تعالى:﴿ وادخلوا الباب سجدا وقولوا حطة نغفر لكم خطاياكم وسنزيد المحسنين ﴾. (سورة البقرة، اية 58). وبالانتقال والدخول الى الباب ذا التزيينات بالأجر المزجج والذي تعلوه كتيبة افقية من الآيات القرأنية يؤدي الى فضاء انتقالي يختلف طوله بحسب امتداد السور ويؤدي الى تنامي الصورة البصرية شيئا فشيئا وتحقيق المفاجأة ويزيد من الشعور بالانتقال بين العام والخاص، عند الدخول الى الفناء المفتوح والذي يحتضن ويوازن كتلة الروضة الممتدة بعموديتها الى السماء وكأنها اكف تتضرع وتطلب الرحمة من بارئها والتي توازن الامتداد الافقي للصحن وسوره، ويتم الدخول بعدها ضمن فضاء انتقالي اخر الى وهو فضاء الروضة ذا الإضاءة الدافئة والألوان الغنية والتي تشعر الانسان بالهدوء والسكينة والراحة وهو داخلها.
11. ان الجانب التزييني في العتبة الكاظمية المقدسة يأخذ دورا أساسيا بجانب للجوانب التخطيطية والفضائية فيها، فمنظومة التزيين هي جزء من الحل المعماري الوظيفي في العتبة ولا تكون إضافة بعدية وانما جزء من القرار المعماري والتخطيطي، وكل معالجة تزيينية تهدف الى تحقيق جانب انطباعي وشعوري يعزز تكامل الجانب الحسي للمتلقي ويتكامل مع التكوين الكتلي والفضائي، وكما لوحظ فأن عملية توظيف الجوانب التزيينية من دون فهم وأدراك للغرض المقصود يؤدي الى تغيير الانطباع والشعور بالفضاء والتكوين ككل. وان اخذ العناصر التزيينية وتجميعها مع بعضها من دون فهم الغرض المقصود منها يلعب جانبا سلبيا في عملية إعادة الانشاء والتصميم.

ان عمارة العتبات والمراقد المقدسة في العراق قد خضعت لعوامل المكان ونشأت متأثرة بها بصورة رئيسية، وهذا ما أثبته تطبيق المؤشرات التي تم استخلاصها من معاينة الأنماط والطرز البنائية المعمارية في العراق ومنذ فجر التأريخ، وهي وأن اصطبغت في بعض الأحيان بمؤثرات من ثقافات وامم مجاورة الا انها استطاعت ان تحافظ على خصوصيتها المكانية وتفردها وتميزها عن غيرها من العمارات الإسلامية في البلدان الأخرى. ولقد ساهمت وحدة مبادئ وثوابت الإسلام في توحيد لغتها المعمارية بالرغم من التنوع والتعدد في التفاصيل. وهذا ما يثبت فرضية البحث القائمة حول تأثير عوامل المكان إضافة الى مفاهيم الإسلام في تشكيل وصياغة عمارة العتبات المقدسة في العراق.

المصادر :

المصادر العربية:

- ﴿ القرآن الكريم ﴾
- ابن بطوطة، تحفة النظار في غرائب الامصار، دار الكتب العلمية، بيروت، الطبعة الأولى، 1987م.
- ابن جبير، رحلة ابن جبير الاندلسي، كتاب الكتروني.
- ابن خلدون، المقدمة، نسخة الكترونيةwww.al-mostafa.com.
- احمد سوسة، بالاشتراك مع مصطفى جواد، دليل خارطة بغداد المفصل في خطط بغداد قديما وحديثا، مكتبة الحضارات، بيروت، 2011م.
- ال ياسين، محمد حسن، تأريخ المشهد الكاظمي، مطبعة المعارف، بغداد، الطبعة الأولى، 1967م.
- الليدي درور، على ضفاف دجلة والفرات، ترجمة؛ فؤاد جميل، دار الوراق للنشر، الطبعة الأولى، 2008م.
- البعلبكي، منير، قاموس المورد (انكليزي-عربي)، دار العلم للملايين، بيروت، 2000م.
- بهنسي، عفيف، جمالية الفن العربي، المجلس الوطني للثقافة والعلوم والآداب، دولة الكويت، سلسلة عالم المعرفة، عدد 14، 1979م.
- ثويني، علي، معجم عمارة الشعوب الإسلامية، بيت الحكمة، بغداد، الطبعة الأولى، 2005م.
- جدو، ينار حسن، المذاهب الفكرية الحديثة والعمارة، دار الطليعة، بيروت، الطبعة الأولى، 1993م.
- جنان عبد الوهاب، جدلية التواصل في العمارة العراقية، دار الشؤون الثقافية العامة، بغداد، الطبعة الأولى، 2002م.
- جواد علي، المفصل في تأريخ العرب قبل الإسلام، ساعدت جامعة بغداد على نشره، الطبعة الثانية، 1993م.
- الحاج قاسم، حسان محمود، تأثير التفاعل الحضاري في العمارة العربية قبل الإسلام، أطروحة دكتوراه غير منشورة، كلية الهندسة، جامعة بغداد، 2007م.
- الحديثي، عطا وهناء عبد الخالق، القباب المخروطية في العراق، مديرية الاثار العامة، بغداد، 1974م.
- حرز الدين، محمد، مراقد المعارف، مطبعة الآداب، النجف الاشرف، 1971م.
- الحسني، عبد الرزاق، العراق قديما وحديثا، دار اليقظة العربية، بغداد، الطبعة السابعة، 1982م.
- الحمداني، عبد الأمير، جذور اجتماعية رافدينية من السهل الرسوبيّ، مقاربة أثنو-آثاريه لبعض الظواهر الاجتماعية في المجتمع العراقي، مجلة الكوفة، العدد الرابع، السنة الثانية، خريف 2013م.
- الحموي، ياقوت، معجم البلدان، دار صادر، بيروت، الطبعة الأولى، 1996م.
- حيدر عبد الأمير رشيد، حوار الأديان في الفن (الإسلام والمسيحية)، مركز حمورابي للبحوث والدراسات الاستراتيجية، الطبعة الأولى، 2012م.
- حيدر ناجي عطية، إمكانات تطوير مواقع المراقد المقدسة في مدينة كربلاء، رسالة ماجستير غير منشورة، كلية الهندسة، جامعة بغداد، 2009م.
- خالد عزب، الرمزية السياسية للعمارة. العمارة لغة للحوار الحضاري، مقال منشور الكترونيا.
- الخليلي، جعفر، وآخرون، موسوعة العتبات المقدسة، مؤسسة الاعلمي، بيروت، الطبعة الثانية، 1987م.
- دوغزي، جرورجي، النسبة الذهبية وتناغم النسب في الطبيعة والفن والعمارة، بتصرف وترجمة واعداد: ياسر عابدين وبيير نانو وياسر الجابي، جامعة دمشق، 2011م.
- رويتر، اوسكار، البيت العراقي في بغداد ومدن أخرى، ترجمة؛ محمود كبيبو، دار الوراق، لندن، الطبعة الأولى، 2006م.
- زكي محمد حسن. اطلس الفنون الزخرفية والتصاوير الإسلامية، دار الرائد العربي، بيروت، 1984م.
- الساعدي، عبد الجواد حسن، تقويم دراسات التطوير والحفاظ للمنطقة المحيطة بصحن الكاظمين الشريفين والتوجهات المطلوبة، رسالة ماجستير غير منشورة، مركز التخطيطي الحضري والإقليمي، جامعة بغداد، 1998م.

- السلطاني، خالد، واقعة تسقيف صحن الروضة الحسينية، موقع صحيفة المدى العراقية الالكتروني.
- سعاد ماهر، مشهد الامام علي في النجف وما به من الهدايا والتحف، دار المعارف، مصر، 1967م.
- سعفان، كامل، معتقدات اسيوية، موسوعة الأديان القديمة، دار الندى، مدينة نصر، جمهورية مصر العربية، الطبعة الأولى، 1999م.
- شافعي، فريد محمود، العمارة العربية الإسلامية ماضيها وحاضرها ومستقبلها، عمادة شؤون المكتبات، جامعة الملك سعود، المملكة العربية السعودية، الطبعة الأولى، 1982م.
- شذى عباس، التواصل المعماري والحضري للتراث العربي الإسلامي، مجلة المخطط والتنمية، العدد 25، 2012م.
- عبد الوهاب حميد رشيد، حضارة وادي الرافدين (العقيدة الدينية، الحياة الاجتماعية، الأفكار الفلسفية)، دار المدى، بغداد، الطبعة الأولى، 2004م.
- عبد الجواد، توفيق احمد، تأريخ العمارة والفنون في العصور الأولى، الطبعة الثانية، 1970م.
- عكاشة، ثروت، القيم الجمالية في العمارة الإسلامية، دار الشروق، القاهرة، الطبعة الأولى، 1994م.
- علام، نعمت إسماعيل، فنون الشرق الأوسط في العصور الإسلامية، دار المعارف، مصر، الطبعة الثانية، 1982م.
- علي ناجي عطية، عمارة العتبات المقدسة نظرة في الجوانب الروحية، قسم الشؤون الفكرية والثقافية، العتبة العلوية المقدسة، 2008م .
- غالب، عبد الرحيم، موسوعة العمارة الإسلامية، جروس برس، طرابلس، لبنان، الطبعة الأولى، 1988م.
- القحطاني، هاني محمد، مبادئ العمارة الإسلامية وتحولاتها المعاصرة، مركز دراسات الوحدة العربية، بيروت، الطبعة الأولى، 2009م.
- قديفة، مالك صبري، صورة العمارة العراقية قبل الإسلام (537ق م–632 م)، أطروحة دكتوراه غير منشورة، كلية الهندسة، جامعة بغداد، 2005م.
- القصيري، اعتماد يوسف، أضواء على التراث الحضاري المعماري الإسلامي في العراق، منشورات المنظمة الإسلامية للتربية والعلوم (ايسيسكو)، كتاب الكتروني، بدون سنة طبع.
- الكرملي، انستاس، مزارات بغداد، تحقيق؛ باسم الياسري؛ مراجعة؛ طالب البغدادي، دار الوراق للنشر، كتاب الكتروني.
- كتانة، لطف الله جنين، دراسات في هندسة العمارة الإسلامية وتخطيط المدن في حاضر العالم الإسلامي، مطبعة انوار دجلة، بغداد، الطبعة الأولى، 2012م.
- الكوراني، علي، الامام الكاظم (ع) سيد بغداد وحاميها وشفيعها، الشؤون الفكرية والثقافية، العتبة الكاظمية المقدسة، دار المرتضى، بيروت، 2012م.
- المالكي، قبيلة فارس، التناسب والمنظومات التناسبية في العمارة العربية الإسلامية، أطروحة دكتوراه غير منشورة، كلية الهندسة، جامعة بغداد، 1996م.
- مازن لطيف وآخرون، موسوعة الاضرحة والمزارات العراقية، دار ميزوبوتاميا، بغداد، 2013م.
- المحمد، وليد، مراقد البصرة لها قصص وحكايات، دار ومكتبة عدنان، بغداد، الطبعة الأولى، 2013م.
- المعموري، حمزة سلمان جاسم، النظام في العمارة العربية الإسلامية وأثر تحولاته في الية انساقها، أطروحة دكتوراه غير منشورة، كلية الهندسة، جامعة بغداد، 2005م.
- الموسوي، مصطفى عباس، العوامل التأريخية لنشأة وتطور المدن العربية الإسلامية، دار الرشيد للنشر، وزارة الثقافة والاعلام، الجمهورية العراقية، الطبعة الأولى، 1982م.
- الموسوي، مسلم السيد حسين، قبس من الكاظمين، الدار العربية، بغداد، الطبعة الأولى، 1986م.
- مؤنس، حسين، المساجد، المجلس الأعلى للثقافة والآداب والفنون، دولة الكويت، عالم المعرفة، 1981م.
- النجار، عبد المجيد، معالم المنهج الحضاري في الإسلام، مجلة ثقافتنا للدراسات والبحوث، العدد الخامس والعشرون، 2010م.
- النجفي، محمد حسن، جواهر الكلام في شرح شرائع الإسلام، دار احياء التراث العربي، بيروت، الطبعة الأولى، 2009م.
- نصار، كريستين، الانسان والتأريخ (أثر التأريخ وتأثره بسيكولوجية الفرد)، جروس برس، طرابلس، لبنان، 1991م.
- النقدي، جعفر، تأريخ الامامين الكاظمين وروضتهما الشريفة، تحقيق: الشيخ غزوان بن الشيخ سهيل الكليدار، إصدارات العتبة الكاظمية المقدسة، دار المرتضى، الطبعة الأولى، 2014م.
- الهروي، ابي بكر، الإشارات الى معرفة الزيارات، تحقيق؛ عمر علي، مكتبة الثقافة الدينية، القاهرة، الطبعة الأولى، 2002م.
- هيكل، محمد حسين، الإمبراطورية الإسلامية والأماكن المقدسة، كلمات للترجمة والنشر، القاهرة، 2013م.
- الوردي، علي، دراسة في طبيعة المجتمع العراقي، دار ومكتبة دجلة والفرات، بيروت، الطبعة الثانية، 2010م.
- وزيري، يحيى، العمارة الإسلامية والبيئة؛ الروافد التي شكلت التعمير الإسلامي، سلسلة عالم المعرفة، عدد304، الكويت، 2004م.
- يوسف، شريف، تأريخ فن العمارة العراقية في مختلف العصور، وزارة الثقافة والاعلام، الجمهورية العراقية، 1982م.

REFERENCES

- Antoniades, Anthony C., Poetics of Architecture Theory of Design, John Wiley & sons, Canada, 1992.
- The Beginnings of Civilization, Electronic book.
- Escrig, F., The Great Structure In Architecture (Antiquity to Baroque), WIT Press, U.K., 2006.
- Foroozani, Principles of aesthetics in Islamic architecture, PBRIODICA POLYTBCHNICA SBR. ARCH. VOL. 35, NO. 3-_}, PP. 189-200 {1991}.
- Frankl, Paul, Principles of Architectural History, The Massachusetts Institute of Technology, second printing, 1973.
- Farah Habib, & others, Christian Norberg-Schulz and the Existential Space, International Journal Of Architecture and Urban Development Vol.1, No.3, Winter 2012.
- Fletcher, Banister, History of Architecture on The Comparative Method, London, fifth edition, MCMV.
- Hoag, John D., Islamic Architecture, Harry N. Abrams Publishers, New York, 1977.
- Harmanşah, Ömür, the Cattle pen and the Sheepfold: Cities, Temples, and Pastoral Power in Ancient Mesopotamia, the Oriental Institute of the University of Chicago, 2012.
- Hillenbrand, Robert, Islamic Art and Architecture, Thames and Hudson, London, 1999.
- Islamic Art and Geometric Design, the Metropolitan Museum of Art, New York, 2004.
- Kadhim Fathel Khalil and Julaihi Wahid, The Proportional Relations System of Islamic Architecture, International Journal of Scientific and Research Publications, Volume 3, Issue 1, January 2013.
- Krunic, J., Iraq; Protection of Cultural Heritage, unesco, 1968.
- Longhurst, C., Theology of a Mosque, the Sacred Inspiring Form, Function and Design in Islamic Architecture, Lonaard Magazine, London, Issue 8, V. 2, March 2012.
- Noghrekar & others, Unison of the phenomenological theory of genius loci and islamic philosophy-Dispositional influence of climate and its consequences on the design of environment, International Journal of Architectural Engineering & Urban Planning, Vol. 22, No. 1, June 2012.
- Park, Chris, RELIGION AND GEOGRAPHY, Chapter 17, Companion to the Study of Religion. London, 2004.
- Petersen, Andrew, Dictionary of Islamic Architecture, Rout ledge, London and New York, 1996.
- Ragavan, Deena, Heaven on Earth; Temples, Ritual, and Cosmic Symbolism in the Ancient World, the Oriental Institute of the University of Chicago, 2012.
- Joedicke, Jurgen, Space and Form in Architecture, karl Kramer verlag, Stuttgart, Germany, 1985.
- Hafsa Ramzi and Maysaa Muffeq, Structure as a Tool of Achieving Human Scale in the Islamic Architecture, International Conference on Transport, Civil, Architecture and Environment engineering, 2012, Dubai.
- Rabah Saoud, Muslim Architecture Under Seljuk Patronage (1038-1327), foundation for science technology and civlisation, 2003.
- Sani, Rafooneh Mokhtarshahi, A Conceptual Understanding for Teaching the History of Islamic architecture; an Iranian (Persian) perspective, Arch net, V. 3, 2009.
- Sidawi, Bhzad, Understanding the vocabulary of the Islamic architectural heritage, GBER Vol. 8, Issue. Two, p. 26 – 39.
- Taghizadeh, Katayoun, Islamic Architecture in Iran; A Case Study on Evolutionary of Minarets of Isfahan, Architecture Research, Department of Architecture, University of Tehran, Tehran, Iran, 2012.
- Warren, John, Fethi, Ihsan, Traditional Houses in Baghdad, Couch publishing House, Horsham, England, 1st published, 1982.

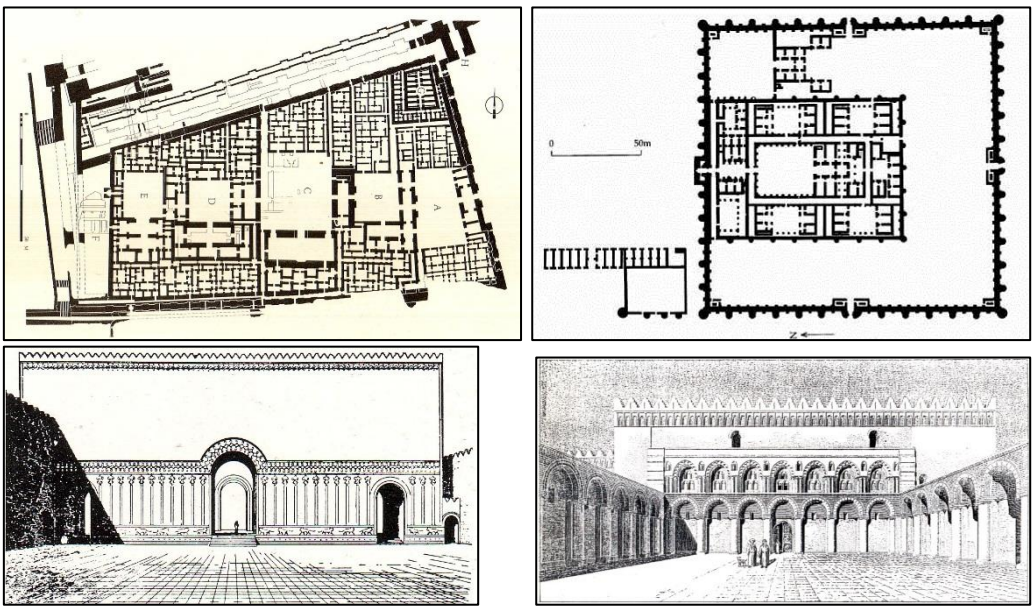

شكل (1-1) مقاربة معمارية لقصرين عراقيين. الأول من جهة اليمين قصر الاخيضر في العراق والذي يعتقد بأن تأريخ انشاءه يعود الى أوائل العصر العباسي والثاني القصر الجنوبي في مدينة بابل والذي يعود تأريخ انشاءه الى عهد الدولة الكلدانية التي حكمت البلاد بما يقارب القرن الخامس قبل الميلاد. مصدر الصورة الأولى (يوسف، 1982م، ص). والثانية (جنان عبد الوهاب، 2003م، ص).

1-3 العتبة الكاظمية المقدسة، مجلة السياحة الاسلامية، عدد1.

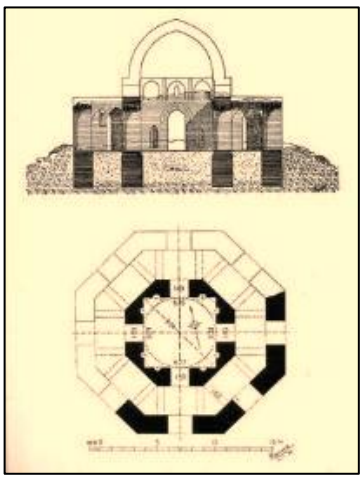

شكل (1-2) قبة الصليبية في سامراء مخطط ومقطع، شريف يوسف، ص132.

شكل 3-2مجسم العتبة الكاظمية المقدسة، من موقع Google Earth

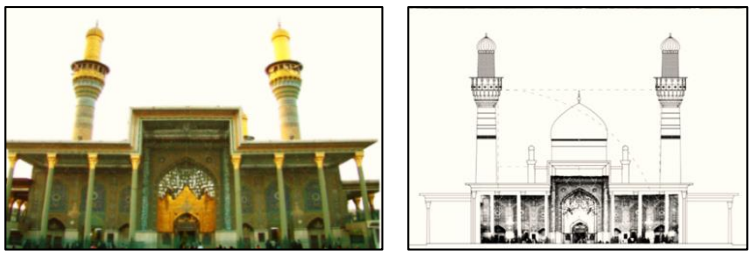

شكل (3-3) الواجهة الجنوبية من العتبة الكاظمية المقدسة وهي او ما يقابل الزائر الداخل للعتبة وتظهر الرسمانية بأعلى صورها من خلال التناظر والشكل التصاعدي الى السماء. اعداد وتصوير الباحث.

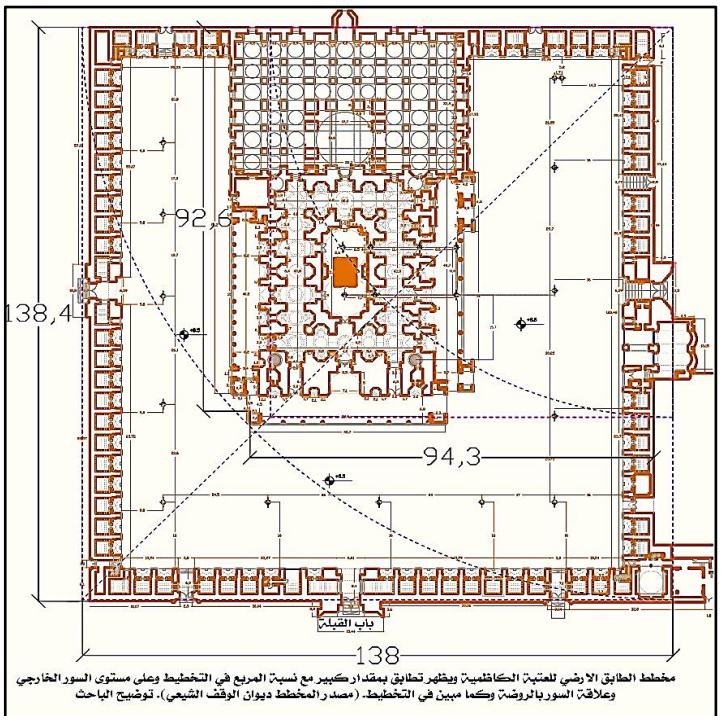

شكل (3-4) مخطط العتبة الكاظمية المقدسة ، ويوضح التناسب المربع، اعداد الباحث.

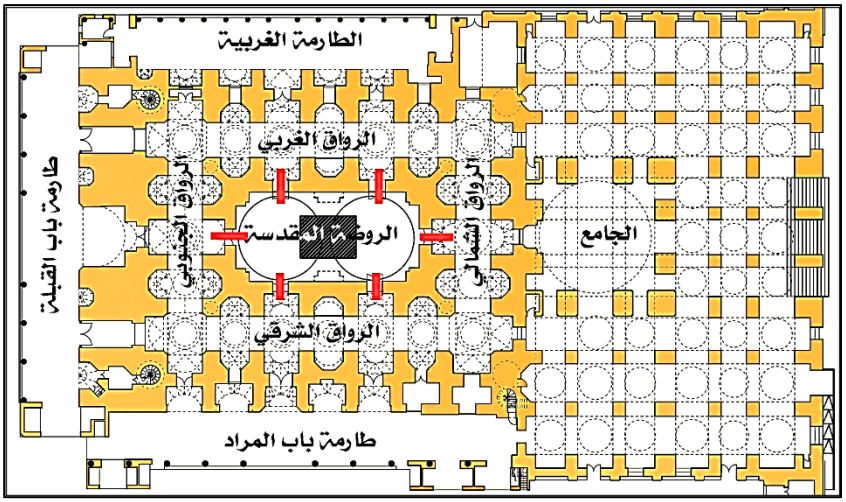

شكل (3-5) مخطط الروضة في العتبة الكاظمية المقدسة ويلاحظ الهيكل المؤشر باللون الغامق وهو بمساحة عالية نسبة لمساحة الروضة. (اعداد الباحث).

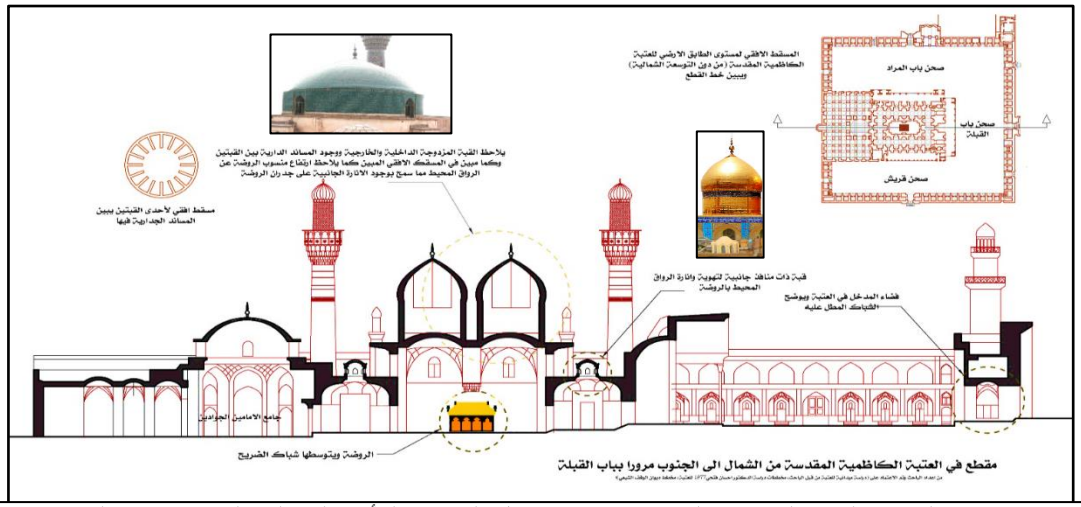

شكل (3-6) مقطع طولي في العتبة الكاظمية المقدسة ويبين تفصيل القباب والمآذن المختلفة الموجودة في العتبة. اعداد الباحث

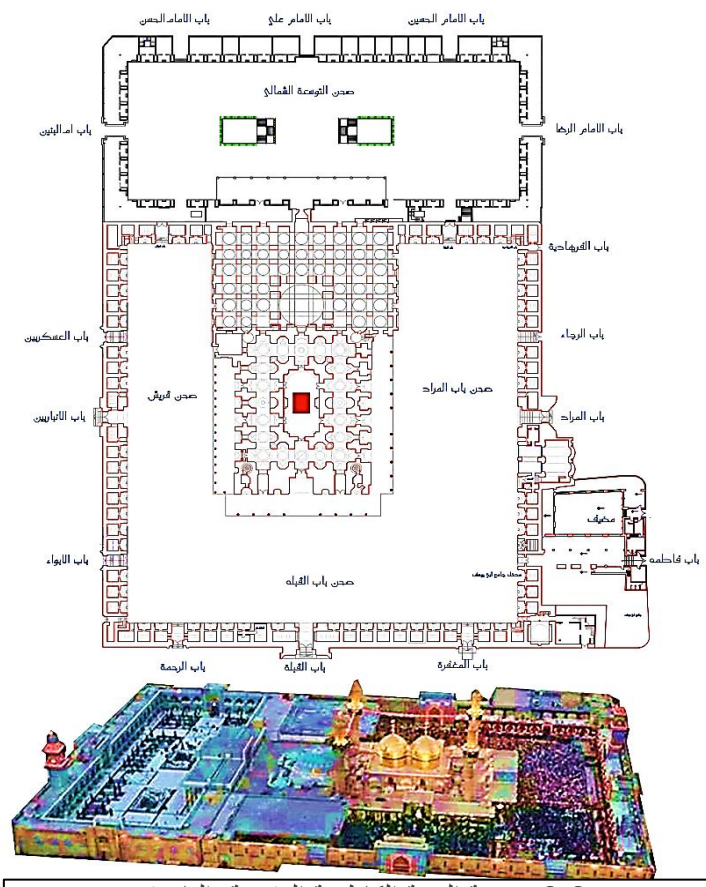

3-8 توسعة العتبة الكاظمية المقدسة، الباحث.

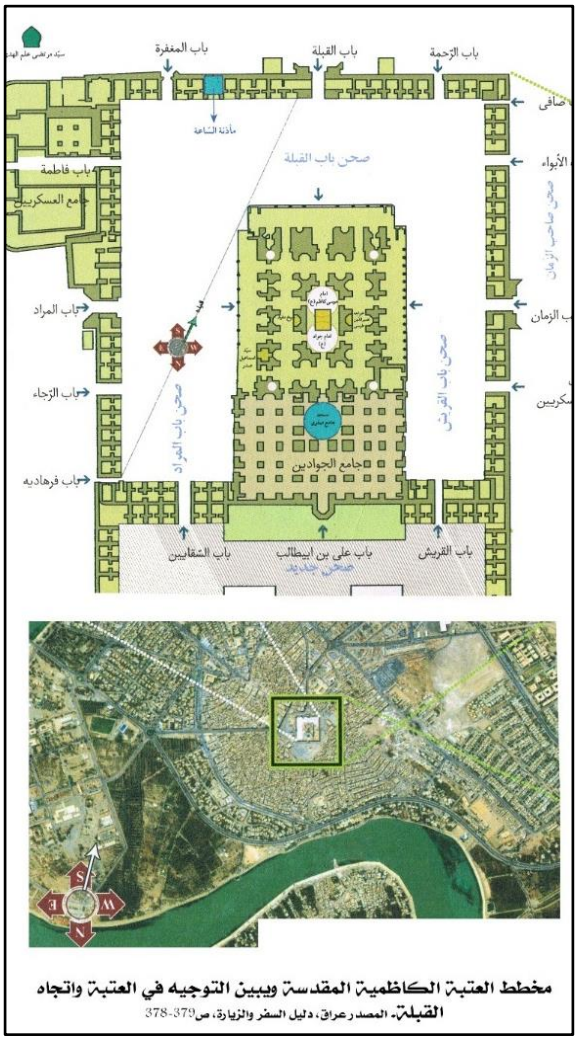

3-7 توجيه العتبة الكاظمية المقدسة.

Journal of Engineering

ISSN 1726-4073

A Scientific Refereed Journal Published by College of Engineering University of Baghdad

December

2015

Number 12

Volume 21

مجلة الهندسة

ISSN 1726-4073

مجلة علمية محكمة تصدرها
كلية الهندسة ـ جامعة بغداد

كانون الاول
2015

العدد 12
المجلد 21